

The copyright of this thesis vests in the author. No quotation from it or information derived from it is to be published without full acknowledgement of the source. The thesis is to be used for private study or non-commercial research purposes only.

Published by the University of Cape Town (UCT) in terms of the non-exclusive license granted to UCT by the author.

TOPICS IN CONTEMPORARY COSMOLOGY

by
Deon Mark Solomons

University of Cape Town

SUBMITTED IN PARTIAL FULFILLMENT OF THE
REQUIREMENTS FOR THE DEGREE OF
DOCTOR OF PHILOSOPHY
AT
UNIVERSITY OF CAPE TOWN
CAPE TOWN, SOUTH AFRICA
JULY 2003

© Copyright by Deon Mark Solomons, 2003

UNIVERSITY OF CAPE TOWN

Date: July 2003

Author: **Deon Mark Solomons**
Title: **Topics in Contemporary Cosmology**
Department: **Mathematics and Applied Mathematics**
Degree: **Ph.D.** Convocation: **December** Year: **2003**

Permission is herewith granted to University of Cape Town to circulate and to have copied for non-commercial purposes, at its discretion, the above title upon the request of individuals or institutions.

Signature of Author

THE AUTHOR RESERVES OTHER PUBLICATION RIGHTS, AND NEITHER THE THESIS NOR EXTENSIVE EXTRACTS FROM IT MAY BE PRINTED OR OTHERWISE REPRODUCED WITHOUT THE AUTHOR'S WRITTEN PERMISSION.

THE AUTHOR ATTESTS THAT PERMISSION HAS BEEN OBTAINED FOR THE USE OF ANY COPYRIGHTED MATERIAL APPEARING IN THIS THESIS (OTHER THAN BRIEF EXCERPTS REQUIRING ONLY PROPER ACKNOWLEDGEMENT IN SCHOLARLY WRITING) AND THAT ALL SUCH USE IS CLEARLY ACKNOWLEDGED.

UNIVERSITY OF CAPE TOWN
DEPARTMENT OF
MATHEMATICS AND APPLIED MATHEMATICS

The undersigned hereby certify that they have read and recommend to the Faculty of Science and Engineering for acceptance a thesis entitled "Topics in Contemporary Cosmology" by Deon Mark Solomons in partial fulfillment of the requirements for the degree of **Doctor of Philosophy**.

Dated: July 2003

External Examiner:

Research Supervisor:

George Ellis and Peter Dunsby

Examining Committee:

UNIVERSITY OF CAPE TOWN

Date: July 2003

Author: Deon Mark Solomons
Title: Topics in Contemporary Cosmology
Department: Mathematics and Applied Mathematics
Degree: Ph.D. Convocation: December Year: 2003

Permission is herewith granted to University of Cape Town to circulate and to have copied for non-commercial purposes, at its discretion, the above title upon the request of individuals or institutions.

Signature of Author

THE AUTHOR RESERVES OTHER PUBLICATION RIGHTS, AND NEITHER THE THESIS NOR EXTENSIVE EXTRACTS FROM IT MAY BE PRINTED OR OTHERWISE REPRODUCED WITHOUT THE AUTHOR'S WRITTEN PERMISSION.

THE AUTHOR ATTESTS THAT PERMISSION HAS BEEN OBTAINED FOR THE USE OF ANY COPYRIGHTED MATERIAL APPEARING IN THIS THESIS (OTHER THAN BRIEF EXCERPTS REQUIRING ONLY PROPER ACKNOWLEDGEMENT IN SCHOLARLY WRITING) AND THAT ALL SUCH USE IS CLEARLY ACKNOWLEDGED.

To Mom, Dad, Julia and Benji.

University of Cape Town

Table of Contents

Table of Contents	v
List of Tables	ix
List of Figures	x
1 Introduction	1
I Observational Cosmology	5
2 Gravitational Lensing and the Shrinking of Area Distances	6
2.1 Introducing Gravitational Lensing and Shrinking	6
2.2 The Gravitational Lens Diagram and its Lensing Equation	7
2.3 Gravitational Lensing causes Shrinking of Area Distances	10
3 Caustics of Compensated Spherical Lens Models	18
3.1 Do Gravitational Lensing Significantly Influence Area Distance Measurements?	18
3.2 The Gravitational Lensing Equations	19
3.2.1 Compensated lenses	20
3.2.2 The lensing equation in scaled variables	21
3.3 Angles and Distances	24
3.3.1 Caustics and Critical Curves	25
3.4 The Top-Hat Matter Distribution	29
3.4.1 Results	32
3.4.2 Galaxy clusters	33
3.4.3 Galaxies	35
3.5 Conclusions	36

II	Pre-Big Bang Cosmology in String Theory	38
4	Pre-Big Bang Cosmology and the Graceful Exit Problem	39
4.1	Overview	39
4.2	The Graceful Exit Problem	40
4.3	Pre-Big Bang Cosmology	42
4.4	Duality Symmetry of the Effective Action	43
4.5	Concluding Remarks	46
5	A Solution to the Graceful Exit Problem in Pre-Big Bang Cosmology	49
5.1	Introduction	49
5.2	String Cosmology Equations	50
5.2.1	Flat Dilaton Potential with Exotic Equation of State	52
5.3	Obtaining Desired Dynamics From a Dilaton Potential	54
5.3.1	The Algorithms	55
5.3.2	Exponential Scale Factor Behaviour with No Matter	56
5.4	“Pre-Big Bang” Behaviour	57
5.4.1	Pre-Big Bang behaviour with radiation equation of state	58
5.4.2	“Pre-big Bang” Behaviour with Exotic Equation of State	60
5.5	Discussion	65
III	Braneworld Cosmology	69
6	Braneworld Cosmology	70
6.1	Some Introductory Remarks	70
6.2	The Braneworld Scenario	71
6.3	Inflation on the Brane	73
6.4	Alternatives to Inflation	75
6.5	Preliminary Considerations	77
6.6	Some Final Remarks	79
7	Braneworld Inflation	80
7.1	Introduction	80
7.2	The FRW Braneworld	81
7.2.1	Matter description	81
7.2.2	Gravitational Equations	82
7.3	Generating Exact Inflation Braneworlds	83
7.3.1	The Reality Condition	83
7.3.2	How to obtain Braneworlds with desired inflationary behaviour	84
7.3.3	Simple examples	85
7.4	Flat Braneworlds with desired inflaton self- interaction	90

7.4.1	The Braneworld Superpotential	90
7.4.2	Power-law inflation	91
7.5	Conclusion	93
8	Bounce Behaviour in Kantowski-Sachs and Bianchi Cosmologies	94
8.1	Introduction	94
8.2	The Key Equations	96
8.3	The No-bounce theorem in BI, BIII and KS models	98
8.3.1	Definition of a Bounce	98
8.3.2	The reality condition at a bounce	98
8.4	No bounce behaviour in other Bianchi models	99
8.5	Bounce behaviour on a Kantowski-Sachs brane	101
8.5.1	Matter description on the Kantowski-Sachs brane	102
8.5.2	Gravitational Equations	104
8.5.3	Feasible Bounce Behaviour	104
8.5.4	Illustration	105
8.5.5	Phase Portrait	106
8.6	Conclusion	108
IV	Higher Order Corrections to Gravity	111
9	Introduction to Higher Derivative Cosmologies	112
9.1	Introduction	112
9.2	Higher Derivative Cosmology	113
9.3	Concluding Remarks	116
10	Bounce Behaviour in Higher Derivative Kantowski-Sachs Cosmology	118
10.1	Introduction	118
10.2	Preliminaries	120
10.3	Gravitational Equations	120
10.4	Bounce behaviour	121
10.4.1	The Weak Energy Condition	121
10.4.2	Equation of state	122
10.4.3	Normalized Variables	122
10.4.4	Vanishing Radiation Density $\Omega_{rad} = 0$	124
10.5	Discussion	127
A	Pre-Big Bang Evolution for Radiation	133
A.1	Introduction	133
A.2	Density evolution with exotic equation of state	135

B	Euclidean quantum wormholes with scalar fields	137
B.1	Introduction	139
B.2	The classical model	141
B.3	The perfect fluid matter model	144
B.3.1	Two examples	146
B.4	The scalar field $V(\phi)$ model	147
B.4.1	Separating the WDW	148
B.4.2	Complex scalar field with $\gamma > 2/3$	150
B.5	Discussion and Conclusions	152
B.6	Appendix	159
B.6.1	Quantum wormholes with $V(\phi) \sim \exp(\lambda\phi)$ and $ \phi \rightarrow \infty$	159
B.6.2	Quantum wormholes with $V(\phi) \sim \phi^{2n}$ and $ \phi \rightarrow 0$	164
C	Classical and quantum wormholes with perfect fluids and scalar fields	173
C.1	Introduction	175
C.2	Carlini-Mijić wormholes	176
C.2.1	Perfect fluid source	176
C.2.2	Scalar field source	177
C.3	Quantum wormholes	178
C.3.1	Perfect fluid source	178
C.3.2	Scalar field source	180
C.4	Classical signature change	180
C.4.1	Perfect fluid source	180
C.4.2	Scalar field source	183
C.5	Conclusions	185
D	Spatially Homogeneous Cosmologies: Geometrical Setting	187
	Bibliography	190

List of Tables

3.1	Area shrinking ratio with actual image redshift.	34
3.2	Cusp angle, cross-over angle and area of shrinking ratio at decoupling.	35
3.3	Area shrinking ratio with actual image redshift.	35
3.4	Cusp angle , cross-over angle and shrinking ratio at decoupling.	37
10.1	Equilibrium points of the four-dimensional <i>invariant submanifold</i> $(\mathcal{Q}, \Sigma, \Omega_R, \Omega_{rad})$ corresponding to $\mathcal{P} = 0$. B_{ϵ_1} represent unstable bounce equilibrium points on the surface $\mathcal{Q} = 0$, for fixed radiation density parameter values $\Omega_{rad} = b \leq 1$. For <i>negative</i> values of b , the higher order theory reproduce the bounce behaviour predicted by braneworld cosmology (chapter 8 and [214]). The constants $\mathcal{Q}_0, \Sigma_0, \Omega_K^0$ and Ω_Λ^0 are defined in terms of $\Omega_R =: c$ in section (10.4.3). The Bianchi III equilibrium points lie outside the domain $\{(\mathcal{Q}, \Sigma) : \mathcal{Q} \in [-1, 1]; \Sigma \in [-1, 1]\}$ and are not relevant.	125
D.1	The Bianchi types for <i>class A</i> . Null Energy Condition (NEC) violation for bounce behaviour in General Relativity is indicated with \mathcal{N} , otherwise \mathcal{Y} . Similarly for the Weak Energy Condition (WEC).	189
D.2	The Bianchi types for <i>class B</i> . Strong Energy Condition violation for bounce behaviour in General Relativity is indicated with \mathcal{N} , otherwise \mathcal{Y} . Similarly for the Weak Energy Condition (WEC).	189

List of Figures

2.1	Gravitational lensing scenario: The lens L located between the source S and the observer O produces two images S_1 and S_2 of the background source. η is the displacement of the source from the optical axis OL in the source plane. ξ is the impact parameter in the lens plane.	7
2.2	The NASA Hubble Space Telescope survey of exotic patterns, rings, arcs and crosses that are all optical mirages produced by a gravitational lens. A quick look at over 500 Hubble fields of sky has uncovered 10 interesting lens candidates in the deepest 100 fields. This is a significant increase in the number of known optical gravitational lenses.	10
2.3	A NASA Hubble Space Telescope image of the galaxy cluster CL1358+62 has uncovered a gravitationally-lensed image of a more distant galaxy located far beyond the cluster. The resulting high redshift ($z_s = 4.92$) corresponds to a very early era when the universe was just beginning to form galaxies.	11
2.4	Giant luminous arcs in cluster CL0024: five images of a high redshift galaxy seen lensed by a galaxy cluster with a redshift of $z_d = 0.39$; the radius of curvature is about 20 arcseconds	12

2.5	Abell 2218 is a rich galaxy cluster composed of thousands of galaxies and a mass equivalent to ten thousand galaxies interspersed throughout the cluster. The cluster is located relatively nearby – at a distance of 2 billion light-years (a redshift $z_d = 0.18$). The gravitational field from this huge concentration of matter distorts and magnifies the light from distant galaxies. The “baby galaxy” has a redshift of $z_s = 5.58$, corresponding to a distance of about 13.4 billion light-years. The galaxy’s light has been magnified more than 30 times by Abell 2218 and split into two “images” by the uneven distribution of matter in the cluster.	13
2.6	Left: The light from the single quasar PG 1115+080 is split and distorted in this infrared image. PG 115+080 is at a distance of about 8 billion light years in the constellation Leo, and it is viewed through an elliptical galaxy lens at a distance of 3 billion light years. Right: In this NICMOS image, the four quasar images and the lens galaxy have been subtracted, revealing a nearly complete ring of infrared light. This ring is the stretched and amplified starlight of the galaxy that contains the quasar, some 8 billion light years away. Credit: Christopher D. Impey (University of Arizona)	14
2.7	A lens L and resulting caustics on the past light cone $C^-(P)$ (2-dimensional section of the full light cone), showing in particular the cross-over line L_2 and cusp lines L_{-1}, L_1 meeting at the conjugate point Q . The intersection of the past light cone with a surface of constant time defines exterior segments C^-, C^+ of the light cone together with interior segments C_1, C_2, C_3	15
2.8	The imaged point moves forward along C_1 from I to the cusp at P_{-1} , backward along C_2 to the cusp at P_1 , and then forward along C_3 to F	16
2.9	Sampling of an inhomogeneity by the observational point at a caustic results in a change of the observed profile, because the same region of the profile is traversed 3 times by the observational point.	17
3.1	Shape of caustics in past light cone showing preferred geodesics and distance traveled.	23

3.2	The bending angle diagram for two different redshifts. (a) one large, so other side of conjugate point Q; (b) One small, so this side of conjugate point Q. The number of images is the number of times the line $y = x$ intersects the bending angle curve. Considering curve (a), firstly, there is one image corresponding to line (c); then there are two images for line (d) which is tangent to the curve and determines the cusp angle; there are three intersections for line (e) which determines the cross-over angles (as it corresponds to no displacement at the source plane); there are 3 images for generic position (f), again two images for line (g) as it passes through the cusp, and finally one image for line (h). Parameters based on the lens +MG1131+0456.	27
3.3	Variation in (a) cusp angle, (b) the crossover angle, and (c) the cut-off angle. The image redshift starts at the limiting value of $z_s = z_d = 0.231$, and increases through the arc redshift of 0.914, up to the value $z_s = 5$. Parameters based on the lens A2390.	33
3.4	The pointwise area shrinking ratio γ for parameters based on the lens +MG1131+0456.	34
3.5	The average area distance shrinking ratio β for the Abell cluster 2390. The average $\langle\beta\rangle$ at (a) $\theta = \theta_1$ (the cusp angle), (b) $\theta = \theta_2$ (the cross-over angle), and (c) $\theta = \theta_3$ (the cut-off angle).	36
4.1	Time evolution of the curvature scale in the standard cosmological scenario, in the conventional inflationary scenario, and in the string cosmology scenario. Courtesy M. Gasperini.	47
4.2	The four branches of a low-energy string cosmology background. Courtesy M. Gasperini.	48
4.3	Time evolution of the curvature scale H and of the string coupling $g_s = \exp(\phi/2) \simeq M_s/M_p$, for a typical self-dual solution of the string cosmology equations. Courtesy M. Gasperini.	48
5.1	Phase portrait representing the solution space of equations (5.2.13–5.2.14) with $\kappa > 0$	53
5.2	Phase portrait representing the solution space of equation (5.4.17).	62

5.3	The evolution of the scalefactor $a(t)$ as a function of time t , with $a(0) = 1$, over the time interval $[-10, 10]$. For negative times $t \leq 0$, there is power-law inflation, $t \geq 0$, followed by a radiation dominated phase of expansion for positive time $t \geq 0$	64
5.4	The function $\exp(\phi(t))$ as a function of time t , with $a(0) = 1$, $\phi(0) = 0$ and $\chi(0) = 0.25$. $\exp(\phi(t))$ increases monotonically from 0 at time $t = -\infty$ to 2 at $t = +\infty$	64
5.5	The dilaton potential $V(\phi)$ as a function of time ϕ . We assume that $a(0) = 1$, $\phi(0) = 0$ and $\chi(0) = 0.25$ and take the density $\rho(t)$ to have value $\rho(\infty) = 0$ at time $t = \infty$. The potential $V(\phi)$ is continuous at all times, but non-differentiable at $\phi = 0$. For $\phi \rightarrow -\infty$, $V(\phi)$ is asymptotically zero. To the right of $\phi = 0$, the potential starts at $V \approx -0.005$ and goes to zero from below as phi goes to $\ln 2$, then increases to $+\infty$ as $\phi \rightarrow \infty$. Around $\phi = \ln 2$, both $V(\phi)$ and its gradient $V'(\phi)$ are zero. As time $t \rightarrow +\infty$, the dilaton field asymptotes to a constant value of $\ln 2$ in our model. The dilaton potential $V(\phi)$ approximates a fixed value of 0 as $\phi \rightarrow \ln 2$ asymptotically for large positive times.	66
8.1	State space R is an invariant submanifold of M that represents general relativity for ${}^{(3)}R \geq 0$. The separatrix $y = Q - \Sigma = 0$ precludes bounce behaviour in Y from occurring.	109
8.2	State space M no longer has a separatrix at $y = Q - \Sigma = 0$ for $\Omega_u > 0$. A <i>blue</i> trajectory that passes through the plane $x = Q + 2\Sigma = 0$ exhibits bounce heavier in X , and a bounce in Y when it passes through the plane $y = Q - \Sigma = 0$	110
10.1	False Vacuum Bounce: The state space \mathcal{R} exhibits bounce behaviour in scale factor X as a blue trajectory that passes through the plane $Q + 2\Sigma = 0$, and a bounce in Y as that same trajectory passes through the plane $Q - \Sigma = 0$	126
B.1	The wave function for a perfect fluid model with $\gamma = 4/3$ (we have plotted the sum in eq. B.3.8 for $n \in [0, 10]$).	169

B.2	The wave function for a perfect fluid model with $\gamma = 0$ (we have plotted eq. B.3.10 for $d_2 = 0$ and $a_0 = 1$).	169
B.3	The potential $V(\phi) = \Omega \cosh^{2n} \lambda \phi$ for $\gamma = 1/2$	170
B.4	The potential $V(\phi) = \Omega \cosh^{2n} \lambda \phi$ for $\gamma = 4/3$	171
B.5	The potential $V(\phi) = \Omega \cos^{2n} \lambda \phi_2$ for $\gamma = 4/3$ and $\lambda \phi_2 \rightarrow \lambda \phi - \pi/2$	172

University of Cape Town

Abstract

There are distinct divisions to this document that separate the bulk of work into four Parts and an Appendix, each dealing with topics in General Relativity, Pre-Big Bang Cosmology in String Theory, the Braneworld Scenario and Higher Derivative Cosmology. The Appendix contains some important results related to these topics, but is mainly composed of two publications in Quantum Cosmology.

The first Chapter is an Introduction to the thesis. PART I reflects upon the effect that Caustic Formation in Gravitational Lensing has on Area Distance Measurements in Observational Cosmology. The claim that caustic formation necessarily leads to *shrinking*, in that distant areas subtend smaller solid angles than they would in a FL universe model and that this effect will remain even when the observations relate to large angles, is illustrated by exact examples with caustics displaying the *shrinking effects* for single spherically symmetric compensated lenses to which we can apply the thin-lens approximation.

In Part II we pay particular attention to attempts at using the Pre-Big Bang Cosmological Scenario to resolve some problems of the Standard Cosmological Model. We highlight issues surrounding the *graceful exit* from an initial Inflationary phase of expansion in the very early Universe. However, the main aim is to solve the equations of String Cosmology in the String Frame, allowing for a dilaton potential $V(\phi)$. We look at cases in which the *equations* have such a scale factor symmetry, when solutions may or may not exhibit the same symmetry, and at cases in which the *solutions obey* the scale factor symmetry, even if the *equations do not*.

After a brief look at recent developments in Braneworld Cosmological Scenario (a derivative of String Theory) in Part III, we derive a code for constructing the self-interacting potential $V(\phi)$ of a Universe in which Inflationary behaviour in FRW expansion is driven by its scalar field ϕ confined to the brane. Bounce Behaviour in Cosmology is an alternative to Inflationary Cosmology that attempts at circumventing certain problems surrounding evolution from a Big Bang singularity. However, Bounce Behaviour in Relativistic Cosmology violates some important Energy Conditions. The Braneworld Scenario is free of these

energy violating anomalies. We therefore investigate Bounce Behaviour in Kantowski-Sachs Braneworld Cosmologies.

Higher Derivative Theories of Gravity of the form $R + \alpha R^2$ (here R is the Ricci scalar, α is constant) is an alternative that allows greater freedom in the choice of underlying geometrical structure that allows for feasible Bounce Behaviour. This is explored in Part IV.

The two publications that are included in the Appendix concentrate on Euclidean Wormholes obtained by the analytic continuation of closed recollapsing FRW universes. The Quantum versions of such Wormholes are consistent with the Hawking-Page (HP) conjecture for Quantum Wormholes as solutions of the Wheeler-De Witt equation. This is contrasted with a classical change of signature approach which, upon quantization gives everywhere oscillatory wave-functions which do not satisfy the HP conjecture. Matter sources giving Quantum Wormholes include a dilaton with a self-interacting exponential potential obtained from String Theory, unlike the classical case where such matter sources do not allow wormhole solutions. Excited states of the Quantum Wormhole spectrum are also derived.

Acknowledgements

I wish to express my sincerest gratitude to Di Loureiro for her unwavering support and timely reminders to complete (and submit!) this thesis.

I owe George Ellis, my supervisor and constant source of inspiration, far more than gratitude. He has been a father-figure when it came to matters of commitment to the task, always endearing, especially at times when I was my most rebellious self, more often than not distracted by trivia. His insight and vast knowledge reaches way beyond the sphere of science, and impress upon me the importance of maintaining good human relations.

Peter Dunsby is the most tolerant of men, and a true friend. His enthusiasm for science is immeasurable. Having had Peter as a supervisor has made the task of writing up this thesis a joy indeed. Needless to say, the final document does not do justice to his scrutinizing eye and keen sense of judgement. I thank him dearly.

To Julia: How quickly eight years of fun and laughter flew by, and upon reflection, what a worthwhile journey. A journey enriched by your charm and grace.

Love for Mathematics and Science is based upon a love for life itself, a love nurtured by trust and tempered faith imparted throughout a glorious youth spent amongst close-knit family and friends, on the dunes and rolling grasslands of the Cape. In my case, I have two wonderful parents to thank.

Chapter 1

Introduction

There are four parts to this thesis, in addition to a rather bulky Appendix. The first two parts are fairly independent in terms of content, while parts III and IV overlap to a large degree. The Appendix contains two publications that deal with topics in the field of Quantum Cosmology, which is fairly disjoint from the rest of the thesis.

Part I deals with the rather swanky notion of *shrinking*. The second chapter introduces the fundamental ideas behind Gravitational Lensing and how it results in this phenomenon (a large portion of this chapter is due to the seminal paper on *shrinking* [49]). Caustic formation in Gravitational Lensing has a significant effect on area distance measurements in Observational Cosmology [49, 171, 53]. We start with a brief introduction to Strong Gravitational Lensing [202, 85, 6], and then present the claim that caustic formation [186] necessarily leads to *shrinking*, in that distant areas subtend smaller solid angles than they would in a Friedmann-Lemaitre (FL) universe model and that this effect will remain even when the observations relate to large angles. In the Chapter 3, this is followed up by exact examples with caustics displaying the shrinking effects. We show how to calculate the magnitude of the effect analytically and numerically for single spherically symmetric compensated lenses to which we can apply the thin-lens approximation, and look in detail at *top hat* lenses, which are the simplest in this class. These were done in the context of observation of luminous arcs and multiple lensed images [146, 216, 217, 218, 122, 180].

Initial impressions of the capacity of the Pre-Big Bang Cosmology [69, 71, 16, 193, 70, 17] proved to be somewhat optimistic. Part II of this thesis starts with a short review of some

of the problems encountered in the Standard Cosmological Scenario, and in particular at attempts to resolve them in the context of the Pre-Big Bang Cosmological Scenario. This is done in Chapter 4. We highlight issues surrounding the *graceful exit* [153, 154, 14, 15, 62, 27] from an initial Inflationary phase of expansion in the very early Universe. In Section 4.3 we review some important aspects of Pre-Big Bang Cosmology. The characteristic Duality symmetry of the Effective Action of String Theory is discussed in Section 4.4.

The equations of String Cosmology in the String Frame allow for a dilaton potential $V(\phi)$ that does not feature naturally in General Relativity. In Chapter 5 we are able to use a code to arrive at *desired* String Cosmology solutions when there is a dilaton potential V not equal to zero, and used it to obtain Pre-Big Bang solutions that seem to have close to the desired properties. Two different cases are considered: In the first case, choice of the exact radiation equation of state (5.4.3) at all times leads to a very unstable situation where extreme fine-tuning of initial conditions is required to attain the desired results, and indeed there may be no initial data leading to the desired behaviour in both the forward and backwards directions of time. In the second case an *exotic equation of state* (5.4.9) links the fluid behaviour to the potential in a way that generalizes the perfect fluid equation of state. The desired solutions are found without the need for fine tuning the initial data set at $t = 0$. The Duality symmetry of the Effective Action of String Theory is discussed in Section 4.4 is reviewed in Section 5.2.1 and Section 5.4. The *equations* have such a scale factor symmetry, when solutions may or may not exhibit the same symmetry, and at cases in which the *solutions obey* the scale factor symmetry, even if the *equations do not*. In the latter case we obtain some solutions that seem to have most of the properties desired in the Pre-Big Bang Scenario.

In Chapter 6 of PART III we describe the underlying geometrical setting of the so-called Braneworld Scenario [2, 113, 131]. In the Randall-Sundrum setting [189] the observable Universe is a 3-brane boundary of a non-compact Z_2 symmetric 5-dimensional Anti-de Sitter (AdS) space. The matter fields are restricted to the brane but gravity exists in the whole Anti-de Sitter (AdS) bulk. We take a brief look at recent developments in Braneworld Inflation in Section 6.3 and in Section 7.1. In Section 7.2 of Chapter 7 we develop a generic scheme (see [155, 52] and Chapter 5 for an outline of this code) for constructing models with a single scalar field that is confined to the brane, and the appropriate potential for different

types of Inflationary behaviour in Friedmann-Robertson-Walker (FRW) Universes. We find that Braneworlds generically possess larger classes of potentials for a particular type of Inflationary behaviour than what is found in General Relativistic Cosmology.

Each of the various Inflationary Cosmological Scenarios has a vested set of problems [84, 141, 124, 140], and so far none of them are sufficiently broad to solve all the problems of the Standard Model of Cosmology. Bounce Behaviour in Cosmology 6.4 is an alternative to Inflationary Cosmology that attempts at circumventing certain problems surrounding evolution from a Big Bang singularity. In Chapter 8 of PART III we show that besides violating the SEC, Bounce Behaviour in Relativistic Cosmology leads to violation of either the NEC or the WEC or both. Once we incorporate the Braneworld Scenario of Randall and Sundrum, however, such energy violations disappear. If one envisage the Universe as emerging from the interior of a collapsing black hole state [226, 39, 211, 44], then the geometry of Kantowski-Sachs Universe models have the desirable property that they share the same symmetries as the spatially homogeneous interior region of the extended (vacuum) Kruskal solution, making them ideal candidates for such a scenario. We therefore investigate Bounce Behaviour in Kantowski-Sachs Braneworld Cosmologies [92].

More over, one may broaden the scope of the discussion by embracing a class of Higher Derivative Theories of Gravity (of which the Randall-Sundrum Braneworld Scenario is a subclass) to demonstrate the feasibility of Bounce Behaviour in a broader sense, without violating either the NEC or the WEC. This we do in a Chapter called Higher Derivative Kantowski-Sachs Cosmology of Part IV. The Introductory Chapter to Part IV contains a section (9.2) that describes recent attempts to use Higher Derivative Cosmologies as an alternative, that may harness the curvature singularities of General Relativity [73, 114]. Significant results such as the *Zero Energy Theorem* [11] and the *Conformal Equivalence Theorem* of Barrow and Cotsakis [4, 30] are additional guidelines toward resolving the problems associated with Higher Order Gravity Theories, and also to help us understand the intrinsic nature of a theory with a Lagrangian which has an alternative functional form.

In Chapter 10 we consider the eventuality of an Alternative Theory with Lagrangian that is a function of the form $f(R) = R + \alpha R^2$. Recent work by Gordon and Turok [172] employs an idea derived from the Ekpyrotic Scenario [220, 123, 221] to provide estimates of the comoving curvature perturbations generated via back-reaction from a *pre-singularity*

phase, and hence resulting in a *semi-classical* bounce. We hope to discuss relation to their work in a forthcoming publication.

We have included two publications in the Appendix that deal with Quantum Cosmology, a subject that falls outside the primary emphasis of this thesis, yet forms part of research performed towards obtaining the degree of PhD.

The first of the two publications by the authors A Carlini, DH Coule and DM Solomons called *Classical and Quantum Wormholes with Perfect Fluids and Scalar Fields* [22] directs attention to Euclidean Wormholes obtained by the analytic continuation of closed recollapsing FRW universes obtained by Carlini and Mijić (CM) [25]. This is demonstrated for a perfect fluid satisfying the SEC. The Quantum versions of such Wormholes are consistent with the Hawking-Page (HP) [248, 90] conjecture for Quantum Wormholes as solutions of the Wheeler-DeWitt equation. This is contrasted with a classical change of signature approach which, although might be consistent with the existence of Classical Wormholes for a given definition of the energy-momentum tensor of the fluid, upon quantization gives everywhere oscillatory wavefunctions which do not satisfy the HP conjecture.

The second publication by the authors A Carlini, DH Coule and DM Solomons, also called contained in the Appendix, is called *Euclidean Quantum Wormholes with Scalar Fields* [22], and further investigates the Quantum analogues of Euclidean Wormholes obtained by Carlini and Mijić (CM). By simulating the equation of state of a perfect fluid with a real scalar field, Quantum Wormholes are also found when the SEC is violated, although generally not Asymptotically Euclidean (AE). The non AE solutions are interpreted as excited states of the Quantum Wormhole spectrum.

These results give support to the claim of HP that Quantum Wormhole solutions are a fairly general property of the WDW equation for various matter sources. Matter sources giving Quantum Wormholes could now include those expected in low-energy effective String Theory: a dilaton with a self-interacting exponential potential. This is unlike the classical case where such matter sources do not allow Wormhole solutions.

Finally, these Quantum Wormhole solutions are contrasted with other boundary conditions of Quantum Cosmology describing an Inflationary earlier behaviour and a resulting large Lorentzian Universe phase. Quantum Wormholes were initially used in an attempt to justify why the Cosmological Constant should be zero [28, 35].

Part I

Observational Cosmology

University of Cape Town

Chapter 2

Gravitational Lensing and the Shrinking of Area Distances

2.1 Introducing Gravitational Lensing and Shrinking

In this Chapter we present an overview of the Gravitational Lens Equation and particularly summarize the latter day impact of Strong Gravitational Lensing upon observations, and how its is applied today (eg. in the search for dark matter).

Thereafter we explain the bearing Gravitational Lensing has upon area distance measurements. We elaborate the claim that observational results using Area Distances may lead to conflicting results, for instance the use of FL area distance formula underestimates area distances on both small and large scales (a phenomenon called *shrinking*).

It is in the presence of caustic formation that area distance measurements veer significantly from angular diameter distance measurements, although the two have the same manifestation in its absence. The areas corresponding to a specific solid angle are invariant if the shear is small in a vacuum region, but there will be a change in area if distortion is significant or if there is matter present, as follows from the null Raychaudhuri equation.

Thus focussing is caused when Strong Lensing takes place. Consequently before cusps have formed, the area of a nearby bundle of geodesics will be less than if the strong lens had not been there, such as in the FL background geometry.

2.2 The Gravitational Lens Diagram and its Lensing Equation

In Figure 2.1 we illustrate the gravitational lensing scenario.

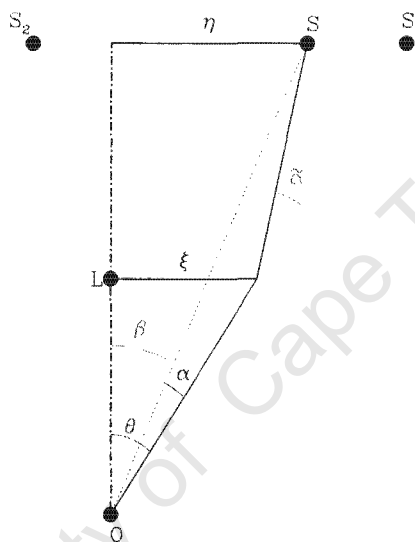


Figure 2.1: Gravitational lensing scenario: The lens L located between the source S and the observer O produces two images S_1 and S_2 of the background source. η is the displacement of the source from the optical axis OL in the source plane. ξ is the impact parameter in the lens plane.

The true deflection is represented by $\tilde{\alpha}$. The observed deflection at the observer's plane is reduced by $\alpha = \frac{D_{ds}}{D_s} \tilde{\alpha}$, where $\tilde{\alpha}(\xi) = \frac{4G}{c^2} \frac{M(\xi)}{\xi}$; $M(\xi)$ is the mass inside a radius ξ . For $\theta, \beta, \alpha \ll 1$, we relate the position of the image to the source by

$$\beta = \theta - \alpha(\theta).$$

The two-dimensional generalization of this result leads to the lens equation

$$\vec{\beta} = \vec{\theta} - \vec{\alpha}(\vec{\theta}). \quad (2.2.1)$$

Clearly the impact vector $\vec{\xi} = D_d \vec{\theta}$. If the source is located exactly on the optical axis,

then $\beta = 0$ so that

$$\theta_E = \sqrt{\frac{4GM}{c^2} \frac{D_{ds}}{D_d D_s}}. \quad (2.2.2)$$

Here θ_E is called the Einstein radius that defines the angular scale of the lensing scenario. For instance, microlensing phenomena inside the Milky Way act over scales $\theta_E \approx 0.5 (h_{50})^{-\frac{1}{2}} \sqrt{\frac{M}{M_\odot}}$ milli-arcsec with timescales typically ranging from weeks to months. Here we have expressed the Hubble constant $H_0 = 50 h_{50} \text{kms}^{-1} \text{Mpc}^{-1}$ where $1 \leq h_{50} \leq 2$. For a galaxy of mass $M = 10^{11} M_\odot$ at a redshift of $z_d = 0.5$ and a source at redshift $z_s = 2.0$, the Einstein radius is

$$\theta_E \approx 0.57 (h_{50})^{-\frac{1}{2}} \sqrt{\frac{M}{10^{11} M_\odot}} \text{ arcsec}, \quad (2.2.3)$$

with timescales extending up to a year if it is cosmological/quasar microlensing. For Strong Lensing events, caustic crossings can be as short as a few weeks. The first images due to Strong Lensing was detected in 1986, as highly elongated curves (so-called luminous ‘arcs’) of low surface brightness were detected in two galaxy clusters, Abell 370 and Cl 2244 reported in Lynds and Petrosian 1986 [146] and Soucail et al. 1987a,b [216], [217], and also Soucail et al. 1988 [218].

Strong lensing is characterized by a source/lens/observer configuration illustrated in Figure 2.1 that may change with time. See pictures 2.2-2.6 for some examples of Strong Lensing. We give a brief summary of recent observations and applications of Strong Lensing:

- 1 Lens images are typically **distorted**, as seen in the Hubble Deep Field [85] giant luminous arcs; Bartelmann [6] gives an up to date overview of the lessons learned from lensing on mass distributions in clusters. Large arcs are usually thin, and some are unresolved even on Hubble Space Telescope images. A giant arc may have radius of curvature larger than the radius of cluster galaxies, and lacks a bright and extended counter-arc. “Straight” arcs are structures in clusters that resemble arcs in there length, brightness and of course high redshift, but lack curvature (first observed by Pelló *et al* 1991 [180]). “Radial” arcs point away from the cluster centers and generally appear very close to the central cluster galaxy (e.g. Fort *et al.* 1992 [89]; Hammer *et al.* 1997 [209]).
- 2 Sources are sometimes **magnified** but most sources are slightly demagnified. **Duplication** may occur, as unresolved multiple images (microlensing) or distinct multiple

quasar or galaxy images observed directly. An **offset in position** is common, as illustrated in Figure 2.1.

- 4 **Cosmic Microwave Background:** Weak gravitational lensing of the cosmic microwave background (CMB) and the cosmic shearing of faint galaxies images will help shed light on quantities hidden from the CMB temperature anisotropies such as dark energy (see Wayne Hu 2001 [104]): lensing power spectra break CMB degeneracies and they can ultimately be used to map structures on the largest scales at high redshift [247, 246, 102, 103]. In its cross correlation with the integrated Sachs-Wolfe effect, CMB lensing offers a unique opportunity for a more direct detection of the dark energy and enables study of its clustering properties. By obtaining source redshifts and cross-correlations with CMB lensing, cosmic shear surveys provide tomographic handles on the evolution of clustering and correspondingly better precision on the dark energy equation of state and density.
- 5 **Gravitational waves:** Ruffa [196] has proposed that the massive black hole at the Galactic center may act as a gravitational lens focusing gravitational wave energy to the Earth. The author considers the gravitational wave signal emitted are galactic spinning pulsars, for which enhancements in the gravitational wave intensity of a few thousand-fold is found. For galactic and extra-galactic sources the intensity enhancement can be as high as 4,000 and 17,000, respectively. De Paolis *et al* [175] determines that the probability of significant signal enhancement from galactic and extra-galactic pulsars, and find it to be negligible.
- 6 **Astrophysical systems such as white dwarfs and galaxies, by spherically symmetric lenses with angular momentum** [205, 20]. **Gravitomagnetism** induces a correction on the deflection angle as large as 0.1%.
- 7 **Supernovae:** Edvard Mörtsell 2001 [166] investigated the possibility of calculating the fraction of compact objects in the Universe by studying gravitational lensing effects on Type Ia supernova observations. Using simulated data sets from one year of operation of the proposed dedicated supernova detection satellite SNAP, they find that it should be possible to determine the fraction of compact objects to an accuracy of less than 5%. Gunnarsson 2001 [83, 167] investigate the effect of gravitational lensing on the

farthest known supernova, SN1997ff with a redshift of $z_s \approx 1.7$ (see Riess 2001 [195]) in the Hubble Deep Field North [85]. Poor knowledge of the properties of the lensing foreground galaxies still makes it difficult to put strong constraints on the cosmological parameters, grey dust obscuration or luminosity evolution of SNIa.

8 General use in the Search for Matter: Gravitational lensing is sensitive to both luminous and dark matter alike. All lensing effects (offset in position, distortion, magnification and multiple images) are used in the search for matter (see e.g. Wambsganss 2002 [238] for a good summary).

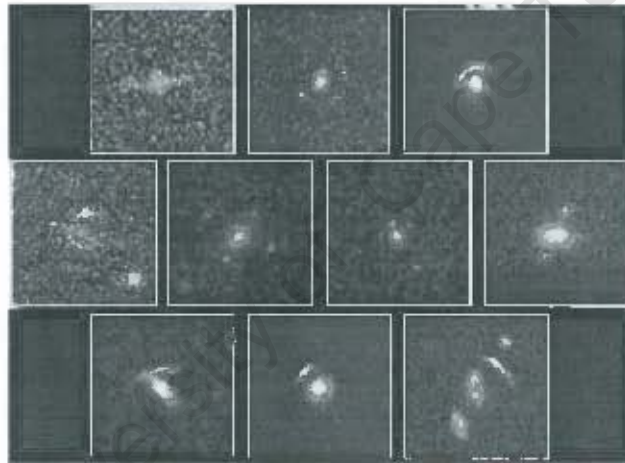


Figure 2.2: The NASA Hubble Space Telescope survey of exotic patterns, rings, arcs and crosses that are all optical mirages produced by a gravitational lens. A quick look at over 500 Hubble fields of sky has uncovered 10 interesting lens candidates in the deepest 100 fields. This is a significant increase in the number of known optical gravitational lenses.

2.3 Gravitational Lensing causes Shrinking of Area Distances

In a Friedmann-Lemaître (FL) universe, an exactly spatially homogeneous and isotropic Robertson-Walker (RW) geometry is some kind of large-scale average of inhomogeneous matter distribution and geometry on smaller scales [54]. Local inhomogeneities cause distortion of bundles of light rays and so alters the angular diameter distance and area distance

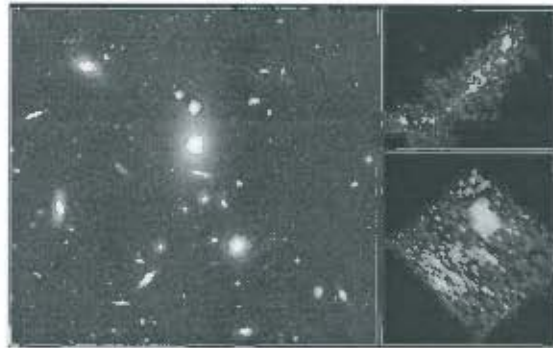


Figure 2.3: A NASA Hubble Space Telescope image of the galaxy cluster CL1358+62 has uncovered a gravitationally-lensed image of a more distant galaxy located far beyond the cluster. The resulting high redshift ($z_s = 4.92$) corresponds to a very early era when the universe was just beginning to form galaxies.

through the resultant gravitational lensing [49]. Bertotti gave a power-series expansion for this effect [8] while the Dyer-Roeder formula [43, 202] can be used at any redshift for those many rays that propagate in the lower density regions between inhomogeneities. However this formula is not accurate for those ray bundles that pass very close to matter, where shearing becomes important [49]. Some null geodesics may pass through regions of low density, while others may through lensing-induced caustics. As a result the cosmological area distances due to combinations of these effects may be significantly altered. In fact, references [49, 171, 53] demonstrate an increase in observed areas corresponding to a given solid angle even when averaged over large angular scales, through the additive effect of increases on all scales, but particularly on micro-angular scales. When caustics occur, area distances and angular-diameter distances no longer coincide. Angular sizes will not be significantly effected on large angular scales [49]. Other studies [204, 42, 99, 86] all indicate that an average source at high redshift in our universe will be demagnified due to caustics, and therefore the area distance is not FL on average. The fact that the area distance of the volume averaged inhomogeneous universe need not be that of the underlying FL model was proven explicitly in [171], and investigated further by Linder [143]. This is contrary to the commonly accepted view (see for instance [241]) that although the area distance will be inaccurately represented by the FL area distance formula on small angular scales due to

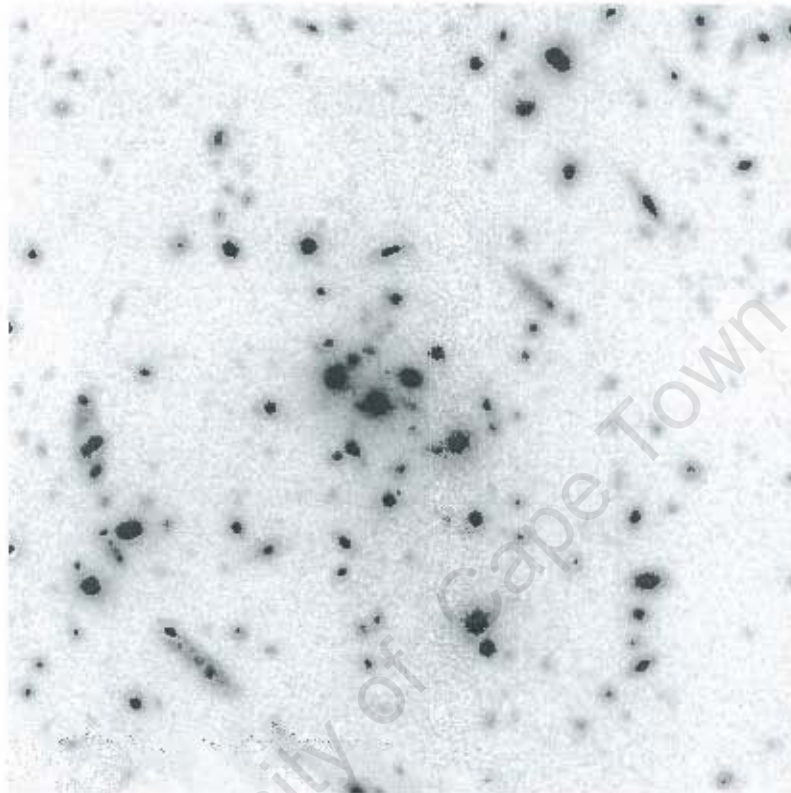


Figure 2.4: Giant luminous arcs in cluster CL0024: five images of a high redshift galaxy seen lensed by a galaxy cluster with a redshift of $z_d = 0.39$; the radius of curvature is about 20 arcseconds

the clumping of matter, when averaged over large enough angular scales that the formula will be exactly correct, essentially due to photon conservation. For a formal rebuttal of this notion, see reference [49] page 3.

In 2.3 we present the generic shape of a 2-dimensional section of the null cone occurring when simple gravitational lensing takes place¹. Bundles of light rays passing through empty space between clustered matter will be less focused than in the corresponding FL

¹This diagram was taken from reference [49]. See also Figure 2 in [173], Figure 5.1 in [202], Figure 4 in [65], and Figure 25 in [192]



Figure 2.5: Abell 2218 is a rich galaxy cluster composed of thousands of galaxies and a mass equivalent to ten thousand galaxies interspersed throughout the cluster. The cluster is located relatively nearby – at a distance of 2 billion light-years (a redshift $z_d = 0.18$). The gravitational field from this huge concentration of matter distorts and magnifies the light from distant galaxies. The “baby galaxy” has a redshift of $z_s = 5.58$, corresponding to a distance of about 13.4 billion light-years. The galaxy’s light has been magnified more than 30 times by Abell 2218 and split into two “images” by the uneven distribution of matter in the cluster.

geometry [43]. However, further down the null geodesics after passing strong sources, conjugate points (and associated multiple images) will occur [203, 128]; the loci of conjugate points in space time is a caustic sheet, a two-dimensional surface to which the rays are tangent [49, 10]. The typical behaviour of null rays near these caustics has been presented in [182] (see Figure 49); the relation to gravitational lensing is discussed *inter alia* in [202]. We now demonstrate how a combination of these effects can change the area-distance relation².

Figure 2.3 illustrates the past light cone $C^-(P)$ of the space-time event ‘here and now’,

²A detailed analysis can be found in reference [49]

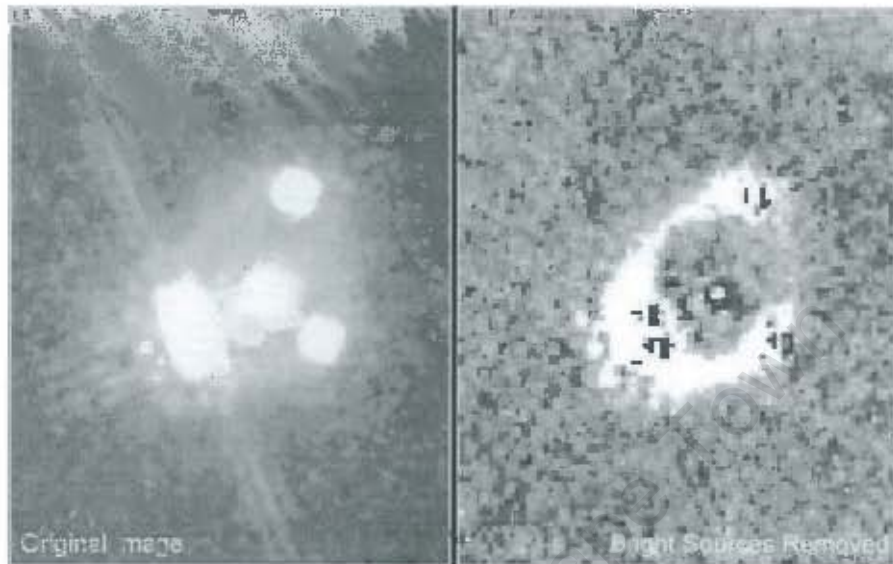


Figure 2.6: Left: The light from the single quasar PG 1115+080 is split and distorted in this infrared image. PG 1115+080 is at a distance of about 8 billion light years in the constellation Leo, and it is viewed through an elliptical galaxy lens at a distance of 3 billion light years. Right: In this NICMOS image, the four quasar images and the lens galaxy have been subtracted, revealing a nearly complete ring of infrared light. This ring is the stretched and amplified starlight of the galaxy that contains the quasar, some 8 billion light years away. Credit: Christopher D. Impey (University of Arizona)

denoted by P . As a bundle of light rays $B(d\Omega)$ generating $C^-(P)$ (and subtending a solid angle $d\Omega$ at P) passes near a lensing mass L , the nearer rays are distorted in towards the central ray γ_L linking P to L . Radial ratios will change (cf. [202], figure 2.3), decreasing as light rays are bent inwards in the case of a spherically symmetric lens (cf [186], Figure 2). The areas corresponding to a specific solid angle are invariant if the shear is small in a vacuum region, because transverse ratios will change in a compensating way, but there will be a change in area if distortion is significant or if there is matter present (as follows from the null Raychaudhuri equation, see e.g. [8, 204]). Thus focussing is caused when Strong Lensing takes place, and this can be examined by ray tracing, by use of the geodesic deviation equation, or by using the optical scalar equations. Consequently before cusps have formed, the area dS of this nearby bundle of geodesics $B(d\Omega)$ beyond L will be less

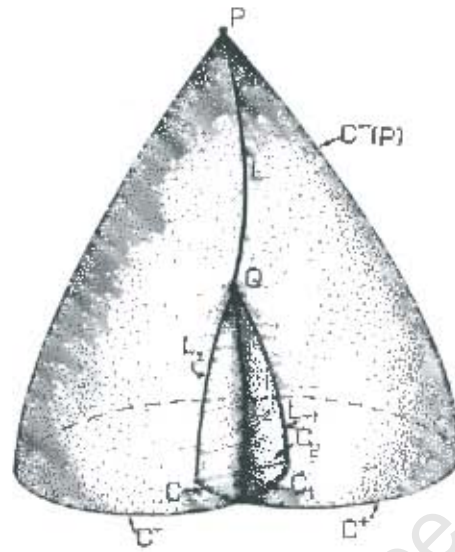


Figure 2.7: A lens L and resulting caustics on the past light cone $C^-(P)$ (2-dimensional section of the full light cone), showing in particular the cross-over line L_2 and cusp lines L_1, L_3 meeting at the conjugate point Q . The intersection of the past light cone with a surface of constant time defines exterior segments C^-, C^+ of the light cone together with interior segments C_1, C_2, C_3 .

than if L had not been there (i.e. in an FL background geometry). Further out from the lens, where the density is less than in the background, the effect will be reversed: areas will be larger [49]. As the observer's direction of view changes at P , the angle of observation θ increases continuously from some arbitrary initial angle θ_I to a final direction θ_F , where the corresponding light rays pass through a transparent lens L centered at θ_L , with $\theta_I < \theta_L < \theta_F$. We assume that the light rays develop caustics before intersecting the spacelike surface Σ . As θ continuously increases at P , the corresponding image point in Σ will trace out an arc along the intersection of $C^-(P)$ with Σ , which consists of a series of forward, backward, and then forward motions; the light-cone has at least two cusps and a cross-over (self-intersection) in it, each of these being projections of the caustic sheet in full space time.

Let us consider the motion of the image point in Σ (see Figure 2.3). Starting at the initial point I on C_- , it moves on C_- from left, through the cross-over point P_2 along C_1

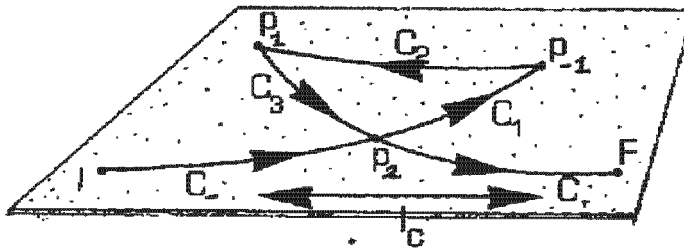


Figure 2.8: The imaged point moves forward along C_1 from I to the cusp at P_{-1} , backward along C_2 to the cusp at P_1 , and then forward along C_3 to F .

to the cusp point P_{-1} , then back along C_2 through the lens point to the cusp point P_1 , and then forward along C_3 through the cross-over point P_2 again and onwards on C_+ to the final point F on C_+ . Hence it effectively traverse the same spatial distance three times. We distinguish *distance traveled* l_t along the full path (calculated as a line integral along the path) from *distance gained* l_g - how far the image point has moved in space from its starting point θ_I to its final point θ_F , calculated by determining the shortest distance between I and F .

What this shows is that after caustics have occurred, area distances and angular size distances are different. The former corresponds broadly to distance traveled, the latter to distance gained. A strongly-lensing object L will cause caustic lines on Σ , defined as the intersection of the caustic sheet with Σ . These will be spherically symmetric if the lensing object is spherically symmetric, and will be centered on the null geodesic γ_L from P through L to Σ ; similarly the critical curves (the images in the lens plane of the caustic lines) will also be circles around γ_L . Considering the full two-dimensional intersection \mathcal{S} of $C^-(P)$ with Σ , in the spherically symmetric lens case, it will be given by rotating the 1-dimensional picture (2.3) about the central geodesic γ_L (see also Figure 2.9 in this regard). In order to calculate the area relations, we need to use the determinant J relating solid angles at the observer to areas in the source plane [202], the key point being sign of J : the regions where angular travel is forward as discussed above will correspond to regions where $|J| > 0$; the regions where angular travel is backwards correspond to where $|J| < 0$. Thus in adding up areas, we have two options: adding up the magnitudes of areas (where we assign a +ve

value to all areas, i.e. we integrate $|J|$ over the relevant solid angle) or adding up signed areas (where we assign a -ve value to areas where $|J| < 0$, i.e. we integrate J itself over the relevant solid angle). The former corresponds to distance gained, the latter to distance traveled (see figure 2.9).

We use the latter to define area distance in the realistic universe model, and hence to determine the area ratio $\langle \beta \rangle$. Hence we take the modulus of areas and solid angles in calculating $\langle \beta \rangle$. The claim in [49] is that when the background model is properly matched to a more realistic lumpy universe model, we will find $\langle \beta \rangle > 1$ on averaging over large angular scales.

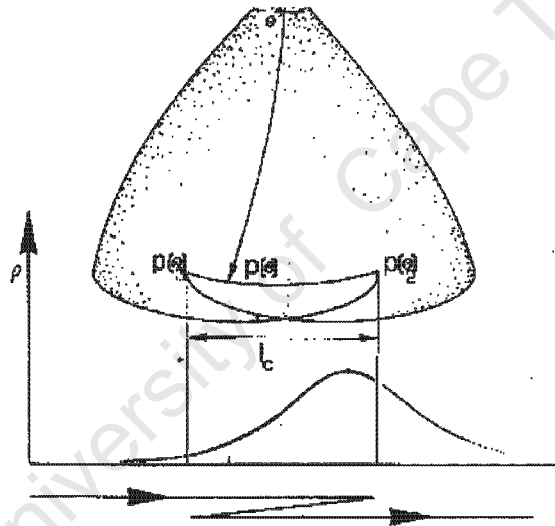


Figure 2.9: Sampling of an inhomogeneity by the observational point at a caustic results in a change of the observed profile, because the same region of the profile is traversed 3 times by the observational point.

Chapter 3

Caustics of Compensated Spherical Lens Models

3.1 Do Gravitational Lensing Significantly Influence Area Distance Measurements?

In this Chapter we consider exact examples with caustics displaying the shrinking effects discussed in Section 2.3 of Chapter 2 and also analyzed in greater detail in reference [49]. In order to calculate the magnitude of the effect analytically and numerically for single spherically symmetric compensated lenses to which we can apply the thin-lens approximation, we look in detail at *top hat* lenses, which are the simplest in this class. We refer to and mainly follow the notation of Schneider, Ehlers and Falco (1992) [202] (SEF).

In a publication by Ellis and Solomons [53] we continue the study of how area distances behave in universes where strong gravitational lensing takes place [49]. Reference [49] considered the claim by S. Weinberg [241] that although individual lensing masses alter area distances for ray bundles that pass near by them, photon conservation guarantees the same area distance-redshift relation as in exact FL universes when averaged over large angular scales. It was shown in [49] that this claimed compensation result is incorrect once one has passed caustics, which are necessarily the result of strong gravitational lensing; consequently (by continuity) the result is not true in general. Indeed it has to be wrong because area distances are determined by the gravitational field equations (essentially through the null

Raychaudhuri equation) quite independently of the issue of photon conservation (which is determined by Maxwell's equations and is valid whatever the space-time curvature). Thus the latter cannot causally determine area distances. In fact at large distances, *shrinking* takes place in that distant areas subtend smaller solid angles than they would in a FL universe model; and this effect will remain even when the observations relate to large angles. The way these small effects for individual lenses add up to give a significant averaged effect over the whole sky is discussed in [49]. This may affect high-redshift number counts and Cosmic Background Radiation (CBR) anisotropy observations at very small angles.

The general argument has been given in reference [49]. Specific spherically symmetric examples (viewed from the centre, and so without caustics) are presented in reference [171], which thereby gives a rigorous proof of the existence of the effect we claim; but the models used are unrealistic as models of the real universe.

3.2 The Gravitational Lensing Equations

We consider compensated spherically symmetric lenses in an Einstein-de Sitter background universe. The effect of the lens will be represented by the usual thin lens approximation, and we use the scaled variables of SEF.

Background Relations

The angular diameter distances between the observer and lens, observer and source, and lens and source in this background are D_d , D_s and D_{ds} respectively. In an Einstein - De Sitter model ($\Omega = 1$, no clumping),

$$D_{ds} = \frac{2c}{H_0} \frac{(1+z_d)^{1/2}(1+z_s) - (1+z_d)(1+z_s)^{1/2}}{(1+z_d)(1+z_s)^2} \quad (3.2.1)$$

[see SEF (4.57)], and D_d (respectively, D_s) is obtainable from D_{ds} by setting $z_d \rightarrow 0$, $z_s \rightarrow z_d$ (respectively, $z_d \rightarrow 0$). In what follows, the dimensionless ratio $\mathcal{R} = \frac{H_0}{2c} \frac{D_d D_{ds}}{D_s}$ is important. For a given lens position z_d , as $z_s \rightarrow \infty$ this has the limiting value $\mathcal{R}_\infty = \frac{(1+z_d)^{1/2}-1}{(1+z_d)^2}$, which has a maximum value of $\frac{2}{3} \frac{9^2}{16^2} = 0.21$ when $z_d = 9/7$.

If a source in a FLRW universe with scale factor $a(t)$ emits a signal at time t_s which is received at time t_0 , then the proper distance at time t_s between the source and observer is

$\ell = a(t_s) \int_{t_s}^{t_0} \frac{dt}{a(t)}$. For an Einstein-de Sitter universe $a(t) = t^{2/3}$, the Hubble parameter is $H(t) = (2/3)t^{-1}$, and $1 + z = t_0^{2/3}/t_s^{2/3}$, so

$$\ell = 3ct_s^{2/3}(t_0^{1/3} - t_s^{1/3}) = (2c/H_0)(1+z)^{-3/2}(\sqrt{1+z} - 1) \quad (3.2.2)$$

is this distance in the background universe.

3.2.1 Compensated lenses

If the energy density is $\rho(\vec{x})$ the fractional matter perturbation $\delta(\vec{x})$ in an inhomogeneity is related to the matter source by

$$\delta(\vec{x}) = \frac{\rho(\vec{x}) - \rho_0}{\rho_0} \Leftrightarrow \rho(\vec{x}) = \rho_0 (\delta(\vec{x}) + 1) . \quad (3.2.3)$$

where ρ_0 is the average energy density over a hypersurface of constant time S , defined by

$$\int_S \rho(\vec{x}) d^3x = \rho_0 . \quad (3.2.4)$$

Integrating (3.2.3) over S , $\int_S \delta(\vec{x}) d^3x = \frac{1}{\rho_0} \int_S [\rho(\vec{x}) - \rho_0] d^3x$; so by (3.2.4),

$$\int_S \delta(\vec{x}) d^3x = 0 , \quad (3.2.5)$$

which is the condition for a compensated perturbation that has been formed by rearrangement of matter in a uniformly distributed background with matter density ρ_0 . Equivalently, the density ρ averages out to the correct background value ρ_0 ; if this is not true, then the background density has been wrongly assigned [50]. Clearly this means that $\delta(\vec{x})$ must be negative in some domains, to compensate for the regions where it is positive. By (3.2.3), no negative densities will occur iff

$$\rho_0 > 0, \quad \delta(x) > -1 \text{ everywhere.} \quad (3.2.6)$$

We will assume these conditions to be true for the matter inhomogeneities causing lensing. Then in the lensing equations that follow, the quantities and relations will all refer to the variation from what they would have been in the background model (i.e. if there had been no lens). Thus the lensing *surface mass density* σ will mean the projected surface mass density in the lens plane arising from the density difference $\delta\rho = \rho - \rho_0$ from the background value, which will be chosen so that the compensation condition (3.2.5) is true;

and the *bending angle* will be the deviation in direction at the lens from what it would have been in the background model. This will be given via the usual thin-lens equations, with the surface mass density as just defined.

Simple compensated lenses

We define a *simple compensated lens (SCL)* to be a spherically symmetric compensated lens where $\delta(\vec{x}) = \delta(|\vec{x}|)$ is positive for an inner domain $0 \leq |\vec{x}| < 1$, negative for an outer domain $1 < |\vec{x}| < \lambda$, ($\lambda > 1$), and zero at larger radii, i.e. for $\lambda < |\vec{x}|$. This configuration would naturally arise by formation of a spherical massive object through gathering together material from an initially uniform substratum. In the sequel we consider a particularly simple form of SCL, namely a top hat lens.

3.2.2 The lensing equation in scaled variables

Given a choice of length scale ξ_0 in the lens plane, there is a corresponding length scale $\eta_0 = \frac{D_s^*}{D_d} \xi_0$ in the source plane. From the position vector $\vec{\eta}$ of the source relative to the optic axis in the source plane, and the impact vector $\vec{\xi} = D_d \vec{\theta}$ in the lens plane, where (vector) $\vec{\theta}$ is the observational angle from the optical axis, we define corresponding scaled variables \vec{x} , \vec{y} by

$$\vec{x} = \frac{\vec{\xi}}{\xi_0}, \quad \vec{y} = \frac{\vec{\eta}}{\eta_0} \quad (3.2.7)$$

[SEF (3.5)]. The surface mass density $\sigma(|\vec{\xi}|)$ for thin spherical lenses can be rescaled as

$$\kappa(x) = \frac{\sigma(\xi_0 x)}{\sigma_{cr}}, \quad \sigma_{cr} := \frac{c^2}{4\pi G} \frac{H_0}{2c\mathcal{R}}, \quad x = |\vec{x}|. \quad (3.2.8)$$

(SEF 5.4, 5.5). The lens equation can then be written in the very simple dimensionless form

$$\vec{y} = \vec{x} - \vec{\alpha}(\vec{x}) \quad (3.2.9)$$

(SEF 5.6, 8.6) where the scaled (vector) deflection angle $\vec{\alpha}$ is related to the true (vector) deflection angle $\vec{\alpha}$ by

$$\vec{\alpha}(\vec{x}) = \frac{2c\mathcal{R}}{H_0\xi_0} \vec{\alpha}(\xi_0\vec{x}) \quad (3.2.10)$$

(SEF 5.7). Because of the spherical symmetry, the deflection is radially inward and of magnitude $y = |\vec{y}|$ given by

$$y = x - \alpha(x) = x - \frac{m(x)}{x} \quad (3.2.11)$$

where

$$m(x) = 2 \int_0^x x' dx' \kappa(x') \quad (3.2.12)$$

is the dimensionless mass $m(x)$ within a circle of radius x (SEF 8.3); its first derivative is the dimensionless surface density (SEF 8.13):

$$m' = \frac{dm(x)}{dx} = 2x\kappa(x). \quad (3.2.13)$$

Also the change $\Delta\ell$ in radial distance traveled by light in a given time, as measured at the source, is equal to the time delay caused by lensing [SEF (4.67), (5.45)]¹, and can be rescaled to

$$Z = \frac{1+z_s}{1+z_d} \left(\frac{2c\mathcal{R}}{H_0 \xi_0^2} \Delta\ell \right) \quad (3.2.14)$$

[SEF (5.11) and following]. This is given by

$$Z = \frac{1}{2} |\vec{\alpha}|^2 - \psi(x), \quad (3.2.15)$$

where $\vec{\alpha}$ is given by (3.2.10) and the (rescaled) deflection potential is

$$\psi(x) = 2 \int_0^x x' \kappa(x') \ln \left(\frac{x}{x'} \right) dx' \Rightarrow \alpha(x) = \frac{d\psi(x)}{dx} \quad (3.2.16)$$

[SEF (8.7)-(8.9)].

The shrinking ratios

Finally, pointwise over the sky, the angular shrinking factor γ which relates observed distances corresponding to a given angle in the real lumpy universe to those in the background smoothed-out universe (as explained in the Introduction 2) is

$$\gamma = |dy/dx| \quad (3.2.17)$$

which can be averaged over a stated angle $\Delta\Theta$ to give the average angular shrinking factor $\langle\gamma\rangle$ over that angle. Similarly the pointwise area shrinking factor β which relates observed areas corresponding to a given solid angle in the real lumpy universe to those in the background smoothed-out universe (as demonstrated in the Introduction 2) is

$$\beta = |\det J|, \quad J = \left| \frac{\partial \vec{y}}{\partial \vec{x}} \right|. \quad (3.2.18)$$

¹The time change calculated in these equations is at most a first order quantity, and so the change in radial distance traveled can be found from it to first order by calculating distance as if light travels on null geodesics in the background geometry.

This can be averaged over a solid angle $\Delta\Omega$ to give the average area shrinking factor $\langle\beta\rangle$ over that solid angle.

The overall effect

Together the radial and transverse equations (3.2.15), (3.2.9) give the deflection of each null ray relative to the background geometry, and hence the shape of the perturbed light cone in the real lumpy space-time. These deflections are not independent: they are related by the fact that the speed of light is locally unity, so that the actual light path is stationary w.r.t. variation of the arrival time delay. Consequently a sideways deflection (which increases the distance to be traveled) is compensated by an inwards deflection (reducing the distance to be traveled), so the (tangential) lensing equation is a consequence of the (radial) time delay equation (SEF pp.146-147, 170-171). It is this combination of radial and tangential effects, implied by the above equations, that gives the light cone caustics their characteristic shapes (see Figure 1).

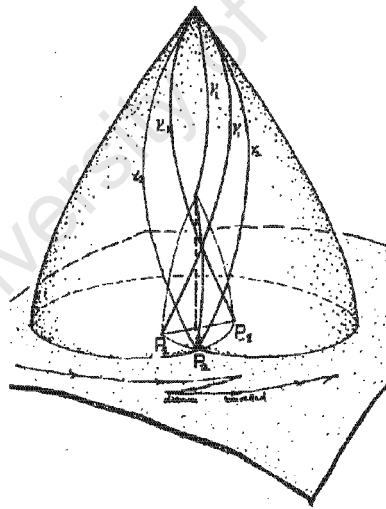


Figure 3.1: Shape of caustics in past light cone showing preferred geodesics and distance traveled.

3.3 Angles and Distances

Consider now angles and distances in the perturbed space-time. We start with angular diameter distance. Consider the source plane of a lens in direction $(\vec{\theta})$. Image points of nearby directions will be displaced from their background position (ℓ, \vec{x}) by the (scaled) displacement $(\Delta\ell, \Delta\vec{\eta})$ $(Z, \vec{y} - \vec{x}) = (Z, -\vec{\alpha})$ where the first part is the radial component of the displacement, given by (3.2.15), and the second is the tangential component (in the source plane) given by (3.2.11). If we move our viewing direction through an arc in the sky, the image point will move; for simplicity we will consider an arc where only one angular component θ only varies. This gives a 2-dimensional section of the full 3-dimensional light cone.

As we vary θ through $d\theta$, the (scaled) tangential distance traveled will be dy^2 , and the radial change of distance dZ^2 will be much less than this. Thus the total *distance traveled* DT due to an angle increase $\Delta\theta$ is, to good approximation,

$$DT(\Delta\theta) = \int_{\Delta\theta} \left| \frac{\partial y(\theta)}{\partial \theta} \right| d\theta, \quad (3.3.1)$$

where we sum all distances with a positive sign, thus determining the total increment in $|y|$ (see the Introduction 2). In terms of normalized magnitudes when spherical lensing takes place, the integrand is just $|\partial y/\partial \theta| = |1 - d\alpha/dx| \partial x/\partial \theta$. By contrast, the background distance is the same expression but with integrand $|\partial x/\partial \theta|$, and *Distance gained* DG is the distance moved from the starting point:

$$DG(\Delta\theta) = \int_{\Delta\theta} \frac{\partial y(\theta)}{\partial \theta} d\theta = y(\theta) - y(0). \quad (3.3.2)$$

In this case we subtract off those regions where $\partial y/\partial \theta$ is negative, ending up simply with the increment of y .

Now when $\frac{\partial y(\theta)}{\partial \theta}$ is positive, distance traveled is the same as distance gained. However when $\frac{\partial y(\theta)}{\partial \theta}$ changes sign, we have cusps forming (see the Introduction 2) and in the formula (3.3.1) for distance traveled the integral is over the curve corresponding to all values of θ and hence traverses the cusp backwards and forwards, see Figure 1. This is different from distance gained; the latter is then given by the integral (3.3.1) but where now the integral is over the (connected) curve γ excluding the cusp sections, so that $\frac{\partial y(\theta)}{\partial \theta}$ is positive over all the curve traversed.

The *Change in Distance Gained* due to the presence of the deflector is small in all cases. The effect for large angular scales does not average to zero when we have a distribution of lenses, but it is very small (the change from the background value is given by the difference of $-D_{ds} \bar{\alpha}(\bar{\xi})$ at the two ends, corresponding to a minute of arc at most). The *Change in Distance Traveled* ΔDT is given by the integral (3.3.1), but now taken over all the closed loops γ_c that are excluded when one calculates distance gained. The effect at each lens is small, but it is cumulative. Hence when there are a large number of lenses, the effect can be large (as discussed in [49]).

We are also interested in the true *Cosmological Area Distance* and so *change in area distance*, where the area distance is determined by the question, as we look over a given solid angle, what area does that cover at the source? This change is given pointwise by the determinant of the lens equation, see (3.2.18). We give explicit expressions for this determinant in the following paragraphs. A radial increase of size will be partly compensated by a transverse decrease of size, see e.g. Gunn and Press [186]), so the area distance will not relate very simply to the (radial) angular size distance.

We see then that before caustics form, distance traveled and distance gained are both very similar (and very close to the background value, on large angular scales). Thereafter, they can be very different (as was argued in [49]). To calculate this, we must locate the cusps and caustics.

3.3.1 Caustics and Critical Curves

Caustics in a source plane are the points in the plane where the Jacobean of the lensing map is singular. *Critical curves* are the points in the lensing plane where the light rays pass that will end up at caustics at the source plane. They can be located by determining the zeros of the Jacobean of the lensing map. The set of caustic points in space-time for all source planes form the space-time caustic set.

The Jacobian

Considering a spherical lens \hat{L} centered at the origin of the Cartesian XY -plane, the Jacobian matrix $J = \left(\frac{\partial \vec{y}}{\partial \vec{x}} \right)$ of the (transverse) lens mapping in the lens plane has determinant

$$\det J = \left(1 - \frac{\alpha(x)}{x} \right) \left(1 - \frac{d\alpha(x)}{dx} \right) \quad (3.3.3)$$

(SEF, equation (8.16)) which vanishes where either the first or the second brackets on the right hand side vanishes.

When the first bracket in (3.3.3) vanishes, the radius x is x_c such that

$$\frac{m(x_c)}{x_c^2} = 1 \Leftrightarrow \frac{\alpha(x_c)}{x_c} = 1 \Leftrightarrow \frac{\hat{\alpha}(r_c)}{r_c} = \frac{1}{\mathcal{R}}. \quad (3.3.4)$$

Such a critical point occurs for example at $\mathbf{r} = (x_c, 0)$; then there is a tangent vector $\Xi_t = (0, 1)$ to the critical curve at this point, and since the curve is tangential, Ξ_t is an eigenvector with zero eigenvalue. Since the tangential critical curves are mapped onto the point $\eta = 0$ in the source plane, there exists a caustic there which degenerates to a single point. The equation of the tangential critical curve in *two dimensions* in the lens plane is then simply $x^2 = x_c^2$, where x_c solves (3.3.4). This corresponds to an Einstein ring [many images, in a circle, of one point in the source plane].

The determinant $\det J$ in (3.3.3) also vanishes where the last bracket is zero, i.e. when $x = x_d$ such that

$$\frac{d\alpha(x_d)}{dx} = 1. \quad (3.3.5)$$

This equation describes radial critical curves. Again it corresponds to a circle in the lens plane. It has a radial eigenvector Ξ_r with eigenvalue zero. For instance, at $\mathbf{r} = (\xi, 0)$, $\Xi_r = (1, 0)$. We see in the next section it corresponds to a caustic in the source plane [and a cusp in the surface of constant distance].

The Cross-over and Cusp Angles

The lensing equation (3.2.9) is a two-dimensional vector equation with (transverse) components y_1 and y_2 while the radial equation gives the 3rd-component for the 2-d section of the past null cone in any surface of constant time. Lensing is radially inward with radial displacement magnitude given by (3.2.11). The first term on the right is the position that would have been with no lens; the second term is the effect of the lens.

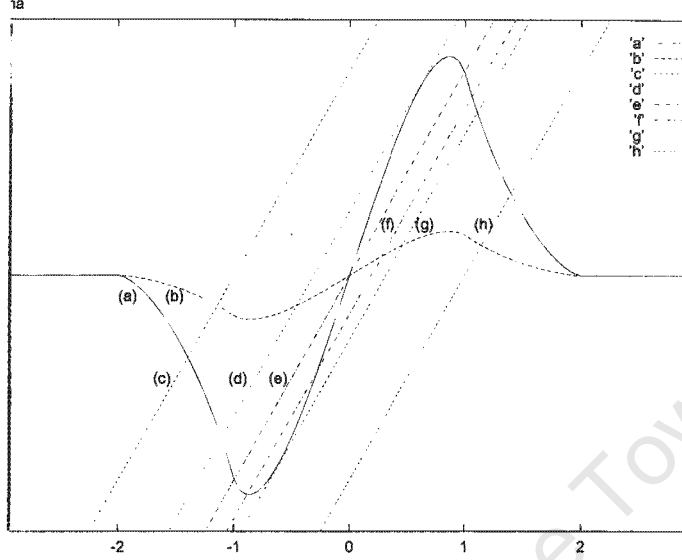


Figure 3.2: The bending angle diagram for two different redshifts. (a) one large, so other side of conjugate point Q; (b) One small, so this side of conjugate point Q. The number of images is the number of times the line $y = x$ intersects the bending angle curve. Considering curve (a), firstly, there is one image corresponding to line (c); then there are two images for line (d) which is tangent to the curve and determines the cusp angle; there are three intersections for line (e) which determines the cross-over angles (as it corresponds to no displacement at the source plane); there are 3 images for generic position (f), again two images for line (g) as it passes through the cusp, and finally one image for line (h). Parameters based on the lens +MG1131+0456.

To express this in terms of the observational angle θ from the optical axis, we note from the relations $\vec{\xi} = D_d \vec{\theta}$, $\vec{x} = \vec{\xi}/\xi_0$ that $\vec{x} = D_d \vec{\theta}/\xi_0$. Hence the magnitude equation takes the form

$$y(\theta) = \frac{D_d}{\xi_0} \left(\theta - \frac{D_{ds}}{D_s} \hat{\alpha}(D_d \theta) \right). \quad (3.3.6)$$

(SEF 4.47b, 5.34). The cusp angles θ_1 and θ_{-1} are determined by

$$\frac{\partial y}{\partial \theta} \Big|_{\theta_1} = 0, \quad \frac{\partial y}{\partial \theta} \Big|_{\theta_{-1}} = 0, \quad (3.3.7)$$

where again by the symmetry, $\theta_1 = -\theta_{-1}$. Differentiating (3.3.6), this occurs when

$$0 = D_s - D_{ds} \frac{\partial \hat{\alpha}}{\partial \xi} (D_d \theta_1) D_d \quad (3.3.8)$$

that is

$$\frac{\partial \hat{\alpha}}{\partial \xi}(D_d \theta_1) = \frac{1}{\mathcal{R}} \quad (3.3.9)$$

determines the cusp angle θ_1 . These angles correspond to the radial critical points in equation (3.3.5). In terms of the bending angle diagram (Figure 2), this occurs where the curves $y - x = y_1$ are tangent to the curve $\alpha(x)$. The cusp physical size is $D_s \theta_1$; twice this distance is the difference between distance gained and distance traveled, to good approximation. θ_2 and θ_{-2} are related by

$$y(\theta_2) = y(\theta_{-2}) = 0, \quad (3.3.10)$$

where by the spherical symmetry $\theta_2 = -\theta_{-2}$ and the self-intersection of the light cone (given by the first equality in this equation) occurs on the central line through the lens (as implied by the second equality). Thus we have from (3.3.6)

$$\theta_{-2} = \frac{D_{ds}}{D_s} \hat{\alpha}(D_d \theta_{-2}) \quad (3.3.11)$$

determines the cross-over angle θ_{-2} . Thus the cross-over angles θ_2 and θ_{-2} correspond to the critical points satisfying equation (3.3.4). In terms of the bending angle diagram (see Figure 2) this occurs where the line $y - x = 0$ intersects the curve $\alpha(x)$.

An angle θ_3 and corresponding impact parameter x_3 yields the same image position as the cusp angle, on the other side of the caustic: $y(x_3) = -y(x_1)$, and it is *this* angle that we treat as the cut-off in the caustic size. Henceforth, we refer to this as the *cut-off angle* θ_3 (and the cut-off on the other side occurs at $\theta_{-3} = -\theta_3$).

Finally, the maximum deflection caused by the lens occurs when $\theta = \pm\theta_m$, where

$$\frac{\partial \hat{\alpha}}{\partial \xi}(D_d \theta_m) = 0. \quad (3.3.12)$$

This does not correspond to either of the other angles; indeed it lies between them. For a SCL centred at $\theta = 0$, if cusps and cross-overs occur then generically

$$0 < \theta_1 < \theta_m < \theta_2 < \theta_3.$$

The two-dimensional picture obtained by suppressing one angular coordinate is as shown in Figure 1 (with one radial coordinate and one angular coordinate). Going to the full 3-dimensional picture, at the source plane, the whole picture is circularly symmetric about

the optical axis at $\theta = 0$. The cross-over angles at $\theta = \pm\theta_2$ correspond to a circle in the lens plane but a point (a degenerate caustic) in the source plane; the cusp angles $\theta = \pm\theta_1$ correspond to circles in both planes.

We now apply the preceding theory to Top Hat models.

3.4 The Top-Hat Matter Distribution

In the simplest case of a *top-hat* SCL, there is a constant inner density δ_+ for $0 \leq |\vec{x}| < 1$ and a constant outer density δ_- for $1 < |\vec{x}| < \lambda$ with $\lambda > 1$. Then the compensation condition (3.2.5) is

$$\delta_- = -(\lambda^3 - 1)^{-1}\delta_+, \quad (3.4.1)$$

Unless otherwise stated, we will assume that δ_+ is positive (so δ_- is negative). Then the positivity condition (3.2.6) demands that

$$0 < \delta_+ < (\lambda^3 - 1) \Leftrightarrow 0 > \delta_- > -1, \quad (3.4.2)$$

using the scaled variables, and $\kappa(x)$ will take the form

$$\kappa(x) = C \left(\lambda^3 \sqrt{1 - x^2} - \sqrt{\lambda^2 - x^2} \right), \quad 0 \leq x \leq 1, \quad (3.4.3)$$

$$\kappa(x) = -C \sqrt{\lambda^2 - x^2}, \quad 1 \leq x \leq \lambda, \quad (3.4.4)$$

$$\kappa(x) = 0, \quad x > \lambda \quad (3.4.5)$$

where $C = -2\rho_0\delta_-/\sigma_{cr}$, with a central value $\kappa(0) = C\lambda(\lambda^2 - 1) > 0$ and a junction value of $\kappa(1) = -C\sqrt{\lambda^2 - 1} < 0$. The surface density will be positive for $0 \leq x < x_+ < 1$, negative for $x_+ < x < \lambda$, and zero for $\lambda < x$, where

$$x_+ = \lambda \sqrt{(\lambda^4 - 1)/(\lambda^6 - 1)} < 1. \quad (3.4.6)$$

Substituting into (3.2.8) and integrating (3.2.12) to find the mass function $m(x)$, we obtain the following:

$$m(x) = Af(x), \quad A = -\frac{4\rho_0}{3}\delta_- \frac{\xi_0 \lambda^3}{\sigma_{cr}}, \quad (3.4.7)$$

where the function $f(x)$ is given by

$$f(x) = \left(1 - \frac{x^2}{\lambda^2}\right)^{3/2} - (1 - x^2)^{3/2}, \quad 0 \leq x \leq 1, \quad (3.4.8)$$

$$f(x) = \left(1 - \frac{x^2}{\lambda^2}\right)^{3/2}, \quad 1 \leq x \leq \lambda, \quad (3.4.9)$$

$$f(x) = 0, \quad \lambda \leq x. \quad (3.4.10)$$

The function $f(x)$ is a continuous positive even function, with $f(0) = df/dx(0) = 0$, a single maximum value of $f(x_m) = (\lambda^2 - 1)^{3/2}/(\lambda^6 - 1)^{1/2}$ at $x_m < 1$ given by $x_m^2 = \lambda^2(\lambda^4 - 1)/(\lambda^6 - 1) = x_+^2$, and junction values $f(1) = (\lambda^2 - 1)^{3/2}/\lambda^3$, $f(\lambda) = 0 = df/dx(\lambda)$. Near zero it has the form

$$f(x) = \frac{3}{2} \frac{(\lambda^2 - 1)}{\lambda^2} x^2 - \frac{3}{8} \left(\frac{\lambda^4 - 1}{\lambda^4}\right) x^4 + O(x^6). \quad (3.4.11)$$

It follows that $m(x)$ is a continuous non-negative function with $m(0) = 0$ and junction values $m(\lambda) = 0$ and $m(1) = A(\lambda^2 - 1)^{3/2}/\lambda^3$. Its maximum value is at $x = x_m = x_+$, where $m(x_m) = Af(x_m)$.

Consequently, because any SCL lens can be built up by a superposition of a sufficient number of top hat lenses, we see that the effective surface deflection mass $M(r)$ is always positive and is exactly zero at the outer edge of the compensating region, that is *the effective 2-dimensional surface density σ is exactly compensated if the 3-dimensional fractional density δ is precisely compensated*. Hence there is no long-range effect due to the lens: precisely because it is correctly compensated, the deflection angle $\alpha = 0$ for impact parameters that lie outside $x = \lambda$ (where the density takes exactly the background value). Thus we note, (1) for compensated lenses, lensing effects occur only for rays that traverse the lens itself and its compensating region; (2) despite the negative values for σ at some radii in such a compensated lens, the deflection angle is always positive.

Collecting formulae resulting from (3.2.11,3.2.12) and (3.4.7-3.4.10), we have that for a spherically symmetric top-hat matter distribution,

$$\alpha(x) = A \frac{f(x)}{x}, \quad (3.4.12)$$

where the constant is

$$A = \left(\frac{16\pi G\rho_0}{3c^2}\right) (\xi_o\delta_+) \left(\frac{\lambda^3}{\lambda^3 - 1}\right) \mathcal{R}, \quad (3.4.13)$$

From (3.3.4) or (3.3.11), cross-overs occur where

$$B(x) := \frac{\alpha(x)}{x} = 1 \quad (3.4.14)$$

and from (3.3.5) or (3.3.9) caustics occur where

$$d\alpha(x)/dx = 1, \quad (3.4.15)$$

The maximum bending angle α_m occurs where $d\alpha/dx = 0$.

Consequently,

1. the bending angle $\alpha(x)$ is a continuous positive odd function with

$$\begin{aligned} \alpha(0) &= 0, \\ d\alpha/dx(0) &= (3A/2) \left(\frac{\lambda^2 - 1}{\lambda^2} \right) \end{aligned}$$

a single maximum value α_m at $x_m < \xi_0$ where

$$x_m^4 = \frac{3\lambda^4(\lambda^2 - 1)}{4(\lambda^6 - 1)},$$

and junction values $\alpha(1) = A(\lambda^2 - 1)^{3/2}/\lambda^3$, $\alpha(\lambda) = 0 = d\alpha/dx(\lambda)$.

2. its slope $d\alpha(x)/dx$ is an even continuous function with maximum value $d\alpha(0)/dx = (3A/2\lambda^2)(\lambda^2 - 1)$ at the centre, positive from $x = 0$ to x_m , negative from $x = x_m$ to λ , and zero thereafter, with junction values $d\alpha(1)/dx = -(A/\lambda^3)(\lambda^2 + 2)\sqrt{\lambda^2 - 1}$ (here it takes its minimum value and its derivative $d/dx(d\alpha/dx)$ is discontinuous, diverging from the left but finite on the right) and $d\alpha(\lambda)/dx = 0$. Hence caustics occur iff

$$(3A/2\lambda^2)(\lambda^2 - 1) \equiv A_{crit} > 1 \quad (3.4.16)$$

(with a degenerate case when equality occurs). If they occur, say at $x = x_2$, then $0 < x_2 < 1$ and x_2 satisfies

$$\frac{d\alpha(x_2)}{dx} = \frac{A}{x_2^2} \left[(1 + 2x_2^2)\sqrt{1 - x_2^2} - \left(1 + \frac{2x_2^2}{\lambda^2}\right)\sqrt{1 - \frac{x_2^2}{\lambda^2}} \right] = 1, \quad (3.4.17)$$

with the corresponding angle θ_2 given by $\theta_2 = x_2\xi_0/D_d$.

3. The function $B(x) = \alpha(x)/x = Af(x)/x^2$ (with $f(x)$ given by (3.4.8-3.4.10)) is even, positive, monotonic decreasing, and continuous, with a maximum value $B(0) = (3A/2\lambda^2)(\lambda^2 - 1)$ at the centre, and junction values $B(1) = (A/\lambda)(\lambda^2 - 1)^{3/2}/\lambda$, $B(\lambda) = 0$. Hence cross-overs also occur iff (3.4.16) is satisfied. They can occur for any value of $x > x_2$ up to λ . If they occur, say at $x = x_1$, then

$$Af(x_1)/x_1^2 = 1 \quad (3.4.18)$$

with the corresponding angle θ_1 given by $\theta_1 = x_1\xi_0/D_d$, where $f(x)$ is given either by (3.4.8) (if $x_1 < 1$) or by (3.4.9) (if $1 < x_1 < \lambda$) (one cannot tell *a priori* in which range it will lie; one has to try to solve one, and if there is no solution, solve the other). Then $\theta_2(z_d, z_s)$ is the angle determining how large a part of the sky is covered by the Einstein circle corresponding to the cross-over surface $z = z_s$ for lenses at z_d (giving multiple images of the central point at z_s). How this scales with z_d (for given z_s) depends on how ρ_0 , ξ_0 , δ_+ , λ and \mathcal{R} scale with z_d .

4. Pointwise over the image, the area shrinking factor is given by $\beta = |\det J|$ given by (3.3.3). This can be evaluated from the formulae given above. Using the expansion (3.4.11) one can evaluate this determinant near the centre-line $\theta = 0$; the result is

$$\det J = (1 - A_{crit}) + O(x^2) \quad (3.4.19)$$

which is 1 near the lens (when A is small) and goes to $-A_{crit}$ (see (3.4.16)) when A is large (the minus sign because images are reversed).

We can determine a value for the lensing parameter M_0 either by directly estimating the quantities in the definition (3.4.13), or by estimating the maximum bending angle α_m for lenses considered. For example, if $\lambda = 2$, the r.h.s. of (3.4.12) has a maximum value of $0.70A$ (when $x = 0.87$). From (3.4.13) with the bending angle relation (3.4.12) and angle scaling relation (3.2.10) we see that then M_0 is determined by the relation

$$M_0 \times 1.14 \times 0.7 = \frac{2c}{H_0} \frac{\alpha_m}{\xi_0}. \quad (3.4.20)$$

3.4.1 Results

We have written a series of Truebasic programmes that compute all the relevant quantities for Tophat lenses, as functions of (i) the determining parameter A , (ii) the source redshift z_s

for fixed lens redshift z_d , (iii) the lens redshift z_d for fixed source redshift z_s . We have experimented with parameter values that correspond to observed gravitational lensing systems; some of the results are given in the following tables and in Figures 3 to 5.

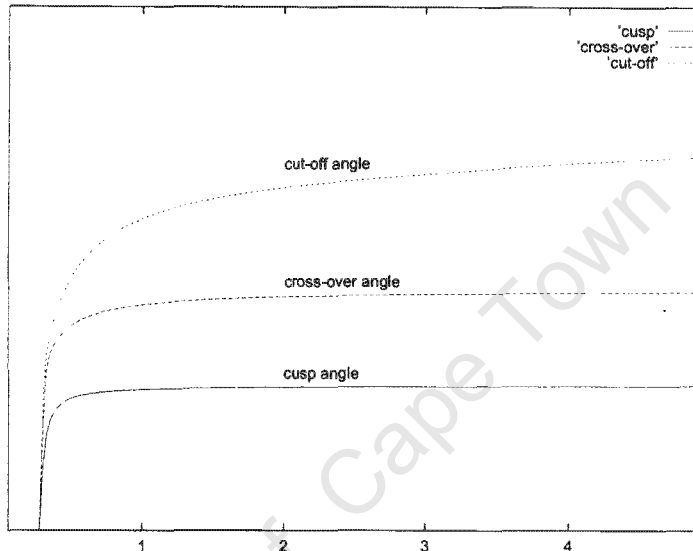


Figure 3.3: Variation in (a) cusp angle, (b) the crossover angle, and (c) the cut-off angle. The image redshift starts at the limiting value of $z_s = z_d = 0.231$, and increases through the arc redshift of 0.914, up to the value $z_s = 5$. Parameters based on the lens A2390.

This area shrinking ratio is about 3 after cusps have occurred, for scales of about 3 times the cusp scale, corresponding to the cusp image point where the deflection is the same size as at the cusp.

3.4.2 Galaxy clusters

We present a table of results for parameters corresponding to four well-known *galaxy clusters* that cause gravitational lensing (note that we are not making detailed models of these objects; rather we are using their observed properties to determine reasonable parameter values in our SCL model). From the cluster Abell 2218 (see refs. [122, 180]) we have selected as images the arcs at redshifts $z_s = 2.6$ and 3.3 respectively, as a case study, where the brackets imply this is evaluated at the angle cut-off angle. We then list the corresponding shrinking factor $\langle\beta\rangle$ for these two images, at the cut-off angle, followed by their cusp and

Table 3.1: Area shrinking ratio with actual image redshift.

LENS	α_{max}	ξ_0	z_d	z_s	shrinking $\langle\beta\rangle$
A2218	90''	160kpc	0.174	3.3/2.6	3.2
A963	76''	130kpc	0.206	0.7	3.2
A370	70''	100kpc	0.374	0.724/1.305	3.1
A2390	75''	160kpc	0.231	0.913	3.3

cross-over angles. The last column is the shrinking factor for the source placed at decoupling redshift $z_s = 1200$. We also consider other lensing clusters Abell 963 (ref. [132]), Abell 370 (refs. [64, 165]), and Abell 2390 (refs. [63, 165]).

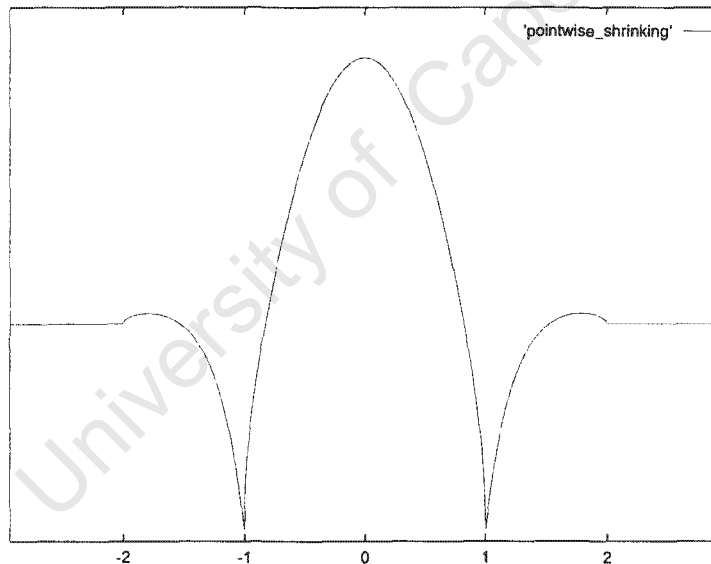


Figure 3.4: The pointwise area shrinking ratio γ for parameters based on the lens +MG1131+0456.

Table 3.2: Cusp angle, cross-over angle and area of shrinking ratio at decoupling.

LENS	Cusp angle θ_2	Cross-over angle θ_1	shrinking $\langle\beta\rangle$ at decoupling
A2218	47/46	77/75	3.2
A963	28	48	3.1
A370	16/25	27/36	3
A2390	24	41	3.35

Table 3.3: Area shrinking ratio with actual image redshift.

LENS	α_{maz}	ξ_0	z_d	z_s	shrinking $\langle\beta\rangle$
+H1413+117	9''	3kpc	1.5	2.55	3
2345+007	20''	15kpc	0.5	2.15	3
+MG2016+112	30''	30kpc	1.01	3.75	3
1635+267	30''	30kpc	0.57	1.96	3
+MG1131+0456	5''	2.5	0.5	1.5	3

3.4.3 Galaxies

We have also used a set of galactic lenses, as evidenced by multiple images of more distant objects, to provide parameters for our model, giving the second table. The first lens is often referred to as the *clover leaf*: +H1413 + 117 has four images of a QSO at redshift $z_d = 2.55$ (See refs. [156, 117]). The second is seen in QSO images A and B for the system 2345 + 007 correspond to a redshift $z_d = 2.15$, despite image A being 1.7mag brighter than image B (ref. [239, 219]). The third is the triple radio source +MG2016 + 112 (see ref. [133]). The fourth is the QSO pair in 1635 + 267 with nearly equal redshift $z_d = 1.96$ [40]. Finally a nearly full Einstein ring was observed in +MG1131 + 0456, albeit somewhat elliptic in shape (ref. [97]).

We find that the caustics shrinking factor tends to an average factor > 3 at large z (as required to get a 3-fold covering factor). However because of the divergence of the light rays within the cusps, it can be much larger when applied to strong lensing (the actual angle corresponding to the cusps is then much smaller than in the equivalent FL model).

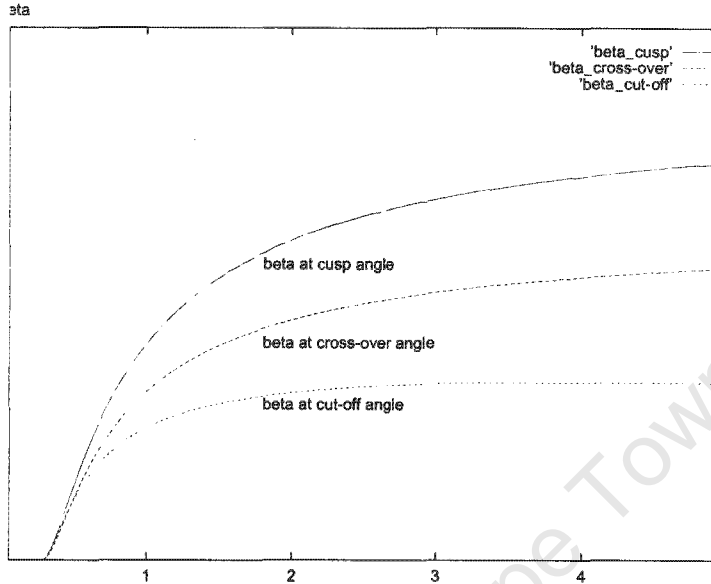


Figure 3.5: The average area distance shrinking ratio β for the Abell cluster 2390. The average $\langle\beta\rangle$ at (a) $\theta = \theta_1$ (the cusp angle), (b) $\theta = \theta_2$ (the cross-over angle), and (c) $\theta = \theta_3$ (the cut-off angle).

3.5 Conclusions

Of particular interest is the way the cusp size and the *shrinking* vary with redshift of the source and of the lensing object. This depends on two things: firstly the variation of angular sizes with redshift, remembering (a) minimum angular apparent diameter occurs at $z = 1.25$, so that the maximum angle θ_c for cusps to form due to lenses of given size and strength will have minimum at that redshift; and (b) that the ratio of distances that enters σ_{cr} saturates with increasing z_s (for given z_d) but has a maximum for each z_s at a z_d of about 0.6 which is thus the optimal distance for the lens in order to create cusps on the last scattering surface.

The models discussed here in [53] are based on specific strong-lensing objects that are not typical of all galaxies or clusters; but they confirm in a concrete way the broad picture proposed in [49]: an area *shrinking* factor of 3 will occur for each lens that causes cusps, on the scale of the cusps (precisely: at the cut-off angle θ_3 which gives the same deflection at the source as the cusp angle, but on the opposite side). The total effect when averaging

Table 3.4: Cusp angle , cross-over angle and shrinking ratio at decoupling.

LENS	Cusp angle θ_2	Cross-over angle θ_1	shrinking $\langle\beta\rangle$ at decoupling
+H1413+117	0.6	0.9	3
2345+007	3	6	3
+MG2016+112	5	8	3
1635+267	6	10	3
+MG1131+0456	0.6	1.0	3

over large angular scales will depend on what fraction of the sky is covered by these angles for all lenses at all smaller scales, as a function of redshift; some simple estimates of this overall effect were given in [49]. To determine realistic multiplicity factors as a function of redshift will require simulations with multiple lensing and more realistic lens models, for example standard elliptical lens models determined by a velocity dispersion parameter and ellipticity parameters as in [122] which allow an increase in the degree of multiple covering (because individual elliptic lenses can have a covering factor of 5). The effect will differ on angular scales, and will almost certainly be substantial due to micro-lensing, with an additional increase due to galactic and cluster lensing. The implication is that it is incorrect to assume a priori that areas average out to the background FL value on large angular scales; one can only know the true area ratios - expressed in the shrinking factors considered here - by detailed calculation.

Part II

**Pre-Big Bang Cosmology in String
Theory**

Chapter 4

Pre-Big Bang Cosmology and the Graceful Exit Problem

4.1 Overview

Matching the classical FRW model of General Relativity with the superinflation of Pre-Big Bang Cosmology of String theory is marred by what is commonly called the *graceful exit problem*. There is a vast literature focused upon repairing this blemish. There are *no-go theorems* that exclude such regular transitions in the presence of a perfect fluid or Kalb-Ramond source terms.

In what follows, we try to shed some light on the intricacies of the graceful exit problem, and the extent to which *Pre-Big Bang Cosmology* impacts the larger debate surrounding various issues related to the early Universe, such as the Singularity Problem, the Cosmological Constant Problem, Flatness Problem etc. So the first section of this Chapter is a brief summary of some of the recent literary contributions to the debate around Graceful Exit Problem.

Then, in Section 4.3 the subject of Pre-Big Bang Cosmology is reviewed in a way similar to various treatises by its founding authors Gasperini, Veneziano and others.

The final Section deals with a significant property of String Theory, namely the *Duality Symmetry of the Stringy Effective Action*, that yields precedence to *a doubling of solutions to the field equations*, an occurrence that has no analogue in the context of

the Einstein cosmology, where there is no *a priori* dilaton, and the duality symmetry cannot be implemented. Key consideration is raised as to symmetries of the equations and whether those same symmetries hold true in their solutions (see Chapter 5). Indeed, there are cases in which the *equations* have such a scale factor symmetry, when solutions may or may not exhibit the same symmetry, and on the other hand cases in which the *solutions* obey the scale factor symmetry, even if the equations do not.

4.2 The Graceful Exit Problem

The Standard (Cosmological) Model gives us a consistent view of a large part of current observations, as far back as the period of nucleosynthesis. Before this period, we postulate an era of accelerated expansion under the Inflationary paradigm [141, 124] to explain such problems as the size of the Universe, its smoothness and flatness on very large scales and the lack of it on smaller scales, the lack of topological relics such as magnetic monopoles, domain walls and cosmic strings. To this list we may add the problem of the smallness of the cosmological constant, and the initial singularity problem. Not only does inflation fail to address the last two issues, there yet remains the task of constructing a plausible dynamical inflationary scenario that is free of internal inconsistencies.

In a classical treatment, the Universe inevitably reaches large curvature scales and ultimately runs into a singularity. In order to see how String Theory cures this problem, one needs to go beyond a classical treatment. The **graceful exit problem** is the issue of matching **pre-big bang cosmology** (see section 4.4) of String Theory with standard FRW cosmology (see for instance [16, 193, 70, 17, 153, 154, 14, 15, 62, 27]). No-go theorems prevent the inclusion of a single potential to catalyze the graceful exit in a vacuum-dilaton cosmology [17, 153, 154]. It appears to be in trend to include higher-order corrections to the string effective action, that incorporate both the classical finite size effects of the string, as well as the quantum string loop corrections [15, 62, 27].

Diamandis *et al.* [163] investigate a toy model two-dimensional string cosmology within the context of a super-critical (Liouville) string where they identify time with the Liouville mode. This also achieves an expanding universe with matter which exhibits an inflationary

phase, and *graceful exit* from it, that tends asymptotically to a flat-metric fixed point characterized by a suitable dilaton configuration in which the string coupling remains bounded during the exit from the inflationary phase.

Kawai & Soda [213] found non-negligible enhancements of both curvature perturbation and gravitational wave in the long wavelength limit during *graceful exit* in a universe dominated by a scalar field coupled to the Gauss-Bonnet term (in a four-dimensional dilaton-gravity model of Antoniadis *et al.* [27], which is really an extension of a two-dimensional model by Rey [193]).

In a paper by C. Park and S-J Sin [179] it was suggested that by using brane scattering in the absence of the Z_2 symmetry, by constructing multi-brane configurations by patching five-dimensional AdS-Schwarzschild solutions, a scenario of a graceful exit of inflation on a brane universe may be attained. Papantonopoulos and Pappa [178] solve the Einstein equations on a 3D-brane with a time dependent cosmological constant. By assuming that at an early epoch the vacuum energy scales as $1/\log t$, they demonstrate how the universe may have passed from an inflationary phase to an expanding phase in a natural way. Bhattacharya *et al.* [109] explore the averaged action of the Randall-Sundrum model with a time dependent metric ansatz, reformulated in terms of a Brans-Dicke action with time dependent Newton's constant and show that the brane metric smoothly exits inflation.

Shapiro and Sola [207, 208, 206] present a model of inflation based on the anomaly-induced effective action of gravity in the presence of a conformally invariant Hilbert-Einstein term first proposed by Starobinsky[208], in which inflation can be stable at the beginning (unlike the Starobinsky model) and unstable at the end. The instability is caused by a slowing down of inflation due to quantum effects associated to the massive fermion fields. In supersymmetric theories this mechanism can be linked to the breaking of SUSY and suggests a natural way to achieve graceful exit from the inflationary to the FLRW phase.

Risi and Gasperini [37] suggested the possibility of a smooth (classical) transition from the pre- to the post-big bang regime by considering *repulsive gravitational effects* due to the back-reaction of the quantum fluctuations outside the horizon, provided the background is higher-dimensional and anisotropic.

We [52] obtain non-singular solutions through the inclusion of a single scalar potential

providing the use of an exotic equation of state (see Chapter 5).

Stefano Foffa [61] considers Pre-Big Bang Cosmology in Braneworld Scenario and recently [hep-th/0304004] obtained a graceful exit at low curvature and low coupling, without violating the Null Energy Condition by means of a regular bouncing universe in the context of a dilaton-gravity brane world scenario. The scale factor starts in a contracting inflationary phase both in the Einstein and in the string frame, it then undergoes a bounce (due to interaction with the bulk Weyl tensor), and subsequently enters into a decelerated expanding era.

4.3 Pre-Big Bang Cosmology

This section provides a brief explanation of the basic ideas underlying the so-called pre-big bang scenario [69] as derived from String Theory.

Figure 4.1 gives a qualitative representation of the main difference between string cosmology and standard, inflationary cosmology can be obtained by plotting the so-called *curvature scale* of the Universe versus time.

In the Standard Model [240], the space time curvature decreases as time increases. As we look back in time, this curvature grows monotonically, and blows up at the initial Big Bang singularity, as illustrated in the top part of Figure 4.1.

The Standard Inflationary Model [141, 124] modifies the Standard Model by allowing for a de Sitter, or “almost” de Sitter phase in the distant past, during which this curvature tends to stay frozen at a nearly constant value. The problem with this scenario is that inflation cannot be extended back in time for ever (see, for instance [234, 232]), since it leads to geodesic incompleteness (see also Guth [84]).

Quantum Cosmology does present an answer, namely that the Universe emerges in a de Sitter state *from nothing* [233] or from an unspecified initial *vacuum state*, via quantum tunnelling. The problem with the Quantum Cosmology explanation is that any computation of the transition probability requires an appropriate choice of the boundary conditions [90], which in the context of standard inflation are imposed *ad hoc* when the Universe is in an unknown state, inside the quantum gravity regime. In String Cosmology, on the contrary, the initial conditions are referred asymptotically to a low-energy, classical state which is

known, and well controlled by the low-energy string effective action [69, 157]. There have been other attempts to use Quantum Cosmology [110, 157]. See for instance the paper by Pinto-Neto and Colistete Jr that uses the Bohm-de Broglie interpretation to construct Gaussian superpositions of the quantum solutions to the corresponding Wheeler-DeWitt equation, to obtain Bohmian trajectories that exhibit a graceful exit from the inflationary Pre-Big Bang epoch to the decelerated expansion phase.

What happens to the Universe before the phase of constant curvature, which cannot last for ever? If the curvature starts growing again, at some point in the past, the Singularity Problem remains unresolved, since it is simply shifted further back in time.

The alternative is for the curvature to start decreasing, as illustrated in the bottom part of Figure 4.1. The String Cosmological Scenario suggests precisely such **dual** behaviour for the curvature around the time $t = 0$. As we look back in time the curvature grows, reaches a maximum controlled by the string scale, and then decreases towards a state which is asymptotically flat and with vanishing coupling constants, and therefore negligible interactions, the so-called *string perturbative vacuum*. A phase of high, but finite (nearly Planckian) curvature replaces the Big Bang singularity of the Standard Model - the **pre-big bang** [230] phase is the initial phase with growing curvature, in contrast to the subsequent, standard, **post-big bang** phase with decreasing curvature.

4.4 Duality Symmetry of the Effective Action

An important property of string theory is the **duality symmetry** of the effective action.

To illustrate this point we start by recalling that in general relativity the solutions of the standard Einstein action,

$$S = -\frac{1}{2\lambda_p^{d-1}} \int d^{d+1}x \sqrt{|g|} R \quad (4.4.1)$$

(d is the number of spatial dimensions, and $\lambda_p = M_p^{-1}$ is the Planck length scale), are invariant under “time-reversal” transformations. Consider, for instance, a homogeneous and isotropic solution of the cosmological equations, represented by a scale factor $a(t)$:

$$ds^2 = dt^2 - a^2(t) dx_i dx^i. \quad (4.4.2)$$

If $a(t)$ is a solution, then also $a(-t)$ is a solution. On the other hand, when t goes into $-t$, the Hubble parameter $H = \dot{a}/a$ changes sign,

$$a(t) \rightarrow a(-t), \quad H = \dot{a}/a \rightarrow -H. \quad (4.4.3)$$

To any standard cosmological solution $H(t)$, describing decelerated expansion and decreasing curvature ($H > 0$, $\dot{H} < 0$), is thus associated a “reflected” solution, $H(-t)$, describing a contracting Universe because H is negative [69].

The String Theory gravi-dilaton effective action (here the fundamental field is represented by the scalar dilaton ϕ) to lowest order in the string coupling and in the higher-derivatives (α') string corrections (see, for instance, Appendices A and B in [69]) can be written as:

$$S = -\frac{1}{2\lambda_s^{d-1}} \int d^{d+1}x \sqrt{|g|} e^{-\phi} \left[R + (\partial_\mu \phi)^2 \right] \quad (4.4.4)$$

($\lambda_s = M_s^{-1}$ is the fundamental string length scale. In addition to the invariance under time-reversal, the above action is also invariant under the **dual** inversion of the scale factor, accompanied by an appropriate transformation of the dilaton (see also [228] and the first paper of Ref. [230]). More precisely, if $a(t)$ is a solution for the cosmological background (4.4.2), then $a^{-1}(t)$ is also a solution, provided the dilaton transforms as:

$$a \rightarrow \tilde{a} = a^{-1}, \quad \phi \rightarrow \tilde{\phi} = \phi - 2d \ln a \quad (4.4.5)$$

This transformation implements a particular case of T -duality symmetry, usually called **scale factor duality** (see Appendix B in [69]).

When a goes into a^{-1} , the Hubble parameter H again goes into $-H$ so that, to each one of the two solutions related by time reversal, $H(t)$ and $H(-t)$, is associated a dual solution, $\tilde{H}(t)$ and $\tilde{H}(-t)$, respectively (see Figure 4.2). The space of solutions is thus richer in a string cosmology context. Indeed, because of the combined invariance under the transformations (4.4.3) and (4.4.5), a cosmological solution has in general four branches: two branches describe expansion (positive H), two branches describe contraction (negative H). Also, as illustrated in Figure 4.2, for two branches the curvature scale ($\sim H^2$) grows in time, with a typical *pre-big bang* behaviour, while for the other two branches the curvature scale decreases, with a typical *post-big bang* behaviour [69].

It follows, in this context, that to any given decelerated expanding solution, $H(t) > 0$, with decreasing curvature, $\dot{H}(t) < 0$ (typical of the Standard Cosmological Model),

is always associated a **dual partner** describing accelerated expansion, $\tilde{H}(-t) > 0$, and growing curvature, $\tilde{H}(-t) > 0$. This doubling of solutions has no analogue in the context of the Einstein cosmology, where there is no dilaton, and the duality symmetry cannot be implemented.

In an isotropic background there are only expanding **pre-big bang** solutions [69], i.e. solutions evolving from the string perturbative vacuum ($H \rightarrow 0, \phi \rightarrow -\infty$), and then characterized by a growing string coupling, $\dot{g}_s = (\exp \phi/2) > 0$. The inversion of the scale factor, in particular, and the associated transformation (4.4.5), is only a special case of a more general, $O(d, d)$ symmetry of the string effective action, which is manifest already at the lowest order. This $O(d, d)$ symmetry holds even in the presence of matter sources, provided they transform according to the string equations of motion in the given background [69, 15]. In the perfect fluid approximation, for instance, the inversion of the scale factor corresponds to a reflection of the equation of state, which preserves however the “shifted” energy $\bar{p} = \rho |\det g_{ij}|^{1/2}$:

$$a \rightarrow \bar{a} = a^{-1}, \quad \bar{\phi} \rightarrow \phi, \quad p/\rho \rightarrow -p/\rho, \quad \bar{p} \rightarrow p \quad (4.4.6)$$

These symmetries supposedly connect in a smooth way the phase of growing and decreasing curvature, and also describe a smooth evolution from the string perturbative vacuum (i.e. the asymptotic no-interaction state in which $\phi \rightarrow -\infty$ and the string coupling is vanishing, $g_s = \exp(\phi/2) \rightarrow 0$), to the present cosmological phase in which the dilaton is frozen, with an expectation value [116] $\langle g_s \rangle = M_s/M_p \sim 0.3 - 0.03$ (see Figure 4.3).

By adding matter sources, in the perfect fluid form, to the action (4.4.4), the string cosmology equations for a $d = 3$, homogeneous, isotropic and conformally flat background can be written as [69]:

$$\begin{aligned} \dot{\phi}^2 - 6H\dot{\phi} + 6H^2 &= e^\phi \rho, \\ \dot{H} - H\dot{\phi} + 3H^2 &= \frac{1}{2}e^\phi p, \\ 2\ddot{\phi} + 6H\dot{\phi} - \dot{\phi}^2 - 6\dot{H} - 12H^2 &= 0. \end{aligned} \quad (4.4.7)$$

For $p = \rho/3$, in particular, they are exactly solved by the standard solution with constant dilaton,

$$a \sim t^{1/2}, \quad \rho = 3p \sim a^{-4}, \quad \phi = \text{const}, \quad t \rightarrow +\infty, \quad (4.4.8)$$

describing decelerated expansion and decreasing curvature scale:

$$\dot{a} > 0, \quad \ddot{a} < 0, \quad \dot{H} < 0. \quad (4.4.9)$$

I.e. the usual radiation-dominated solution of the Standard Cosmological Model, based on the Einstein equations. In String Cosmology there is an associated **dual complement**, i.e. an additional solution which can be obtained by applying on the background (4.4.8) a time-reversal transformation $t \rightarrow -t$, and the duality transformation (4.4.6):

$$a \sim (-t)^{-1/2}, \quad \phi \sim -3 \ln(-t), \quad \rho = -3p \sim a^{-2}, \quad t \rightarrow -\infty. \quad (4.4.10)$$

This is still an exact solution of the equations (4.4.7), describing however accelerated (i.e. inflationary) expansion, with growing dilaton and growing curvature scale:

$$\dot{a} > 0, \quad \ddot{a} > 0, \quad \dot{H} > 0. \quad (4.4.11)$$

The two solutions (4.4.8) and (4.4.10) provide an explicit representation of the scenario illustrated in Figure 4.3, in the two asymptotic regimes of t large and positive, and t large and negative, respectively.

4.5 Concluding Remarks

In this Chapter we have given a broad overview of the current issues surrounding the Graceful Exit Problem in the context of Pre-Big Bang models of String Theory, and the alternative routes various authors propose to circumvent this impasse.

The loop and high curvature corrections dictated by String Theory violate the Null Energy Condition, but this is generally considered to be acceptable, although our understanding of these effective sources is still incomplete.

For this reason the Pre-Big Bang model itself has lost much of the luster it thrived upon with its inception during the early Nineties. Recent work on Pre-Big Bang Cosmology are done in the context of Braneworld Scenario (a subject treated in Part III of this thesis.) Here, an Einstein frame bounce that represents the smooth exit from the pre- to the post-big bang phase can be done without the need for quantum gravity or high curvature effects. In brane worlds, the bounce is obtained from interaction between the brane and the bulk, without violating the Null Energy Condition.

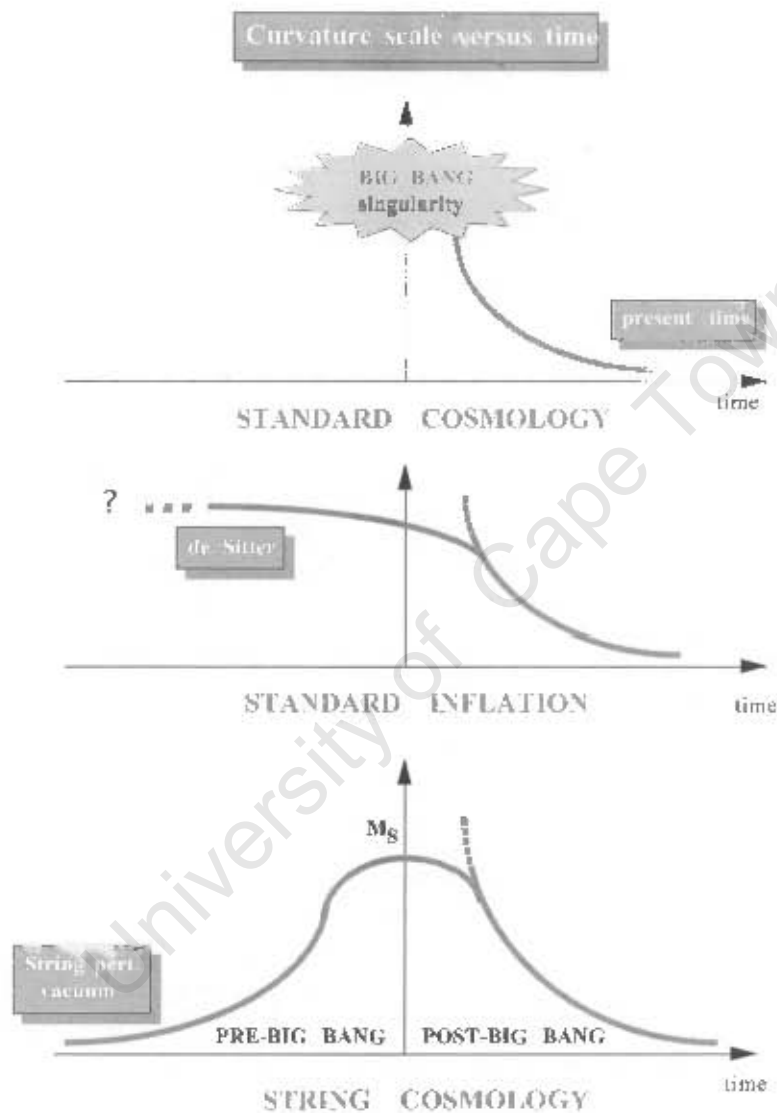


Figure 4.1: Time evolution of the curvature scale in the standard cosmological scenario, in the conventional inflationary scenario, and in the string cosmology scenario. Courtesy M. Gasperini.

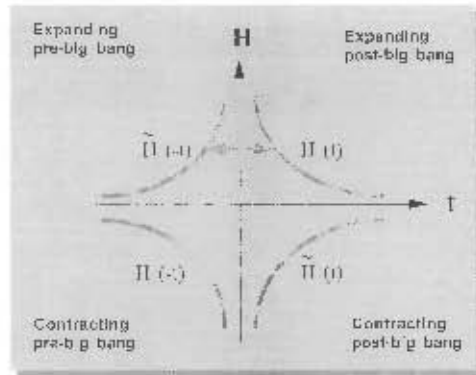


Figure 4.2: The four branches of a low-energy string cosmology background. Courtesy M. Gasperini.

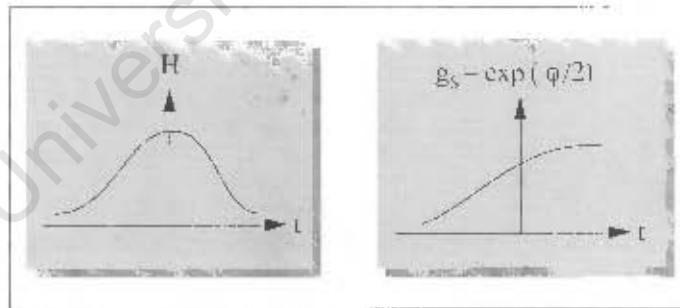


Figure 4.3: Time evolution of the curvature scale H and of the string coupling $g_s = \exp(\phi/2) \sim M_s/M_p$, for a typical self-dual solution of the string cosmology equations. Courtesy M. Gasperini.

Chapter 5

A Solution to the Graceful Exit Problem in Pre-Big Bang Cosmology

5.1 Introduction

In this chapter (as in the paper by Ellis *et al.* [52]), we investigate the equations of string cosmology [69], [137] in the string frame, allowing for a dilaton potential $V(\phi)$. The Pre-Big Bang Scenario is motivated by the search for cosmological solutions with an $a(t) \rightarrow 1/a(-t)$ symmetry in the scale factor $a(t)$, which implements an analogue of the T-duality symmetry of M-theory. However one must distinguish between symmetries of the equations and those of their solutions. We look at cases in which the *equations* have such a scale factor symmetry, when solutions may or may not exhibit the same symmetry, and at cases in which the *solutions* obey the scale factor symmetry, even if the equations do not. In the latter case we obtain some solutions that seem to have most of the properties desired in the Pre-Big Bang scenario, in that they have the desired scale factor symmetry, the desired evolution of the dilaton field, and continuity at $t = 0$ of $a(t)$, $\phi(t)$, $\dot{\phi}(t)$, and the Hubble parameter $H(t) \equiv \dot{a}(t)/a(t)$ (but allowing a discontinuity in $\dot{H}(t)$ and $\ddot{\phi}(t)$ there, implying a corresponding discontinuity in $\partial V/\partial\phi$), thus providing a solution to the graceful exit problem [153, 154, 14]. However, to obtain the desired dilaton behaviour at recent times,

we need to employ an ‘exotic’ equation of state as discussed below.

There are *no-go theorems* that exclude such regular transitions in the presence of a perfect fluid and Kalb-Ramond sources. A ‘lowest order’ Einstein frame analysis by [14] discusses graceful exit in generalized phase-space, and derives a set of necessary conditions for transition from a classical dilaton-driven inflationary pre-big bang phase to a radiation-dominated era, joined at $t = 0$ in a Planck epoch of maximal finite curvature $\dot{H}(t)$. They show that a successful exit requires violation of the null energy condition (NEC). Classical sources tend to obey NEC, but various new kinds of effective sources generating non-singular evolution have been considered that do not. Thus failing invocation of higher order curvature terms, some kind of exotic behaviour of matter is necessary in order to obtain a graceful exit from the pre-big bang phase.

Here we follow Gasperini *et al.* [69] by working in the string frame. The relation to the Einstein frame is left for further investigation. It should be made clear from the start that our solutions are rather special in the spectrum of pre-big bang models; those we concentrate on in the main show an exact scale factor duality in the solutions, and thus we do not consider here the more exciting possibility of a phase of early kinetic-dilaton dominated inflation which leads to an early phase which is not radiation dual but is genuinely stringy inflationary vacuum. Nevertheless the set of solutions investigated here help to understand the spectrum of possibilities available within the broad Pre-Big Bang set of ideas.

5.2 String Cosmology Equations

One can determine the general equations of string cosmology by extremizing the lowest order effective action of dilaton gravity,

$$S = -\frac{1}{2\lambda_s^{d-1}} \int d^{d+1}x \sqrt{|g|} e^{-\phi} \left[R + (\nabla\phi)^2 - \frac{1}{12} H^2 + V(\phi) \right] + \int d^{d+1}x \sqrt{|g|} L_m, \quad (5.2.1)$$

where ϕ is the scalar dilaton, $H = dB$ (antisymmetric tensor field strength), $V(\phi)$ is the dilaton potential, λ_s is the fundamental string length scale, and L_m is the Lagrangian density of other matter sources. To derive string cosmology equations for the $d = 3$, homogeneous, isotropic, conformally flat background we will follow Gasperini [69] in assuming $B = 0$, a perfect fluid minimally coupled to the dilaton, and a Bianchi I type metric (see Appendix C of [69] for details). Unlike Gasperini we assume $V(\phi) \neq 0$, to obtain the string cosmology

equations in the following canonical form:

$$H^2 = \frac{e^\phi}{6}\rho + H\dot{\phi} + \frac{V}{6} - \frac{\dot{\phi}^2}{6}, \quad (5.2.2)$$

$$\dot{H} + H^2 = e^\phi\left(\frac{p}{2} - \frac{\rho}{3}\right) - H\dot{\phi} + \frac{\dot{\phi}^2}{3} - \frac{V'}{2} - \frac{V}{3}, \quad (5.2.3)$$

$$\ddot{\phi} = -3H\dot{\phi} + \dot{\phi}^2 - V - V' + e^\phi\left(\frac{3p}{2} - \frac{\rho}{2}\right), \quad (5.2.4)$$

where $V' = \frac{\partial V}{\partial \phi}$. When combined, these imply the standard energy conservation equation:

$$\dot{\rho} = -3H(\rho + p). \quad (5.2.5)$$

In a relationship analogous to that between the classical Friedmann equation and Raychaudhuri equation,

Eq.(5.2.2) is the first integral of eq.(5.2.3) provided that eq.(5.2.4) and eq.(5.2.5) hold. (5.2.6)

These four equations will be the basis for the analysis in this paper.

One of the primary motivations for the pre-big bang scenario [71] is that when $V(\phi) = 0$, these equations are invariant under the following transformation:

$$a(t) \rightarrow \hat{a}(t) = a^{-1}(t) \quad (5.2.7)$$

provided that the dilaton transforms as $\phi \rightarrow \hat{\phi} = \phi - 6 \ln a$ and the energy density and pressure as $\rho \rightarrow \rho' = a^6 \rho$, $p \rightarrow p' = -pa^{-6}$. Thus if $a(t)$ is a solution, so is $\hat{a}(t)$ for suitable ϕ, ρ, p . Since the string cosmology equations are also invariant under time reversal symmetry,

$$a(t) \rightarrow \bar{a}(t) = a(-t) \quad (5.2.8)$$

the deceleration associated with standard post-big bang cosmology can be associated with an accelerated evolution prior to the big bang by the generalized transformation

$$a(t) \rightarrow \tilde{a}(t) = a^{-1}(-t). \quad (5.2.9)$$

where $\tilde{a}(t)$ is a solution for suitable ϕ, ρ, p because $a(t)$ is. The solution has T-duality symmetry if for each t ,

$$a(t) = \bar{a}(t) = a^{-1}(-t). \quad (5.2.10)$$

However, if we assume $V(\phi) \neq 0$ as in eqs.(5.2.2-5.2.4), then in general the equations are not invariant under the symmetry eq.(5.2.10) even if the solutions are. We will look at both cases in what follows, but generically allowing a potential that does not preserve the symmetry. Note that if we assume matter with *the same* equation of state before and after $t = 0$, then the matter equations also will not be invariant under the scale factor symmetry. One has to decide what is more physically meaningful: matter with a universal equation of state applicable at all times, or that has a discontinuous equation of state that preserves this symmetry. In what follows, we adopt the first option. We return to discuss this choice in the conclusion.

5.2.1 Flat Dilaton Potential with Exotic Equation of State

To obtain equations of motion preserving the scale factor symmetry eq.(5.2.10), we assume the simplest potential, namely a flat potential:

$$V(\phi) = \kappa \quad (5.2.11)$$

where κ is a constant, and then investigate the behaviour of the universe. In order to reliably obtain proper limiting behaviour of the dilaton, we assume that the equation of state

$$p = \frac{\rho}{3} + \frac{2}{3}e^{-\phi}\kappa \quad (5.2.12)$$

holds at all times (this choice, which is not invariant under the duality symmetry, is discussed further in the following sections). One can immediately see that at late times if $\phi \rightarrow$ constant, as we will show follows from this choice, then this equation of state simply reduces to radiation plus a constant.

We are interested in getting satisfactory dynamics for $H(t)$ and $\phi(t)$, or equivalently for $\chi(t) \equiv \dot{\phi}$. To see when this occurs, we manipulate the string cosmology equations (5.2.2-5.2.4) subject to eqs.(5.2.11,5.2.12) to obtain the two-dimensional phase space with coordinates (χ, H) governed by the following equations:

$$\dot{H} = \frac{\chi^2}{6} - 2H^2 + \frac{\kappa}{6}, \quad (5.2.13)$$

$$\dot{\chi} = \chi(\chi - 3H), \quad (5.2.14)$$

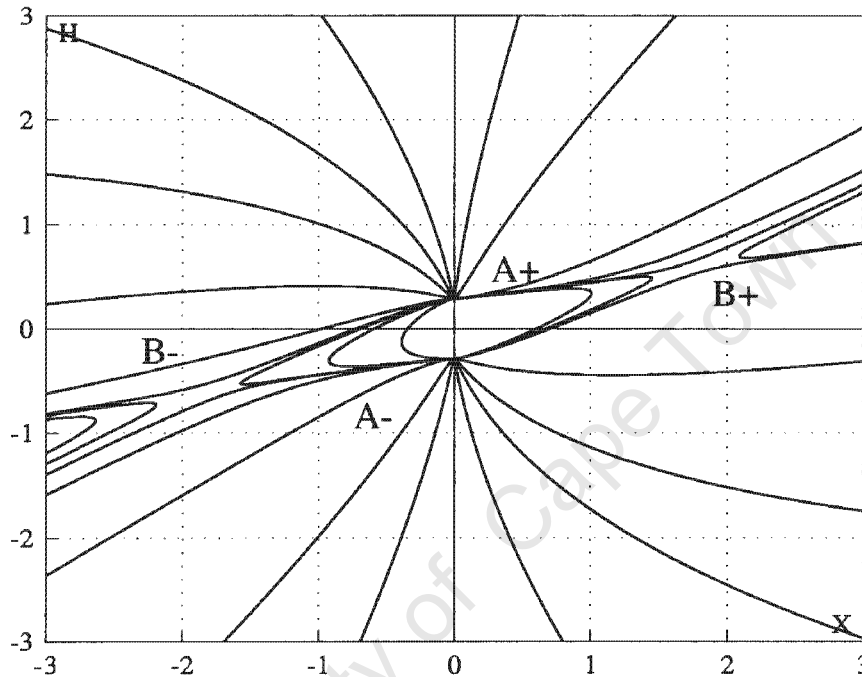


Figure 5.1: Phase portrait representing the solution space of equations (5.2.13–5.2.14) with $\kappa > 0$.

the latter following because of choice (5.2.12). Having chosen the constant κ , we can set initial conditions (χ_0, H_0) at $t = 0$, and then extend the solution to positive and negative values of t by use of these equations. For $\kappa < 0$, there are no fixed points in the phase plane, and on every trajectory both H and χ diverge as $|t| \rightarrow \infty$. For $\kappa = 0$, i.e. no dilaton potential, there is one fixed point at the origin, but for any initial condition (set at $t = 0$), χ and H will diverge either as you run time forwards or run time backwards.

The interesting dynamics is obtained when $\kappa > 0$. There are then fixed points at A_+ : $(0, \sqrt{\kappa/12})$ (a source), A_- : $(0, -\sqrt{\kappa/12})$ (a sink), B_+ : $(\sqrt{3\kappa}, \sqrt{\kappa/3})$ (a saddle point), and B_- : $(-\sqrt{3\kappa}, -\sqrt{\kappa/3})$ (a saddle point). In the phase plane depicted in Figure 1 above, we claim the initial conditions in the region I bounded by A_+ , B_+ and A_- and the separatrices joining them give satisfactory dynamics of both H and χ which include $\chi \rightarrow 0$ as $|t| \rightarrow \infty$,

$\chi > 0$ for all times so $\phi(t)$ is monotonic, H remains finite, and a “bounce” occurs that avoids the initial singularity. Since region I is bounded by fixed points that have coordinates proportional to $\sqrt{\kappa}$, increasing κ will give one a larger region of initial conditions that lead to a nonsingular universe with proper dilaton dynamics. We can obtain a solution on the boundary of region I (evolving along the line joining A_- to A_+ , which does not lie in I) that is invariant under symmetry (5.2.8) by setting $\chi_0 = 0$, $H_0 = 0$ at $t = 0$, but this solution, given explicitly by $a(t) = \cosh^{1/2}(\sqrt{\kappa/3}t)$, is not invariant under the symmetry (5.2.10). A drawback of all these models is that inflation will not stop at $t > 0$, but as discussed in the conclusion, the string cosmology equations derived in section 5.2 do not apply to the present cosmological regime without modification, so it is possible that a radiation dominated evolution started after the time when these equations no longer apply. In any case this gives a specific family of solutions where the equations display the desired symmetry (5.2.10) but the solutions do not - which is not very surprising, given the prevalence of broken symmetries in physics.

5.3 Obtaining Desired Dynamics From a Dilaton Potential

In this section, we generalize the method introduced by Ellis and Madsen [155] through which they obtain a classical scalar potential associated with a specified $a(t)$ in the standard gravitational equations. No field has been observed that coincides with a dilaton potential $V(\phi)$, so we assume that it is a freely disposable function. We show that by suitable choice of $V(\phi)$ one can obtain almost any behaviour for $a(t)$, or alternatively for $\phi(t)$. We first present an algorithm for determining $V(\phi)$ from a desired $a(t)$ or a desired $\phi(t)$, and then present an analytically smooth solvable example. This solution illustrates our main point, but has little physical relevance (although it does satisfy the symmetry (5.2.10)). In the following section we use these methods to obtain two solutions that resemble the standard “pre-big bang scenario”, but with continuity of $a(t)$ and $H(t)$ and with satisfactory dynamics of $\phi(t)$. The associated dilaton potentials are *ad hoc* because they are derived from the desired behaviour of the universe, rather than from a field theory model; as discussed in many inflationary and quintessence studies, see e.g. [136],[200].

5.3.1 The Algorithms

We proceed by providing the following *general algorithm* for determining a dilaton potential $V(\phi)$ that produces a desired $a(t)$:

- 1) Specify a desired monotonic function for the scale parameter $a(t)$, consequently determining $H(t)$ and $\dot{H}(t)$,
- 2) Choose an equation of state and solve for $\rho(a)$ from eq.(5.2.5)¹; as $a(t)$ is known, this determines $\rho(t)$.
- 3) Eliminate V and V' from eq.(5.2.4) by use of eqns.(5.2.2) and (5.2.3) to obtain a differential equation relating $H(t)$, $\phi(t)$, $\rho(t)$, and their time derivatives.
- 4) Solve the equation obtained in step 3) for $\phi(t)$.
- 5) Substitute the now known functions $\phi(t)$, $\rho(t)$, and $H(t)$ and $a(t)$ into the rearranged version of eq.(5.2.2)

$$V(t) = 6H^2 - e^\phi \rho - 6H\dot{\phi} + \dot{\phi}^2 \quad (5.3.1)$$

to obtain $V(t)$.

- 6) Invert $\phi(t)$ to obtain $t(\phi)$, and
- 7) Transform $V(t)$ as follows: $V(t) = V(t(\phi)) \Rightarrow V(\phi)$. This is possible for each range of t on which $\phi(t)$ is monotonic (if it is not monotonic on some range of t , in general $V(\phi)$ will not be well-defined because it will not be single valued for the corresponding values of ϕ).

Thus, provided $\phi(t)$ determined from step 3) is monotonic, we find a $V(\phi)$ that corresponds to a given monotonic function $a(t)$. Because we have now satisfied eqs.(5.2.5), (5.2.2) and the equation obtained in step 3), the latter depending essentially on eq.(5.2.4), it follows from statement (5.2.6) that eq.(5.2.3) will be true also, so we have satisfied all the equations of the theory for this matter description (c.f. [155]); hence we have a solution of the desired form.

Alternatively, we can give an algorithm for determining a dilaton potential $V(\phi)$ that produces a desired dilaton evolution $\phi(t)$ ² by proceeding in the same way as above, except for minor changes: replace step 1) by

¹If the equation of state is a function of V or V' , then you will have to eliminate these quantities using eqs.(5.2.2) and (5.2.3) before solving eq.(5.2.5).

²It is important to note that one has freedom to choose only $a(t)$ or $\phi(t)$, not both.

1') specify the desired monotonic function for the dilaton, $\phi(t)$, in step 2), leave ρ in the form $\rho(a)$, and replace step 4) by

4') solve the equation obtained in step 3) for $a(t)$ (or for $H(t)$).

The rest of the algorithm is as before.

Finally, note that we can carry out these procedures piecewise: for example we can specify $a(t)$ for some range of t and $\phi(t)$ for some adjoining range of t , or different behaviours for $a(t)$ for different ranges of t , then join the solutions together, ensuring that $a(t)$, $H(t)$, $\phi(t)$ and $\chi(t)$ are continuous where these ranges meet.

5.3.2 Exponential Scale Factor Behaviour with No Matter

To demonstrate the procedure, we give a simple analytically solvable example with a pure scalar field, i.e. $\rho = p = 0$. Consider an exponential expansion as in classical inflation,

$$a(t) = e^{wt} \Rightarrow H = w, \dot{H} = 0, \quad (5.3.2)$$

where w is a positive constant. This solution has the desired symmetry (5.2.10).

In this case the differential equation for $\phi(t)$ takes the form:

$$\ddot{\phi} = H\dot{\phi} \quad (5.3.3)$$

Using eq.(5.3.3) and eq.(5.3.1) we obtain

$$\phi(t) = \phi_0 + \frac{\dot{\phi}_0}{w}(e^{wt} - 1), \quad (5.3.4)$$

a monotonic function as required, and

$$V(t) = 6w^2 - 6\dot{\phi}_0 w e^{wt} + \dot{\phi}_0^2 e^{2wt}. \quad (5.3.5)$$

After inserting the inverted eq.(5.3.4),

$$t(\phi) = \frac{1}{w} \log \left[\frac{w}{\dot{\phi}_0} \left(\phi - \phi_0 + \frac{\dot{\phi}_0}{w} \right) \right], \quad (5.3.6)$$

into eq.(5.3.5), one obtains

$$V(\phi) = w^2 \left(\phi - \phi_0 + \frac{\dot{\phi}_0}{w} \right)^2 - 3w^2 \quad (5.3.7)$$

which is simply a quadratic potential plus a constant. Clearly the behaviour for $\phi(t)$ is unphysical since $\phi(t) \rightarrow \infty$ instead of asymptoting to a constant. However, this gives a transparent example where even though the scale factor symmetry (5.2.10) is broken in the equations (because $V(\phi)$ is not constant), the solution obeys that symmetry.

5.4 “Pre-Big Bang” Behaviour

In this section we try to use the methods just explained to obtain solutions that resemble the “pre-big bang scenario” but with satisfactory dynamics of $\phi(t)$ and a continuous transition from the pre-big bang to post-big bang phases. In these examples, we seek solutions that evolve from a string perturbative vacuum, i.e. $H \rightarrow 0$ and $e^\phi \rightarrow 0$ (no interactions), to the present scenario where e^ϕ , which acts as the coupling constant, asymptotes to a constant. We will assume the following behaviour of the universe:

$$a(t) = (t+1)^{\frac{1}{2}}, t \geq 0 \Rightarrow H(t) = \frac{1}{2(t+1)} \quad (5.4.1)$$

determining $a(t)$ for $t \geq 0$, and by the symmetry (5.2.10)

$$a(t) = (-t+1)^{-\frac{1}{2}}, t \leq 0 \Rightarrow H(t) = \frac{1}{2(-t+1)} \quad (5.4.2)$$

determining $a(t)$ for $t \leq 0$. Both $a(t)$ and $H(t)$ are continuous at $t = 0$ with $a(0) = 1$, $H(0) = 1/2$, but $\dot{H}(t)$ is not continuous there.

This behaviour, which is essentially radiation dominated evolution of the universe for positive times and power-law inflation for negative times, is motivated by the “pre-big bang” scenario introduced in [71], and exactly obeys the scale factor symmetry (5.2.10). Note that we have shifted the origin of time in each branch from that customarily used, in order to get a smooth evolution through $t = 0$; this of course makes no difference to the desired physical behaviour, for we can choose the origin of time to be wherever we want (and the equations are invariant under time translation $t \rightarrow t' = t + c$). Although the power law inflation ends with the scale-factor value $a(0) = 1$, required by continuity together with the symmetry (5.2.10), the solution has sufficient inflation for any purpose because it involves an infinite number of e-foldings (it starts with the asymptotical value $a = 0$ as $t \rightarrow -\infty$).

5.4.1 Pre-Big Bang behaviour with radiation equation of state

First we assume the radiation equation of state holds at all times, that is,

$$p = \frac{\rho}{3}, \quad (5.4.3)$$

which, using eqs.(5.2.5) and (5.4.1,5.4.2), implies

$$\rho(\pm t) = \rho_0(\pm t + 1)^{\mp 2} \quad (5.4.4)$$

where ρ_0 is a positive constant and '+t' refers to the post-big bang era, '-t' to the pre-big bang era. Notice that both ρ and $\dot{\rho}$ are continuous at $t = 0$.

The equation for ϕ now takes the form

$$\ddot{\phi} = \frac{2}{3}e^{\phi}\rho + H\dot{\phi} + 2\dot{H}. \quad (5.4.5)$$

Substituting in eqs. (5.4.1) and (5.4.4), we could not find an analytical solution to eq.(5.4.5), so we investigate the three dimensional phase space with coordinates (t, ϕ, χ) , given from eqs. (5.4.5,5.4.1,5.4.2,5.4.4) by

$$\dot{\phi} = \chi, \quad \dot{\chi} = \frac{2}{3}e^{\phi}\rho_0(\pm t + 1)^{\mp 2} + \frac{\chi}{2(\pm t + 1)} \mp \frac{1}{(\pm t + 1)^2}, \quad (5.4.6)$$

where the top sign holds for $t > 0$ and the bottom sign for $t < 0$. We can set initial data at $t = 0$, and then investigate the phase plane orbits as we run the trajectory forward and backwards in time in such a way that χ and ϕ are continuous through $t = 0$. Then $\dot{\chi}$ is discontinuous there, but we have no problem in joining the solutions for $t > 0$ and $t < 0$.

For $t > 0$, there is an exceptional integral curve $\gamma(t)$ given by $(t, \tilde{\phi}_0, 0)$, where $\tilde{\phi}_0 \equiv \ln(\frac{3}{2\rho_0})$; this is the only integral curve with a fixed value of ϕ and χ . Note that setting ϕ_0 and χ_0 determines the initial point in the phase space, and specifying ρ_0 determines the location of this exceptional curve. In the 2-dimensional sub-spaces $t = \text{const}$ with coordinates (ϕ, χ) , the curve $\gamma(t)$ has coordinates $(\tilde{\phi}_0, 0)$ for all t , and represents a set of saddle points parametrised by t . To get exactly the desired dilaton dynamics in the future ($\chi > 0$, $e^{\phi} \rightarrow \text{constant} \Rightarrow \chi \rightarrow 0$ as $t \rightarrow \infty$), one must restrict the initial conditions (ϕ_0, χ_0) to start precisely on the stable branch of these saddle points, which intersects the surface $t = 0$ in a single curve $(0, \gamma_+(\chi), \chi)$ passing through the exceptional point $\gamma_0 = (0, \tilde{\phi}_0, 0)$ (for more details, see A.1). However there is actually slightly more freedom than this in

finding physically relevant initial conditions because if a trajectory starts close enough to the stable branch (but not exactly on it), then the trajectory will stay close to the fixed point for an arbitrarily long period of time before ϕ and χ diverge, and this may suffice for physical purposes even if the solution eventually diverges (cf. the discussion of intermediate isotropisation in [235]). Nevertheless, the physically relevant set of solutions is very unstable and requires very precise fine tuning, in order to obtain the desired dilaton dynamics, lying in a small open neighbourhood \mathcal{D}_+ of the curve $\phi_0 = \gamma_+(\chi_0)$ in the initial data set at $t = 0$. Indeed we have found it very difficult to obtain numerical solutions with the desired behaviour because of this instability.

For $t < 0$ there are no points with a fixed value of ϕ and χ (because we assume $\rho_0 > 0$). To get the desired dilaton dynamics in the past ($\chi > 0$, $e^\phi \rightarrow 0$ as $t \rightarrow -\infty$) one must further restrict the initial conditions, the problem being that eq.(5.4.6) is an inhomogeneous equation for χ with a time-varying source function (albeit a source function that decays away as $t \rightarrow \pm\infty$). We can obtain the desired behaviour if $y_0 = \frac{2}{3}e^{\phi_0}\rho_0 \ll 1$, i.e. $\phi_0 \ll \ln(\frac{3}{2\rho_0})$ (details are given in A.1). This is a sufficient condition; there will be a wider domain \mathcal{D}_- of initial data at $t = 0$, containing this set, that will ensure that at early enough times the desired behaviour is attained.

To get a satisfactory solution for all time, for a given choice of ρ_0 , one must set the initial conditions to lie in both \mathcal{D}_+ and \mathcal{D}_- , so the crucial issue is whether they intersect or not. We have not attained finality on this point. It may be that the ‘no-go’ theorems with a potential [153, 154] imply they do not intersect, but this implication is not entirely clear, as the conditions of those theorems may not correspond precisely to the conditions we contemplate here. If they do intersect, we can attain the desired behaviour $\chi \rightarrow 0$ and $e^\phi \rightarrow 0$ when time runs backwards as well as $e^\phi \rightarrow const$ as time runs forward and in principle, one can obtain a continuous $V(\phi)$ associated with the unstable solution described above because every function is continuous on the right hand side of eq.(5.3.1). Furthermore, $\phi(t)$ is monotonic and continuous, and therefore invertible, so one can complete Step 6 of the algorithm set out in section 5.3.1. However attaining such solutions will require extreme fine-tuning of the initial data, and this is very difficult to do because one does not know where the stable branch of the saddle point intersects $t = 0$. Thus if such solutions do exist, the extreme fine tuning required for their initial data make them seem impracticable

as cosmologies despite their other desirable properties.

5.4.2 “Pre-big Bang” Behaviour with Exotic Equation of State

Finally, we assume the identical “pre-big bang” behaviour of the last example (eqs. (5.4.1, 5.4.2)), but we obtain a stable solution with a different equation of state. The instability in the last example arises because of our choice of the equation of state, as can be seen by inspection of eq.(5.2.4), which we write now as

$$\dot{\chi} = -3H\chi + \chi^2 + \beta, \quad (5.4.7)$$

where

$$\beta \equiv -V - V' + e^\phi \left(\frac{3p}{2} - \frac{\rho}{2} \right). \quad (5.4.8)$$

As mentioned before, we want to obtain $e^\phi \rightarrow \text{constant}$, i.e. $\chi \rightarrow 0$, at late times, which implies $\beta \rightarrow 0$ in eq.(5.4.7). If we choose the radiation equation of state as in the last example, (eq.(5.4.3)), then $\beta = -V - V'$. Therefore, requiring $\beta \rightarrow 0$ as $t \rightarrow \infty$ puts a heavy restriction on the dilaton potential, namely $V \rightarrow e^{-\phi}$ at late times. Consequently, there is a fine-tuning problem if you use the radiation equation of state.

In the present example, we assume $\beta = 0$ for all times, which from eq.(5.4.7) demands the exotic equation of state,

$$p = \frac{\rho}{3} + \frac{2}{3}e^{-\phi}(V + V'), \quad (5.4.9)$$

at all times (note that eq.(5.2.12) is the special case resulting when $V' = 0$). Using this equation of state implies,

$$\rho(t) = \int 2He^{-\phi}(12H\dot{\phi} + 6\dot{H} - 3\dot{\phi}^2)dt \quad (5.4.10)$$

which allows the density to go through zero and become negative. We discuss this equation further in the *Conclusion*.

The differential equation that relates $H(t)$ to $\phi(t)$ is simply eq.(5.4.7) with $\beta = 0$,

$$\ddot{\phi} = -3H\dot{\phi} + \dot{\phi}^2, \quad (5.4.11)$$

For arbitrary $a(t)$, this can be solved (with $a_0 = 1$ and $\chi_0 \equiv \dot{\phi}_0$) by

$$\exp(\phi_0 - \phi(t)) = 1 - \chi_0 \int_0^t a^{-3}(t)dt. \quad (5.4.12)$$

For the specific case given by eqs.(5.4.1,5.4.2) we obtain from this the analytical solution

$$\phi(t) = +\phi_0 - \ln \left| 1 - 2\chi_0 [1 - (1+t)^{-\frac{1}{2}}] \right| \quad (5.4.13)$$

for $t > 0$ and

$$\phi(t) = +\phi_0 - \ln \left| 1 - \frac{2\chi_0}{5} [1 - (1-t)^{\frac{5}{2}}] \right| \quad (5.4.14)$$

for $t < 0$. Inverting eq.(5.4.13) we obtain

$$t(\phi) = \frac{4\chi_0^2 e^{2(\phi-\phi_0)}}{[(1-2\chi_0)e^{\phi-\phi_0} - 1]^2} - 1 \quad (5.4.15)$$

and inverting eq.(5.4.14) we obtain

$$t(\phi) = 1 - \left[\frac{5e^{\phi-\phi_0} - 5 + 2\chi_0}{2\chi_0} \right]^{2/5} \quad (5.4.16)$$

Now we can solve eq.(5.4.10) to obtain $\rho(a)$ and so $\rho(t)$ (see A.2 for one particular case), and substitute our results into eq.(5.3.1) to obtain the dilaton potential $V(\phi)$ that is associated with our specified “pre-big bang” behaviour. This is straightforward but tedious, and results in very complex analytic expressions (the real complexity coming through the expressions for $\rho(t)$ that occur consequent on the choice of the exotic equation of state). Rather than giving these analytic expressions, we give a graph of the potential for one particular case below.

To discuss the relevant initial conditions, it is instructive to look at the phase plane (Figure 2 below) with coordinates (t, χ) , where $\chi = \dot{\phi}$ is governed by the equation:

$$\dot{\chi} = -\frac{3}{2(\pm t + 1)}\chi + \chi^2 \quad (5.4.17)$$

where we again use $+$ to represent $t > 0$ and $-$ to represent $t < 0$. One can easily see that $\chi = 0$ ($\Rightarrow \dot{\chi} = 0$) is an attractor, and represents a physically uninteresting solution with $\phi = \text{const}$. Also $\chi = \frac{3}{2(\pm t + 1)}$ is a nullcline, characterising the other points where $\dot{\chi} = 0$. This curve starts at $(0, \frac{3}{2})$ and drops symmetrically away to zero as $t \rightarrow \pm\infty$. Now we can solve eq.(5.4.17) analytically for $t > 0$, finding

$$\chi = \frac{1}{2(t+1)(1+C_+\sqrt{t+1})} \quad (5.4.18)$$

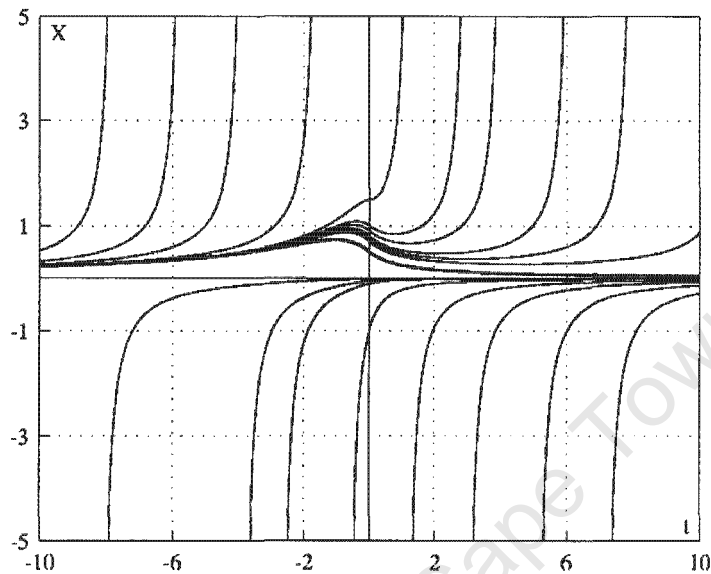


Figure 5.2: Phase portrait representing the solution space of equation (5.4.17).

where $C_+ = (\frac{1}{2\chi_0} - 1)$ is positive iff $\chi_0 < 1/2$. The separatrix between the solutions that diverge and those that go asymptotically to zero as $t \rightarrow \infty$ is the special solution with $C_+ = 0$ which goes through $(0, \frac{1}{2})$, that is,

$$\chi = \frac{1}{2(t+1)} \quad (5.4.19)$$

which itself goes to zero as $t \rightarrow \infty$. If we specify the initial conditions at $t = 0$ such that ϕ_0 is free and $0 < \chi_0 < \frac{1}{2} \Leftrightarrow C_+ > 0$, then as we run the trajectories forward in time $\chi \rightarrow 0$. In this case, for large positive values of t , eq.(5.4.18) will be approximately

$$\chi = \frac{1}{2C_+ t\sqrt{2t}} > 0 \quad (5.4.20)$$

(note that $\phi(t)$ is monotonic for $t > 0$ because $\chi > 0$ on these trajectories). Let T_+ be such that eq.(5.4.20) is valid for all $t > T_+ > 0$. Then for $t > T_+$,

$$\phi(t) \simeq \int_{T_+}^t \frac{1}{2C_+ t\sqrt{2t}} dt + \phi_{T_+} = \frac{1}{C_+ \sqrt{2}} [T_+^{-1/2} - t^{-1/2}] + \phi_{T_+}. \quad (5.4.21)$$

Thus as $t \rightarrow \infty$, for all χ_0 , $\phi(t) \rightarrow$ a constant value, say ϕ_∞ , and $\exp \phi(t) \rightarrow \exp(\phi_\infty)$. (Note that it is essential to check this result even though $\chi \rightarrow 0$, cf. the discussion below of what happens as $t \rightarrow -\infty$). If we specify the initial conditions at $t = 0$ such that ϕ_0 is free and $\frac{1}{2} < \chi_0 \Leftrightarrow C_+ < 0$, as we run the trajectories forward in time then $\chi \rightarrow \infty$ as $t \rightarrow t_0$ given by $1 + C_+ \sqrt{t_0 + 1} = 0$, that is $t_0 = \frac{(2\chi_0)^2 - 1}{(2\chi_0 - 1)^2}$. In this case for large values of χ , eq.(5.4.17) can be approximated as follows:

$$\chi \gg \frac{3}{2(t+1)} \Rightarrow \dot{\chi} \simeq \chi^2 \Rightarrow \chi \simeq 1/(t - t_0). \quad (5.4.22)$$

The solution diverges as $t \rightarrow t_0$ and the approximation eq.(5.4.20) never applies. This behaviour conforms to that implied by eq.(5.4.13), and may be seen clearly on the phase plane.

If we run the trajectories backward in time, starting from initial data with $\chi_0 > 0$, they will cross the nullcline and then drop to zero, never becoming negative because $\chi = 0$ is an exceptional solution of the equations. Then $\phi(t)$ is monotonic for $t < 0$ also because $\chi > 0$ on these trajectories. Solving eq.(5.4.17) analytically for $t < 0$ gives

$$\chi = -\frac{5}{2} \frac{(t-1)\sqrt{-t+1}}{(t^2 - 2t + 1)\sqrt{-t+1} + C_-} \quad (5.4.23)$$

where $C_- = (\frac{5}{2\chi_0} - 1)$. This expression goes to zero for all $C_- > -1$, corresponding to $\chi_0 > 0$ (note that it does not matter if C_- is positive or negative). For large negative t its value, for all C_- , will be approximately

$$\chi = d\phi/dt \simeq -\frac{5}{2t}. \quad (5.4.24)$$

Let T_- be such that eq.(5.4.24) is valid for $t < T_- < 0$. Then for $t < T_-$,

$$\phi(t) \simeq \int_{T_-}^t \left(-\frac{5}{2t}\right) dt + \phi_{T_-} = \frac{5}{2} \ln\left(\frac{T_-}{t}\right) + \phi_{T_-} \Rightarrow \exp \phi(t) \propto \left(\frac{T_-}{t}\right)^{5/2}. \quad (5.4.25)$$

Thus as $t \rightarrow -\infty$, for all χ_0 , $\phi(t) \rightarrow -\infty$ even though $\chi \rightarrow 0$, and $\exp \phi(t) \rightarrow 0$, which is the dynamics we desire [69], and indeed is indicated already by eq.(5.4.14). The value of C_- corresponding to the separatrix eq.(5.4.19) is $C_- = 4$, which does not give any special behaviour for $t < 0$.

Typical results of the integrations for this case are given in Figures 3-5 below.

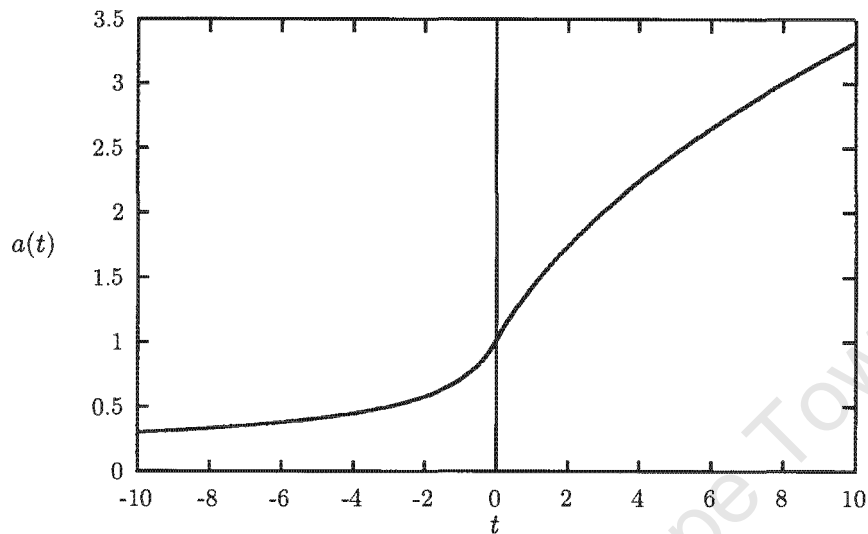


Figure 5.3: The evolution of the scalefactor $a(t)$ as a function of time t , with $a(0) = 1$, over the time interval $[-10, 10]$. For negative times $t \leq 0$, there is power-law inflation, $t \geq 0$, followed by a radiation dominated phase of expansion for positive time $t \geq 0$.

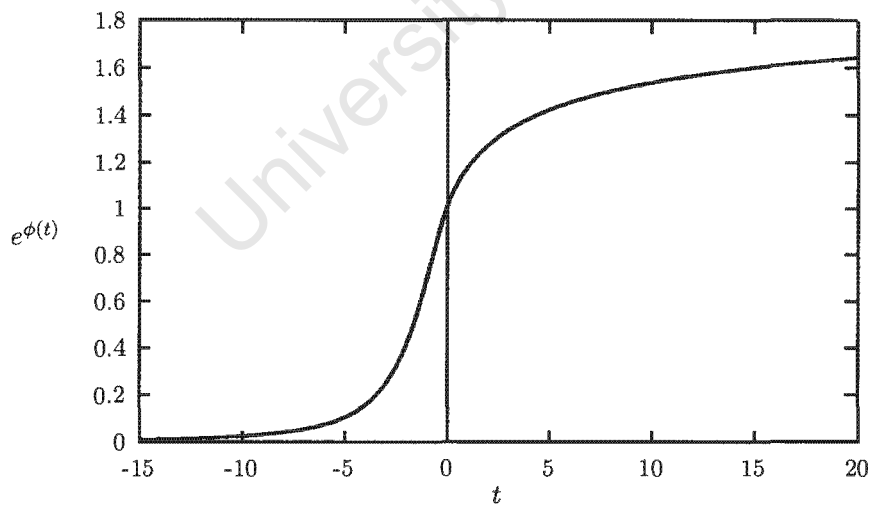


Figure 5.4: The function $\exp(\phi(t))$ as a function of time t , with $a(0) = 1$, $\phi(0) = 0$ and $\chi(0) = 0.25$. $\exp(\phi(t))$ increases monotonically from 0 at time $t = -\infty$ to 2 at $t = +\infty$.

In summary, one gets a stable solution for $0 < \chi_0 < 1/2$, as one can see from the phase plane, with good “pre-big bang” behaviour and the desired dynamics for $\phi(t)$ for both large and small t . The shape of the potential is a bit unusual, but results directly from the specific requested ‘pre-big bang’ evolution eqs.(5.4.1,5.4.2) and the chosen initial conditions. Smoothing out that behaviour at $t = 0$, so that the solution departs from the ‘radiation’ form eq.(5.4.1) at very early times while preserving the symmetry (5.2.10), will result in a smoothed out potential $V(\phi)$; we can choose $a(t)$ in this way so that $H(t)$ and hence $V(\phi)$ are continuous at $t = 0$. Initial conditions can be set so that the matter has the desired late time behaviour: $p/\rho \rightarrow 1/3, \rho \rightarrow 0$; however it then has unusual behaviour at early times in that both ρ and $h \equiv \rho + p$ go negative for some values of $t < 0$. It is unclear if this should be regarded as a serious defect of the model or not, remembering that with the unusual equation of state adopted, the properties of matter are different than usual, and in particular the speed of sound will no longer be given by the usual expression. This needs further investigation. What is clear is that these solutions are not physically reliable as $t \rightarrow +\infty$ (see below), and they will have to be joined on to some other solution to give an adequate model of the universe with ordinary matter behaviour at late times. However, as discussed below, that problem occurs in the entire family of pre-big bang models, and so is not restricted to the models considered here.

5.5 Discussion

We have given examples making very clear the distinction between the equations and the solution having the desired ‘pre-big bang’ symmetry. We have given a broad method of attaining desired string cosmology solutions when there is a dilaton potential V not equal to zero, and used it to obtain ‘Pre-Big Bang’ solutions that seem to have close to the desired properties. In the first case considered, choice of the exact radiation equation of state (5.4.3) at all times leads to a very unstable situation where extreme fine-tuning of initial conditions is required to attain the desired results, and indeed there may be no initial data leading to the desired behaviour in both the forward and backwards directions of time. In the second case we impose an ‘exotic’ equation of state (5.4.9) that links the fluid behaviour to the potential in a way that generalises the perfect fluid equation of state, and we obtain solutions of the desired type without the need for fine tuning the initial data set at $t = 0$.

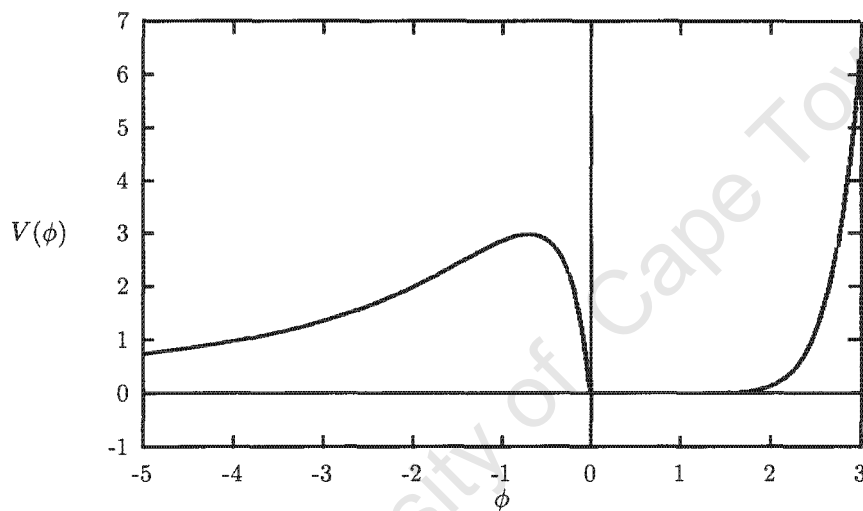


Figure 5.5: The dilaton potential $V(\phi)$ as a function of time ϕ . We assume that $a(0) = 1$, $\phi(0) = 0$ and $\chi(0) = 0.25$ and take the density $\rho(t)$ to have value $\rho(\infty) = 0$ at time $t = \infty$. The potential $V(\phi)$ is continuous at all times, but non-differentiable at $\phi = 0$. For $\phi \rightarrow -\infty$, $V(\phi)$ is asymptotically zero. To the right of $\phi = 0$, the potential starts at $V \approx -0.005$ and goes to zero from below as ϕ goes to $\ln 2$, then increases to $+\infty$ as $\phi \rightarrow \infty$. Around $\phi = \ln 2$, both $V(\phi)$ and its gradient $V'(\phi)$ are zero. As time $t \rightarrow +\infty$, the dilaton field asymptotes to a constant value of $\ln 2$ in our model. The dilaton potential $V(\phi)$ approximates a fixed value of 0 as $\phi \rightarrow \ln 2$ asymptotically for large positive times.

This equation of state looks strange, and the resulting matter behaviour is certainly unusual, but we have no solid handle to use in restricting equations of state in this early era; and we suggest that *it is essential to choose such an equation if one wants the solution to reliably tend to the classical form at late times*. This is because of the form of the equation for $\ddot{\phi}$; if we do not set $\beta = 0$, where β is defined by eq.(5.4.8) then almost always that desired classical state will not be attained, because of eq.(5.4.7); but setting $\beta = 0$, which leads to the desired behaviour, leads immediately to our *exotic* equation of state. Insofar as that equation of state and resulting behaviour is unsatisfactory, this indicates that *there is a problem with the form of the equation for $\ddot{\phi}$* , which comes directly from the standard variational principle employed in the context of the pre-big bang scenario. The remedy probably lies in finding other scenarios with alternative forms of the variational principle, leading to other equations for $\ddot{\phi}$.

This is also indicated because the present form of the equations does not accommodate ordinary matter, the point being that the above analysis applies even if there is no dilaton potential. Suppose $V = 0$; then eq.(5.4.7) remains true, but now

$$\beta = e^{\phi} \left(\frac{3p}{2} - \frac{\rho}{2} \right), \quad (5.5.1)$$

so a reliable approach of the dilaton to a classical solution at late times, requiring $\beta = 0$, demands the radiation equation of state (5.4.3); a baryon dominated epoch is not allowed³. This is usually dealt with by stating that eqs.(5.2.2-5.2.5) don't apply at late times in the history of the universe - a different set of equations are to be used then, and the solutions for early times obtained from eqs.(5.2.2-5.2.5) must be suitably joined on to that late time evolution. However given the vision of M-theory as representing the fundamental theory of gravity, it should be able to describe that epoch too; this apparently requires some modified scenario and associated variational principle (note that although we have discussed the issue in the string frame, it also arises in essentially the same form in the Einstein frame). In any case, whether one accepts this argument or not, given the standard variational principle and equations, we argue that the 'exotic' equation of state implied by setting $\beta = 0$ is *necessary* to give the desired behaviour; when adopted, it enables obtaining that behaviour reliably (i.e it eliminates the need for extreme fine-tuning of data set at $t = 0$).

³Although of course by the algorithm given above, we can simulate a matter dominated phase by suitable choice of the potential V .

However one should note here that we have perhaps been somewhat extreme in imposing this equation of state at all times. It is only really needed, on our approach, near the time of the turnaround, and one could obtain far more general behaviours by modifying what we have here in that light; what is required is that the quantity β must go to zero in the period when the dilaton is stabilised. It has also been pointed out to us that it is not clear why the deviation from its vanishing point should be absorbed completely in the pressure, and then promoted into the conservation equation; other models of the transition [15, 62, 27] successfully stabilise the dilaton at late times without this requirement, with suggestions for classical and quantum corrections in the effective action taking the place of the exotic fluid. Hence our proposal must just be seen as one of a range of possibilities in this regard.

Because we have not made the usual separation of our solution into a '+' and a '-' branch, it is not immediately clear why these solutions are not ruled out by the *no-go theorems* involving a dilaton potential [153, 154]; this is presumably because those theorems exclude fluids with the equation of state we have assumed. We also have not examined the relation of these string-frame solutions to the corresponding Einstein-frame versions. These issues await investigation.

Part III

Braneworld Cosmology

University of Cape Town

Chapter 6

Braneworld Cosmology

6.1 Some Introductory Remarks

The Braneworld Scenario of recent years [2] have dramatically influenced our view of the Universe, and implies completely new scenarios for the cosmology [113, 131]. The cosmological implications of string theory have significantly improved the understanding of topics in string theory itself, eg. the explicit calculation of the black hole entropy and the identification of the AdS/CFT correspondence and its impact on the realization of the holographic principle [158]. Quintessence has led to the discussion of string theory in a de Sitter background [244]. Here we shall describe the effectiveness of the Braneworld Scenario (Section 6.2) and its basic geometrical setting.

In Section 6.3 we elaborate upon the application of this Scenario in the context of Inflation, particularly with the use of D-branes.

S-branes, the *ekpyrotic universe scenario* and bouncing branes are briefly reviewed in Section 6.4.

We lay the groundwork for two Chapters (7 and 8) by outlining some geometrical and mathematical Preliminaries of the Braneworld Scenario of Randall and Sundrum in Section 6.5. This is a necessary precursor to (i) the ideas of braneworld inflation contained in Chapter 7, where we formulate a standard code for deriving the analytic form of a single self-interacting potential of a dilatonic field, and (ii) for further exploring an Alternative to Inflation, viz. the Cosmological Bounce in Chapter 8.

As a precursor to an outline of the context of Braneworld Cosmology in Modern Cosmology performed in the next section, here we briefly elaborate on the historical rôle that extra dimensions has played in Twentieth Century Physics, and innovative attempts to formulate a 1+3 approach cosmological perturbations in Braneworlds, and its applications to CMB anisotropies of late.

Already in the early part of the previous century did Nordstrom and then Kaluza and Klein [112] posit the idea of extra dimensions, and subsequently it started to reappear in various attempts to combine the principles of Quantum Mechanics and Relativity. In its earlier form, String Theories contains more than four dimensions; only after Kaluza-Klein compactification on a manifold of microscopic scale does four dimensional physics reemerge in its standard form [185].

6.2 The Braneworld Scenario

New revelations in String Theory now suggest another approach to compactify extra spatial dimensions. In its most recent spin-off called M-theory, an old idea first motivated by authors such as Akama, Rubakov and Shaposhnikov, Visser, Squires, Gibbons and Wiltshire (see [2] and references there-in) has been resurrected. Here-in lies the main thrust: the Standard Model phenomenology is confined to a hypersurface (the *brane*) that is embedded in a higher dimensional space (the *bulk*). Gravity and all exotic forms of matter propagate in the bulk, while the Standard Model particles propagate only in the three dimensional brane. This scenario weakens the constraints previously exercised upon the size of extra dimension (ie. in the Kaluza-Klein setting). Newton's law of gravity has been tested only on scales larger than a tenth of a millimeter, so there is no reason to exclude possible deviations from this law on smaller scales, suggesting that gravity may in fact be sensitive to the presence of *large* extra dimensions as first proposed by Antoniadis and subsequently by Arkani-Hamed, Dimopoulos and Dvali [2].

The initial proposal by Arkani-Hamed, Dimopoulos and Dvali contained a *flat bulk geometry* in $(4 + d)$ dimensions, with the extra d dimensions are compact with radius R (toroidal topology). The four dimensional Planck mass M_P is related to the fundamental gravitational scale of the extra dimensional theory, called the $(4 + d)$ dimensional Planck

mass M_{fund} , by the equation

$$M_P^2 = M_{fund}^{2+d} R^d .$$

Gravity deviates from Newton's law only on scales smaller than R , where R could be as large as a fraction of a millimeter!

It is possible to localize matter fields in a 3-brane world embedded in a higher-dimensional space if gravity is allowed to propagate away from the brane in the extra dimensions, that were compactified to a finite volume. It was Randall and Sundrum [189] who proposed gravity to be confined to the vicinity of the brane by the warp of one extra dimension. In the Randall-Sundrum brane world scenario the observable Universe is a 3-brane boundary of a non-compact Z_2 symmetric 5-dimensional Anti-de Sitter (AdS) space. The matter fields are restricted to the brane but gravity exists in the whole AdS bulk (see for instance [147] for further detail; we employ this scenario in Chapters 6 and 7).

This *warped bulk geometry* was introduced by Randall and Sundrum [189] (called RSII) as a slice of a space-time with a negative cosmological constant (Anti-de Sitter space time, or AdS in short), and precisely because of the non-flat bulk, they obtained Newton's law of gravity on a brane of positive tension embedded in an *infinite fifth dimension*. In order to explain the large hierarchy between the Planck scale and the electro-weak energy-scale, they also proposed a two-brane scenario [189], called RSI. In this picture, the Standard Model Phenomenology occurs on a negative-tension brane, while there is another positive-tension brane living inside the AdS bulk. The large hierarchy is as a result of the high curvature of the AdS background bulk, represented by the appropriate inter-brane distance, the *radion*.

It was Lukas, Ovrut and Waldram [145] who first who first recognised the possible modification of the Friedmann equation at very high energy, before the time of nucleosynthesis. For a fairly neat pedagogy on the different aspects of Braneworlds, we refer the reader to Brax and van de Bruck [13].

We now divert attention to the early Universe and how the gravitational dynamics lead to imprints on the CMB and other cosmological perturbations.

Fundamental questions such as the Initial Singularity problem, the Hierarchy problem, the Origin of Inflation (or maybe formulating an alternative to the Inflationary Paradigm),

and the Cosmological Constant problem still remain unresolved in Modern Cosmology. Perturbative (and in part, some aspects of non-perturbative) String Theory has been developed to the point where it could finally confront physical testing [212], and in high precision Cosmic Microwave Background experiments such as WMAP [58] and PLANCK. In principle, the Braneworlds phenomenology serves as a means for testing the validity of M-theory in the high precision arena of Early Universe Cosmology.

Up until now, there is no clear understanding of the evolution of cosmological perturbations [13, 148]. The various approaches have been outlined by Nathalie Deruelle [148]. More recently, Roy Maartens [148] outlined the 1+3 covariant approach to cosmological perturbations in Braneworlds, and its application to CMB anisotropies. A new formulation to calculate the CMB spectrum based upon solving the bulk geometry using a low energy approximation has been proposed by Kazuya Koyama [125](see references inside). Unfortunately the ambiguity of the boundary condition is still an open question, even though Koyama uses the RSI model by regarding the second brane as a regulator. Density perturbations with *dark radiation* were investigated by Gumjudpai, Maartens and Gordon [148]. In the radiation era the large-scale density perturbations are *suppressed* by a small amount, and at the same time those in the dark radiation *grows* at late times. For matter with a stiff equation of state, the suppression becomes strong.

6.3 Inflation on the Brane

If the early Universe undergoes a small period of exponential expansion that last sufficiently long, then most of the problems encountered in the Standard Model would be explained [84, 141, 124, 140]. The basic model of inflation includes a scalar field ϕ with a potential $V(\phi)$, whose value acts as a cosmological constant, provided that it is flat, so that the scale factor $a(t)$ in an FRW Universe increases exponentially. The Friedmann equation for such a Universe is

$$\left(\frac{\dot{a}}{a}\right)^2 + \frac{k}{a^2} = \frac{8\pi G}{3} \left(\frac{1}{2}\dot{\phi}^2 + V(\phi)\right), \quad (6.3.1)$$

where the dot denotes a first derivative with respect to time t , whereas the scalar field equation is

$$\ddot{\phi} + 3\frac{\dot{a}}{a}\dot{\phi} = -\frac{\partial V}{\partial \phi}. \quad (6.3.2)$$

The conditions for inflation to be realized can be summarized in two slow-rolling conditions, viz.

$$\epsilon \equiv \frac{M_{\text{Planck}}^2}{2} \left(\frac{1}{V} \frac{\partial V}{\partial \phi} \right) \ll 1 \quad (6.3.3)$$

$$\eta \equiv M_{\text{Planck}}^2 \left(\frac{1}{V} \frac{\partial^2 V}{\partial \phi^2} \right) \ll 1, \quad (6.3.4)$$

in terms of the parameters ϵ and η , that have become the standard way to parameterize the physics of inflation:- If condition (6.3.3) is satisfied, the potential is flat enough to guarantee an exponential expansion; if condition (6.3.4) is satisfied, the friction term $3\frac{\dot{a}}{a}\dot{\phi}$ dominates and therefore implies the slow-rolling of the field on the potential, guaranteeing that the inflationary era lasts for some time. The number of e-foldings is given by

$$N \equiv \int_{a_{\text{init}}}^{a_{\text{end}}} \frac{da}{a} = \frac{1}{M_{\text{Planck}}^2} \int_{\phi_{\text{init}}}^{\phi_{\text{end}}} \frac{V}{\partial V / \partial \phi} d\phi. \quad (6.3.5)$$

In order to solve the Horizon problem successfully one needs at least $N \geq 60$. Hybrid inflation [139] solves the *graceful exit problem* by utilizing a second field that becomes massless and then tachyonic after inflation, signalling an instability in that direction. The field rolls fast towards its true vacuum, thus ending inflation. In this scenario, the inflaton field need not acquire values greater than the Planck scale, as usually happens in single field potentials. This type of potential is easy to realize in models from supersymmetric or string theories. The strong attributes of inflation are (1) an explanation for the density perturbations of CMB and therefore indirect account for large structure formation and (2) a scale invariant, Gaussian and adiabatic spectrum of temperature fluctuations consistent with observations at COBE [140, 60].

The so-called **Cosmological Moduli Problem** [188] stems from any scalar field that has gravitational strength interactions and acquires a non-zero mass after supersymmetry breaking that is of the order of the gravitino mass. If the scalar field happens to be stable, it will over-close the Universe. If the field decays, it will do so very late in the history of the Universe (due to the weakness of its coupling) and drastically decrease the relative abundance of ${}^4\text{He}$ and D by destroying their nuclei, hence ruining the results of nucleosynthesis. This also applies to the gravitino and fermionic partners of the moduli.

The discovery of D-branes and the Horava-Witten scenario [100] of M-theory have further led to the discovery that the brane world appears naturally in string constructions,

allowing its cosmology to be investigated while bearing in mind its particular string realization. The physical implications of the five dimensional brane world scenario of Randall and Sundrum [189] quickly drew the interest of cosmologists. Binetruy *et al.* [113] made the first concrete description of a five-dimensional cosmology with branes, with interesting consequences. Bowcock *et al.* [12, 127, 105] soon revealed that the present expansion of the Universe could be an illusion and that it is actually moving with some non-vanishing velocity in a higher-dimensional static bulk (the so-called *mirage cosmology* [118]).

Dvali and Tye [41] proposed a mechanism for deriving inflation between two D-branes in BPS state. However, they failed to address the issue of what happens after the branes collide and how to exit inflation. Nor is their string potential computable. The D-brane/Antibrane inflation model of Burgess *et al.* [174] (parallel branes with negligible velocity effects) has a completely computable potential, with the inflation field representing the distance between the brane/antibrane pair along the extra dimension. Its authors also claims to solve the *graceful exit problem*: Hybrid inflation is achieved by the appearance of an open string tachyon at a critical distance. Any monopoles or domain walls that appear before inflation, are diluted away during inflation, and are not produced after inflation either since the Kibble mechanism is not at work in the extra dimensions.

Intersecting branes [106] may require less fine-tuning than brane/antibrane systems. The end result of tachyon condensation may also be different from brane/antibrane systems. A more realistic model at the end of inflation can be achieved if the condensate is a configuration of intersecting branes endowed with supersymmetry. Both models suffer from the Moduli problem, and the details of reheating [229]. See also Herdeiro *et al.* [98] for a scenario of attraction of D3 and D7 branes with magnetic fluxes, where the tachyon condensate mechanism leads to a D3/D7 supersymmetric bound state.

6.4 Alternatives to Inflation

S-Branes are topological defects for which all of the longitudinal dimensions are space-like, and therefore exist for only a moment in time. They were introduced in [224] to bring the de Sitter / CFT correspondence closer to the Anti-de Sitter / CFT correspondence, with the s-brane plying the role of the D-brane. In a very recent reprisal by Dyson, Lindsay and Susskind, the existence of such a duality is scrutinized [224].

Burgess *et al.* 2002 [78] argue that a general class of solutions to Einstein-dilaton-Maxwell theory, presented in Grojean *et al.* (see the same reference) with hyperbolic or planar symmetry describe the gravitational interactions of a pair of **negative-tension q -branes**.¹ These spacetimes are static near each brane, but become time-dependent and expanding at late epoch in response to the branes' presence. These time-dependent regions provide *inter alia* explicit examples of cosmological spacetimes with past horizons (interpreted as S-branes) and no past naked singularities, interpreted as a cosmological bounce.

The **ekpyrotic universe** of Khoury *et al.* [220] is based upon the Horava-Witten scenario of M-theory [100] compactified on an interval S^1/\mathbb{Z}_2 for which the two 10-dimensional endpoints are further compactified on a 6-dimensional Calabi-Yau manifold to leave two 4-dimensional worlds at the ends of the interval in the 5-dimensional bulk. Besides these two worlds, there are also in the compactifications 5 branes that are free to move through the bulk. In the original scenario [220] an almost BPS bulk brane moves from one boundary of the interval to the other end and collides with the second boundary brane to produce the big-bang. The attraction of the branes is described by a *negative* potential, proposed to have the form $V(\phi) = -e^{-\alpha\phi}$. Small quantum fluctuations induce some ripples on the bulk brane which then collide with the visible brane to produce the density fluctuations measured in the CMB. The scale factor depends upon the position of the brane in the bulk, and goes from a contraction before the collision to an expansion after the collision (ie. a bounce). The problem of attaining the initial BPS state has been much debated [123]. The main problem with this scenario is the violation of the null energy condition at the bounce in the scale factor (see Khoury *et al.* [221], as well as Chapter 7 later.)

One way in which to avoid this is to simply consider a collision between the boundary branes (no bulk brane) [123]. In this so-called **pyrotechnic universe** the singularity is only in the extra dimension, while the scale factors of the brane remain finite throughout the bounce. The third version is known as the **cyclic universe** [221]. In this scenario the two branes keep separating and passing through each other an infinite number of times.

There has been a debate over the issue of the spectrum of perturbations [161]. The other issue is the contrived use of negative potentials (not derived from theory). See Linde [142]

¹Giovannini [78] derives an effective lower dimensional theory where the gauge-invariant vector fields associated with the fluctuations of the metric are always massless and localized on a **negative tension brane**.

for a comparison of this scenario and its comparison with inflation. See also Musing *et al.* [172] for the most recent contributions to braneworld bounce scenarios. In particular, C. Gordon and N. Turok investigates a bouncing Universe in which neither General Relativity nor the Weak Energy Condition is violated, and discuss the evolution and matching of comoving perturbations through and around the bounce. Lecture notes by Quevedo and Langlois [131] were useful in providing an overview of recent developments in the field.

6.5 Preliminary Considerations

Motivated by developments in Superstring and M-theory [100, 210, 145] have led to the notion that gravity could be a higher dimensional theory, that becomes 4-dimensional at low energies. In the Randall-Sundrum scenario [189] gravity can be localized on a 3-brane while a fifth dimension may remain noncompact. Observers are bound to a brane, which may have a more general metric than the induced Minkowski metric that Randall and Sundrum [189] assumed. A covariant geometric approach was first given by Shiromizu, Maeda and Sasaki [210] and also by Maartens [147]. In Chapters 6 and 7 we shall assume that a scalar field ϕ is bound to the brane, and that higher-dimensional modifications of the standard Einstein field equations are imprinted via (i) local quadratic energy-momentum corrections that arise from the extrinsic curvature, and (ii) non-local effects from the free gravitational field in the bulk, transmitted via a projection of the bulk Weyl tensor onto the brane [147]. The 5-dimensional field equations [189, 147] are Einstein's equations, with a (negative) bulk cosmological constant $\tilde{\Lambda}$ and the brane energy-momentum providing the source:

$$\tilde{G}_{AB} = \tilde{\kappa}^2 \left[-\tilde{\Lambda} \tilde{g}_{AB} + \delta(\chi) \{-\lambda g_{AB} + T_{AB}\} \right]. \quad (6.5.1)$$

The tildes denote the bulk (5-dimensional) generalization of standard general relativity quantities, and $\tilde{\kappa}^2 = 8\pi/\tilde{M}_p^3$, where \tilde{M}_p is the fundamental 5-dimensional Planck mass, which is typically much less than the effective Planck mass on the brane, $M_p = 1.2 \times 10^{19}$ GeV. The brane is given by $\chi = 0$, so that a natural choice of coordinates is $x^A = (x^\mu, \chi)$, where $x^\mu = (t, x^i)$ are spacetime coordinates on the brane. The brane tension is λ , and $g_{AB} = \tilde{g}_{AB} - n_A n_B$ is the induced metric on the brane, with n_A the spacelike unit normal to the brane. Matter fields confined to the brane make up the brane energy-momentum

tensor T_{AB} (with $T_{AB}n^B = 0$).

The modification to the standard Einstein equations[147], with the new terms carrying bulk effects onto the brane are

$$G_{\mu\nu} = -\Lambda g_{\mu\nu} + \kappa^2 T_{\mu\nu} + \tilde{\kappa}^4 S_{\mu\nu} - \mathcal{E}_{\mu\nu}, \quad (6.5.2)$$

where $\kappa^2 = 8\pi/M_p^2$. We choose units in which $\kappa^2 = 1$, and $\lambda = 6 \left(\frac{\kappa^2}{\tilde{\kappa}^4} \right)$. Then the energy scales are related as follow:

$$\Lambda = \frac{4\pi}{M_p^3} \left[\tilde{\Lambda} + \left(\frac{4\pi}{3M_p^3} \right) \lambda^2 \right].$$

The tensor $S_{\mu\nu}$ represents local quadratic energy-momentum corrections of the matter fields, and the $\mathcal{E}_{\mu\nu}$ is the projected bulk Weyl tensor transmitting non-local gravitational degrees of freedom from the bulk to the brane. All the bulk corrections may be consolidated into effective total energy density ρ^{tot} , pressure p^{tot} , anisotropic stress $\pi_{\mu\nu}^{tot}$ and energy flux q_μ^{tot} , as follows. The modified Einstein equations take the standard Einstein form with a redefined energy-momentum tensor:

$$G_{\mu\nu} = -\Lambda g_{\mu\nu} + \kappa^2 T_{\mu\nu}^{tot}, \quad (6.5.3)$$

where

$$T_{\mu\nu}^{tot} = T_{\mu\nu} + \frac{\tilde{\kappa}^4}{\kappa^2} S_{\mu\nu} - \frac{1}{\kappa^2} \mathcal{E}_{\mu\nu}. \quad (6.5.4)$$

Then

$$\rho^{tot} = \rho + \frac{\tilde{\kappa}^4}{\kappa^6} \left[\frac{\kappa^4}{24} (2\rho^2 - 3\pi_{\mu\nu}\pi^{\mu\nu}) + \mathcal{U} \right] \quad (6.5.5)$$

$$p^{tot} = p + \frac{\tilde{\kappa}^4}{\kappa^6} \left[\frac{\kappa^4}{24} (2\rho^2 + 4\rho p + \pi_{\mu\nu}\pi^{\mu\nu} - 4q_\mu q^\mu) + \frac{1}{3}\mathcal{U} \right] \quad (6.5.6)$$

$$\pi_{\mu\nu}^{tot} = \pi_{\mu\nu} + \frac{\tilde{\kappa}^4}{\kappa^6} \left[\frac{\kappa^4}{12} \{ -(\rho + 3p)\pi_{\mu\nu} + \pi_{\alpha\langle\mu}\pi_{\nu\rangle}{}^\alpha + q_{(\mu}q_{\nu)} \} \right] \quad (6.5.7)$$

with non-local energy flux \mathcal{Q}_μ and non-local anisotropic stress $\mathcal{P}_{\mu\nu}$ both on the brane. (Note that $\tilde{\kappa}^4/\kappa^6$ is dimensionless.)

These general expressions simplify in the case of a perfect fluid (or minimally coupled scalar field, or isotropic one-particle distribution function), i.e., for cases where the energy flux and anisotropic stress both vanish

$$q_\mu = 0 = \pi_{\mu\nu} . \quad (6.5.8)$$

However, the total energy flux and anisotropic stress do not necessarily vanish:

$$q_\mu^{\text{tot}} = \frac{\tilde{\kappa}^4}{\kappa^6} \mathcal{Q}_\mu , \quad \pi_{\mu\nu}^{\text{tot}} = \frac{\tilde{\kappa}^4}{\kappa^6} \mathcal{P}_{\mu\nu} .$$

We use this formalism in Chapter 6 and Chapter 7 Section 8.5.1 (see also [214, 215]).

6.6 Some Final Remarks

To conclude this Chapter, we would like to bring attention to the fact that more recent literature has re-enforced the key point that Bouncing Universes in a Braneworld Scenario (see for instance [61, 170]) exploit *a nonvanishing projected Weyl tensor* $\mathcal{E}_{\mu\nu}$, without *exotic* forms of matter.

It is precisely this idea that we employ in Chapter 8. What is in fact unique about these solutions is that they obviate the need for *quantum foam*, in other words, the brane never exits the region of validity of low energy String Theory.

Chapter 7

Braneworld Inflation

7.1 Introduction

The braneworld scenario has important consequences for the standard model of cosmology and in particular for the inflationary paradigm - which has successfully explained many of the standard cosmological problems.

Braneworlds with a homogeneous and isotropic cosmology have recently been explored by a number of authors [9, 113, 127, 105, 96, 59] and in particular, solutions of the Friedmann - Robertson - Walker (FRW) dilatonic Braneworlds have been investigated [245].

Recent work on inflation [150] has demonstrated that the modified braneworld Friedmann equation leads to a stronger condition for inflation that amounts to violation of the strong energy condition. At high energies, feedback from the bulk dampens the rolling of the scalar field, in effect easing the condition for slow-rolling inflation for a given self-interaction, and increasing the number of e-foldings. Furthermore, the perturbation spectral index is driven towards the Harrison - Zel'dovich value $n = 1$ - a very desirable feature of this model.

An algorithm for generating a class of exact braneworld inflationary models has been recently presented by Hawkins and Lidsey [96], in the case where the *dark radiation* component has been neglected¹. It follows that the field equations have a simple *Hamilton - Jacobi* form and Hubble variable, which is written as a function of the inflaton, is then used as

¹This is motivated by the fact that the dark radiation rapidly redshifts away and soon becomes dynamically unimportant.

a solution-generating function for the self-interaction and scale factor evolution $a(t)$ (as proposed in [59, 134, 26]).

Adopting the proposal by Randall and Sundrum [189], where the dynamical equations on the three-brane differ from the general relativity equations by terms that carry the effects of embedding and of the free gravitational field in the five-dimensional bulk, we follow a two-tier approach² for finding exact inflationary FRW solutions to the braneworld Einstein field equations that does not explicitly assume the slow-rolling approximation.

We [214] present two ways in which exact solutions to the covariant non-linear dynamical equations for the gravitational and matter fields on the brane can be obtained. In the first approach, which is based on a paper by Ellis and Madsen [155], we examine the constraints on the dynamical relationship between the cosmological scale factor and the inflaton driving self-interaction potential, imposed by the weak energy condition. The second approach then investigates inflationary solutions obtained from a scalar field superpotential (applied recently to the case of standard inflation by Feinstein [59]). Both these techniques of solving the braneworld field equations are illustrated by flat curvature models.

7.2 The FRW Braneworld

7.2.1 Matter description

A homogeneous scalar field $\phi(t)$ on the brane has an energy-momentum tensor

$$T_{\mu\nu} = \rho u_\mu u_\nu + p h_{\mu\nu}, \quad (7.2.1)$$

with $\rho = \frac{1}{2}\dot{\phi}^2 + V(\phi)$ and $p = \frac{1}{2}\dot{\phi}^2 - V(\phi)$ where $\dot{\phi}^2$ is the kinetic energy and $V(\phi)$ is the potential energy. The effective total energy-momentum tensor then also has

$$\rho^{\text{tot}} = \rho + \frac{6}{\lambda} \left[\frac{1}{12}\rho^2 + \mathcal{U} \right] \quad (7.2.2)$$

$$p^{\text{tot}} = p + \frac{6}{\lambda} \left[\frac{1}{12}\rho(\rho + 2p) + \frac{1}{3}\mathcal{U} \right]. \quad (7.2.3)$$

An FRW braneworld is characterized by vanishing shear, acceleration, vorticity, non-local anisotropic stress and non-local energy flux (see section V equation (61) in [147]):

$$\sigma_{\mu\nu} = A_\mu = \omega_\mu = \mathcal{P}_{\mu\nu} = \mathcal{Q}_\mu = 0, \quad (7.2.4)$$

²See [96, 59, 134, 26, 155] where this program was first outlined in detail.

then

$$\pi_{\mu\nu}^{\text{tot}} = 0 \quad (7.2.5)$$

$$q_{\mu}^{\text{tot}} = 0. \quad (7.2.6)$$

The bulk spacetime could for instance be Schwarzschild-Anti de Sitter with *dark radiation* coming from the black hole if the brane metric is FRW, but as [147] pointed out, more general bulk metrics are in principle possible. The matter fields are constrained to a single brane (a four dimensional hypersurface embedded in the bulk) [127, 105, 147, 12].

The standard conservation equation of general relativity holds on the brane, together with a simplified propagation equation for the non-local energy density \mathcal{U} [147]

$$\dot{\rho} + \Theta(\rho + p) = 0, \quad (7.2.7)$$

$$\dot{\mathcal{U}} + \frac{4}{3}\Theta\mathcal{U} = 0, \quad (7.2.8)$$

where Θ is the expansion parameter.

7.2.2 Gravitational Equations

The Einstein Field equations with $\Lambda = 0$ then become

$$\dot{\Theta} + \frac{1}{3}\Theta^2 = -\frac{1}{2}(\rho^{\text{tot}} + 3p^{\text{tot}}), \quad (7.2.9)$$

$$\frac{1}{3}\Theta^2 + 3\mathcal{K} = \rho^{\text{tot}}, \quad (7.2.10)$$

$$\mathcal{U} = \mathcal{U}_0 \left(\frac{a_0}{a} \right)^4, \quad (7.2.11)$$

where $\mathcal{K} = k/a(t)^2$, $k = 0, \pm 1$, we let $a(t)$ represent the scale factor at a time t with real constants \mathcal{U}_0 and a_0 evaluated at some time $t = t_0$. As per usual, the expansion $\Theta = 3\dot{a}(t)/a$.

7.3 Generating Exact Inflation Braneworlds

7.3.1 The Reality Condition

The effects of embedding the free gravitational field in the five-dimensional bulk are represented by the correction terms to the energy-momentum tensor $T_{\mu\nu}$, as expressed in equations (7.2.2) and (7.2.3). In the absence of anisotropic stress ($\pi_{\mu\nu}^{\text{tot}} = 0$) the non-local energy density \mathcal{U} takes the form of *dark radiation* with its behaviour given by equation (7.2.11).

As a first step to specifying a desired model, we note that the following combination of field equations (7.2.9)–(7.2.10) gives the sum of the effective (total) energy density and pressure:

$$\rho^{\text{tot}} + p^{\text{tot}} = 2 \left(\mathcal{K} - \frac{1}{3} \dot{\Theta} \right). \quad (7.3.1)$$

Adding equations (7.2.2) and (7.2.3) and factorizing the resulting expression, we find

$$\rho^{\text{tot}} + p^{\text{tot}} = \dot{\phi}^2 \left(1 + \frac{1}{\lambda} \rho \right) + \frac{6}{\lambda} \mathcal{U}, \quad (7.3.2)$$

and substituting this relation into (7.3.1) and rearranging terms we obtain an expression for $\dot{\phi}^2$:

$$\dot{\phi}^2 \left(1 + \frac{1}{\lambda} \rho \right) = 2 \left(\mathcal{K} - \frac{1}{3} \dot{\Theta} \right) - \frac{6}{\lambda} \mathcal{U}. \quad (7.3.3)$$

Definition: The Reality Condition holds iff $\dot{\phi}^2 \geq 0$. This statement is equivalent to the *Null Energy Condition* $\rho + p \geq 0$ and requires

$$\left(1 + \frac{1}{\lambda} \rho \right) > 0 \quad (7.3.4)$$

and

$$2 \left(\mathcal{K} - \frac{1}{3} \dot{\Theta} \right) - \frac{6}{\lambda} \mathcal{U} \geq 0 \quad (7.3.5)$$

to hold at all times t . The factor $\left(1 + \frac{1}{\lambda} \rho \right)$ is determined by equations (7.2.2) and (7.2.10):

$$\frac{1}{2\lambda} \rho^2 + \rho + \frac{6}{\lambda} \mathcal{U} - \frac{1}{3} \Theta^2 - 3\mathcal{K} = 0. \quad (7.3.6)$$

In order to satisfy condition (7.3.4) we take the positive root of equation (7.3.6):

$$1 + \frac{1}{\lambda} \rho = \sqrt{1 + \frac{2}{\lambda} \left[(3\mathcal{K} + \frac{1}{3} \Theta^2) - \frac{6}{\lambda} \mathcal{U} \right]}. \quad (7.3.7)$$

Note that the Weak Energy Condition, viz. $\rho \geq 0$ and $\rho + p \geq 0$ holds if

$$3\mathcal{K} + \frac{1}{3}\Theta^2 - \frac{6}{\lambda}\mathcal{U} \geq 0 \quad (7.3.8)$$

since this inequality ensures that ρ is non-negative in equation (7.3.7). The Weak Energy Condition is violated if $\rho < 0$, i.e.:

1. if condition (7.3.8) does not hold,
2. or if both inequalities (7.3.4) and (7.3.5) are reversed³.

7.3.2 How to obtain Braneworlds with desired inflationary behaviour

We now present inflationary braneworld solutions based upon the Reality Conditions (7.3.4) and (7.3.5). Using equations (7.3.3) and (7.3.7) $\dot{\phi}^2$ can be written in the following useful form:

$$\dot{\phi}^2 = \frac{\Phi}{\Delta}, \quad (7.3.9)$$

where

$$\Phi = -\frac{8}{\lambda}U + 2(\mathcal{K} - \frac{1}{3}\dot{\Theta}) \quad (7.3.10)$$

and

$$\Delta = \sqrt{1 + \frac{2}{\lambda} \left(\frac{1}{3}\Theta^2 + 3\mathcal{K} - \frac{6}{\lambda}U \right)}. \quad (7.3.11)$$

An expression for the potential $V(\phi)$ is determined by equations (7.3.7) and (7.3.9),

$$V(\phi) = \lambda(\Delta - 1) - \frac{\Phi}{2\Delta}. \quad (7.3.12)$$

In order to obtain the desired inflationary dynamics we proceed as follows. (i) Specify a (monotonic) function $a(t)$ as desired, provided the *Braneworld Reality Condition* is satisfied; (ii) choose k (and therefore determine \mathcal{K}); (iii) determine the expansion parameter $\Theta = 3\dot{a}(t)/a(t)$ and its derivative $\dot{\Theta}$. Integrating equation (7.3.9) gives $\phi(t)$ and inverting gives $t(\phi)$. Finally equation (7.3.12) gives $V(t) = V(t(\phi)) \Rightarrow V(\phi)$. Thus the above procedure will determine $V(\phi)$ describing a model which satisfies the exact inflationary equations on the brane (with no slow-rolling approximation) with the desired scale factor $a(t)$ behaviour.

³Notwithstanding violation of the Weak Energy Condition, the Reality Condition may in fact still hold, due to this double change in sign.

It should be pointed out that this procedure is consistent as all the above dynamical equations are satisfied at all times.

We present solutions for which the non-local energy density or *dark energy* may be negative (i.e. allowing naked singularities in the bulk, which seems unphysical). Nevertheless, discussions related to the sign of the *dark radiation* and of bulk effects on the cosmological dynamics can be seen elsewhere [127, 147, 19, 12].

7.3.3 Simple examples

The de-Sitter model

There are elementary solutions to equations (7.3.9-7.3.12) which yield the simple exponential inflationary solution representing a de-Sitter universe⁴:

$$a(t) = a_0 \exp(\omega t), \quad \dot{\omega} = 0. \quad (7.3.13)$$

(i) $k = 0, \mathcal{U} = 0$:

Flat models with a constant potential and vanishing non-local energy density

$$V(\phi) = \lambda \left[\sqrt{1 + \frac{6\omega^2}{\lambda}} - 1 \right], \quad \dot{\phi}(t) = 0, \quad \mathcal{U} = 0. \quad (7.3.14)$$

(ii) $k = +1, \mathcal{U} < 0$:

Closed models with a quadratic potential and with *negative* non-local energy density

$$\begin{aligned} \mathcal{K}_0 &= 2\sqrt{\frac{-\mathcal{U}_0}{3} \left(1 + \frac{6\omega^2}{\lambda}\right)}, \\ \phi(t) &= \phi_0 \pm 2\sqrt[4]{\frac{-\mathcal{U}_0}{3}} \left(\frac{1 - e^{-\omega t}}{\omega}\right), \\ V(\phi) &= \lambda \left[\sqrt{1 + \frac{6\omega^2}{\lambda}} - 1 \right] \\ &\quad + \left[2\sqrt[4]{\frac{-\mathcal{U}_0}{3}} \mp \omega(\phi - \phi_0) \right]^2. \end{aligned} \quad (7.3.15)$$

This solution asymptotes to the GR result [155] as $\lambda \rightarrow \infty$, since $V \rightarrow 3\omega^2$ and $\mathcal{U} \rightarrow 0$.

⁴This has already been derived by other authors, see eg. [127].

de-Sitter expansion from a singularity

Consider now inflationary de-Sitter expansion from a singularity ($a(0) = 0$):

$$a(t) = a_0 \sinh(\omega t), \quad \dot{\omega} = 0. \quad (7.3.16)$$

We illustrate exact solutions with

(i) $k = -1, \mathcal{U} = 0$:

Open models with a cosmological constant and vanishing non-local energy density

$$\begin{aligned} \mathcal{K}_0 &= -\omega^2 \\ V(\phi) &= \lambda \left[\sqrt{1 + \frac{6\omega^2}{\lambda}} - 1 \right], \quad \dot{\phi} = 0, \quad \mathcal{U} = 0. \end{aligned} \quad (7.3.17)$$

(ii) $k = \pm 1, \mathcal{U} < 0$:

Open or closed models with *negative* non-local energy density

$$\begin{aligned} \mathcal{K}_0 &= -\omega^2 + 2\sqrt{-\frac{\mathcal{U}_0}{3}} \left(1 + \frac{6\omega^2}{\lambda} \right) : \\ \dot{\phi}^2 &= 4\sqrt{-\frac{\mathcal{U}_0}{3}} \sinh^{-2}(\omega t), \\ \phi &= \phi_\infty \pm 2\sqrt[4]{-\frac{\mathcal{U}_0}{3}} \frac{\ln \left[\tanh \left(\frac{\omega t}{2} \right) \right]}{\omega}, \\ \Phi &= 4\sqrt{-\frac{\mathcal{U}_0}{3}} \sinh^{-2}(\omega t) \Delta, \\ \Delta &= \sqrt{1 + \frac{6\omega^2}{\lambda}} + \frac{6}{\lambda} \sqrt{-\frac{\mathcal{U}_0}{3}} \sinh^{-2}(\omega t), \\ V(\phi) &= \lambda \left[\sqrt{1 + \frac{6\omega^2}{\lambda}} - 1 \right] \\ &\quad + 4\sqrt{-\frac{\mathcal{U}_0}{3}} \sinh^2 \frac{1}{2} \left[\sqrt[4]{-\frac{3}{\mathcal{U}_0}} \omega(\phi - \phi_0) \right]. \end{aligned} \quad (7.3.18)$$

de-Sitter expansion from a bounce

We next consider inflationary de-Sitter expansion from a bounce:

$$a(t) = a_0 \cosh(\omega t), \quad \dot{\omega} = 0. \quad (7.3.20)$$

Exact solutions exist if we choose

(i) $k = +1, \mathcal{U} = 0$:

Closed models with vanishing non-local energy density. If $\mathcal{K}_0 = \omega^2$, we find that

$$V(\phi) = \lambda \left[\sqrt{1 + \frac{6\omega^2}{\lambda}} - 1 \right], \quad \dot{\phi}(t) = 0, \quad \mathcal{U} = 0. \quad (7.3.21)$$

(i) $k = +1, \mathcal{U} < 0$:

This is an example of a closed model with *negative* non-local energy density. For

$$\begin{aligned} \mathcal{K}_0 &= \omega^2 + 2\sqrt{-\frac{\mathcal{U}_0}{3} \left(1 + \frac{6\omega^2}{\lambda}\right)} : & (7.3.22) \\ \dot{\phi}^2 &= 4\sqrt{-\frac{\mathcal{U}_0}{3}} \cosh^{-2}(\omega t), \\ \phi &= \phi_0 \pm 2\sqrt{-\frac{\mathcal{U}_0}{3}} \frac{\arctan[\sinh(\omega t)]}{\omega}, \\ \Phi &= 4\sqrt{-\frac{\mathcal{U}_0}{3}} \cosh^{-2}(\omega t) \Delta, \\ \Delta &= \sqrt{1 + \frac{6\omega^2}{\lambda}} + \frac{6}{\lambda} \sqrt{-\frac{\mathcal{U}_0}{3}} \cosh^{-2}(\omega t), \\ V(\phi) &= \lambda \left[\sqrt{1 + \frac{6\omega^2}{\lambda}} - 1 \right] \\ &\quad + 4\sqrt{-\frac{\mathcal{U}_0}{3}} \cos^2 \frac{1}{2} \left[\sqrt{-\frac{3}{\mathcal{U}_0}} \omega(\phi - \phi_0) \right]. \end{aligned} \quad (7.3.23)$$

The coasting solution

Consider linear expansion

$$a(t) = \omega t, \quad \dot{\omega} = 0. \quad (7.3.24)$$

Flat, open or closed models with *negative* non-local energy density such that

$$\mathcal{U}_0 = -\frac{3}{4} \left(1 + \frac{k}{\omega^2}\right)^2 \leq 0. \quad (7.3.25)$$

Then

$$\begin{aligned}
 \Delta &= 1 + \frac{6}{\lambda} \sqrt{-\frac{\mathcal{U}_0}{3}} t^{-2}, \\
 \Phi &= 4 \sqrt{-\frac{\mathcal{U}_0}{3}} t^{-2} \Delta, \\
 \dot{\phi}^2 &= 4 \sqrt{-\frac{\mathcal{U}_0}{3}} t^{-2}, \\
 \phi(t) &= \phi_0 \pm 2 \sqrt[4]{-\frac{\mathcal{U}_0}{3}} \ln |t|, \\
 V(\phi) &= 4 \sqrt{-\frac{\mathcal{U}_0}{3}} \exp\left(\mp \sqrt[4]{-\frac{3}{\mathcal{U}_0}} (\phi - \phi_0)\right). \tag{7.3.26}
 \end{aligned}$$

An interesting feature of this solution is that it is identical to the GR case (see equation (54) in [155]) for $\phi_0 = 0$, $k = 0$ and $\mathcal{U}_0 = -\frac{3}{4}$.

Coasting/radiation solution

Now consider the expansion

$$a(t) = a_0 \sqrt{1 + 2\omega t}, \quad \dot{\omega} = 0. \tag{7.3.27}$$

Exact solutions occur if we choose

(i) $k = 0, \rho(t) = 0, \mathcal{U} > 0$:

Flat models with *positive* non-local energy density

$$\dot{\phi} = 0, \quad \Phi = 0, \quad V = 0, \quad \mathcal{U}_0 = \frac{9}{2} \lambda a_0^4 \omega^2. \tag{7.3.28}$$

(ii) $k = +1$:

Closed models with *positive or negative* non-local energy density provided that

$$\begin{aligned}
\mathcal{U}_0 &> -\frac{3}{4a_0^2} : \\
\omega &= \frac{1}{2a_0\sqrt{\lambda}} \sqrt{1 + \frac{4\mathcal{U}_0 a_0^2}{3}}, \quad \dot{\phi}^2 = 2\mathcal{K}_0(1 + 2\omega t)^{-1}, \\
\phi(t) &= \phi_0 \pm \frac{\sqrt{2} \sqrt{1 + 2\omega t} - 1}{a_0 \omega}, \\
\Delta &= 1 + \frac{3\mathcal{K}_0}{\lambda(1 + 2\omega t)}, \\
\Phi &= 2\mathcal{K}_0(1 + 2\omega t)^{-1} \Delta, \\
V(\phi) &= \frac{2}{a_0^2 \left(1 \pm \frac{a_0\omega}{\sqrt{2}}(\phi - \phi_0)\right)^2}. \tag{7.3.29}
\end{aligned}$$

At very early times, the scale factor approximates to a coasting solution $a(t) \approx 1 + \omega t$, while at a later stage the model is radiation-dominated $a(t) \sim \sqrt{t}$.

Power-law expansion

Finally let us consider the power-law expansion

$$a(t) = a_0 \sqrt{1 + \omega t^2}, \quad \dot{\omega} = 0. \tag{7.3.30}$$

Various scenarios occur for different curvatures, depending on the sign of ω . We present a general class of solutions. Put

$$\begin{aligned}
x &:= \frac{1}{1 + \omega t^2}, \\
\mathcal{U}_0 &= -\frac{1}{4} (2\lambda\omega + 3(\mathcal{K}_0 + \omega)^2), \\
\dot{\phi}^2 &= 2(\mathcal{K}_0 + \omega) x, \quad \Delta = 1 + \frac{3}{\lambda}(\mathcal{K}_0 + \omega) x, \\
\Phi &= 2(\mathcal{K}_0 + \omega) x \Delta. \tag{7.3.31}
\end{aligned}$$

The scalar field evolves as

$$\phi = \phi_0 \pm \begin{cases} \sqrt{\frac{2(\mathcal{K}_0 + \omega)}{\omega}} \ln(\sqrt{\omega t} + \sqrt{1 + \omega t^2}) & \text{if } \omega > 0 \\ \sqrt{\frac{2(\mathcal{K}_0 + \omega)}{-\omega}} \arcsin(\sqrt{-\omega t}) & \text{if } \omega < 0 \end{cases} \tag{7.3.32}$$

The potential is given by

$$V(\phi) = 2(\mathcal{K}_0 + \omega) \begin{cases} \cosh^{-2} \sqrt{\frac{\omega}{2(\mathcal{K}_0 + \omega)}}(\phi - \phi_0) & \text{if } \omega > 0 \\ \cos^{-2} \sqrt{\frac{-\omega}{2(\mathcal{K}_0 + \omega)}}(\phi - \phi_0) & \text{if } \omega < 0 \end{cases} \tag{7.3.33}$$

In this case we are able to discuss two types of models, viz bouncing universes and recollapsing ones.

(i) $k = 0, \mathcal{U} < 0, \omega > 0$:

Flat models with $\omega > 0$ exhibit a power-law bounce $a(t) \sim a_0(1 + \frac{\omega}{2}t^2)$ around $t = 0$, and later undergoes coasting $a(t) \sim t$.

(ii) $k = -1, \rho = 0, \omega > 0$:

Open models that have $\mathcal{K}_0 = \omega^2, \rho = \dot{\phi} = V(\phi) = 0$, and provided that $\mathcal{U}_0 < \frac{\lambda}{2}\omega$ for $\omega > 0$, have identical causal structure as (i).

(iii) $k = -1, \mathcal{U} > 0, \omega < 0$:

Open models with *positive* non - local energy density start off at a singularity and recollapse after a time $2/\sqrt{-\omega}$ provided that ω is negative and $a_0 > \sqrt{\frac{6}{\lambda}}$.

(iv) $k = +1, \mathcal{U} = 0, \omega < 0$:

Closed models that have $\omega = -(a_0^2 + \frac{\lambda}{3}) + \frac{\sqrt{6\lambda}}{3}\sqrt{a_0^4 + \frac{\lambda}{6}} < 0$ also recollapse.

7.4 Flat Braneworlds with desired inflaton self - interaction

We now demonstrate how the superpotential formalism developed by Feinstein [59] and introduced in a more subtle way via the Hamilton - Jacobi equations in [96] also yield solutions to the braneworld field equations starting from the general ansatz $\Theta = \Theta(\phi)$. The first step is to ensure that the Reality Conditions (7.3.4) and (7.3.5) are met for any value of \mathcal{K} . We then derive a system of non - linear differential equations variable in ϕ , that are equivalent to the Einstein field equations (7.2.9) - (7.2.11). This system is solved for the flat curvature case $\mathcal{K} = 0$, with the specific ansatz $\Theta = \theta_0 e^{m\phi}$ ($\theta_0 = 0 = \dot{m}$). In this way we recover the asymptotic power - law inflationary solution in the limit $\lambda \rightarrow \infty$, or alternatively, for $m\phi \ll 0$.

7.4.1 The Braneworld Superpotential

The superpotential ansatz is

$$\Theta \equiv \Theta(\phi)$$

in terms of the scalar field ϕ . We start again with Δ defined by equation (7.3.11):

$$\Delta^2 := 1 + \frac{2}{\lambda} \left(\frac{1}{3}\Theta^2 + 3\mathcal{K} - \frac{6}{\lambda}\mathcal{U} \right), \quad (7.4.1)$$

then the local energy density is give by

$$\rho = \lambda(\Delta - 1), \quad (7.4.2)$$

and therefore the kinetic energy of the scalar field $\psi = \dot{\phi}$ is a solution of the quadratic equation ⁵

$$\Delta\psi^2 + \frac{2}{3}\Theta'\psi + \frac{8}{\lambda}\mathcal{U} - 2\mathcal{K} = 0, \quad (7.4.3)$$

which yields two solutions for ψ . Together with energy conservation (7.2.7)

$$\rho' + \Theta\psi = 0, \quad (7.4.4)$$

one can obtain solutions for $\rho(\phi)$ and then for $\phi(t)$. The solutions to equations (7.4.3) and (7.4.4) are real for

$$\frac{1}{9}\Theta'^2 + \Delta(2\mathcal{K} - \frac{8}{\lambda}\mathcal{U}) \geq 0, \quad (7.4.5)$$

$$\frac{1}{3}\Theta^2 + 3\mathcal{K} - \frac{6}{\lambda}\mathcal{U} \geq 0 \quad (7.4.6)$$

the first of which corresponds to the Reality Condition, while the second ensures that the RHS of equation (7.4.2), and therefore ρ , is positive. The non-linear differential equations for the scale factor $e^{\alpha(\phi)}$ is

$$a'(\phi) = \frac{\Theta}{3\psi_{\pm}} a(\phi), \quad (7.4.7)$$

with the temporal equation

$$t' := \frac{1}{\psi_{\pm}}. \quad (7.4.8)$$

The non-local energy density and the curvature are then readily obtained.

7.4.2 Power-law inflation

For flat curvature the Reality Condition (7.4.5) and condition (7.4.6) are trivially satisfied. In the absence of *dark radiation*, equation (7.4.3) reduces to

$$\left(1 + \frac{1}{\lambda}\rho\right)\psi^2 + \frac{2}{3}\Theta'\psi = 0. \quad (7.4.9)$$

⁵prime (') denotes differentiation with respect to ϕ .

Now if $\psi = 0$, we recover the *de Sitter* solutions of section (7.3.3) provided that $\rho = \text{constant} > 0$. For $\psi \neq 0$, equation (7.4.9) together with (7.4.4), leads to the system

$$\begin{aligned}\dot{\phi} &= \frac{-2\Theta'}{3\left(1 + \frac{1}{\lambda}\rho\right)}, \\ \rho' &= -\Theta\psi.\end{aligned}\quad (7.4.10)$$

If we assume that

$$\Theta = \theta_0 e^{m\phi} \quad (7.4.11)$$

for constants θ_0 and m , the local energy density

$$\rho = \lambda \left(\sqrt{1 + \frac{2\theta_0^2}{3\lambda} e^{2m\phi}} - 1 \right), \quad (7.4.12)$$

and (7.4.10) integrates to give

$$\begin{aligned}\frac{2m^2\theta_0}{3}t &= \sqrt{\frac{2\theta_0^2}{3\lambda} + e^{-2m\phi}} - \frac{2\theta_0}{\sqrt{6\lambda}}m\phi \\ &- \frac{2\theta_0}{\sqrt{6\lambda}} \ln \left[\frac{2\theta_0}{\sqrt{6\lambda}} + \sqrt{\frac{2\theta_0^2}{3\lambda} + e^{-2m\phi}} \right].\end{aligned}\quad (7.4.13)$$

This asymptotes to $e^{-m\phi}$ for $m\phi \ll 0$. Alternatively, we recover the General Relativity result (see [155]) in the limit $\lambda \rightarrow \infty$. This asymptotic solution implies that $\Theta \sim \frac{3}{2m^2 t}$, which in turn means that

$$a(t) \sim t^{1/2m^2} \quad (7.4.14)$$

i.e., the model exhibits power-law inflation for $m^2 < \frac{1}{2}$.

The potential is then obtained using

$$V(\phi) = \rho - \frac{1}{2}\dot{\phi}^2 \quad (7.4.15)$$

together with equation (7.4.10) and has the form

$$\begin{aligned}V(\phi) &= \lambda \left[\sqrt{1 + \frac{2\theta_0^2}{3\lambda} e^{2m\phi}} - 1 \right] \\ &- \frac{2}{9}m^2\theta_0^2 e^{2m\phi} \left(1 + \frac{2\theta_0^2}{3\lambda} e^{2m\phi} \right)^{-1}\end{aligned}\quad (7.4.16)$$

which asymptotes to $V \sim \frac{3-2m^2}{9}\theta_0^2 e^{2m\phi}$ during power-law inflation.

7.5 Conclusion

In conclusion, we have presented two codes for solving the braneworld generalizations of the FRW equations for a single classical non-minimally coupled scalar field which is confined to the brane, embedded in five dimensional Einstein gravity. The first approach, which mirrors the one followed by Madsen and Ellis [155], does not assume any slow rolling approximation however breaks down when the field oscillates about the minimum of the potential well. The second approach extends recent work by Feinstein [59] where a superpotential method, inspired by studies in supergravity, is used to generate standard inflationary solutions.

These codes are utilized in a number of simple examples, including the Braneworld analogue of de-Sitter exponential inflation and power-law inflation. All our solutions reduce to the standard result in the appropriate limit.

Chapter 8

Bounce Behaviour in Kantowski-Sachs and Bianchi Cosmologies

8.1 Introduction

Already in the 1930's, Tolman [226] proposed that closed ($k = +1$) FL universe models might re-expand after collapsing towards a high density state in the future; it was already known then that this was not possible for $k = 0$ and $k = -1$ models. This idea of a *phoenix universe* has remained popular (see Dicke and Peebles [39] for a discussion), and has re-appeared recently in new forms, for example specifically in Smolin's idea of collapse to a black hole state resulting in re-expansion into a new expanding universe region [211] and more recently Easson and Brandenberger [44] have discussed the general features all such scenarios have in common. Thus it is interesting to investigate under what conditions such a bounce might take place within the context of General Relativity.

Essentially because of the Raychaudhuri equation [191, 45, 47], such bounces are not possible in FL models if the active gravitational mass is positive: that is, if $\rho + 3p > 0$. On the other hand quantum fields and indeed classical scalar fields can violate this condition [92] - indeed that is the major discovery underlying the concept of inflationary universe models. Hence such fields can in principle allow bounce behaviour in FL models. However

there are still other conditions that must be satisfied by such fields, for example the *reality condition* $\dot{\phi}^2 \geq 0$ which is equivalent to requiring that the inertial mass density $\rho + p \geq 0$ (if this is not true, very anomalous physical behaviour can occur). Thus it is interesting to see when bounces can occur without violating such conditions.

Models with $\dot{\phi}^2 \leq 0$ are gaining popularity, and is known as **Phantom Matter** See for instance [18], where it is shown that a simple analysis of CM anisotropies and large scale structure arguably favour such models. We stress that consistency with the reality condition nevertheless remains a good criterion for ruling out strange models.

It is not only FL models that are of interest. The geometry of the universe at a bounce might be very different than the completely isotropic and spatially homogeneous Robertson-Walker (RW) spacetimes; indeed because some spatially homogeneous modes are unstable [235], some more general geometry might be expected. Thus it is interesting to examine also what happens in models such as Bianchi models which are anisotropic and spatially homogenous, in order to start exploring the full phase-space of possibilities. Additionally, in the scenario of black hole collapse and subsequent re-expansion, we might expect the geometry at the bounce to be that of a Kantowski-Sachs $k = +1$ model [115, 48], because this model has the same symmetries as the spatially homogeneous interior region of the extended (vacuum) Kruskal solution that represents the late stage of evolution of an isotropic black hole when the matter can be neglected. We may indeed expect that at late stages of collapse such a vacuum approximation will be valid, because in many Bianchi universes anisotropy dynamically dominates over matter at early and late times [235].

For these reasons we are interested in the bounce behaviour not only of FL models but also of Bianchi and Kantowski-Sachs universes. (In Appendix D we present a complete classification of Bianchi types A and B.) In this chapter, we prove a number of relevant results. Specifically, bounce behaviour in LRS Bianchi types I (BI) and III (BIII) or Kantowski-Sachs (KS) models with scalar fields violate the reality condition $\dot{\phi}^2 = \rho + p \geq 0$ (we assume that the energy flux and anisotropic pressure vanish: $\pi_{\mu\nu} = 0 = q_\mu$ which follows for fields observed relative to the normal congruence of curves). For scalar field models with arbitrary self-interaction we prove a *no-bounce* theorem to this effect, viz. *bounce behaviour in LRS BI, BIII or KS models violates the reality condition*¹.

¹It has been known for some time that flat and open FLRW scalar field models do not admit bounce solutions [155].

We then present additional results that restrict bounce behaviour in other spatially homogeneous models to closed FLRW and Bianchi type IX. Open FLRW and all (untilted) spatially homogeneous models all violate the weak energy condition $\rho \geq 0$ and $\rho + p \geq 0$ at the time of a bounce. The strong energy condition is violated in all such models, including flat FLRW models. The reality condition and the null energy condition are violated in all spatially homogeneous models with the exception of Bianchi type IX and closed FLRW models.

Finally we turn our attention to the braneworld scenario of Randall and Sundrum [189]. For a Kantowski-Sachs, BI or BIII metric confined to a single three-brane embedded in a five-dimensional bulk, a non-local anisotropic pressure and negative non-local energy density (e.g. *dark radiation*) projected from the bulk onto the brane via the bulk Weyl tensor modifies the Einstein field equations sufficiently for bounce behaviour to be consistent with the reality condition.

Efforts to solve the standard cosmological puzzles such as that of flatness, homogeneity and monopole excess via ekpyrotic models [220] in the braneworld context as potential alternatives to inflation are plagued by difficulties. A more recent discussion by Martin *et al*[161] considered bounce behaviour in ekpyrotic models, but that is not directly related to the aims of this chapter.

8.2 The Key Equations

In this section we set up the equations needed to investigate whether or not the dynamics of LRS BI, BIII and KS models admit bounce behaviour in the presence of a classical non-minimally coupled scalar field ϕ with a self-interaction potential $V(\phi)$. The metric tensor for these models can be written in the following form:

$$ds^2 = -dt^2 + X(t)^2 dr^2 + Y(t)^2 (d\theta^2 + S^2(\theta) d\phi^2), \quad (8.2.1)$$

where

$$S(\theta) = \begin{cases} \sin \theta & \text{for } k = +1, \\ \theta & \text{for } k = 0, \\ \sinh \theta & \text{for } k = -1, \end{cases} \quad (8.2.2)$$

$X(t)$ and $Y(t)$ are the expansion scale factors and we have chosen standard units where $8\pi G = c = 1$.

Relative to a normal congruence of curves with tangent vector u^μ , the energy - momentum tensor $T_{\mu\nu}$ for a scalar field takes the form of a perfect fluid (See [235] page 17 for details):

$$T_{\mu\nu} = \rho u_\mu u_\nu + p h_{\mu\nu}, \quad (8.2.3)$$

with

$$\rho = \frac{1}{2}\dot{\phi}^2 + V(\phi) \quad (8.2.4)$$

and

$$p = \frac{1}{2}\dot{\phi}^2 - V(\phi). \quad (8.2.5)$$

It is easy to show that for the above metric and choice of u^μ , the Einstein Field equations can be written in terms of propagation equations for the usual expansion Θ , shear $\sigma^2 = \frac{1}{2}\sigma^{\mu\nu}\sigma_{\mu\nu}$ and 3-curvature ${}^{(3)}R$ scalars:

$$\dot{\Theta} + \frac{1}{3}\Theta^2 + 2\sigma^2 + \dot{\phi}^2 - V(\phi) = 0 \quad (8.2.6)$$

$$\dot{\sigma} + \Theta\sigma - \frac{1}{2\sqrt{3}}{}^{(3)}R = 0 \quad (8.2.7)$$

$${}^{(3)}\dot{R} + \frac{2}{3}\Theta{}^{(3)}R - \frac{2}{\sqrt{3}}{}^{(3)}R\sigma = 0, \quad (8.2.8)$$

and the Gauss - Codazzi constraint

$${}^{(3)}R = \dot{\phi}^2 + 2V(\phi) + 2\sigma^2 - \frac{2}{3}\Theta^2, \quad (8.2.9)$$

where

$$\Theta = \frac{\dot{X}}{X} + \frac{2\dot{Y}}{Y}, \quad \sigma = \frac{1}{\sqrt{3}}\left(\frac{\dot{X}}{X} - \frac{\dot{Y}}{Y}\right), \quad {}^{(3)}R = \frac{2k}{Y^2}, \quad (8.2.10)$$

and k is a constant taking the values $k = 0, -1, +1$ for BI, BIII and KS models respectively.

The above set of equations together with the Klein - Gordon equation

$$\ddot{\phi} + \Theta\dot{\phi} + \frac{\partial V}{\partial\phi} = 0 \quad (8.2.11)$$

give a complete description of the dynamics of these universe models and solutions may be obtained once $V(\phi)$ has been specified. The expansion may also be expressed in terms of a volume scale factor $a(t)$, viz. $\Theta = \frac{3\dot{a}}{a}$.

It is worth mentioning that there is an alternate route to finding solutions by noticing that equations (8.2.6) and (8.2.9) can be combined to give expressions for the potential and momentum density of the scalar field:

$$V(\phi) = \frac{1}{3}(\dot{\Theta} + \Theta^2 + {}^{(3)}R), \quad (8.2.12)$$

$$\dot{\phi}^2 = -\frac{2}{3}\dot{\Theta} - 2\sigma^2 + \frac{1}{3}{}^{(3)}R, \quad (8.2.13)$$

so that in principle $V(\phi)$ can be determined by first specifying the scale factor dependence $X(t)$ and $Y(t)$ and then running the field equations backwards to determine the potential. This method has been used to generate exact FLRW inflationary solutions [155].

The aim here is not to attempt to find exact solutions but examine whether it is possible to find solutions that exhibit bounce behaviour subject to the reality condition: $\dot{\phi}^2 \geq 0$. Hence we need a precise definition of what a bounce is, together with a careful examination of equation (8.2.13). This is discussed in the next section.

8.3 The No-bounce theorem in BI, BIII and KS models

8.3.1 Definition of a Bounce

Defining the expansion parameters

$$x = \dot{X}/X, \quad y = \dot{Y}/Y, \quad (8.3.1)$$

a bounce in X occurs at time $t = t_0$ iff $x(t_0) = 0$ and $\dot{x}(t_0) > 0$ while a bounce in Y occurs at time $t = t_1$ iff $y(t_1) = 0$ and $\dot{y}(t_1) > 0$. It is clear that although it may be possible to have a bounce in one of the scale factors but not the other, this does not lead to a new expanding universe region. We therefore require that a bounce occurs both in X and Y scale-factors, even though they may in general occur at different times.

8.3.2 The reality condition at a bounce

Let us now determine whether the reality condition for the scalar field is satisfied at a bounce. In order to do this we need to write equation (8.2.13) in terms of x and y and their derivatives. This is most easily done by first substituting for the spatial curvature

${}^{(3)}R$ using equation (8.2.7):

$$\dot{\phi}^2 = -\frac{2}{3}\dot{\Theta} - 2\sigma^2 + \frac{2}{\sqrt{3}}\dot{\sigma} + \frac{2}{\sqrt{3}}\Theta\sigma. \quad (8.3.2)$$

Now using

$$\sigma = \frac{1}{\sqrt{3}}(x - y), \quad \Theta = x + 2y, \quad (8.3.3)$$

we obtain

$$\dot{\phi}^2 = -2(\dot{y} + y^2 - xy). \quad (8.3.4)$$

We can now state and prove the main result of this section².

Theorem: In the absence of anisotropic pressure and energy flux ($\pi_{\mu\nu} = 0 = q_{\mu}$), bounce behavior in LRS Bianchi type I, III and Kantowski-Sachs models dominated by a scalar field is not permitted unless the reality condition $\dot{\phi}^2 \geq 0$ is violated.

Proof: The proof follows immediately from equation (8.3.4) when evaluated for a bounce in the Y direction at time $t = t_1$. In this case $y(t_1) = 0$ and $\dot{y}(t_1) > 0$ so (8.3.4) simplifies to give $\dot{\phi}(t_1)^2 = -2\dot{y}(t_1) < 0$, so that even if a bounce occurs in the X direction it is only possible in the Y direction if the reality condition is violated.

8.4 No bounce behaviour in other Bianchi models

We now examine the extent to which energy conditions preclude bounce behaviour in isotropic, spatially homogeneous Bianchi models of class A and B. We refer the reader to Wainwright and Ellis [235] for an interesting review and classification of Bianchi type universes. Wald's no-hair theorem for global anisotropy can be found in [236].

Not all Bianchi type models isotropize at large times. Specifically, those types which do not admit FLRW solutions become highly anisotropic[29]. Models that do admit FLRW solutions; Bianchi I and VII_0 admits $k=0$ solutions, Bianchi V and VII_h admits $k = -1$ solutions, and Bianchi IX admits $k = +1$ solutions. Type VII_h will in general *not* approach isotropy, while the type IX models will recollapse after a finite time.

²It has been brought to our attention that Toporensky and Ustiansky [227] has given an almost identical proof in the appendix to their paper.

From the outset it is clear that bounce behaviour in the volume scale factor $a(t)$ violates the Strong Energy Condition. This can be seen from the Raychaudhuri equation for spatially homogeneous cosmologies

$$\dot{\Theta} + \frac{1}{3}\Theta^2 + 2\sigma^2 = -\frac{1}{2}(\rho + 3p) \quad (8.4.1)$$

which simplifies to

$$-\frac{1}{2}(\rho + 3p) = \dot{\Theta}(t_0) + 2\sigma^2(t_0) > 0 \quad (8.4.2)$$

since $\Theta = 0$ at the bounce in the volume scale factor, and positivity results from σ^2 being non-negative and the requirement that $\dot{\Theta} > 0$ at the bounce. Hence

$$\rho + 3p < 0,$$

violating SEC at the bounce.

In addition to this, bounce behaviour in spatially homogeneous models with negative spatial curvature ${}^{(3)}R$ violates the Weak Energy Condition $\rho \geq 0$ and $\rho + p \geq 0$. To show this we use the Friedmann constraint for spatially homogeneous cosmologies³

$$\rho + \sigma^2 = \frac{1}{3}\Theta^2 + \frac{1}{2}{}^{(3)}R \quad (8.4.3)$$

which simplifies to

$$\rho + \sigma^2 = \frac{1}{2}{}^{(3)}R < 0$$

at the bounce, implying that $\rho < 0$, since σ^2 is non-negative. This violates WEC in class A types II, VI_0 , VII_0 (except for a very special case) and VIII. Bounce behaviour can be obtained in type IX, which can have positive curvature. In class B, the spatial curvature is negative for all models, hence the WEC is violated in all of class B.

Finally, spatially homogeneous cosmologies satisfy the Reality Condition $\dot{\phi}^2 = \rho + p \geq 0$ provided that

$$\dot{\phi}^2 = \frac{1}{3}{}^{(3)}R - \frac{2}{3}\dot{\Theta} - 2\sigma^2 \geq 0. \quad (8.4.4)$$

This constraint is obtained by subtracting equations (8.4.1) and (8.4.3), and then rearranging terms. Bounce behaviour implies that $\frac{2}{3}\dot{\Theta} + 2\sigma^2 > 0$, since the shear σ^2 is

³See Wainwright and Ellis [235].

non-negative. Hence we can write condition (8.4.4) in a somewhat weaker form, viz. *Models satisfying RC necessarily have ${}^{(3)}R > 0$* . Therefore, spatially homogeneous cosmologies with ${}^{(3)}R \leq 0$ violate RC. This does not mean models with positive spatial curvature necessarily satisfy RC, since they have to meet the stronger condition (8.4.4), in cases where the shear is non-vanishing at the time of the bounce. However, for isotropic models, it is necessary and sufficient that the spatial curvature is positive.

Bianchi class A types II, VI_0 and VIII all have negative spatial curvature, and for type I it is zero. Type VII_0 is negative or zero. Hence all these cases violate the RC, by virtue of the above argument. Type IX violates RC for cases in which the spatial curvature is negative or zero.

In class B, since types IV, V, VI_h and VII_h have negative spatial curvature. Bianchi III is the special case of $h = -1$ in Bianchi VI_h , and the *exceptional* case Bianchi $VI_{-1/9}^*$ has $h = -1/9$. They all violate RC.

8.5 Bounce behaviour on a Kantowski-Sachs brane

Recent ideas in string and M-theory [100, 210, 145] have led to the notion that gravity could be a higher dimensional theory, that becomes 4-dimensional at low energies. In the Randall-Sundrum scenario [189] gravity can be localized on a 3-brane while a fifth dimension may remain noncompact. Observers are bound to a brane, which may have a more general metric than the induced Minkowski metric that Randall and Sundrum [189] assumed. A covariant geometric approach was first given by Shiromizu, Maeda and Sasaki [210] and also by Maartens [147]. We shall assume that a scalar field ϕ is bound to the brane, and that higher-dimensional modifications of the standard Einstein field equations are imprinted via (i) local quadratic energy-momentum corrections that arise from the extrinsic curvature, and (ii) non-local effects from the free gravitational field in the bulk, transmitted via a projection of the bulk Weyl tensor onto the brane [147].

In five dimensions, the field equations [189, 147] are Einstein's equations, with a (negative) bulk cosmological constant $\tilde{\Lambda}$ and the brane energy-momentum providing the source:

$$\tilde{G}_{AB} = \tilde{\kappa}^2 \left[-\tilde{\Lambda} \tilde{g}_{AB} + \delta(\chi) \{-\lambda g_{AB} + T_{AB}\} \right]. \quad (8.5.1)$$

The tildes denote the bulk (5-dimensional) generalization of standard general relativity quantities, and $\tilde{\kappa}^2 = 8\pi/\tilde{M}_p^3$, where \tilde{M}_p is the fundamental 5-dimensional Planck mass, which is typically much less than the effective Planck mass on the brane, $M_p = 1.2 \times 10^{19}$ GeV. The brane is given by $\chi = 0$, so that a natural choice of coordinates is $x^A = (x^\mu, \chi)$, where $x^\mu = (t, x^i)$ are spacetime coordinates on the brane. The brane tension is λ , and $g_{AB} = \tilde{g}_{AB} - n_A n_B$ is the induced metric on the brane, with n_A the spacelike unit normal to the brane. Matter fields confined to the brane make up the brane energy-momentum tensor T_{AB} (with $T_{AB}n^B = 0$).

The modification to the standard Einstein equations[147], with the new terms carrying bulk effects onto the brane are⁴

$$G_{\mu\nu} = -\Lambda g_{\mu\nu} + T_{\mu\nu} + \tilde{\kappa}^4 S_{\mu\nu} - \mathcal{E}_{\mu\nu}. \quad (8.5.2)$$

If $\lambda = \frac{6}{\tilde{\kappa}^4}$, then the energy scales are related as follow:

$$\Lambda = \frac{1}{2}\tilde{\kappa}^2 \left(\tilde{\Lambda} + \frac{1}{6}\tilde{\kappa}^2 \lambda^2 \right).$$

The tensor $S_{\mu\nu}$ represents local quadratic energy-momentum corrections of the matter fields, and the $\mathcal{E}_{\mu\nu}$ is the projected bulk Weyl tensor transmitting non-local gravitational degrees of freedom from the bulk to the brane. All the bulk corrections may be consolidated into effective total energy density ρ^{tot} , pressure p^{tot} , anisotropic stress $\pi_{\mu\nu}^{tot}$ and energy flux q_μ^{tot} . The modified Einstein equations take the standard Einstein form with a redefined energy-momentum tensor:

$$G_{\mu\nu} = -\Lambda g_{\mu\nu} + T_{\mu\nu}^{tot}, \quad (8.5.3)$$

where

$$T_{\mu\nu}^{tot} = T_{\mu\nu} + \tilde{\kappa}^4 S_{\mu\nu} - \mathcal{E}_{\mu\nu}. \quad (8.5.4)$$

8.5.1 Matter description on the Kantowski-Sachs brane

For a homogeneous scalar field $\phi(t)$ on the brane has an energy-momentum tensor given by equations (8.2.3)–(8.2.5), and in the absence of local anisotropic pressure and energy flux

⁴Note that we set $\kappa^2 = 8\pi G = c = 1$

$\pi_{\mu\nu} = 0 = q_\mu$, effective total energy-momentum tensor has

$$\rho^{\text{tot}} = \rho + \frac{\rho^2}{2\lambda} + \frac{6U}{\lambda}, \quad (8.5.5)$$

$$p^{\text{tot}} = p + \rho\left(p + \frac{\rho}{2\lambda}\right) + \frac{2U}{\lambda} \quad (8.5.6)$$

with a non-local energy density $U = -\frac{6}{\lambda}\mathcal{E}_{\mu\nu}u^\mu u^\nu$. A thorough analysis of the dynamics of FLRW, Bianchi I and V obeying a barotropic equation of state on the brane was done by Campos and Sopuerta [19]. A Kantowski-Sachs brane is characterized by vanishing acceleration, vorticity and non-local energy flux (similar to that for a Bianchi I brane, but with positive 3-curvature; see for instance [147, 149])

$$A_\mu = \omega_\mu = \mathcal{Q}_\mu = 0, \quad (8.5.7)$$

hence the total energy flux vanishes

$$q_\mu^{\text{tot}} = 0. \quad (8.5.8)$$

However, the anisotropic stress does not necessarily vanish:

$$\pi_{\mu\nu}^{\text{tot}} = \frac{6}{\lambda}\mathcal{P}_{\mu\nu}.$$

Here $\mathcal{P}_{\mu\nu} = -\frac{6}{\lambda}(h_\mu^\alpha h_\nu^\beta - \frac{1}{3}h^{\alpha\beta}h_{\mu\nu})\mathcal{E}_{\alpha\beta}$. There is no evolution equation for $\mathcal{P}_{\mu\nu}$ on the brane, since the non-local anisotropic stress carry bulk degrees of freedom that cannot be determined by brane observers. In general, the projection of the five-dimensional field equations onto the brane, together with the Z_2 symmetry, does not lead to a closed system. The standard conservation equation of general relativity holds on the brane, together with a simplified propagation equation for the non-local energy density U [147, 149]

$$\dot{\rho} + \Theta(\rho + p) = 0, \quad (8.5.9)$$

$$\dot{U} + \frac{4}{3}\Theta U + \sigma_{\mu\nu}\mathcal{P}^{\mu\nu} = 0, \quad (8.5.10)$$

where Θ is the expansion parameter. Both U and $\mathcal{P}_{\mu\nu}$ are homogeneous on the brane.

8.5.2 Gravitational Equations

The Einstein Field equations (8.2.6)-(8.2.9) of Section 8.2 are modified:

$$\dot{\Theta} + \frac{1}{3}\Theta^2 + 2\sigma^2 + \frac{1}{2}(\rho + 3p) = -\frac{1}{2\lambda}\rho(2\rho + 3p) - \frac{6U}{\lambda}, \quad (8.5.11)$$

$$\dot{\sigma} + \Theta\sigma - \frac{1}{2\sqrt{3}}{}^{(3)}R = \frac{3}{\lambda} \frac{\sigma_{\mu\nu}\mathcal{P}^{\mu\nu}}{\sigma}, \quad (8.5.12)$$

$${}^{(3)}\dot{R} + \frac{2}{3}\Theta{}^{(3)}R - \frac{2}{\sqrt{3}}{}^{(3)}R\sigma = 0, \quad (8.5.13)$$

$$\frac{1}{3}\Theta^2 + \frac{1}{2}{}^{(3)}R - \sigma^2 = \rho \left(1 + \frac{\rho}{2\lambda}\right) + \frac{6U}{\lambda}. \quad (8.5.14)$$

The effects of embedding the free gravitational field in the five-dimensional bulk are represented by the correction terms to the energy-momentum tensor $T_{\mu\nu}$, as expressed in equations (8.5.11), (8.5.12) and (8.5.14).

8.5.3 Feasible Bounce Behaviour

If we subtract equation (8.5.14) from $2 \times$ equation (8.5.11):

$$\left(1 + \frac{\rho}{\lambda}\right)(\rho + p) = \frac{1}{3}{}^{(3)}R - \frac{2}{3}\dot{\Theta} - 2\sigma^2 - \frac{8U}{\lambda}$$

then substitute ${}^{(3)}R$ using equation (8.5.12), together with new variables x and y given by equations (8.3.3), to obtain

$$\left(1 + \frac{\rho}{\lambda}\right)(\rho + p) = -2(\dot{y} + y^2 - xy) - \frac{8U}{\lambda} + \frac{2\sqrt{3}}{\lambda} \frac{\sigma_{\mu\nu}\mathcal{P}^{\mu\nu}}{\sigma}. \quad (8.5.15)$$

The quantity $\frac{2\sqrt{3}}{\lambda}\sigma_{\mu\nu}\mathcal{P}^{\mu\nu}/\sigma$ is generally non-zero. We then assume the induced metric for the brane is given by equations (8.2.1) and (8.2.2), which apply to Kantowski-Sachs, Bianchi I or III models. (The bulk metric for a Kantowski-Sachs or Bianchi braneworld is not known [149].) It is evident that a bounce in Y (see the definition in Section (8.3.1)) becomes feasible by virtue of (i) the anisotropic pressure contracted with shear term, or (ii) in the absence of this contraction⁵, provided the energy density is sufficiently negative.

The bounce in X is readily achieved, provided that non-local contributions are of such

⁵In that case the non-local energy propagates as *dark radiation* $U = U_0(a/a_0)^{-4} < 0$.

a nature that

$$\begin{aligned}
 \dot{x} &= -(x+2y)x + \frac{1}{2}\left(\rho - p - \frac{\rho p}{\lambda}\right) + \frac{2U}{\lambda} + \frac{2\sqrt{3}}{\lambda} \frac{\sigma_{\mu\nu}\mathcal{P}^{\mu\nu}}{\sigma} \\
 &= \frac{1}{2}\left(\rho - p - \frac{\rho p}{\lambda}\right) + \frac{2U}{\lambda} + \frac{2\sqrt{3}}{\lambda} \frac{\sigma_{\mu\nu}\mathcal{P}^{\mu\nu}}{\sigma} \\
 &> 0
 \end{aligned} \tag{8.5.16}$$

at the bounce.

8.5.4 Illustration

In the case of a bare cosmological constant $\Lambda > 0$ with $\sigma_{\mu\nu}\mathcal{P}^{\mu\nu} = 0$, the reality condition is marginally satisfied, since $\rho + p = 0$. We shall assume that the non-local anisotropic pressure contracted with the shear vanishes $\sigma_{\mu\nu}\mathcal{P}^{\mu\nu} = 0$. From equation (8.5.15)

$$\dot{y} + y^2 - xy = -\frac{4U}{\lambda}. \tag{8.5.17}$$

A bounce in scale factor Y occurs at $y = 0$, $\dot{y} > 0$, then equation (8.5.17) implies that

$$\frac{U}{\lambda} < 0. \tag{8.5.18}$$

Equation (8.5.16) gives

$$\dot{x} + x^2 + 2xy = \Lambda + \frac{2U}{\lambda} \tag{8.5.19}$$

and since a bounce in X occurs at $x = 0$, $\dot{x} > 0$, we have

$$-\frac{\Lambda}{2} < \frac{U}{\lambda} < 0. \tag{8.5.20}$$

This corresponds with the result of Santos *et al* [149] where it is shown that Bianchi branes are *stable* in this regime, but unstable if $\frac{U}{\lambda} < -\frac{\Lambda}{2}$. However, a bouncing Kantowski Sachs brane requires a stronger constraint. This is seen by casting equation (8.5.14) as

$$\frac{1}{2}{}^{(3)}R = -(2x+y)y + \Lambda + \frac{6U}{\lambda}. \tag{8.5.21}$$

Hence a bounce in Y also means that $\frac{1}{2}{}^{(3)}R = \Lambda + \frac{6U}{\lambda}$, and since the 3-curvature is positive, $\frac{U}{\lambda} > -\frac{\Lambda}{6}$. The KS brane bounce therefore constrains the non-local energy density to

$$-\frac{\Lambda}{6} < \frac{U}{\lambda} < 0. \tag{8.5.22}$$

8.5.5 Phase Portrait

In the Friedmann equation (8.5.14), define the non-negative quantity

$$D^2 = \frac{1}{9}\Theta^2 + \frac{1}{6}{}^{(3)}R - \frac{2U}{\lambda} = \frac{1}{3}\sigma^2 + \frac{1}{3}\Lambda \quad (8.5.23)$$

and employ this to redefine variables

$$Q^2 = \frac{\Theta^2}{9D^2}, \quad \Sigma^2 = \frac{\sigma^2}{3D^2}, \quad \tau = Dt. \quad (8.5.24)$$

Clearly $Q, \Sigma \in [-1, 1]$. There are three non-negative density parameters

$$\Omega_u := -\frac{2U}{\lambda D^2}, \quad \Omega_\Lambda := \frac{\lambda}{3D^2}, \quad \Omega_k = \frac{{}^{(3)}R}{6D^2} \quad (8.5.25)$$

with the property that $\Omega_u, \Omega_\Lambda, \Omega_k \in [0, 1]$. The Friedmann constraint (8.5.23) separates into two equations

$$\Sigma^2 + \Omega_\Lambda = 1, \quad Q^2 + \Omega_u + \Omega_k = 1 \quad (8.5.26)$$

hence the state space is compact [79, 235]. If we use the deceleration parameter

$$q := -\frac{3}{\Theta^2}(\dot{\Theta} + \frac{1}{3}\Theta^2) \quad (8.5.27)$$

then the Raychaudhuri equation (8.5.11) becomes

$$qQ^2 = 2\Sigma^2 - \Omega_u - \Omega_\Lambda. \quad (8.5.28)$$

The non-local energy density equation (8.5.10), the shear and curvature evolution equations (8.5.12) and (8.5.13), together with (8.5.26) and (8.5.27) yield a closed system of ode's

$$D' = (\Omega_k - 3Q\Sigma)\Sigma D \quad (8.5.29)$$

$$Q' = -(1+q)Q^2 - (\Omega_k - 3Q\Sigma)\Sigma Q \quad (8.5.30)$$

$$\Sigma' = (1 - \Sigma^2)(\Omega_k - 3Q\Sigma) \quad (8.5.31)$$

$$\Omega'_u = -2[2Q + (\Omega_k - 3Q\Sigma)\Sigma]\Omega_u \quad (8.5.32)$$

$$\Omega'_\Lambda = -2(1 - \Sigma^2)(\Omega_k - 3Q\Sigma)\Sigma \quad (8.5.33)$$

$$\Omega'_k = -2[Q - \Sigma + (\Omega_k - 3Q\Sigma)\Sigma]\Omega_k \quad (8.5.34)$$

Since D does not appear in equations (8.5.30)-(8.5.34) we shall omit equation (8.5.29) from the rest of the discussion. The state space is now 5-dimensional. After replacing q, Ω_k

and Ω_Λ from equations (8.5.26) and (8.5.28), the state space is reduced to three dimensions (Q, Σ, Ω_u) .

$$Q' = (1 - Q^2)(1 - Q\Sigma - 3\Sigma^2) + (1 + Q\Sigma)\Omega_u \quad (8.5.35)$$

$$\Sigma' = (1 - \Sigma^2)(1 - Q^2 - 3Q\Sigma - \Omega_u) \quad (8.5.36)$$

$$\Omega'_u = -2[2Q + (1 - Q^2 - 3Q\Sigma - \Omega_u)\Sigma] \Omega_u. \quad (8.5.37)$$

The boundaries $Q = \pm 1$ represent BI models with a cosmological constant, while the boundaries $\Sigma = \pm 1$ correspond to (vacuum) Kasner models in the invariant submanifold

$$\mathcal{R} = \{(Q, \Sigma, \Omega_u) : |Q| \leq 1, |\Sigma| \leq 1, \Omega_u = 0\}$$

that represents general relativity. Table 1 contains a listing of all critical points, their characterization and eigenvalues. The points $K_{\pm\pm}$ and $K_{\pm\mp}$ are Kasner metrics that form the vertices of \mathcal{R} . The critical points K_{++} and K_{+-} are *repellers*, while K_{--} and K_{-+} are *attractors*. de Sitter spacetime dS_+ is an *attractor* and dS_- (anti-de Sitter) is a *repeller* located on the respective boundaries $Q = 1$ and $Q = -1$ of the submanifold \mathcal{R} . There are two saddle points F_\pm located on the separatrix $y = Q - \Sigma = 0$ inside \mathcal{R} . The saddle points F_\pm have $\{{}^{(3)}R = 2\Lambda, \Theta = \sqrt{3}\sigma = \pm\sqrt{\Lambda}, U = 0\}$. From Figure 1 it is clear that no trajectory emerging from dS_- inside \mathcal{R} can reach dS_+ due to the separatrix $y = Q - \Sigma = 0$. In Figure 2 we demonstrate how the presence of non-local density parameter Ω_u alters the picture. The saddle points M_\pm represent static braneworld models with $\{{}^{(3)}R = 0, \Theta = 0, \sigma = \pm\sqrt{2\Lambda}, \frac{U}{\chi} = -\frac{\Lambda}{2}\}$. Since $\Omega_u = 1$ these models are located inside the greater state space

$$\mathcal{M} = \{(Q, \Sigma, \Omega_u) : |Q| \leq 1, |\Sigma| \leq 1, 0 \leq \Omega_u \leq 1\}$$

but outside \mathcal{R} . A trajectory emerging from dS_- may now *exit* \mathcal{R} and cross the plane $y = Q - \Sigma = 0$ (which is no longer a separatrix for $\Omega_u > 0$) as it evolves toward, and eventually away from the static model M_\pm , and enters dS_+ . Such a trajectory passes through $Q = 0$ and close to M_\pm , indicative of bounce behaviour in the volume scale factor a , since Q' remains positive.

Model	Coordinates	Eigenvalues
dS_{\pm}	$(\pm 1, 0, 0)$	$(\mp 2, \mp 3, \mp 4)$
$K_{\pm\pm}$	$(\pm 1, \pm 1, 0)$	$(\pm 2, \pm 6, \pm 6)$
$K_{\pm\mp}$	$(\pm 1, \mp 1, 0)$	$(\pm 2, \pm 2, \pm 6)$
F_{\pm}	$(\pm \frac{1}{2}, \pm \frac{1}{2}, 0)$	$(\pm \frac{3}{2}, \mp 2, \mp 3)$
M_{\pm}	$(0, \pm \sqrt{\frac{2}{3}}, 1)$	$(\pm 2\sqrt{\frac{2}{3}}, 2, -2)$

Starting at dS_- a trajectory passes through the plane $y = Q - \Sigma = 0$, with y changing sign from negative to 0 to positive, and through the plane $x = Q + 2\Sigma = 0$ with x changing sign from negative to 0 to positive. It terminates at the attractor dS_+ . Note that the bounce definition (8.3.1) requires the trajectory to cut both the x - and y -planes (the order may be reversed, depending on the path chosen), entering from the negative side of each plane, and exiting the positive side. If it passes through $(0, 0, \Omega_u)$ then the bounce in X and Y is synchronous, i.e. the shear σ and the expansion Θ both vanish there.

8.6 Conclusion

We have shown that LRS Bianchi type I, III and Kantowski-Sachs scalar field models that exhibit bounce behaviour violate the *reality condition* for the momentum density $\dot{\phi}^2 \geq 0$.

Thus Smolin's idea of collapse to a black hole state resulting in re-expansion into a new expanding universe region is not viable if the end-state of the universe after collapse into a black hole is described by a Kantowski-Sachs model, even in situations where the matter is dominated by a scalar field.

None of the LRS Bianchi models besides closed FLRW and B IX can support bounce behaviour without significant energy violations. We have analyzed this phenomenon in the Randall-Sundrum type braneworld scenario. There are non-local effects transmitted via the bulk Weyl tensor from the gravitational field in the bulk, onto the brane, that makes Kantowski-Sachs brane exhibit bounce behaviour, assuming that the such non-local effects required do indeed lead to a physical higher-dimensional bulk (an issue that still remains unresolved). A Kantowski-Sachs braneworld bounce requires *negative non-local energy density* if $\sigma_{\mu\nu}\mathcal{P}^{\mu\nu} = 0$, as demonstrated in section 8.5.

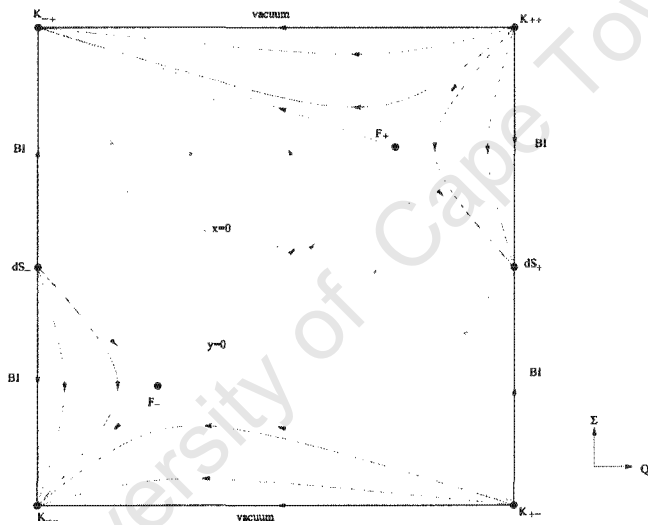


Figure 8.1: State space R is an invariant submanifold of M that represents general relativity for ${}^{(3)}R \geq 0$. The separatrix $y = Q - \Sigma = 0$ precludes bounce behaviour in Y from occurring.

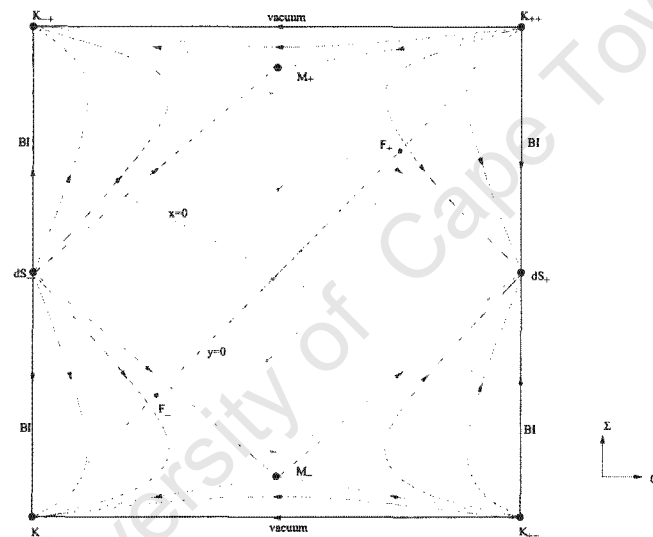


Figure 8.2: State space M no longer has a separatrix at $y = Q - \Sigma = 0$ for $\Omega_u > 0$. A *blue* trajectory that passes through the plane $x = Q + 2\Sigma = 0$ exhibits bounce heavier in X , and a bounce in Y when it passes through the plane $y = Q - \Sigma = 0$.

Part IV

**Higher Order Corrections to
Gravity**

Chapter 9

Introduction to Higher Derivative Cosmologies

9.1 Introduction

This is a short comment on the implications of generalizing the standard Einstein-Hilbert action commonly associated with improving Einstein Gravity to include semi-classical and/or quantum gravity effects to the lowest order. We review some of the more significant results obtained in recent years, with emphasis on correspondence with String theory, Supergravity and M-theory where-ever any such links may exist.

In addition to finding an Alternative Theory of Gravity that is possibly more accurate than Einstein Gravity, such a need has arisen due to various *no go theorems* surrounding the Singularity Problem in particular. For instance, bounce behaviour at the time of the Big Bang is predicated by various degrees of Energy density violations (especially the Null Energy Condition). The question arises: Is there a feasible theoretical framework from which a programme of Bounce Behaviour may be launched, that is regular in the vicinity of the bounce, and coherent with observations of the era preceding nucleosynthesis?

Various mechanisms may adhere to such a framework, and since almost all the calculations are done well below the Planck scale, it may be premature to single out a preferred mechanism or Cosmological Scenario. Needless to say there are various candidates such as Braneworlds as was illustrated in Chapter 8 and reference [157], and the Einstein frame

Pre-Big Bang Braneworlds by Stefano Foffa [61].

9.2 Higher Derivative Cosmology

Einstein's theory is the simplest geometrical theory of gravity based upon the equivalence principle and the general covariance of physical covariance of the physical laws. There is no reason why the gravitational Lagrangian ought to be linear, nor why other more complicated settings that are suitable generalizations of the Einstein-Hilbert action would not lead to more accurate theories. Moreover, Stelle [222] rigorously proved the renormalizability of the general fourth-order action

$$S = \int d^4x \sqrt{-g} (\alpha R^2 - \beta C^2 + \gamma L_{GB} + \delta \square R) \quad (9.2.1)$$

where C^2 denotes the contracted quadratic product of the Weyl tensor, L_{GB} the Gauss-Bonnet term (topological invariant), and the \square the d'Alembertian differential operator. Indeed, such alternative theories may provide the semi-classical of a quantum theory of gravity. The low-energy effective action of some versions of string theory, supergravity and M-theory contain such higher-derivative terms (see for instance [73] for reviews.)

We look at higher derivative cosmologies as an alternative, that may tame the curvature singularities of general relativity. Such singularity-free cosmological solutions were found in a general field theory of a scalar field coupled to gravity through a quadratic Gauss-Bonnet term $\xi(\phi)R_{GB}^2$, with the coupling function has the form $\xi(\phi) = \phi^n$, where n is a positive integer studied by Kanti *et al* [114]. In the presence of the quadratic Gauss-Bonnet term, for the dual case of even n , the set of solutions of the classical equations of motion in a curved FRW background includes singularity-free cosmological solutions. The singular solutions are shown to be confined in a part of the phase space of the theory allowing the non-singular solutions to fill the rest of the space.

The geometrical structure of any theory is intimately connected to the formalism, be it Lagrangian or Hamiltonian, and the variational principle from where the field equations originate. It is significant that alternative theories of gravity may non the less have possible interconnections between their respective solution spaces. The drawback of higher-order gravity theories are

- that the solutions of the classical theory are expected to have no lower energy bound and therefore exhibit instabilities, namely *runaway solutions* in the form of:
- negative energy modes (ghosts)
- and possibly tachyons [177].

There are, however, some significant *nonperturbative* results that offer remedy [11]. For instance, the *zero energy theorem* states that all exact solutions representing isolated, asymptotically flat systems have precisely zero energy, despite the existence of linearized solutions with negative energy.

According to the *Conformal Equivalence Theorem* of Barrow and Cotsakis [4, 30] any higher order system may be regarded as GR with additional fields in conformal space; if the Lagrangian is an analytic function $f(R)$ of the Ricci scalar curvature R , then a conformal transformation of the type

$$f(R) + T_m \quad \bar{g} = \Omega^2 g \quad \tilde{R} + T_\phi + \tilde{T}_m$$

$$\iff$$

where T_m contains the matter terms, and T_ϕ is the contribution of an effective scalar field ϕ . The new system has a symmetric hyperbolic form which is easier to analyze.

Conformal gravity is the purely quadratic theory based on an action that contains only a square of the Weyl curvature, the C^2 -term. It satisfies Birkhoff's theorem and nonperturbative effects can confine the ghosts [194]. The conformal fourth-order field equations [3] have regained popularity as a physically viable alternative theory of gravity that resolves some of the problems that GR alone is unable to address without ad hoc assumptions, eg. the dark matter hypothesis [159]. Unfortunately there are open problems that require further attention [121].

It is well known that more general gravity theories such as quadratic or scalar-tensor theories possess solutions exhibiting an inflationary phase. Such theories could also provide us with a more satisfactory mechanism to trigger inflation. If we were to relax the stringent symmetry requirement that the Universe is isotropic *ab initio*, then we enter the realm of spatially homogeneous and anisotropic models (such as the Kantowski-Sachs cosmology) in higher-order gravity. This would allow deeper investigation of specific issues such as the

asymptotic approach towards the initial singularity and the related genericness of oscillatory, chaotic dynamical regimes (see for instance [187]).

The search of brane-world cosmology (with AdS bulk) in higher order gravity presented in a paper by Nojiri and Odintsov [199], found the wide range of theory parameters where such cosmology may be realized. The quantum effects of conformal field theory living on the brane (via the corresponding conformal anomaly induced effective action) may qualitatively change the results of classical analysis. In the AdS/CFT correspondence, the addition of such CFT effective action (in some energy region) is naturally explained in terms of holographic renormalization group, and results in the possibility of quantum creation of inflationary brane Universe.

Meissner and Olechowski 2001 [111] consider a class of higher order corrections with arbitrary power n of the curvature tensor to the standard gravity action in arbitrary space-time dimension D . This class of corrections allows for domain wall solutions since, despite the presence of higher powers of the curvature tensor, the singularity structure at the wall is of the same type as in the standard gravity. However, models with higher order corrections have a larger set of domain wall solutions and the existence of these solutions no longer depends on the presence of cosmological constants. They find for example that the Randall-Sundrum scenario [189] can be realized without any need for bulk and/or brane cosmological constant. In Meissner and Olechowski 2002 they explicitly solve the linearized equation of motion for gravity fluctuations around the domain wall background.

Jakobek *et. al.* [107] subsequently consider the higher order gravity with dilaton and with the leading string theory corrections to investigate domain wall type solutions for arbitrary number of space-time dimensions. They analyze and classify solutions with finite effective gravitational constant, noting in particular the existence of *a class of such solutions which have no singularities*. A detailed discussion around the relation between fine tuning and self tuning helps them to clarify in which sense the solutions are fine-tuning free. The stability of such solutions is also discussed.

Why is the Universe so much less anisotropic than Einstein's field equations allow it to be in principle? Maybe, as Penrose surmises, the initial conditions logically entail a vanishing Weyl tensor, to ensure an isotropic Universe from its very inception. The other possibility is to drop the assumption of isotropy, as we do. A third possibility would be to

drop the assumption of homogeneity, an option that is gaining popularity [126]. In section D we give the geometrical setting that allows one to define and classify spatially homogeneous anisotropic Bianchi cosmologies.

Kluske [198] investigates classes of higher order theories where the de Sitter space-time is an attractor solution in the set of the spatially flat FRW models. The isotropisation problem is due to the well-known theorem of Collins and Hawking [29]: *The set of spatially homogeneous cosmologies that can approach isotropy at late times is of measure zero in the space of all spatially homogeneous initial data.* However, in higher order gravity theories such as Bianchi types I, V and VII an isotropic end-state is reached [30] thus satisfying theorem I of Collins and Hawking.

The *almost-homogeneity of the universe* in $R + \alpha R^2$ higher-order gravity was discussed by Taylor and Maartens [225] in extension of the significant proof by Stoeger, Maartens and Ellis [223] that the observed almost-isotropy of the CMBR implies that the Universe since photon decoupling is almost spatially homogeneous and isotropic, i.e. almost FRW.

Gordon and Turok [172] explores the idea that density perturbations apparent in today's universe could have been generated in a *pre-singularity* epoch before the big bang so as to provide explicit mechanisms whereby a scale invariant spectrum of adiabatic perturbations may be generated without the need for cosmic inflation. They study a bouncing Universe model in which neither General Relativity nor the WEC is violated, and show that a perturbation which is pure growing mode before the bounce does not match to a pure decaying mode perturbation after the bounce. Analytical estimates of when the comoving curvature perturbation varies around the bounce are given. It is found that in general it is necessary to evaluate the evolution of the perturbation through the bounce in detail rather than using matching conditions.

9.3 Concluding Remarks

In chapter 10 of this thesis (and the corresponding paper [215]) we further explore an idea already presented in chapter 8, namely that the Universe may be the end-state of a collapsing black hole that leads to another phase of re-expansion; the Universe emerges from an early, anisotropic bounce with space time geometry similar to that of a Kantowski-Sachs model, expands and becomes almost FRW (de Sitter) at late times. Since various *no-go theorems*

(particularly those stated in Chapter 8) preclude Bounce Behaviour in Einstein Gravity, we lean towards a broader class of theories with an alternative geometrical structure that is perhaps better suited to the task.

Chapter 10

Bounce Behaviour in Higher Derivative Kantowski-Sachs Cosmology

10.1 Introduction

Here we intend to study Bounce Behaviour in Kantowski -Sachs Cosmology in a generic (higher dimensional) geometry, as a continuation of the discussion initiated in Chapter 8 of this thesis and pursued in Chapter 9. The four dimensional Universe emerges from an anisotropic initial state in Higher Order Gravity , and evolves toward an end-state that is de Sitter in flat Einstein Gravity. We decline from specifying any higher dimensional background such as RSI or RSII. Instead we represent any String / M-theory modifications as a higher-order correction to the action for gravity.

After stating some preliminaries in Section 10.2, we present the field equations for the Kantowski-Sachs model in Section 10.3. In Section 10.4.1 we formulate the weak energy condition in order for a Higher Derivative Kantowski-Sachs Cosmology to exhibit Bounce Behaviour in both scale factors X and Y . The remainder of Section 10.4 concentrates on identifying such a class of solutions. This is followed by concluding remarks in Section 10.5.

Under the assumption that the action for gravity is

$$\mathcal{S}_g = \frac{1}{16\pi G} \int R \sqrt{-g} d^4x \quad (10.1.1)$$

and that matter satisfies the *dominant energy condition* $\rho \geq 0$ and $\rho + 3p \geq 0$ where ρ is the energy density and p is the pressure, the Penrose-Hawking [181] singularity theorems prove that spacetime manifolds in general relativity are geodesically incomplete. This signifies a possible breakdown of the theory at large curvatures. Spatially homogeneous bounce solutions to the Einstein field equations also violate some important energy conditions [214]. For instance in Kantowski-Sachs cosmologies, bounce behaviour along all scale factor directions violate the *null energy condition* $\rho + p \geq 0$. More generally, the construction of viable models of geodesically complete re-collapsing universes or black hole interiors are precluded by such energy conditions.

Various hypotheses have been formulated [44, 183] to address the singularity problem: The ‘limiting curvature hypothesis’ ensures that *all* curvature invariants such as R , $R_{\mu\nu}R^{\mu\nu}$, $R_{\mu\nu\alpha\beta}R^{\mu\nu\alpha\beta}$ and $C_{\kappa\rho\tau\sigma}C^{\kappa\rho\tau\sigma}$ are bounded, to guarantee that spacetime manifolds are geodesically complete (here $C_{\kappa\rho\tau\sigma}$ is the Weyl tensor). Penrose’s ‘vanishing Weyl curvature hypothesis’ allows for otherwise anisotropic universe models to isotropize ($C^2 \rightarrow 0$) in their asymptotic regions. Of note is the Collins-Hawking theorem [29], which restrict models that isotropize to a set of measure zero in the space of all spatially homogeneous initial data (see previous chapter).

We [214] address the Singularity Problem in a different light by investigating bounce behaviour along all scale factors in spatially homogeneous cosmologies where feasible (i.e. where there is no need for a negative mass density source at any stage). The only models for which this can be done are closed FRW and Bianchi IX [214]. In the Randall-Sundrum braneworld scenario [189] the matter action is modified since the higher dimensional bulk back-reacts on the brane so as to modify the matter side of the Einstein field equations. This feed-back mechanism introduces an extra degree of freedom at high curvatures, and as a result allows more solutions to the field equations than in general relativity.

As opposed to *a priori* inclusion of higher space time dimensions, we shall consider higher derivative correction terms to the Einstein gravitational action, in concordance with string theory and quantum gravity requirements, viz.

$$S_g = \frac{1}{16\pi G} \int f(R, R_{\mu\nu}R^{\mu\nu}, C_{\kappa\rho\tau\sigma}C^{\kappa\rho\tau\sigma}, \dots) \sqrt{-g} d^4x \quad (10.1.2)$$

provided that the leading term in f is simply R at low curvatures.

The simplest higher derivative theory

$$S_g = \frac{1}{16\pi G} \int (R + \alpha R^2) \sqrt{-g} d^4x \quad (10.1.3)$$

gives rise to higher order equations of motion than the usual Einstein theory of gravity, and therefore has more cosmological solutions. There are classes of solutions that are nonsingular without violating the weak energy condition.

10.2 Preliminaries

Varying the matter action (10.1.3) yields the modified Einstein field equations

$$R_{\mu\nu} - \frac{1}{2}Rg_{\mu\nu} + 2\alpha [R (R_{\mu\nu} - \frac{1}{4}Rg_{\mu\nu}) + R_{;\kappa\lambda} (g^{\kappa\lambda}g_{\mu\nu} - \delta_{\mu}^{\kappa} \delta_{\nu}^{\lambda})] = 8\pi GT_{\mu\nu} \quad (10.2.1)$$

with a perfect fluid stress-energy-momentum tensor

$$T_{\mu\nu} = (\rho + p)u_{\mu}u_{\nu} + pg_{\mu\nu}, \quad (10.2.2)$$

for a homogeneous energy density ρ and pressure p in co-moving coordinates $u_{\mu} = \delta_{\mu}^0$, and a Kantowski-Sachs metric

$$ds^2 = -dt^2 + X^2 dr^2 + Y^2 d\theta^2 + Y^2 \sin^2 \theta d\phi^2 \quad (10.2.3)$$

Vorticity and acceleration both vanish, $\omega = 0 = a^{\mu}$.

The law of conservation of energy is expressed in the form

$$T^{\mu}_{\nu;\mu} = 0 \Rightarrow \dot{\rho} + \Theta(\rho + p) = 0. \quad (10.2.4)$$

10.3 Gravitational Equations

The trace of equation (10.2.1) leads to a Klein-Gordon equation of the Ricci scalar

$$\ddot{R} + \Theta\dot{R} + \frac{1}{6\alpha}R = \frac{1}{6\alpha}(\rho - 3p), \quad (10.3.1)$$

since the trace of the energy tensor $T \equiv T^{\mu}_{\mu} = 3p - \rho$. The tt -component of equation (10.2.1) results in the Raychaudhuri equation

$$\dot{\Theta} + \frac{1}{3}\Theta^2 + 2\sigma^2 = \frac{-2\rho + R + \alpha(R^2 + 4\Theta\dot{R})}{2(1 + 2\alpha R)}. \quad (10.3.2)$$

The rr -component yields

$$\frac{1}{3}\dot{\Theta} + \frac{1}{3}\Theta^2 + \frac{2}{\sqrt{3}}(\dot{\sigma} + \Theta\sigma) = \frac{2\rho + R + \alpha[3R^2 - 4(\Theta + 2\sqrt{3}\sigma)\dot{R}]}{6(1+2\alpha R)} . \quad (10.3.3)$$

The $\theta\theta$ - and $\phi\phi$ -components yield the same equation up to a factor of $\sin^2\theta$

$$\begin{aligned} \frac{1}{3}\dot{\Theta} + \frac{1}{3}\Theta^2 - \frac{1}{\sqrt{3}}(\dot{\sigma} + \Theta\sigma) + \frac{1}{2} {}^{(3)}R \\ = \frac{2\rho + R + \alpha[3R^2 - 4(\Theta - \sqrt{3}\sigma)\dot{R}]}{6(1+2\alpha R)} \end{aligned} \quad (10.3.4)$$

with 3-curvature ${}^{(3)}R = \frac{2}{\sqrt{3}}$. Subtract equation (10.3.4) from equation (10.3.3) results in the shear evolution equation

$$\dot{\sigma} + \left(\Theta + \frac{2\alpha\dot{R}}{1+2\alpha R} \right) \sigma = \frac{1}{2\sqrt{3}} {}^{(3)}R \quad (10.3.5)$$

Use this expression to replace $\dot{\sigma}$ in equation (10.3.3), and use equation (10.3.2) to substitute $\dot{\Theta}$, then re-arrange terms to find the Gauss-Codacci equation

$$\frac{1}{3}\Theta^2 + \frac{1}{2} {}^{(3)}R = \sigma^2 + \frac{2\rho + \alpha(R^2 - 4\Theta\dot{R})}{2(1+2\alpha R)} . \quad (10.3.6)$$

Together with the energy conservation equation (10.2.4) this system is self-consistent, provided that we incorporate the 3-curvature evolution identity

$${}^{(3)}\dot{R} + \frac{2}{3}(\Theta - \sqrt{3}\sigma) {}^{(3)}R = 0 . \quad (10.3.7)$$

10.4 Bounce behaviour

10.4.1 The Weak Energy Condition

Subtract equation (10.3.6) from equation (10.3.2) and replace the 3-curvature using equation (10.3.5), then rearrange terms to arrive at

$$\begin{aligned} \frac{1}{2}(\rho + p) = -(\dot{y} + y^2 - xy)(1 + 2\alpha R) \\ + \frac{1}{3}\alpha \left((2x + y)\dot{R} - 3\ddot{R} \right) . \end{aligned} \quad (10.4.1)$$

Note that we have defined $x = \frac{\dot{X}}{X}$, $y = \frac{\dot{Y}}{Y}$. The Weak Energy Condition $\rho + p \geq 0$ amounts to the reality of a scalar field gradient $\dot{\phi}$ defined in the usual way: $\rho = \frac{1}{2}\dot{\phi}^2 + V(\phi)$, $p = \frac{1}{2}\dot{\phi}^2 - V(\phi)$ for a homogeneous scalar field ϕ with a self-interacting potential $V(\phi)$.

For $\alpha = 0$ we have the standard general relativity weak energy condition expressed as $\frac{1}{2}(\rho + p) = -(\dot{y} + y^2 - xy) \geq 0$, which is violated for bounce behaviour in the scale factor Y , since $y = 0$, $\dot{y} > 0$ imply that $\frac{1}{2}(\rho + p) < 0$.

It is clear from equation (10.4.1) that the higher order correction to general relativity allows for bounce behaviour in Y provided that $-\dot{y}(1 + 2\alpha R) + \frac{1}{3}\alpha(2x\dot{R} - 3\ddot{R}) \geq 0$ at the time of the bounce.

10.4.2 Equation of state

We shall assume an equation of state $\rho = 3p + 4\Lambda$, so that the energy conservation equation (10.4.7) implies that the energy density $\rho = \rho_r + \Lambda$ and pressure $p = \frac{1}{3}\rho_r - \Lambda$ in terms of the radiation density $\rho = \rho_{r0}a_0^4/a^4$, for constants ρ_{r0} , a_0 and the cosmological constant Λ . The weak energy condition is satisfied for provided the energy density is positive, while the strong energy condition $\rho + 3p = 2\rho_r - 2\Lambda$ is violated in regions far away from the bounce, hence resulting in a de Sitter expansion for models in which Λ remains positive.

10.4.3 Normalized Variables

Introduce Normalized Variables $(\mathcal{D}, \tau, \xi, \chi, \mathcal{P}, \mathcal{Q}, \Sigma, \Omega_K, \Omega_R, \Omega_{rad}, \Omega_\Lambda, \Omega_\rho)$:

$$\begin{aligned} \frac{1}{-2\alpha}\mathcal{D}^2 &\equiv \frac{1}{3}\left(\Theta + \frac{3\alpha\dot{R}}{1+2\alpha R}\right)^2 + \frac{1}{2}({}^3R) - \frac{\alpha R^2}{2(1+2\alpha R)} = \sigma^2 + \frac{\rho + 3\alpha^2\dot{R}^2}{1+2\alpha R}, \quad d\tau := \frac{1}{\sqrt{-6\alpha}}\mathcal{D}dt \\ \xi &:= -\alpha(R - 4\Lambda), \quad \chi := \frac{-\alpha R}{\mathcal{D}^2(1+2\alpha R)}, \quad \mathcal{P} := \frac{-\alpha\dot{R}}{\sqrt{-6\alpha}\mathcal{D}(1+2\alpha R)} \\ \Theta &:= \frac{3}{\sqrt{-6\alpha}}\mathcal{D}\mathcal{Q}, \quad \sigma := \frac{1}{\sqrt{-6\alpha}}\mathcal{D}\Sigma, \quad ({}^3R) := \frac{1}{-\alpha}\mathcal{D}^2\Omega_K \\ \Omega_R &:= \frac{\alpha^2 R^2}{\mathcal{D}^2(1+2\alpha R)}, \quad \Omega_{rad} := \frac{-2\alpha\rho_r}{\mathcal{D}^2(1+2\alpha R)}, \quad \Omega_\Lambda := \frac{-2\alpha\Lambda}{\mathcal{D}^2(1+2\alpha R)} \end{aligned} \quad (10.4.2)$$

and that the total energy density $\Omega_\rho = \Omega_{rad} + \Omega_\Lambda$ is positive definite provided that $-1 \ll \alpha < 0$, while ρ_r and Λ are positive. In terms of these variables, equations (10.2.4),(10.3.1),

(10.3.2) and (10.3.5–10.3.7) become a closed system of ode's

$$\mathcal{D}' = \mathcal{D}\Delta \quad (10.4.3)$$

$$\begin{aligned} \Delta &:= (\mathcal{Q} - \mathcal{P})[2\Omega_\Lambda - 2 + \Omega_K - \mathcal{Q}\mathcal{P} - \Sigma^2] \\ &\quad - (\mathcal{Q} - \Sigma)\Omega_K - \left(1 + \frac{1}{\lambda + \xi}\right)\Omega_R\mathcal{P} \end{aligned} \quad (10.4.4)$$

$$\xi' = (1 - 2\lambda - 2\xi)\mathcal{P} \quad (10.4.5)$$

$$\chi' = -\chi \left[2\Delta - \frac{1}{\lambda + \xi}\right] \quad (10.4.6)$$

$$\mathcal{P}' = -\mathcal{P}[\Delta - 2\mathcal{P} + 3\mathcal{Q}] + (\chi - 2\Omega_\Lambda) \quad (10.4.7)$$

$$\mathcal{Q}' = -\mathcal{Q}[\Delta + 2\mathcal{Q}] - \Sigma^2 + \chi - \Omega_K - 2\Omega_R \quad (10.4.8)$$

$$\Sigma' = -\Sigma[\Delta + 3\mathcal{Q} - 2\mathcal{P}] + \Omega_K \quad (10.4.9)$$

$$\Omega'_K = -2\Omega_K[\Delta + 2(\mathcal{Q} - \Sigma)] \quad (10.4.10)$$

$$\Omega'_R = -2\Omega_R \left[\Delta + \left(1 - \frac{1}{\lambda + \xi}\right)\mathcal{P}\right] \quad (10.4.11)$$

$$\Omega'_{rad} = -2\Omega_{rad}[\Delta + 2\mathcal{Q} - \mathcal{P}] \quad (10.4.12)$$

$$\Omega'_\Lambda = -2\Omega_\Lambda[\Delta - \mathcal{P}] \quad (10.4.13)$$

where we have set $\lambda := -4\alpha\Lambda$. The Friedmann constraint separates into two constraints

$$(\mathcal{Q} + \mathcal{P})^2 + \Omega_K + \Omega_R = 1 \quad , \quad \mathcal{P}^2 + \Sigma^2 + \Omega_{rad} + \Omega_\Lambda = 1 \quad (10.4.14)$$

There are in fact three additional differential equations with which one obtains the scale factors X , Y and their geometric mean $a = \sqrt[3]{XY^2}$

$$X' = (3\mathcal{Q} + 2\Sigma)X \quad , \quad (10.4.15)$$

$$Y' = (3\mathcal{Q} - \Sigma)Y \quad , \quad (10.4.16)$$

$$a' = \mathcal{Q}a \quad . \quad (10.4.17)$$

Note that equation (10.4.15) is equivalent to equation (10.4.10) because ${}^{(3)}R = \frac{2}{Y^2}$. None of equations (10.4.5)-(10.4.17) terms involving \mathcal{D} we may omit its evolution equation from the discussion. The dimensionality can be further reduced by the two constraints (10.4.14). Bounce behaviour may be illustrated for constant scalar curvature R by imposing the condition

$$\mathcal{P} = 0 \quad \iff \quad \xi' = 0 \quad (10.4.18)$$

upon the system. One may then substitute for the curvature density parameter Ω_K and the cosmological density parameter Ω_Λ respectively, using the now reduced form of the constraints (10.4.14)

$$\Omega_K = 1 - \Omega_R - \mathcal{Q}^2, \quad \Omega_\Lambda = 1 - \Omega_{rad} - \Sigma^2, \quad \chi = 2\Omega_\Lambda$$

to realize a four-dimensional *invariant submanifold* $(\mathcal{Q}, \Sigma, \Omega_R, \Omega_{rad})$

$$\mathcal{Q}' = (1 - \mathcal{Q}^2)(1 - \mathcal{Q}\Sigma - 3\Sigma^2 - 2\Omega_{rad}) + \Omega_R(1 + \mathcal{Q}\Sigma), \quad (10.4.19)$$

$$\Sigma' = (1 - \Sigma^2)(1 - 3\mathcal{Q}\Sigma - \mathcal{Q}^2 - \Omega_R) + 2\Omega_{rad}\mathcal{Q}\Sigma, \quad (10.4.20)$$

$$\Omega_R' = -2\Omega_R[(1 - 3\mathcal{Q}\Sigma - \mathcal{Q}^2 - \Omega_R)\Sigma - 2\mathcal{Q}\Omega_{rad}], \quad (10.4.21)$$

$$\Omega_{rad}' = -2\Omega_{rad}[(1 - 3\mathcal{Q}\Sigma - \mathcal{Q}^2 - \Omega_R)\Sigma + 2\mathcal{Q}(1 - \Omega_{rad})], \quad (10.4.22)$$

We present a table of all equilibrium points with their respective classifications. We have defined new equilibrium points $\tilde{F}_{\epsilon_1\epsilon_2\epsilon_3}$ in terms of the numbers

$$\begin{aligned} \mathcal{Q}_0^2 &= \frac{1}{8}[5 + c - \epsilon_3\sqrt{(3-c)(3+15c)}] \quad , \quad \Sigma_0^2 = \frac{1}{24}[3 + 7c + \epsilon_3\sqrt{(3-c)(3+15c)}] \quad , \\ \Omega_K^0 &= \frac{1}{8}[3(1-3c) + \epsilon_3\sqrt{(3-c)(3+15c)}] \quad , \quad \Omega_\Lambda^0 = \frac{1}{24}[7(3-c) - \epsilon_3\sqrt{(3-c)(3+15c)}] \end{aligned}$$

where $c := \Omega_R$ and $\epsilon_i = \pm 1$, $i = 1, 2, 3$.

10.4.4 Vanishing Radiation Density $\Omega_{rad} = 0$

If the radiation density vanishes $\Omega_{rad} = 0$, the above system results in

$$\mathcal{Q}' = (1 - \mathcal{Q}^2)(1 - \mathcal{Q}\Sigma - 3\Sigma^2) + \Omega_R(1 + \mathcal{Q}\Sigma), \quad (10.4.23)$$

$$\Sigma' = (1 - \Sigma^2)(1 - 3\mathcal{Q}\Sigma - \mathcal{Q}^2) + 2\Omega_{rad}\mathcal{Q}\Sigma, \quad (10.4.24)$$

$$\Omega_R' = -2\Omega_R\Sigma(1 - 3\mathcal{Q}\Sigma - \mathcal{Q}^2), \quad (10.4.25)$$

so that equations (10.4.24) and (10.4.25) may be combined to obtain the first integral

$$\Omega_R = \Omega_R^0(1 - \Sigma^2), \quad (10.4.26)$$

for a constant of motion $\Omega_R^0 > 0$. This further reduces the system to an autonomous two-dimensional phase portrait in the (\mathcal{Q}, Σ) - plane

$$\mathcal{Q}' = (1 - \mathcal{Q}^2)(1 - \mathcal{Q}\Sigma - 3\Sigma^2) + \Omega_R^0(1 - \Sigma^2)(1 + \mathcal{Q}\Sigma), \quad (10.4.27)$$

$$\Sigma' = (1 - \Sigma^2)[1 - 3\mathcal{Q}\Sigma - \mathcal{Q}^2 - \Omega_R^0(1 - \Sigma^2)]. \quad (10.4.28)$$

Cosmology	Model	\mathcal{Q}	Σ	Ω_R	Ω_{rad}	Ω_K	Ω_Λ
Bianchi I	$K_{\epsilon_1\epsilon_2}$	ϵ_1	ϵ_2	0	0	0	0
Bianchi I	dS_{ϵ_1}	ϵ_1	0	0	0	0	1
KS	F_{ϵ_1}	$\frac{\epsilon_1}{2}$	$\frac{\epsilon_1}{2}$	0	0	$\frac{3}{4}$	$\frac{3}{4}$
Bianchi I	R_{ϵ_1}	ϵ_1	0	0	1	0	0
Bianchi I	B_{ϵ_1}	0	$\epsilon_1\sqrt{\frac{2}{3}(1-b)}$	1	b	0	$\frac{1}{3}(1-b)$
Bianchi I	$\tilde{K}_{\epsilon_1\epsilon_2\epsilon_3}$	$\epsilon_1\mathcal{Q}_0$	$\epsilon_2\Sigma_0$	c	0	Ω_K^0	Ω_Λ^0
Bianchi III	F_{ϵ_1}	ϵ_1	$-\epsilon_1$	3	0	-3	0
Bianchi III	$F_{2\epsilon_1}$	$2\epsilon_1$	$-\epsilon_1$	0	0	-3	0
Bianchi III	$F_{\epsilon_1/2}$	$\frac{\epsilon_1}{2}$	$-\epsilon_1$	$\frac{9}{4}$	0	$-\frac{3}{2}$	0

Table 10.1: Equilibrium points of the four-dimensional *invariant submanifold* $(\mathcal{Q}, \Sigma, \Omega_R, \Omega_{rad})$ corresponding to $\mathcal{P} = 0$. B_{ϵ_1} represent unstable bounce equilibrium points on the surface $\mathcal{Q} = 0$, for fixed radiation density parameter values $\Omega_{rad} = b \leq 1$. For *negative* values of b , the higher order theory reproduce the bounce behaviour predicted by braneworld cosmology (chapter 8 and [214]). The constants $\mathcal{Q}_0, \Sigma_0, \Omega_K^0$ and Ω_Λ^0 are defined in terms of $\Omega_R =: c$ in section (10.4.3). The Bianchi III equilibrium points lie outside the domain $\{(\mathcal{Q}, \Sigma) : \mathcal{Q} \in [-1, 1]; \Sigma \in [-1, 1]\}$ and are not relevant.

In the event that $\Omega_R^0 = 0$, then we have the usual no-bounce phase-portrait of General Relativity. For $\Omega_R^0 > 0$ the bounce behaviour is illustrated in Figure 10.1. One may set $\Omega_R^0 =: c$ in order to obtain all the equilibrium points of the state space $(\mathcal{Q}, \Sigma, \Omega_R, \Omega_K, \Omega_\Lambda)$, defined in Table 10.1 by the models $\tilde{F}_{\epsilon_1\epsilon_2\epsilon_3}$ for $\epsilon_i = \pm 1, i = 1, 2, 3$. Although this is only the false vacuum case, since we set $\Omega_{rad} = 0$, this result extends to the case of non-vanishing radiation and cosmological constant (both of which may assume positive-definite values without violating neither NEC nor WEC). Such bounce behaviour are characterized by positive values of $\Omega_{rad} =: b$ of the equilibrium points B_{ϵ_1} in phase space.

The braneworld bounce discussed in chapter 8 and the paper [214] is naturally a higher derivative cosmology if the Ricci scalar is constant $\dot{R} = 0$. The presence of the cosmological constant enforces the equality $R = 4\Lambda$ (this is easily seen from equation (10.3.1)) and the radiation density parameter $\Omega_{rad} = -2\alpha\rho_r/[D^2(1+2\alpha R)]$ is strictly negative for $\alpha < 0$ provided that $1+2\alpha R = 1+8\alpha\Lambda < 0$ since ρ_r has to remain non-negative. In the braneworld context, this model corresponds to a *negative brane tension* $1+2\alpha R$ while maintaining positive radiation density, as opposed to *dark radiation* with $\rho_r < 0$. In phase space the bounce corresponds to equilibrium points B_{ϵ_1} for negative values of b .

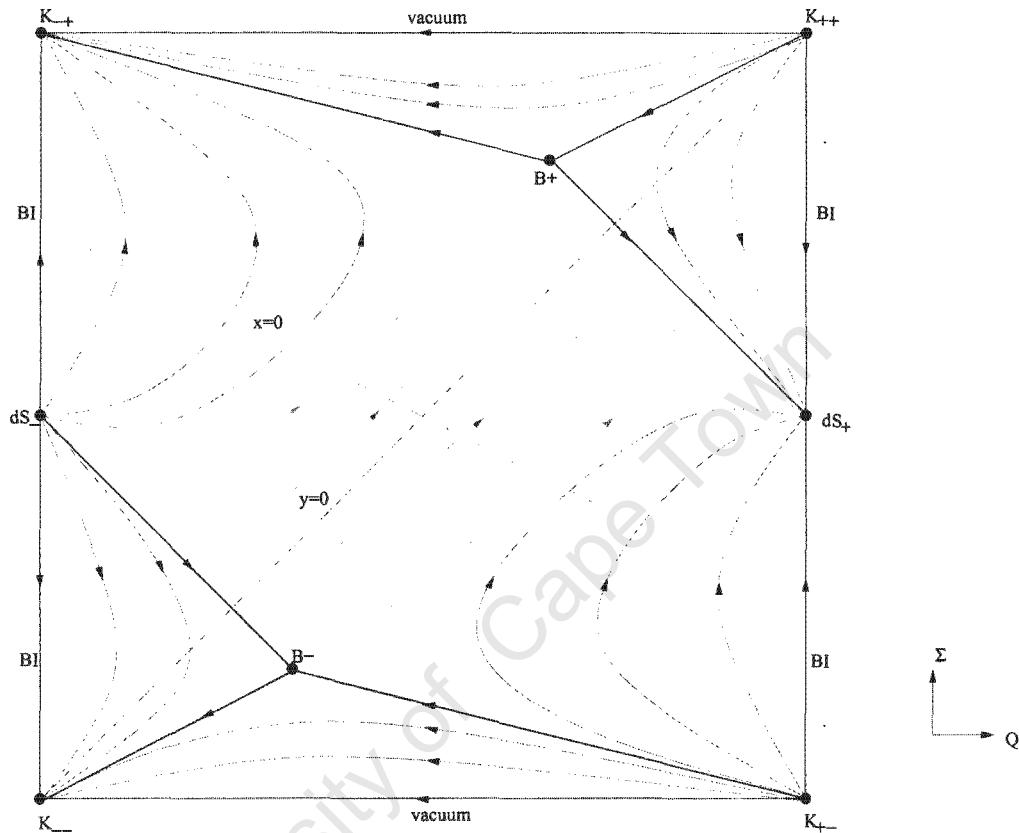


Figure 10.1: False Vacuum Bounce: The state space \mathcal{R} exhibits bounce behaviour in scale factor X as a blue trajectory that passes through the plane $Q + 2\Sigma = 0$, and a bounce in Y as that same trajectory passes through the plane $Q - \Sigma = 0$.

In chapter 8 we discussed the nature of such bounce behaviour in the braneworld scenario. We now present an equivalent discussion for higher derivative bounce behaviour.

The boundaries $Q = \pm 1$ represent Bianchi I models with a cosmological constant, while the boundaries $\Sigma = \pm 1$ correspond to (vacuum) Kasner models in the invariant submanifold

$$\mathcal{R} = \{(Q, \Sigma) : |Q| \leq 1, |\Sigma| \leq 1\}$$

that represents general relativity. The points $K_{\pm\pm}$ and $K_{\pm\mp}$ are Kasner metrics that form the vertices of \mathcal{R} . The critical points K_{++} and K_{+-} are *repellers*, while K_{-+} and K_{--} are *attractors*. de Sitter spacetime dS_{+} is an *attractor* and dS_{-} (anti-de Sitter) is a *repeller* located on the respective boundaries $Q = 1$ and $Q = -1$ of the submanifold \mathcal{R} . There are

two saddle points F_{\pm} located on the separatrix $y = Q - \Sigma = 0$ inside \mathcal{R} . The saddle points F_{\pm} have $\{^{(3)}R = 2\Lambda, \Theta = \sqrt{3}\sigma = \pm\sqrt{\Lambda}, \Omega_R^0 = 0\}$. From Figure 8.1 in chapter 8 it is clear that no trajectory emerging from dS_- inside \mathcal{R} can reach dS_+ due to the separatrix $y = Q - \Sigma = 0$. In Figure 10.1 we demonstrate how the presence of density parameter Ω_R broadens the parameter space to allow bounce behaviour. The saddle points B_{ϵ_1} represent static cosmological models with $\{^{(3)}R = 0, \Theta = 0, \sigma = \epsilon_1\sqrt{\frac{2}{3}(1-b)}, \Omega_R = 1, \Omega_{rad} = b, \Omega_{\Lambda} = \frac{1}{3}(1-b)\}$. Since $\Omega_R = 1$ these models are located inside the greater state space

$$\mathcal{M} = \{(Q, \Sigma, \Omega_R) : |Q| \leq 1, |\Sigma| \leq 1, 0 \leq \Omega_R \leq 1\}$$

containing \mathcal{R} . A trajectory emerging from dS_- may now leave \mathcal{R} and cross the plane $y = Q - \Sigma = 0$ (which is no longer a separatrix for $\Omega_R > 0$) as it evolves toward, and eventually away from the static model B_{ϵ_1} , and enters dS_+ . Such a trajectory passes through $Q = 0$ and close to B_{ϵ_1} , indicative of bounce behaviour in the volume scale factor a , since Q' remains positive.

Starting at dS_- a trajectory passes through the plane $y = Q - \Sigma = 0$, with y changing sign from negative to 0 to positive, and through the plane $x = Q + 2\Sigma = 0$ with x changing sign from negative to 0 to positive. It terminates at the attractor dS_+ . Note that the bounce definition (8.3.1) requires the trajectory to cut both the x - and y -planes (the order may be reversed, depending on the path chosen), entering from the negative side of each plane, and exiting the positive side. If it intersects the line $(0, 0, \Omega_R)$ then the bounce in X and Y is synchronous, i.e. the shear σ and the expansion Θ both vanish there.

10.5 Discussion

To fashion a singularity-free Kantowski-Sachs Cosmology to serve as the interior to a collapsing black hole whose exterior is the true vacuum [44, 243] calls for a suitable modification of Einstein Gravity. The singularity located at $r = 0$ to an external observer may then correspond to a bounce at time $t = 0$ in an expanding baby universe. It is not possible to construct an anisotropic, spatially homogeneous bounce in ordinary General Relativity due to violation of the NEC and WEC in the vicinity of the bounce. In conceiving a higher order effective action that does allow such behaviour, we are compelled to assign a *negative* value to the higher order correction constant α . We investigate a simple model

consisting of a mixture radiation fluid and false vacuum energy (here in the form of a positive cosmological constant) before the onset of primordial nucleosynthesis, and possibly even before Electroweak transition, and confine the discussion to a period when the Universe was radiation-dominated (during the first second). Thereafter the Universe reaches isotropy and drifts toward a de Sitter attractor.

For fixed Ricci scalar $R = 4\Lambda$ such that $1 + 2\alpha R$ remains negative for $\alpha < 0$, the *dark energy* Braneworld Bounce of Chapter 8 is replicated. That this is indeed feasible is visible from equation (10.4.1) whence

$$\frac{2}{3}\rho_{rad} = -(1 + 8\alpha\Lambda)(\dot{y} + y^2 - xy) \quad (10.5.1)$$

becomes negative at the bounce in Y , signifying that the radiation fluid has an *effective dark energy density* $\frac{\rho_{rad}}{1+8\alpha\Lambda} < 0$. This result is indicative of a correspondence between Higher Order Gravity and tree-level String (Membrane) Theory.

For a negative value of α , the radiation $+\Lambda$ fluid mixture is free of anomalous behaviour in physical variables. In the case of $\alpha > 0$, peculiarity in for instance the 3-curvature may occur, due to the presence of unstable equilibrium points in higher order phase space.

Conclusion

University of Cape Town

The somewhat voluminous document that comprises this thesis has been divided into four Parts, and a large Appendix. The preponderance of the work is in published form, or has recently been submitted for publication.

Contemporary Cosmology enjoys the venerable status of a precision science, mainly due to remarkable success of lucrative ventures such as Hubble Space Telescope and the Deep Survey, the Chandra X-Ray Observatory, SALT and the planned Square Kilometre Array Radio Telescope in Observational Astronomy; COBE, BOOMERANG, WMAP, and the planned launch of PLANCK in the first quarter of 2007 together with the Herschel satellite, in CMB observations.

The first Part of this thesis is a sojourn into the fascinating field of Gravitational Lensing, a topic that has captured the public's imagination due to marvellous pictures from the Hubble Space Telescope, such as the Deep Field and the Deep Survey, X-ray multiple images of lensed quasars from Chandra, and a host of other radio telescope images. We scrutinized the subject of *shrinking*, in that distant areas subtend smaller solid angles than they would in a Friedmann-Lemaitre (FL) universe model and that this effect will remain even when the observations relate to large angles. This phenomenon has yet to live up to its promise. Possible reasons for its muted impact on Area Distance measurements are two-fold: (a) Strong-lensing is still a relatively rare occurrence in Observational Cosmology, this despite observation of various luminous arcs and multiple lensed images [146, 216, 217, 218, 122, 180], and (b) very few objects have surface mass densities in excess of $10^{12}M_{\odot}$ per square kpc, a critical number for caustic-formation. In Chapter 3 of Part I, exact examples with caustics displayed the posited shrinking effects analytically and numerically for single spherically symmetric compensated lenses to which we can apply the thin-lens approximation.

CMB anisotropy measurements by WMAP and PLANCK will hopefully shed some light on the viability of Pre-Big Bang Cosmological Scenario. In Chapter 4 of Part II we reviewed some important aspects of Pre-Big Bang Cosmology, and we mentioned the Duality symmetry of the Effective Action of String Theory in its customary rôle. The Universe eschews *graceful exit* from an initial Inflationary phase of expansion at high curvature [153, 154, 14, 15, 62, 27].

In Chapter 5 we purport a code that elicit *desired* String Cosmology solutions when there

is a dilaton potential V not equal to zero, and used it to obtain Pre-Big Bang solutions that appear to display the desired hallmarks. Two different cases are analyzed: In the first case, an exact radiation equation of state (5.4.3) maintained throughout history leads to capricious behaviour, where only *extreme fine-tuning* of initial conditions attain the desired results, and indeed there may be no initial data leading to the desired behaviour in both the forward and backwards directions of time. In the second case an *exotic equation of state* links the fluid dynamics to the potential in a way that generalizes the perfect fluid equation of state. The fancied solutions are found without the need for fine tuning. Duality symmetry is reviewed in Section 5.2.1 and Section 5.4. The *equations* have such a scale factor symmetry, when solutions may or may not exhibit the same symmetry. There are cases in which the *solutions* obey the scale factor symmetry, even if the *equations do not*. Then there are some solutions that seem to have most of the properties fancied in the Pre-Big Bang Scenario.

The Braneworld Scenario II suffers the ignominy of an impasse re junction conditions across the brane, stalling CMB predictions. Of late various authors engage in generalizing the RSII model, eg. the introduction of a second brane (RSI), bulk scalar fields, alternatives to inflation generated by the bulk scalar potentials causing branes to collide, as seen in the *ekpyrotic* and *cyclic* models. In Section 7.2 of Chapter 7 we commission a code seen previously in [155, 52] and Chapter 5 to engineer an FRW Universe model with a brane-bound scalar field, and an adapted potential for suitable Inflationary behaviour. Braneworlds admit generic potentials for different Inflationary Scenarios.

Inflationary Cosmology has vested issues destitute for some clarification. Bounce Behaviour in Cosmology 6.4 has been formulated as an alternative to inflation *and* to elude the problems associated with the Big Bang. The geometry of a black hole interior matches that of an Kantowski-Sachs Universe, since the two models share the same symmetries as the spatially homogeneous interior region of the extended (vacuum) Kruskal solution. In Chapter 8 of Part III we show that besides violating the SEC, Bounce Behaviour in Relativistic Cosmology leads to violation of either the NEC or the WEC or both, in almost all of the anisotropic, spatially homogeneous models, particularly the Kantowski-Sachs model. However, in the Braneworld Scenario of Randall and Sundrum (II), such energy violations disappear (or at least, they are relegated to the bulk).

Higher Derivative Theories of Gravity (of which the Randall-Sundrum Braneworld Scenario is a subclass) can manifest Bounce Behaviour without violating either the NEC or the WEC. In Part IV we reviewed some recent publications that visit Higher Derivative Cosmologies simply to veer from the curvature singularities of General Relativity, and state some of the problems associated with Higher Order Gravity Theories themselves. An alternative theory of gravity with a Lagrangian of the form $f(R) = R + \alpha R^2$ is one such instance. We use a phase portrait to demonstrate that Bounce Behaviour is intrinsic to such theories. In a forthcoming publication we hope to outline a 3+1 covariant approach to cosmological perturbations in bouncing higher derivative theory, and its application to CMB anisotropies.

Quantum Wormhole solutions are a fairly general property of the WDW equation for various matter sources. Sources that admit Quantum Wormholes include those expected in low-energy effective String Theory, such as a scalar field with a self-interacting exponential potential. This is unlike the classical case where such matter sources do not allow Wormhole solutions. Two publications by the authors A Carlini, DH Coule and DM Solomons (see the Appendix) derive these Quantum Wormhole solutions, and contrast them with other solutions that are subject to appropriate choice of boundary conditions of Quantum systems describing an Inflationary Scenario followed by a large Lorentzian Universe phase.

Appendix A

Pre-Big Bang Evolution for Radiation

This is an Appendix to Chapter 6. In this section we try to obtain solutions that resemble the “pre-big bang scenario” but with satisfactory dynamics of $\phi(t)$ and a continuous transition from the pre-big bang to post-big bang phases. In these examples, we seek solutions that evolve from a string perturbative vacuum, i.e. $H \rightarrow 0$ and $e^\phi \rightarrow 0$ (no interactions), to the present scenario where e^ϕ , which acts as the coupling constant, asymptotes to a constant. This behaviour, which is essentially radiation dominated evolution of the universe for positive times and power-law inflation for negative times, is motivated by the “pre-big bang” scenario introduced in [71], and exactly obeys the scale factor symmetry (5.2.10).

A.1 Introduction

For given ρ_0 , it is convenient to define $y = \frac{2}{3}e^\phi\rho_0$ and change variables to (t, y, χ) . The equations (5.4.6) for $t > 0$ become

$$\dot{y} = \chi y, \quad \dot{\chi} = \frac{y-1}{(t+1)^2} + \frac{\chi}{2(t+1)}, \quad (\text{A.1.1})$$

In the 2-dimensional sub-spaces $t = \text{const}$ with coordinates (y, χ) , the curve $\gamma(t)$ has coordinates $(1, 0)$ for all t , and represents a set of saddle points parametrised by t . To get exactly the desired dilaton dynamics in the future ($\chi > 0$, $e^\phi \rightarrow \text{constant} \Rightarrow \chi \rightarrow 0$ as $t \rightarrow \infty$), one

must restrict the initial conditions (y_0, χ_0) to start precisely on the stable branch of these saddle points, which intersects the surface $t = 0$ in a curve $(0, \gamma_+(\chi), \chi)$ passing through the exceptional point $\gamma_0 = (0, 1, 0)$. One can obtain approximate solutions by rewriting the second of eqs.(A.1.1) in the form

$$\left(\frac{\chi}{(1+t)^{1/2}} \right)' = \frac{y-1}{(t+1)^{5/2}}$$

Suppose y is almost constant for $t > T_+$, implying χ is close to zero then. Then we can integrate to get

$$t > T_+ \Rightarrow \chi = -\frac{2y-1}{3} \frac{1}{1+t} + C_+ \sqrt{1+t}$$

where C_+ determines the magnitude of χ at time T_+ . The first part decays away as desired, but the second part grows with time unless $C_+ = 0$; this is the fine-tuning required to attain the desired behaviour of χ .

To investigate $t < 0$, it is again convenient to define $y = \frac{2}{3} e^\phi \rho_0$ and change variables to (t, y, χ) . The equations for $t < 0$ become

$$\dot{y} = \chi y, \quad \dot{\chi} = y(-t+1)^2 + \frac{\chi}{2(-t+1)} + \frac{1}{(-t+1)^2}, \quad (\text{A.1.2})$$

implying that $\dot{\chi} > 0$ for all $t < 0$; hence χ necessarily decreases at all times in the past. The problem is that it can become negative, because $\chi = 0$ is not an invariant set of the equation. We want a solution where χ remains positive for all time so that ϕ decreases for all time; this means we need χ to go to a positive value or zero, but not to become negative, and y to go to zero. As in the previous case one can obtain approximate solutions by rewriting the second of eqs.(A.1.2) in the form

$$\left(\chi(1-t)^{1/2} \right)' = \frac{1}{(-t+1)^{3/2}} (1 + y(-t+1)^4).$$

Suppose

$$y(-t+1)^4 \ll 1 \text{ for } t < T_-. \quad (\text{A.1.3})$$

Then we can ignore the second term on the right and integrate to get

$$t < T_- \Rightarrow \chi = \frac{2}{1-t} + \frac{C_-}{\sqrt{1-t}}, \quad y = y_0 \frac{1}{(1-t)^2} \exp(-2C_- \sqrt{1-t})$$

where C_- , y_0 represent the magnitude of χ , y at time T_- . This decays away as desired, and consistently preserves the inequality (A.1.3) for all earlier times because the exponential always dominates the power law terms. The question then is whether for suitable initial conditions we can attain this inequality at some time T_- , requiring $y(T_-) \ll (1 - T_-)^{-4}$. We can satisfy this with $T_- = 0$ if $y_0 = \frac{2}{3}e^{\phi_0}\rho_0 \ll 1$, i.e. $\phi_0 \ll \ln(\frac{3}{2\rho_0})$.

A.2 Density evolution with exotic equation of state

The 'pre-big bang' evolution (5.4.1,5.4.2) implies H and \dot{H} in terms of a :

$$t \geq 0: H(a) = \frac{1}{2a^2}, \dot{H}(a) = \frac{-1}{2a^4}, \quad (\text{A.2.1})$$

$$t \leq 0: H(a) = \frac{a^2}{2}, \dot{H}(a) = \frac{a^4}{2}. \quad (\text{A.2.2})$$

Assuming the exotic equation of state (5.4.9) implied by setting $\beta = 0$ at all times, from (5.4.12) we find ϕ in terms of a :

$$t \geq 0: \exp(\phi(a)) = \exp(\phi_0) \frac{a}{a(1-2\chi_0)+2\chi_0}, \quad (\text{A.2.3})$$

$$t \leq 0: \exp(\phi(a)) = \exp(\phi_0) \frac{a^{5/2}}{a^{5/2}(1-\frac{2}{3}\chi_0)+\frac{2}{3}\chi_0}, \quad (\text{A.2.4})$$

and from (5.4.18,5.4.23) we find χ in terms of a :

$$t \geq 0: \chi(a) = \frac{\chi_0}{a^2(2\chi_0+(1-2\chi_0)a)}, \quad (\text{A.2.5})$$

$$t \leq 0: \chi(a) = -\frac{5a\chi_0}{2\chi_0+(5-2\chi_0)a^{5/2}}. \quad (\text{A.2.6})$$

A particularly simple case occurs when $\chi_0 = \frac{1}{4}$. Then

$$t \geq 0: \exp(\phi(a)) = \exp(\phi_0) \frac{2a}{a+1}, \quad (\text{A.2.7})$$

$$t \leq 0: \exp(\phi(a)) = \exp(\phi_0) \frac{10a^{5/2}}{9a^{5/2}+1}. \quad (\text{A.2.8})$$

and

$$t \geq 0: \chi(a) = \frac{1}{2a^2(1+a)}, \quad (\text{A.2.9})$$

$$t \leq 0: \chi(a) = -\frac{5a}{2(1+9a^{5/2})}. \quad (\text{A.2.10})$$

Now $\rho(t)$ is determined by (5.4.10); using the above expressions, for $t > 0$ and $\chi_0 = \frac{1}{4}$ this becomes

$$\frac{d\rho}{da} = -\frac{3}{a^5} - \frac{3}{4a^6(1+a)}$$

which can be solved to give

$$\rho(a) = C + \frac{3}{20a^5} + \frac{9}{16a^4} + \frac{1}{4a^3} - \frac{3}{8a^2} + \frac{3}{4a} + \frac{3}{4} \ln\left(\frac{a}{1+a}\right).$$

This implies $\rho(t) \rightarrow C + \frac{107}{80} - \frac{3}{4} \ln 2 = C + 0.81764\dots$ as $t \rightarrow 0_+$ and $\rho(t) \rightarrow C$ as $t \rightarrow \infty$; hence choosing $C = 0$, $\rho(t) \rightarrow 0.81764\dots$ as $t \rightarrow 0_+$ and $\rho(t) \rightarrow 0$ as $t \rightarrow \infty$. Also $p/\rho \rightarrow 1/3$ as $t \rightarrow \infty$. The expression for $V(\varphi)$ in this case follows on putting this into (5.3.1) and using (5.4.15), (5.4.1), and the various expressions above. Similar (more complicated) expressions can be obtained for $t < 0$.

Appendix B

Euclidean quantum wormholes with scalar fields

Appeared in *Int. Journal of Mod. Phys. A* Vol **20** No 20 (1997) 3517 - 3544.

A. Carlini \diamond \dagger 1 D.H. Coule * and D.M. Solomons \ddagger 2

\diamond NORDITA, Blegdamsvej 17, DK-2100 Copenhagen Ø, Denmark

\dagger Tokyo Institute of Technology, Physics Department,
Oh-Okayama, Meguro-ku, Tokyo 152, Japan

* School of Mathematical Sciences, University of Portsmouth,
Mercantile House, Portsmouth P01 2EG, UK

\ddagger Department of Applied Mathematics, University of Cape Town,
Rondebosch 7700, Republic of South Africa

Abstract

We consider the quantum analogues of Euclidean wormholes obtained by Carlini and Mijić (CM), who analytically continued recollapsing closed universe models. Using a perfect fluid matter source we obtain asymptotically Euclidean (AE) wormholes when the strong

1 Email: carlini@th.phys.titech.ac.jp

2 Email: deon@maths.uct.ac.za

energy condition is satisfied. Such wormholes are found to be consistent with the Hawking-Page (HP) conjecture for quantum wormholes as solutions of the Wheeler-DeWitt (WDW) equation.

By simulating the equation of state of a perfect fluid with a real scalar field, quantum wormholes are also found when the strong energy condition is violated, although generally not AE. The non AE solutions are interpreted as excited states of the quantum wormhole spectrum.

Our results give support to the claim of HP that quantum wormhole solutions are a fairly general property of the WDW equation for various matter sources. Matter sources giving quantum wormholes could now include those expected in low-energy effective string theory: a dilaton scalar field with exponential potential. This is unlike the classical case where such matter sources do not allow wormhole solutions.

We finally contrast quantum wormhole solutions with other boundary conditions of quantum cosmology describing an inflationary earlier behaviour and a resulting large Lorentzian universe phase.

B.1 Introduction

In recent years there has been considerable interest in the use of Euclidean wormholes. This is because they might affect the value of coupling constants in our universe. For the cosmological constant Λ the effect of wormholes is to make Λ a dynamical variable given by a distribution function $P(\Lambda)$. If such a distribution is peaked around $\Lambda \rightarrow 0$, it could help explaining why the cosmological constant is zero in our universe [28].

Because wormholes contain information that is not necessarily accessible to outside observers, one would have to sum over all their possible internal states and the global quantum state appears to be mixed. This is reminiscent of black holes, and so wormholes were also suggested to eventually play a role in understanding Hawking radiation from black holes and their resulting evaporation [93]. Further, quantum Euclidean wormholes might describe properties of the “vacuum foam” structure of space time on Planck length scales. These properties could include topological fluctuations since the ‘no-go’ theorems about (classically) changing topology in Lorentzian space [72] are no longer valid.

Originally, classical wormholes were constructed using axions. Without reviewing all the cases that have since been found, we consider some of their general features. A necessary (but not sufficient) condition for the existence of wormholes is that the Ricci tensor should have at least a negative eigenvalue somewhere on the manifold [75]. For instance, in the case of a minimally coupled real scalar field the Ricci tensor is given by ³

$$R_{\mu\nu} = \partial_\mu\phi\partial_\nu\phi + g_{\mu\nu}V(\phi) . \quad (\text{B.1.1})$$

Because in Euclidean space the signature of the 4-d metric is $g_{\mu\nu} = (+ + + +)$, $R_{\mu\nu} > 0$ for $V(\phi) > 0$ and wormholes do not occur for, say, a real massive scalar field with potential $V(\phi) = m^2\phi^2$. However, if we consider an imaginary scalar field, i.e. let $\phi \rightarrow i\phi$, then $R_{\mu\nu}$ can become negative. For an imaginary free massive scalar field we now get

$$R_{\mu\nu} = -\partial_\mu\phi\partial_\nu\phi - g_{\mu\nu}m^2\phi^2 , \quad (\text{B.1.2})$$

and a wormhole solution might be possible now. For this imaginary massive scalar field the wormhole solution is given in ref. [36]. A similar reasoning is valid with other classical

³We are using the notation and conventions of Wald [237].

wormholes based on scalar fields. However, this is quite unsatisfactory, since if we consider a Hermitian theory then the Ricci tensor (for a free massless scalar field)

$$R_{\mu\nu} = \partial_\mu\phi\partial_\nu\phi^\dagger \quad (\text{B.1.3})$$

is always positive, even when $\phi \rightarrow i\phi$. One exception is the axion, which being a pseudo-scalar does pick up a “wrong sign” on going to Euclidean space [75].

Instead of looking for special matter sources that give wormholes, CM [24] considered an analytic continuation of closed Friedman-Robertson-Walker (FRW) universes. For a perfect fluid equation of state $p = (\gamma-1)\rho$, (p and ρ are the pressure and energy density respectively) recollapsing closed universes require that the strong energy condition be satisfied, i.e. $\gamma > 2/3$. By using an adaptation of an approach by Ellis and Madsen (EM) [155], they worked with a scalar field model with a potential $V(\phi)$ which simulates a certain value of γ . Or one might say that, by altering the parameter γ , the slope of the scalar field potential can be altered. If the slope is too shallow the strong energy condition would be violated and one would not expect wormholes to be possible. By being able to alter the slope of the scalar potential it should give a more systematic way of investigating when wormhole solutions can occur than by just choosing certain potentials, for example a massive scalar field $V(\phi) = m^2\phi^2$.

Originally, CM used an asymmetric analytic continuation to find the corresponding Euclidean wormhole from a recollapsing closed universe. The lapse in the matter and gravitational parts was Wick rotated in different directions as the transition to the Euclidean region was done. This is similar to the procedure of Linde [138] for obtaining a positive gravitational action S which could describe the quantum creation of the universe through tunneling, with probability $\sim \exp(-S)$. Later this continuation was extended in ref. [21], where the lapse and the scalar field ϕ were analytically continued a’ la Wick in opposite directions. These methods have the advantage of avoiding discontinuities in the scalar potential and the kinetic energy at the 3-d surface where Euclidean and Lorentzian signature regions join, and they ensure that the Ricci tensor has negative eigenvalues. However, this means that these wormholes are still rather restrictive, this aspect being “hidden” in the form of the continuation.⁴

⁴We note in passing that some wormholes (e.g. $R + \epsilon R^2$) are more closely related to the analytic continuation of bounces (where the singularity in open Lorentzian $k = -1$ universes is avoided [35]).

In a different vein, because the number of known classical wormhole solutions had appeared so restrictive, Hawking and Page (HP) considered that solutions of the Wheeler-DeWitt (WDW) equation could more generally represent wormholes [95]. They hoped that all reasonable matter sources would have the possibility of realizing quantum wormholes. For such wormholes they suggested that the wavefunction Ψ should decay exponentially for large scale factors a so as to represent Euclidean space, and that Ψ be well behaved as $a \rightarrow 0$, so that no singularities are present.

Because the WDW equation is independent of the lapse, the Euclidean region is already ‘included’ in the formalism. In this way the quantum versions of the CM wormholes should be automatically included in the solutions of the WDW equation, so avoiding the ad-hoc continuation required for the classical wormholes. There is some hope of expecting that this is possible: the WDW equation has both Hartle-Hawking (HH) [91] and Tunneling [138, 231] boundary condition solutions. As already mentioned, when dealing with the classical action the Tunneling case appears to correspond to an asymmetric continuation. This is rather analogous to what will be required to give quantum CM wormhole solutions.

As well as finding the quantum analogues of bulk matter wormholes that occur when the strong energy condition is satisfied, we also wish to explore if wormholes are even more general. We will do this by using a scalar potential $V(\phi)$ that simulates a certain value of γ . Hawking and Page constructed quantum wormholes for a real massive scalar field and a ϕ^n potential. But, depending on where the scalar field is on such potentials, the effective value of γ can be anywhere in the range $0 \leq \gamma \leq 2$ and it was not clear if the strong energy condition was violated in such cases. If quantum wormholes can also occur when the strong energy condition is violated, this would extend the viability of wormholes in mediating processes where this condition is probably violated, for example in the early universe with dynamics driven by effective low energy string theory, or during black hole evaporation.

B.2 The classical model

We first review the classical closed universe models from which we are going to derive the corresponding WDW equations. For a more detailed description of the features of the classical CM wormholes, we refer to the original results presented in ref. [24].

First we take a bulk matter source with a perfect fluid equation of state $p = (\gamma - 1)\rho$ and work in a Lorentzian FRW ansatz

$$ds^2 = \hat{\sigma}^2[-N^2 dt^2 + a^2 d\Omega_3^2] = \hat{\sigma}^2[-a^{4-3\gamma} dt^2 + a^2 d\Omega_3^2], \quad (\text{B.2.1})$$

where the lapse is chosen to aid calculations as in ref. [24], $d\Omega_3^2$ is the metric of the three-sphere and $\hat{\sigma}^2 \doteq 2G/3\pi$. The scale factor a is given by

$$a = a_0 \left[1 - \left(\frac{3\gamma - 2}{2} \right)^2 \frac{t^2}{a_0^{3\gamma-2}} \right]^{1/(3\gamma-2)}, \quad (\text{B.2.2})$$

with a_0 an arbitrary constant which is the maximum size of the FRW universe when $\gamma > 2/3$. Using the same approach as in EM, one can convert to a scalar field ϕ whose trajectory is given by

$$\phi - \phi_0 = \frac{\sqrt{2\gamma}}{3\gamma - 2} \tanh^{-1} \left[\frac{(3\gamma - 2)}{2a_0^{(3\gamma-2)/2}} t \right]. \quad (\text{B.2.3})$$

The classical potential for the scalar field ($\phi_0 = 0$) is

$$V(\phi) = \Omega \cosh^{2n}(\lambda\phi), \quad (\text{B.2.4})$$

where we have defined ⁵

$$\lambda \doteq \frac{3\gamma - 2}{\sqrt{2\gamma}}, \quad n \doteq \frac{3\gamma}{3\gamma - 2}, \quad \Omega \doteq \frac{(2 - \gamma)}{2a_0^2}. \quad (\text{B.2.5})$$

The classical CM wormhole is obtained by analytically continuing the time variable as $t \rightarrow -i\tau$ in eqs. (B.2.1)–(B.2.3), and the scalar field variable as $\phi \rightarrow +i\phi$ in eqs. (B.2.3)–(B.2.4) (cf. ref. [21]). These classical wormholes appear to have a nontrivial potential term, and so do not possess any conserved charge. The fact that they exhibit a periodicity in the Euclidean time was interpreted as evidence that wormholes of size a_0 should have a finite temperature $T \sim 1/a_0$ [24]. Inclusion of a small bare cosmological constant was also considered in ref. [21]. Furthermore, the analytic continuation to the Euclidean regime was shown to be consistent with the reality of the Euclidean path integral at one-loop [23].

⁵Note the difference in the previous expressions with their Euclidean counterparts in ref. [24]. In the Euclidean region, which is reached in ref. [24] by a Wick rotation of both t and ϕ , one has to replace the hyperbolic functions with the corresponding trigonometric ones in eqs. (B.2.3)–(B.2.4).

We then note that, by using eqs. (B.2.2)–(B.2.4), classically the scalar potential can be written as a function of the scale factor

$$V(a) \equiv V(\phi) = \frac{V_m}{a^{3\gamma}}, \quad (\text{B.2.6})$$

where the constant $V_m \doteq \Omega a_0^{3\gamma}$. Essentially, in doing this identification one has “frozen” the kinetic degree of freedom of the scalar field and is now dealing with a perfect fluid matter source with $\rho = \rho(a)$. From the conservation equation of the energy-momentum tensor the energy density behaves as

$$\rho = \frac{\rho_0}{a^{3\gamma}}, \quad (\text{B.2.7})$$

which is equivalent to the identification $V(\phi) \rightarrow \rho \equiv \rho_0/a^{3\gamma}$.

Before we go on to consider the quantum versions of these wormholes, let us make a few comments about what has been done:

a) the equivalence between the potential $V(\phi)$ and the perfect fluid source $\rho(a)$, eq. (B.2.6), is only valid “on shell” when all the classical equations are satisfied. This equivalence needs not to occur in the quantum theory when only the WDW equation has to be satisfied (see ref. [168]). In the quantum case the potential $V(\phi)$ will contain possibilities of extra solutions since it is not constrained by an additional classical equation;

b) later we will use the general potential $V(\phi)$, which simulates a certain value of γ . However it only does this for a finite time as the scalar field ‘rolls down’ the potential. Eventually the simulation breaks down and either the kinetic or potential energy will dominate, i.e. the effective γ related to the “roll down” along the potential will tend to two or zero. For instance, when $\gamma > 2/3$ the scalar potential has a (positive) cosmological constant ground state as $|\phi| \rightarrow 0$, and the effective γ there is zero. This effect can be overcome by introducing a second scalar field (or equivalently using a complex scalar field) as was also done in ref. [51] when extending the EM approach. A similar problem occurs for the $V(\phi)$ potential when $\gamma < 2/3$. Although in this case there is no cosmological constant ground state, however, on reaching the minimum as $|\phi| \rightarrow \infty$, the potential energy is lost and the effective γ tends to two (the kinetic dominated case), and again the simulation breaks down. Because of this limitation one can not really claim that wormholes with $\gamma < 2/3$ occur in the limit $a \rightarrow \infty$, but only up to a finite scale factor a_{max} . However, this size can be made much greater than the Planck scale, and for all practicality this is not a serious limitation.

B.3 The perfect fluid matter model

We will start our quantum analysis of the CM wormholes for the case in which the matter content of the theory is given by a perfect fluid, i.e. when the kinetic part of the scalar field is “frozen” and the scale factor a becomes the only effective degree of freedom. As mentioned, this will not exhaust all the possible solutions which could be obtained using the more general potential $V(\phi)$.

The WDW equation for a closed universe filled with a perfect fluid matter source takes the form (see, e.g., ref. [197])

$$\left(a^2 \frac{d^2}{da^2} + pa \frac{d}{da} + \rho_0 a^{6-3\gamma} - a^4 \right) \Psi(a) = 0, \quad (\text{B.3.1})$$

where we have substituted from the conservation equation the energy density $\rho = \rho_0/a^{3\gamma}$, with $\rho_0 = a_0^{3\gamma-2}$, and p represents part of the operator ordering ambiguities. A similar ansatz has been considered recently in the context of models for the quantum birth of the universe [130].

We must impose some boundary condition in order to select (if any) the solutions of the WDW which represent quantum wormholes. Here we follow the proposal of HP:

(a) Ψ should decay exponentially as the radius $a \rightarrow \infty$, in fact like $\sim \exp(-a^2/2)$ if the wormhole is asymptotically Euclidean (AE);

(b) Ψ should be well-behaved (regular) at the origin. This is because there should be no singularities as $a \rightarrow 0$.

Moreover, there should be no divergences in the wave function due to the matter content.

In the conclusions we will discuss how the boundary condition for quantum wormholes is related to others used in quantum cosmology, i.e. the HH and Tunneling boundary conditions.

We can get a preliminary idea as to when an Euclidean domain occurs at large a by studying the WDW equation (B.3.1) as an ordinary Schrödinger equation (for the factor ordering $p = 0$)

$$\left[\frac{d^2}{da^2} + U(a) \right] \Psi(a) = 0, \quad (\text{B.3.2})$$

which represents the motion of a ‘particle’ of unit mass and zero energy in the potential $U(a) = \rho_0 a^{4-3\gamma} - a^2$. When $U > 0$ the wave function for large a is oscillating, implying the

existence of a Lorentzian phase (see, e.g., ref. [88]). Therefore, in order to have a quantum wormhole, it is necessary that, at least, $U < 0$. Returning to eq. (B.3.1), and setting the (unimportant in this regard) factor $p = 0$, this occurs for

$$\rho_0 a^{4-3\gamma} - a^2 < 0. \quad (\text{B.3.3})$$

Therefore for the usual case of a positive energy density source ($\rho_0 > 0$, $\gamma < 2$) we require $2 > 4 - 3\gamma$, i.e. $\gamma > 2/3$ for such behaviour. In particular, neglecting the $a^{4-3\gamma}$ term in eq. (B.3.2), it is straightforward to check that the asymptotic behaviour of the wave function for $a \rightarrow \infty$ is, in fact,

$$\Psi(a) \simeq a^{1/2} K_{1/4}(a^2/2) \sim \exp[-a^2/2], \quad (\text{B.3.4})$$

which satisfies the boundary condition **(a)** of HP, giving AE quantum wormholes for $2/3 < \gamma < 2$. This strong energy condition is the same as that obtained by CM for the occurrence of their classical wormhole solutions. It is stronger than (but consistent with) the result of Kim and Page (KP) [120] that quantum wormholes are incompatible with a cosmological constant.

A quantum wormhole also requires a suitable behaviour for small a . As $a \rightarrow 0$ we can ignore the a^4 term, since $4 > 6 - 3\gamma$ when $\gamma > 2/3$. In this case the WDW equation (B.3.1) (for $\gamma \neq 2$) simplifies to a Bessel equation with solution

$$\Psi(a) \simeq a^{(1-p)/2} \left[a_1 J_\nu \left(\frac{2\sqrt{\rho_0}}{3(2-\gamma)} a^{3-3\gamma/2} \right) + a_2 Y_\nu \left(\frac{2\sqrt{\rho_0}}{3(2-\gamma)} a^{3-3\gamma/2} \right) \right], \quad (\text{B.3.5})$$

where $\nu \doteq |1 - p|/[3(2 - \gamma)]$.

Using the asymptotes $J_\nu(z) \sim z^\nu$ and $Y_\nu(z) \sim -z^{-\nu}$, as $z \rightarrow 0$ (see ref. [1]), the wave function can be expressed as

$$\Psi(a) \sim \begin{cases} b_1 a^{1-p} + b_2 & ; p < 1 \\ b_1 + b_2 a^{1-p} & ; p > 1, \end{cases} \quad (\text{B.3.6})$$

which satisfies the regularity boundary condition **(b)** of HP, apart from a possible divergence due to the factor ordering term $\sim a^{1-p}$ when $p > 1$.⁶

For the particular case $\gamma = 2$, the solution of the WDW equation (B.3.1) is a linear combination of Bessel functions, $J_{\pm i\sqrt{\rho_0}/2}(ia^2/2)$, which oscillate an infinite number of times

⁶It has been suggested [119] that even wave functions with this mild divergent behaviour as $a \rightarrow 0$ should still be considered to satisfy the HP condition for wormholes.

at the origin (see ref. [95]), and therefore cannot satisfy the required regularity condition of HP. However, this problem can be overcome using a massless scalar field (see Ref. [95], section 4.1 and the Appendix to this paper).

B.3.1 Two examples

We conclude this first section by giving two explicit examples of solutions of the WDW equation for the “on shell” potential $V(a)$ of a perfect fluid matter model. Although the WDW equation has been simplified to an ordinary differential equation, it is still not straightforward to obtain analytic solutions for all γ . One could proceed by finding approximate WKB solutions. But instead we consider two cases of γ : one satisfying and one violating the strong energy condition. This enables us to emphasize the main properties that any solution in the range $0 \leq \gamma < 2$ should have.

- $\gamma = 4/3$

This example classically represents a radiation (or, equivalently, that of a conformally coupled scalar field) dominated FRW geometry. In this case the WDW equation (B.3.1), for the factor ordering $p = 0$, can be rewritten as

$$\left\{ \frac{d^2}{da^2} + a_0^2 - a^2 \right\} \Psi(a) = 0, \quad (\text{B.3.7})$$

which can be thought of as the Schrödinger equation for a harmonic oscillator with energy a_0^2 . The general solution of eq. (B.3.7) can be expressed as a linear superposition of harmonic wave functions as

$$\Psi(a) = \sum_n c_n \exp(-a^2/2) H_n(a), \quad (\text{B.3.8})$$

where H_n are the Hermite polynomials. Such wave functions are regular at the origin and exponentially damped at infinity, and according to the HP boundary conditions they represent quantum AE wormholes, see fig. (1). The minimum ‘throat’ of the wormholes is quantized, $a_0 = \sqrt{2n+1}$.

- $\gamma = 0$

This example is equivalent to having a cosmological constant as the matter source. In this case the WDW equation (B.3.1), for the factor ordering $p = 0$, can be rewritten as

$$\left\{ \frac{d^2}{da^2} + \frac{a^4}{a_0^2} - a^2 \right\} \Psi(a) = 0. \quad (\text{B.3.9})$$

This is reminiscent of the Schrödinger equation for an anharmonic oscillator, and it can be exactly solved, by a suitable redefinition of variables, in terms of Airy functions as

$$\Psi(a) = d_1 \text{Ai} \left[2^{-2/3} \left(1 - \frac{a^2}{a_0^2} \right) \right] + d_2 \text{Bi} \left[2^{-2/3} \left(1 - \frac{a^2}{a_0^2} \right) \right]. \quad (\text{B.3.10})$$

The wave function (B.3.10) is oscillating for large a (see fig. (2)), and clearly does not resemble a quantum wormhole (as we expected, since $\gamma < 2/3$). Actually, it may be thought as representing the quantum nucleation at the radius a_0 of an expanding Lorentzian inflationary universe.

B.4 The scalar field $V(\phi)$ model

So far we have obtained quantum wormholes with the restriction that the strong energy condition is satisfied. We next extend our analysis of the quantum solutions by studying the WDW equation with the scalar potential $V(\phi)$. This potential gives a wider possibility of solutions and so might also give quantum wormholes when the strong energy condition is violated, i.e. when $\gamma < 2/3$.

This potential is plotted for various values of the parameter γ in figs. (3-5). For $\gamma > 2/3$ a positive minimum occurs when $\phi = 0$. At this point the simulation of γ breaks down and the effective value of γ becomes zero. The potential $V(\phi)$ behaves as a cosmological constant. In order to analyse this region we would have to add an extra field, or equivalently “complexify” the scalar field, to enable the ground state to correspond to $V(\phi) = 0$. We later briefly outline how this should proceed. On the other hand, the simulation of the cases with $\gamma > 2/3$ is still valid in the minisuperspace region of large $|\phi|$, and in this region it is also possible to show the existence of quantum wormholes which are not AE but which still satisfy the HP boundary conditions. These states can be interpreted as representing the excited part of the spectrum of quantum wormholes.

Anyway, as we already know from the analysis of the bulk matter case that wormholes occur for $\gamma > 2/3$, the most interesting case is when $\gamma < 2/3$. In this case, taking the potential $V(\phi)$ for $|\phi| \simeq 0$ would imply an expansion around an (unstable) positive cosmological constant, which KP already showed is inconsistent with the existence of wormholes. However, the scalar potential has a zero ground state $V(\phi) \rightarrow 0$ as $|\phi| \rightarrow \infty$, and we expect quantum wormholes to be possible there. Similarly to the $\gamma > 2/3$ case, again we have to ensure that the simulation of $\gamma < 2/3$ does not break down before the wormhole has an arbitrary large size a . This restriction on the scaling for a , as $a \rightarrow \infty$, also turns out to be a necessary (but not sufficient) condition for the existence of (non AE) quantum wormholes.

B.4.1 Separating the WDW

The WDW equation for a real scalar field model (see, e.g., ref. [88]) in a FRW closed universe is

$$\left[a^2 \frac{\partial^2}{\partial a^2} + pa \frac{\partial}{\partial a} - \frac{\partial^2}{\partial \phi^2} + a^6 V(\phi) - a^4 \right] \Psi(a, \phi) = 0, \quad (\text{B.4.1})$$

where, as in the previous section, p is a factor ordering correction and $V(\phi)$ is given by eq. (B.2.4). As mentioned before, the only minisuperspace region where we can hope to find quantum wormhole solutions with the potential (B.2.4) is where $|\phi| \rightarrow \infty$, i.e. where

$$V(\phi) \simeq [\Omega/2^{2n}] \exp[\lambda_0 |\phi|], \quad (\text{B.4.2})$$

with

$$\lambda_0 \doteq [2n\lambda] \text{sign}(3\gamma - 2) = [3\sqrt{2\gamma}] \text{sign}(3\gamma - 2), \quad (\text{B.4.3})$$

and where the parameters Ω , n and λ are given by eq. (B.2.5). The potential $V(\phi)$ is approximated by an exponential in the case of large $|\phi|$. For simplicity, due to the symmetry of the WDW constraint (B.4.1) with potential (B.4.2) under the reflection $\phi \rightarrow -\phi$, we will only consider the minisuperspace region of positive scalar field, $\phi > 0$.

In order to separate the WDW eq. (B.4.1), we make the following transformation of coordinates in minisuperspace:

$$\begin{aligned} x &\equiv a^\alpha \cosh \alpha \phi, \\ y &\equiv a^\alpha \sinh \alpha \phi, \end{aligned} \quad (\text{B.4.4})$$

where α is an arbitrary constant parameter. This is essentially a generalization of the coordinate transformation originally introduced in ref. [68]. In terms of the new variables x and y , the WDW eq. (B.4.1) becomes (choosing the factor ordering $p = 1$)

$$\left[\frac{\partial^2}{\partial x^2} - \frac{\partial^2}{\partial y^2} + \frac{\Omega(x^2 - y^2)^{3/\alpha-1}}{(2^n \alpha)^2} \left(\frac{x+y}{x-y} \right)^{\lambda_0/2\alpha} - \frac{(x^2 - y^2)^{2/\alpha-1}}{\alpha^2} \right] \Psi(x, y) = 0. \quad (\text{B.4.5})$$

Eq. (B.4.5) can be further simplified by going to the 'null coordinate' ansatz

$$\begin{aligned} u &\equiv x + y = (ae^\phi)^\alpha, \\ v &\equiv x - y = (ae^{-\phi})^\alpha, \end{aligned} \quad (\text{B.4.6})$$

for which we finally obtain

$$\left[\frac{\partial^2}{\partial u \partial v} + \frac{\Omega}{(2^{n+1} \alpha)^2} u^{(6-2\alpha+\lambda_0)/2\alpha} v^{(6-2\alpha-\lambda_0)/2\alpha} - \frac{(uv)^{(2-\alpha)/\alpha}}{(2\alpha)^2} \right] \Psi(u, v) = 0. \quad (\text{B.4.7})$$

In general, due to the presence of the non trivial exponents in the terms u, v in the WDW equation (B.4.7), this equation is not yet exactly separable for an arbitrary value of γ .⁷

Our main idea is then to solve the WDW equation (B.4.7) in the new variables u, v in the minisuperspace regions where, respectively, the third (potential) or last (curvature) term in eq. (B.4.7) dominate. In other words, we can define the ratio

$$R \doteq \frac{\Omega}{2^{2n}} (x^2 - y^2)^{1/\alpha} \left(\frac{x+y}{x-y} \right)^{\lambda_0/2\alpha} = \frac{\Omega}{2^{2n}} u^{1+\lambda_0/2\alpha} v^{1-\lambda_0/2\alpha} = \frac{\Omega}{2^{2n}} a^2 e^{\lambda_0 \phi}, \quad (\text{B.4.8})$$

and separately study the regions where either $R \gg 1$ or $R \ll 1$, neglecting the smaller term in the WDW equation. In particular, as we show in detail in the Appendix to this paper, one can further simplify the WDW in each of these regions by using the freedom in the choice of the parameter α .

As a result of this analysis (see the Appendix to this paper), it is easy to show that, for the case of $2/3 < \gamma \leq 2$ and the potential (B.4.2), the asymptotic behaviour of Ψ is damped but not AE because of the presence of the large potential $V(\phi)$ in the

⁷Although, for some special values of γ , this might be possible. For instance, when $\gamma < 2/3$, for $\lambda_0 = -\alpha = -2$ (i.e. $\gamma = 2/9$) and $\Omega/2^{2n} = 1$ (i.e. $a_0 = 4/3$), our eqs. (B.4.4),(B.4.5) reduce to the (separable) case described by eqs. 2.4, 2.11 of ref. [68] for their potential 2.6 with their $\alpha = -\beta = 1$.

limit of large $|\phi|$, see fig. (4). The resulting solutions can be interpreted, instead, as representing excited states of the quantum wormhole spectrum.

For the case $0 < \gamma < 2/3$ (which is of most interest), non AE excited quantum wormhole states are obtained in different regions of minisuperspace. Only when a cosmological constant is present ($\gamma = 0$) is a quantum wormhole prevented from occurring. In this case, the wavefunction Ψ oscillates for large a , representing a Lorentzian de Sitter universe. However, we should stress that many of these quantum wormholes have been found as particular solutions of the WDW equation in specific regions of minisuperspace, and also some integration constants had to be chosen properly so as to avoid an oscillatory behaviour. Moreover, our choices of coordinates have also facilitated finding wormholes (compare with ref. [190], where a similar exponential potential model was analysed, but where only inflationary solutions were given). This is a consequence of the more general problem of finding a complete set of solutions of the WDW equation, and is related to the ambiguity in the (possible) definition of a corresponding Hilbert space (for a review of these difficulties in quantum gravity see, e.g., ref. [129]). Given the general solution to eq. (B.4.7), it might be interesting to try and quantify, for instance, the number of favourable solutions (i.e. wormholes) to unfavourable ones in a manner reminiscent of ref. [74]. Until then we can at least say that wormholes are less 'robust' when $V(\phi) \gg 0$, although they are still possible.

B.4.2 Complex scalar field with $\gamma > 2/3$

The $V(\phi)$ potential when $\gamma > 2/3$ suffers from the presence of a cosmological constant in its minimum. We have seen that this prevents an AE quantum wormhole from occurring in the minisuperspace region $|\phi| \rightarrow 0$ (see also ref. [120]).

However, by adding a second scalar field, or equivalently taking a single complex scalar field, we can ensure that the potential has a zero minimum, thus providing a good simulation of the $\gamma > 2/3$ equation of state as $|\phi| \rightarrow 0$. A similar method was used by Ellis, Lyth and Mijić [51] to alter the ground state of the potential $V(\phi)$. One should not think of this as implying that a complex scalar field is necessary to have wormhole solutions, but rather as one way of removing the cosmological constant caused by a

limitation of the EM procedure in this case.

If we consider a complex scalar field, its Hermitian Lorentzian Lagrangian is formally given by

$$\mathcal{L} = \partial_\mu \phi \partial^\mu \phi^\dagger - V(\phi \phi^\dagger), \quad (\text{B.4.9})$$

where the complex scalar field is defined as $\phi = \phi_1 + i\phi_2$, with both ϕ_1 and ϕ_2 real. Taking for the potential in eq. (B.4.9)

$$V(\phi) = \Omega \left[\cosh[\lambda\phi] \cosh[\lambda\phi^\dagger] \right]^n, \quad (\text{B.4.10})$$

in the limit that the real part ϕ_1 of the complex scalar field ϕ dominates this becomes

$$V(\phi) \simeq \Omega \cosh^{2n}(\lambda\phi_1), \quad (\text{B.4.11})$$

which is the CM potential of eq. (B.2.4). On the other hand, in the limit that the imaginary part ϕ_2 of the scalar field ϕ dominates, the potential (B.4.10) becomes

$$V(\phi) \simeq \Omega \cos^{2n}(\lambda\phi_2), \quad (\text{B.4.12})$$

see fig. (6).

Let us now concentrate on the form (B.4.12) of the potential (B.4.10), and for simplicity from now on drop the subscript and let $\phi_2 \equiv \phi$. If we expand about the minimum at $\phi = \pi/2$, then the potential (B.4.12) approximates to the power law form

$$V(\phi) \simeq \Omega \lambda^{2n} \phi^{2n}. \quad (\text{B.4.13})$$

Note that a singularity in the scalar potential ($V(\phi) \rightarrow \infty$, as $|\phi| \rightarrow 0$) for $n < 0$ prevents considering the case $\gamma < 2/3$.

The corresponding WDW equation for this scalar field potential is given by

$$\left[a^2 \frac{\partial^2}{\partial a^2} + pa \frac{\partial}{\partial a} - \frac{\partial^2}{\partial \phi^2} + a^6 \Omega \lambda^{2n} \phi^{2n} - a^4 \right] \Psi(a, \phi) = 0, \quad (\text{B.4.14})$$

where p represents, as usual, part of the operator ordering ambiguities.

Quantum wormholes are known to occur for such potentials - (see, e.g., refs. [36], [95], [120], [119], and the Appendix top this paper for details of a simplified derivation of

this result, where we explicitly show the existence of both AE and non AE solutions satisfying the HP boundary conditions).

The form (B.4.12) of the scalar potential is the same as that found by CM (in the Euclidean region) in obtaining their classical wormholes, but there is a difference in the form of the WDW equation. The classical wormholes of CM were achieved using a particular asymmetric Wick rotation for the lapse and the scalar field in going from the Lorentzian to the Euclidean signature regions. Quantizing the Hamiltonian constraint starting from the CM Euclidean action after using this rotation would then correspond to a plus sign in front of the kinetic term $\partial^2/\partial\phi^2$ in equation (B.4.14).

However, it can be shown that quantum wormholes when this different sign is present can also be obtained. The only slight difference between the two cases (when a minus or a plus sign in front of $\partial^2/\partial\phi^2$ is present in eq. (B.4.14)) is when $\gamma = 2$. Taking the plus sign we get quantum wormholes for a massless scalar field without the need of a change of basis for the solutions (or, alternatively, the requirement of an integration of the global wave function $\Psi(a, \phi)$ over the separation constant), which was instead necessary in ref. [95].

B.5 Discussion and Conclusions

We have obtained the quantum analogues of the classical CM wormholes. There are several advantages which make these quantum solutions more general than their classical counterparts. The requirement that the Ricci tensor has a negative eigenvalue, in order to produce a wormhole throat, is no longer necessary in the quantum wormhole. In the classical CM wormhole this requirement was accomplished by using an asymmetric analytic continuation of the matter source. This aspect is included “automatically” in the WDW equation, which does not depend explicitly on the spacetime signature. Quantum wormholes will occur also when a “wrong sign” is imposed in front of the kinetic term in the WDW equation, but this is not necessary, unlike for classical wormholes.

Quantum wormholes occur, for example, when ordinary radiation is present. We saw this using a perfect fluid matter source which does not give all the possible

solutions but does enable many of the known quantum wormholes to be found (e.g. that of radiation or equivalently a conformally coupled scalar field). Other quantum wormholes can be found for any $\gamma > 2/3$, although in general they will not have a simple analytic solution. But, in analogy to the classical case, there is a CM quantum wormhole for any value of γ in the range $2/3 < \gamma < 2$.

We next used the potential $V(\phi)$ which allows a wider set of quantum solutions to be found. By choosing a region of phase space where $|\phi|$ is large, the potential is approximated by an exponential and the WDW equation can be solved by separation of variables. Although this method would not give a general solution it is sufficient to achieve our aim: of showing that wormhole solutions are possible. Using this $V(\phi)$ potential, wormholes could be also obtained when the strong energy condition is violated: something which is not possible for a classical CM wormhole. Only when a cosmological constant is present ($\gamma = 0$) are we unable to find a wavefunction that obeys the HP conditions for a quantum wormhole, so consistent with the results of KP. Even then, the second condition **(b)** regarding the behaviour as $a \rightarrow 0$ is rather easily satisfied for Planck sized wormholes. Looking at the WDW equation (B.4.1) one sees that the potential $V(\phi)$ can be ignored (even if it is constant) for $a < 1$, and this case behaves like a massless scalar field in this limit. One might say that the massless scalar field is the ‘archetypal’ wormhole for small scale factors. However, if wormholes are to play a role in black hole evaporation, it is suspected that their throat should be much larger than the Planck size $a \sim 1 \sim 10^{-33} \text{cm}$. It is therefore necessary to try and satisfy condition **(a)** up to, say, values of $a \sim 10^3$. For a perfect fluid matter source this was found not to be possible when the strong energy condition is violated. However, with a scalar field, although the matter source was violating the strong energy condition, quantum wormholes could still be found, except for the case of a cosmological constant. There exist both AE and non AE quantum wormholes, the latter being interpreted as representing excited states of the wormhole spectrum. Since classical CM wormholes are only possible for $\gamma > 2/3$, these wavefunctions represent an entirely quantum “off shell” phenomena.

It was not really necessary to solve the WDW equation with $V(\phi)$ and $\gamma > 2/3$, since the existence of wormholes had already been established working with a perfect

fluid matter source. If one works with a complex scalar field, then the cosmological groundstate as $|\phi| \rightarrow 0$ can be removed and both AE and non AE quantum wormholes are obtained. Finally, in the minisuperspace region where $|\phi| \gg 1$, for a generic equation of state, we also proved the existence of quantum wormhole states which are not AE.

Because wormholes can be obtained for such a broad range of γ , this suggests, in agreement with HP, that quantum wormholes should be a general phenomena that can occur for a large class of matter sources. One should recall that any actual potential coming from a particle theory, e.g. $V(\phi) = m^2\phi^2$ or $\lambda\phi^4$, has an effective γ in the range $0 \leq \gamma \leq 2$. As the minimum $V(\phi) \rightarrow 0$ is approached, such ϕ^n potentials typically have an effective $\gamma \sim 1$, so satisfying the strong energy condition: the quantum wormholes found by HP for a massive scalar field or $\lambda\phi^4$ can be understood in this way.

Instead, using an exponential potential we have been able to keep the potential “shallow” on approaching the minimum so that the strong energy condition is violated. This extends the viability of quantum wormholes to a much larger class of matter sources. The closed $k = 1$ restriction could also be relaxed to $k = 0$, although it does not seem possible to take open models $k = -1$, probably for reasons given in ref. [176], i.e. the unboundedness of Ψ in open models.

Exponential potentials typically arise in string theories and also in scalar (tensor) higher derivative gravity actions after transforming to the ‘Einstein-Hilbert’ frame (see, e.g., refs. [87]). The string dilaton field (for a constant axion field) could now be a possible source for the quantum wormhole; whereas it usually prevents (depending on the strength of its coupling to the axion field) the classical axion wormhole from occurring, see refs. [75] and [34]. In ref. [34] it was shown that the introduction of an extra (non-minimally coupled to the scalar curvature) scalar field could restore the axion wormhole. Later it was realized [32] that a non-minimally coupled scalar field alone can have wormhole solutions, these can in turn be quantized and quantum wormholes obeying the HP conditions can be obtained, see refs. [32]-[201]. In the context of low energy string theory, Lidsey [135] has also obtained quantum wormholes, although with a value of γ that allows eq. (B.4.7) to be exactly separable. In particular, Lidsey showed that quantum wormholes are still present even after the

addition of extra massless scalar fields, which should also occur in an extension of our model. Only if the low-energy string effective potential behaves like a cosmological constant ($\gamma \simeq 0$) would quantum wormholes be prevented. The next interesting step might be to consider the case of ‘multiplicative’ potentials eg. $V(\phi, \psi) \sim \phi^n \exp(\lambda\psi)$, which typically occur when the dilaton has a non-zero potential in the ‘Jordan’ frame, cf. ref. [87].

We have found that wormhole states can be obtained by imposing the HP boundary condition. In doing so we seem to be losing the possibility of choosing other wavefunctions which might have other favourable characteristics. We have in mind the presence of a Lorentzian regime with wavefunctions that represent inflationary behaviour (i.e., with $V(\phi) \gg 0$).

This point can be understood further by considering the problem of caustics in the WDW equation (for a 2-d minisuperspace FRW ansatz with a homogeneous scalar field) with HH boundary conditions discussed by Grishchuk and Rozhansky [82] (see also ref. [144]). In order to have a realistic model with a Lorentzian region they required the existence of a caustic for the classical Euclidean trajectories. Below a certain value of the scalar field the caustic does not develop and the model remains Euclidean even for large scale factors. But this aspect (of no caustic) is exactly what is required to have the possibility of a wormhole. In other words, the lack of a caustic was first considered a potential problem for the HH boundary condition, but is now being used as a condition for the existence of quantum wormholes in the HP ansatz. However, it is well known that the HH wavefunction grows exponentially like $\sim \exp(a^2)$, in contrast to the exponential decay of the HP one.

The HP boundary condition also differs in a crucial way with the Tunneling boundary condition. Whereas the Tunneling wave function is peaked at a large potential $V(\phi)$, which will tend to produce a Lorentzian regime and inflationary behaviour for $\gamma < 2/3$, the wormhole boundary condition suggests a small potential $V(\phi)$. However, the Tunneling boundary condition does give a wave function which decays exponentially in the Euclidean region, similarly to the HP case.

Recently, the wormhole boundary condition has been claimed to be the more fundamental one [162], requiring the dropping or modification of the other (e.g. HH or

Tunneling) boundary conditions. This was based on the claim that our universe is asymptotically flat and this could be a prediction of the wormhole boundary condition. As our universe is not asymptotically flat (it appears FRW) and is also Lorentzian, other boundary conditions would appear necessary. Especially if we required an inflationary phase during the early history of the universe.⁸ In our view the choice of the ‘correct’ boundary condition in quantum cosmology is still an open issue. The analysis of the so called 3rd quantization [77] of the WDW equation might give some useful hints, since more than one type of solution could be present at once. Otherwise, if there is a correct universal boundary condition for the WDW equation, it is difficult to see how the possibility of wormholes is compatible with an earlier inflationary regime which presumably caused our universe. If during the early universe $V(\phi) \gg 0$, we would expect the universe to be driven large (by an inflationary phase) before quantum wormholes could anyway occur. Could they still influence the resulting large, essentially classical, Lorentzian universe ?

Consider further the implications for the Coleman mechanism for the setting to zero of the cosmological constant. In an earlier version of this paper [35] we had only considered the $V(a)$ potential and had missed seeing the possibility of having wormholes when the strong energy condition is violated. We had argued that there was a contradiction in that wormholes are incompatible with a Λ term. What we notice is that, as mentioned in ref. [77], the wormhole mechanism might first require $\Lambda \ll 1$, this initial constraint presumably coming from some other mechanism, e.g. supersymmetry. Once Λ attains this “small” value, wormholes would then be possible and could proceed in setting Λ infinitesimally close to zero [28]. Recall that one is trying to explain the current value of $\Lambda \sim 10^{-120}$. However, we are still left with the problem of how the boundary conditions responsible for wormholes are compatible with Lorentzian or inflationary behaviour. A related problem is that: if the Tunneling boundary condition and wormholes could coexist, the Coleman mechanism would work in the opposite direction, setting $\Lambda \sim 1$, i.e. large [31]. Note that while the boundary conditions that enable the Coleman mechanism to proceed, given wormholes, are fairly general (the Tunneling boundary condition is an exception) we have found that obtaining

⁸Some authors do not seem to have a problem with this, saying a “dynamical” value for Λ , unaffected by the wormhole mechanism, could occur, cf. ref. [66].

wormholes themselves is a more restrictive requirement. Restrictive, in the sense that they might preclude other things from occurring, e.g. inflation. Within the Coleman mechanism, it might be preferable to try and do without wormholes *per se*, and rather other things, e.g. axions, torsion [38], could simulate their effects. One would then not have to impose the restrictive wormhole boundary condition, but rather concentrate on the boundary conditions explaining our large Lorentzian universe with its possible past inflationary epoch.

University of Cape Town

Acknowledgements

We would like to thank Prof. G.F.R. Ellis for helpful comments and suggestions during the course of this work. We should also thank Drs. L.J. Garay, G. A. Mena Marugan and D. Wands for various interesting and helpful discussions. A.C. is deeply indebted to Dr. M. Mijić for having shared his original ideas on classical wormholes.

A.C. research was mainly supported by an individual EEC fellowship in the 'Human Capital and Mobility' program, under contract No. ERBCHBICT930313, and, since February 1996 by the JSPS postdoctoral fellowship No. P95196.

University of Cape Town

B.6 Appendix

B.6.1 Quantum wormholes with $V(\phi) \sim \exp(\lambda\phi)$ and $|\phi| \rightarrow \infty$

We wish to study the WDW eq. (B.4.7) in the limit of large $\phi > 0$ by considering the minisuperspace regions where the ratio defined in eq. (B.4.8) is either $R \gg 1$ or $R \ll 1$. In each of these regions, in fact, the WDW eq. (B.4.7) can now be easily solved with the variables u, v . In order to prove that quantum wormholes are present within these solutions, we need to show that the two conditions **(a)** and **(b)** of HP can be satisfied. There is enough freedom to achieve this, since, within the ratio (B.4.8), we can have different scaling behaviours of the a and ϕ variables, which are not constrained by the general solutions (this is because u and v are functions of both a and ϕ).

- $2/3 < \gamma \leq 2$

– $a \rightarrow \infty$

When $2/3 < \gamma < 2$, we see from eq. (B.4.3) that $\lambda_0 > 0$ and, therefore, in the limit of large scale factor $a \rightarrow \infty$, only the case $R \gg 1$ for the ratio (B.4.8) is possible. In this limit we are effectively ignoring the spatial curvature term, that is the last term in the WDW eq. (B.4.7), which then becomes

$$\left[\frac{\partial^2}{\partial u \partial v} + \frac{\Omega}{(2^{n+1}\alpha)^2} u^{(6-2\alpha+\lambda_0)/2\alpha} v^{(6-2\alpha-\lambda_0)/2\alpha} \right] \Psi(u, v) \simeq 0. \quad (\text{B.6.1})$$

It is straightforward to find that a particular solution of eq. (B.6.1) is given by

$$\Psi(u, v) \simeq A \exp \left[B u^{(6+\lambda_0)/2\alpha} - (CB)^{-1} v^{(6-\lambda_0)/2\alpha} \right], \quad (\text{B.6.2})$$

where A and B ($B \neq 0$) are two arbitrary integration constants and we have defined $C \doteq [3 \cdot 2^{(n+1)} a_0]^2$ ($C > 0$). One can immediately check (just using eq. (B.4.3)) that the exponents of the u, v variables in eq. (B.6.2) are such that $6 \pm \lambda_0 > 0$, for any $0 < \gamma \leq 2$. Then, using the definitions (B.4.6) for the variables u and v , it can be easily shown that, in the minisuperspace region of large scale factor (with large ϕ) and for $\gamma > 2/3$, we always have $u^{(6+\lambda_0)/2\alpha} \gg v^{(6-\lambda_0)/2\alpha}$. In

other words, the dominant contribution to the asymptotic wave function (B.6.2) is given by the u term and reads, in the variables a and ϕ

$$\Psi(a, \phi) \simeq A \exp \left[B(ae^\phi)^{(6+\lambda_0)/2} \right]. \quad (\text{B.6.3})$$

Therefore, since in this minisuperspace region $a \exp[\phi] \rightarrow \infty$, the asymptotic wave function can be damped for large scale factors and thus satisfy the boundary condition (a) of HP provided that $B < 0$.

– $a \rightarrow 0$

In the case when $a \rightarrow 0$, from eq. (B.4.6) we clearly have that $v \rightarrow 0$. On the other hand, we can have two possibilities for the ratio (B.4.8), i.e. either $R \gg 1$ or $R \ll 1$.

In the former case, or in the minisuperspace region where $a \exp[\lambda_0 \phi/2] \rightarrow \infty$, the WDW equation again can be approximated by formula (B.6.1), with the general solutions given by eq. (B.6.2). There are still further possibilities for the asymptotics of eq. (B.6.2), depending on the relative scaling of a and ϕ , since, for $2/3 < \gamma < 2$ we have that $\exp[-\lambda\phi/2] \ll \exp[-6\phi/\lambda] \ll \exp[-\phi]$ (see eq. (B.4.3)). In particular, in the minisuperspace region where $a \exp[6\phi/\lambda] \rightarrow \infty$ the u term dominates in the wave function (B.6.2), whose asymptotics is then given again by eq. (B.6.3). The wave function (B.6.3) can be regular for small a (and thus be consistent with the boundary condition (b) of HP) either for $\exp[-6\phi/\lambda] \ll a \ll \exp[-\phi]$, or for $a \exp[\phi] \rightarrow \infty$ and $B < 0$. Moreover, in the region where $\exp[-\lambda\phi/2] \ll a \ll \exp[-6\phi/\lambda]$, it is the v term which dominates in eq. (B.6.2), whose asymptotics in terms of the a and ϕ variables is given by

$$\Psi(a, \phi) \simeq A \exp \left[-(CB)^{-1} (ae^{-\phi})^{(6-\lambda)/2} \right]. \quad (\text{B.6.4})$$

Since we have that $a \exp[-\phi] \rightarrow 0$, the wave function (B.6.4) is always regular for small scale factor and thus satisfies condition (b) of HP.

The other possibility is that we have the scaling $a \exp[\lambda\phi/2] \rightarrow 0$. In this region of minisuperspace we can neglect the potential term in the WDW eq. (B.4.7), and if we make the further choice of the parameter

$$\alpha \doteq 1, \quad (\text{B.6.5})$$

the WDW equation simplifies, in the x, y coordinates, to the form

$$\left[\frac{\partial^2}{\partial x^2} - \frac{\partial^2}{\partial y^2} - x^2 + y^2 \right] \Psi(x, y) \simeq 0, \quad (\text{B.6.6})$$

which is easily separated as a system of two coupled harmonic oscillators in the variables x and y . This system has already been extensively studied in the literature (see, for instance, refs. [95] and [67]). In particular, one can express the solutions of the WDW eq. (B.6.6) as a linear combination of

$$\Psi_n(x, y) \simeq \psi_n(x)\psi_n(y) \quad ; \quad \psi_n(x) \doteq (n!2^n)H_n(x)e^{-x^2/2}, \quad (\text{B.6.7})$$

which, in the variables a and ϕ , read

$$\Psi_n(a, \phi) \simeq \left[(n!2^n)H_n\left(\frac{ae^\phi}{2}\right) \right]^2 \exp[-a^2e^{2\phi}/4]. \quad (\text{B.6.8})$$

It is easy to see that these wave functions, for any relative scaling of the variables a and ϕ , are bounded and regular as $a \rightarrow 0$, i.e. they satisfy the boundary condition (b) of HP.

In conclusion, the scalar field potential $V(\phi)$ given by eq. (B.4.2) can be consistent with the existence of quantum wormholes in the sense of HP for $2/3 < \gamma \leq 2$.⁹ The global asymptotic wave function is given by eq. (B.6.3) in the minisuperspace region of large scale factor a , and in that of small scale factor where $a \exp[6\phi/\lambda] \rightarrow \infty$, while it is given by eq. (B.6.4) in the region of small scale factor where $\exp[-\lambda\phi/2] \ll a \ll \exp[-6\phi/\lambda]$. Finally, it is given by (B.6.8) in the minisuperspace region where $a \rightarrow 0$ and $a \exp[\lambda\phi/2] \rightarrow 0$. Since the asymptotic form of the wave function at large scale factor is always damped but not AE, we interpret these solutions as representing excited states of the quantum wormhole spectrum. Note that the wormhole requirements can be satisfied within in the regime $R \gg 0$ when the spatial curvature term has been ignored. This suggests that the spatial curvature may not be a necessary condition for such solutions, cf. ref. [135].

- $0 < \gamma < 2/3$

⁹The special case $\gamma = 2$, representing the model of a massless, minimally coupled scalar field, corresponds to the ansatz $R = 0$, for which the solutions (B.6.7)–(B.6.8) are exact (see refs. [95] and [67]).

– $a \rightarrow \infty$

In the case of large a , since $\lambda_0 < 0$ for $\gamma < 2/3$ (cf. eq. (B.4.3)), we can see from eq. (B.4.8) that there are two possibilities, i.e. either $R \rightarrow \infty$ or $R \rightarrow 0$, depending on the relative scaling of a and ϕ .

In particular, for the case when $R \gg 1$, i.e. for the scaling $a \exp(-|\lambda|\phi/2) \rightarrow \infty$, the WDW reduces again to eq. (B.6.1), with solutions (B.6.2). As in the previous paragraph, we can have two further possibilities depending on the behaviour of the two terms in the argument of the exponential in eq. (B.6.2), since, for $\gamma < 2/3$, we have that $\exp(|\lambda|\phi/2) \ll \exp(6\phi/|\lambda|)$. When the u term part dominates in eq. (B.6.2), i.e. when $\exp(|\lambda|\phi/2) \ll a \ll \exp(6\phi/|\lambda|)$, the asymptotic wave function is again given by eq. (B.6.3), and is damped and consistent with condition (a) of HP for $B < 0$. On the other hand, when the v term part dominates, i.e. when we have the scaling $a \exp(-6\phi/|\lambda|) \rightarrow \infty$, the asymptotic wave function for large scale factor is given by eq. (B.6.4). Since in this minisuperspace region we have that $a \exp[-\phi] \rightarrow \infty$, also this wave function can be damped for large factor and thus satisfies condition (a) of HP provided that $B > 0$.

Finally, we have the minisuperspace region in which $R \ll 1$, i.e. where we have the scaling $a \exp(-|\lambda|\phi/2) \rightarrow 0$. In this case the WDW equation again approximates to formula (B.6.6), which is then solved in terms of the harmonic oscillator wave functions (B.6.8). This wave function is clearly damped for large scale factor a (although not AE due to the presence of the extra scalar field contribution in the exponential), and thus satisfies the boundary condition (a) of HP.

– $a \rightarrow 0$

In the case when $a \rightarrow 0$ one can see that, for $\gamma < 2/3$, the only possibility for the ratio (B.4.8) is that $R \ll 1$, i.e. that we have the scaling $a \exp(-|\lambda|\phi/2) \rightarrow 0$. This is the same case as the one considered in the last paragraph, leading to the harmonic oscillator solutions (B.6.8), which are clearly regular for small scale factor and satisfy condition (b) of HP.

In conclusion, the scalar field potential (B.4.2) is consistent with the existence of quantum HP wormholes also in the case $0 < \gamma < 2/3$. The global asymptotic wave function is given by eq. (B.6.4) in the minisuperspace region where, for $a \rightarrow \infty$, $a \exp(-6\phi/|\lambda|) \rightarrow \infty$, by eq. (B.6.3) in the minisuperspace region where $a \rightarrow \infty$ and $\exp(|\lambda|\phi/2) \ll a \ll \exp(6\phi/|\lambda|)$, and finally by eq. (B.6.8) in the region where $a \rightarrow \infty$ and $a \exp(-|\lambda|\phi/2) \rightarrow 0$, or where $a \rightarrow 0$. Since the asymptotic form of the wave function at large scale factor is never AE, also these solutions are interpreted to represent excited quantum wormhole states.

Additional power-series solutions of the WDW equation

Additional solutions to eq. (B.6.1) can be obtained in the form of power series, $\Psi(u, v) = \sum_{m=0}^{\infty} \Phi_m(u, v)$, by using the method of successive approximations and quadratures, as done by Lidsey [135]. In fact, if we first rescale the variables u, v such that

$$V = v^{(6-\lambda_0)/(6+\lambda_0)} \quad ; \quad U = u, \quad (\text{B.6.9})$$

then eq. (B.6.1) can be recast in the form

$$\left[\frac{\partial^2}{\partial U \partial V} + K^2 (UV)^{(6-2\alpha+\lambda_0)/2\alpha} \right] \Psi(U, V) = 0, \quad (\text{B.6.10})$$

where we have defined $K^2 \equiv \Omega(6 + \lambda_0)/(6 - \lambda_0)(2^{n+1}\alpha)^2 > 0$. Eq. (B.6.10) is now in the 'canonical form' of eq. 3.6 in ref. [135], provided we identify

$$\alpha_L^2 = -4K^2 \quad ; \quad D_L = \frac{6 + 2\alpha + \lambda_0}{2\alpha}, \quad (\text{B.6.11})$$

where the subscript L denotes quantities defined in ref. [135]. The series solutions are given in our case (cf. eq. 4.11 in ref. [135]) by

$$\Psi(U, V) = \Phi_0(U, V) \left[1 + \sum_{m=1}^{\infty} \frac{(-1)^m \left[2K\alpha (UV)^{\frac{\zeta_{\pm}}{4\alpha}} \right]^{2m}}{\zeta_+^m m!(\zeta_+ + a)(2\zeta_+ + a) \cdots (m\zeta_+ + a)} \right], \quad (\text{B.6.12})$$

where we have defined $\zeta_{\pm} \equiv \lambda \pm 6$ and $a \equiv 2b\alpha$, and for $\Phi_0(U, V) \equiv U^b + V^b$, with b constant. In particular (turning to the a and ϕ variables via eqs. (B.4.4), (B.4.6) and (B.6.9)), closed solutions can be given in the following cases:

$$b = 0 \quad ; \quad \Psi_I(a, \phi) = J_0 \left(\frac{4K\alpha (ae^{\lambda\phi/6})^3}{\zeta_+} \right); \quad (\text{B.6.13})$$

$$b = \frac{\zeta_+}{4\alpha} \quad ; \quad \Psi_{II} = \left[(ae^\phi)^{-\zeta_+/4} + (ae^{-\phi})^{\zeta_-/4} \right] \sin \left(\frac{4K\alpha(ae^{\lambda\phi/6})^3}{\zeta_+} \right) ; \quad (\text{B.6.14})$$

$$b = -\frac{\zeta_+}{4\alpha} \quad ; \quad \Psi_{III} = \left[(ae^\phi)^{-\zeta_+/4} + (ae^{-\phi})^{\zeta_-/4} \right] \cos \left(\frac{4K\alpha(ae^{\lambda\phi/6})^3}{\zeta_+} \right) . \quad (\text{B.6.15})$$

In particular, $\Psi_I(a, \phi)$ is simply the Hartle-Hawking wavefunction for this model (see, e.g., ref. [94]), which is oscillating for large scale factor independently of γ . Moreover, for $\gamma > 2/3$, it is fairly easy to see that the remaining two solutions $\Psi_{(II,III)}$ are also oscillating for large a . However, in the case $\gamma < 2/3$, one can still find some restricted minisuperspace regions where the wave function Ψ_{II} can satisfy the HP boundary conditions. In particular, a straightforward computation shows that this solution can be damped as $a \rightarrow \infty$ provided that $a \exp[-|\lambda|\phi/6] \rightarrow 0$ (with the exponentially suppressed asymptotics being of the form $(a \exp[-\phi])^{(6+|\lambda|)/4}$), and regular as $a \rightarrow 0$ provided that $a \exp[\phi] \rightarrow 0$ (with asymptotics of the form $(a \exp[\phi])^{(6-|\lambda|)/4}$).¹⁰

B.6.2 Quantum wormholes with $V(\phi) \sim \phi^{2n}$ and $|\phi| \rightarrow 0$

We wish to explicitly show the existence of quantum wormholes with a power law scalar field potential of the form

$$V(\phi) \simeq \Omega \lambda^{2n} \phi^{2n} \doteq \epsilon \phi^{2n} , \quad (\text{B.6.16})$$

with $|\phi| \rightarrow 0$ and $n > 0$ (i.e., $\gamma > 2/3$).¹¹ Also in this minisuperspace region, the problem of solving the WDW equation (B.4.14) can be simplified by using the new coordinates (B.4.4). This time, however, it turns out more convenient to start with the following choice for the parameter α , i.e.

$$\alpha \doteq \frac{3}{n+1} . \quad (\text{B.6.17})$$

Rewriting the WDW eq. (B.4.14) in terms of the variables x, y , with the potential (B.6.16) and using formula (B.6.17), we obtain

$$0 = \left[\frac{\partial^2}{\partial x^2} - \frac{\partial^2}{\partial y^2} + \Omega \left[\frac{\lambda^n (n+1)}{3} \right]^2 (x^2 - y^2)^n \left[\left(\frac{n+1}{3} \right) \tanh^{-1} \left(\frac{y}{x} \right) \right]^{2n} - \left(\frac{n+1}{3} \right)^2 (x^2 - y^2)^{(2n-1)/3} \right] \Psi(x, y) . \quad (\text{B.6.18})$$

¹⁰Because these wormholes have been obtained while neglecting the curvature term, this suggests wormholes may also be allowed for $k \neq 1$, see ref. [82].

¹¹Again, for simplicity, due to the explicit symmetric form of the WDW operator under the transformation $\phi \rightarrow -\phi$, we confine ourselves to the case $\phi > 0$.

Eq. (B.6.18) can be further simplified by noting that, in the (relevant) minisuperspace region where $\phi \rightarrow 0^+$, from eqs. (B.4.4) we have $y/x \simeq 3\phi/(n+1) \ll 1$. In other words, one can make a Taylor expansion in the WDW eq. (B.6.18) in the small variable $z \equiv y/x$, thus finally getting

$$\left[\frac{\partial^2}{\partial x^2} - \frac{\partial^2}{\partial y^2} + \rho^2 y^{2n} - \tau^2 x^{2(2n-1)/3} \right] \Psi(x, y) \simeq 0, \quad (\text{B.6.19})$$

where we have defined the parameters $\rho^2 \doteq \Omega \lambda^{2n} \tau^{2(n+1)}$ and $\tau \doteq (n+1)/3$ (and neglected terms of order $y^{2n}(y/x)^2$ and $x^{2(2n-1)/3}(y/x)^2$).

Eq. (B.6.19) is then easily separated as

$$\left[\frac{d^2}{dx^2} - \tau^2 x^{2(2n-1)/3} - \nu^2 \right] \psi(x) \simeq 0, \quad (\text{B.6.20})$$

$$\left[\frac{d^2}{dy^2} - \rho^2 y^{2n} - \nu^2 \right] \Phi(y) = 0, \quad (\text{B.6.21})$$

where ν^2 is a separation constant. We can now study the solutions of the system of equations (B.6.20)–(B.6.21) separately in the regions of large and small scale factor a for $\gamma > 2/3$.

- $2/3 < \gamma \leq 2$

– $a \rightarrow \infty$

When $a \rightarrow \infty$, $\phi \rightarrow 0^+$ and $\gamma > 2/3$, it is easy to see from eqs. (B.2.5) and (B.4.4) that, since $n + 1 > 0$ and $x \simeq a^{3/(n+1)}$, the only possibility for x is that $x \rightarrow \infty$. On the other hand, for the variable $y \simeq 3a^{3/(n+1)}\phi/(n + 1)$ we can have two possibilities, either $y \rightarrow 0$ or $y \rightarrow \infty$, depending on the relative scaling between a and ϕ in the combination $a^{3/(n+1)}\phi$.

Let us consider the x -dependent part of the wave function first. Checking from eq. (B.2.5) that also $2n - 1 > 0$ for $\gamma > 2/3$, as $x \rightarrow \infty$ we can neglect the ν^2 term in eq. (B.6.20), which is then solved in terms of the modified I and K Bessel functions as

$$\psi(x) \simeq x^{1/2} \left[l_1 K_{1/4\tau} \left(\frac{x^{2\tau}}{2} \right) + l_2 I_{1/4\tau} \left(\frac{x^{2\tau}}{2} \right) \right]. \quad (\text{B.6.22})$$

Let us then study the y -dependent part of the wave function in the case of the scaling $a^{3/(n+1)}\phi \rightarrow 0$, i.e. when $y \rightarrow 0$. In this limit, since from eq. (B.2.5) we have that $n > 0$, we can neglect the y^{2n} term in eq. (B.6.21), and we get the solution

$$\Phi(y) \simeq m_1 e^{\nu y} + m_2 e^{-\nu y}. \quad (\text{B.6.23})$$

It is straightforward to check that the global asymptotic wave function, which is the product of eqs. (B.6.22) and (B.6.23), can be damped at large scale factors provided one chooses $l_2 = 0$ in eq. (B.6.22), and in terms of the variables a and ϕ explicitly reads

$$\begin{aligned} \Psi(a, \phi) \simeq & a^{(1-2n)/2(n+1)} \left[m_1 \exp \left(-(a^2/2)[1 - 6\nu a^{(1-2n)/(n+1)}\phi/(n+1)] \right) \right. \\ & \left. + m_2 \exp \left(-(a^2/2)[1 + 6\nu a^{(1-2n)/(n+1)}\phi/(n+1)] \right) \right]. \quad (\text{B.6.24}) \end{aligned}$$

In this case, the wave function satisfies the boundary condition (a) of HP for a quantum wormhole, and it is of AE form.

In the other scaling limit, i.e. in the minisuperspace region where $a^{3/(n+1)}\phi \rightarrow \infty$, or $y \rightarrow \infty$, we can instead neglect the ν^2 term in eq. (B.6.21), and we get the y -dependent part of the solution expressed in terms of modified K and I Bessel functions

$$\Phi(y) \simeq y^{1/2} \left[n_1 K_{1/2(n+1)} \left(\frac{\rho}{(n+1)} y^{n+1} \right) + n_2 I_{1/2(n+1)} \left(\frac{\rho}{(n+1)} y^{n+1} \right) \right]. \quad (\text{B.6.25})$$

In this case, the form of the global wave function in the limit of large scale factor is the product of the functions (B.6.22) and (B.6.25). There are still two more possibilities in this case, depending on the scaling of a and ϕ . In particular, in the limit $a^{3/(n+1)}\phi \rightarrow \infty$, but with $a^{1/(n+1)}\phi \rightarrow 0$ (for $a \rightarrow \infty$ and $\phi \rightarrow 0^+$), the global wave function can be asymptotically damped in this minisuperspace region provided we take $l_2 = 0$ in eq. (B.6.22), and in the variables a and ϕ explicitly reads

$$\begin{aligned} \Psi(a, \phi) \simeq & a^{(1-5n)/2(n+1)} \phi^{-n/2} \left[p_1 \exp \left(-(a^2/2)[1 + 2\xi a \phi^{n+1}] \right) \right. \\ & \left. + p_2 \exp \left(-(a^2/2)[1 - 2\xi a \phi^{n+1}] \right) \right], \end{aligned} \quad (\text{B.6.26})$$

where we have introduced the parameter $\xi \doteq \sqrt{3\Omega} \lambda^n / (n+1)^{3/2}$. The wave function (B.6.26) satisfies the boundary condition (a) of HP for an AE quantum wormhole.

Finally, in the region of large y , there is also the possible scaling $a^{1/(n+1)}\phi \rightarrow \infty$ (for $a \rightarrow \infty$ and $\phi \rightarrow 0^+$), and in this case the global wave function is still asymptotically damped provided we take $n_2 = 0$ in eq. (B.6.25), and explicitly reads, in the variables a and ϕ ,

$$\begin{aligned} \Psi(a, \phi) \simeq & a^{(1-5n)/2(n+1)} \phi^{-n/2} \left[q_1 \exp \left(-\xi a^3 \phi^{n+1} [1 + (2\xi a \phi^{n+1})^{-1}] \right) \right. \\ & \left. + q_2 \exp \left(-\xi a^3 \phi^{n+1} [1 - (2\xi a \phi^{n+1})^{-1}] \right) \right]. \end{aligned} \quad (\text{B.6.27})$$

Although this wave function satisfies the HP boundary condition (a), it is clearly not AE.

– $a \rightarrow 0$

In the case when $a \rightarrow 0$ (and $\phi \rightarrow 0^+$), one clearly sees from eqs. (B.4.4) (for $\gamma > 2/3$ and for α given by eq. (B.6.17)) that the only possibility is that both $x \rightarrow 0$ and $y \rightarrow 0$. In other words (since $n, 2n - 1 > 0$), one can study the solutions of eqs. (B.6.20)–(B.6.21) by neglecting the contributions of the terms, respectively, $x^{2(2n-1)/3}$ and y^{2n} . While the y -dependent part of the wave function is still given by eq. (B.6.23), the x -dependent part now reads

$$\psi(x) \simeq r_1 e^{\nu x} + r_2 e^{-\nu x} . \quad (\text{B.6.28})$$

The global wave function in the limit of small scale factor is then the product of eqs. (B.6.23) and (B.6.28), and in the variables a and ϕ reads

$$\begin{aligned} \Psi(a, \phi) &\simeq \left[r_1 \exp[\nu a^{3/(n+1)}] + r_2 \exp[-\nu a^{3/(n+1)}] \right] \\ &\times \left[m_1 \exp\left(3\nu a^{3/(n+1)}\phi/(n+1)\right) \right. \\ &\left. + m_2 \exp\left(-3\nu a^{3/(n+1)}\phi/(n+1)\right) \right] , \end{aligned} \quad (\text{B.6.29})$$

which is regular for $a \rightarrow 0$ and thus satisfies the boundary condition (b) of HP for the existence of quantum wormholes.

In conclusion, also the scalar field potential $V(\phi)$ given by eq. (B.6.16) is consistent with the existence of quantum wormholes in the sense of HP for $2/3 < \gamma \leq 2$. The global asymptotic wave function for $a \rightarrow 0$ is always given by eq. (B.6.29), while for $a \rightarrow \infty$ it is given by eq. (B.6.24) in the minisuperspace region where $a^{3/(n+1)}\phi \rightarrow 0$, and by eq. (B.6.26) in the minisuperspace region where $a^{3/(n+1)}\phi \rightarrow \infty$ and $a^{1/(n+1)}\phi \rightarrow 0$. In these cases the wave function represents AE quantum wormholes in the sense of HP. Finally, in the minisuperspace region where, for $a \rightarrow \infty$, $a^{1/(n+1)}\phi \rightarrow \infty$, the global asymptotic form of the wave function for large scale factor is given by eq. (B.6.27). Since this wave function is damped, but not AE, we again interpret this solution as representing an excited state of the HP quantum wormhole spectrum.

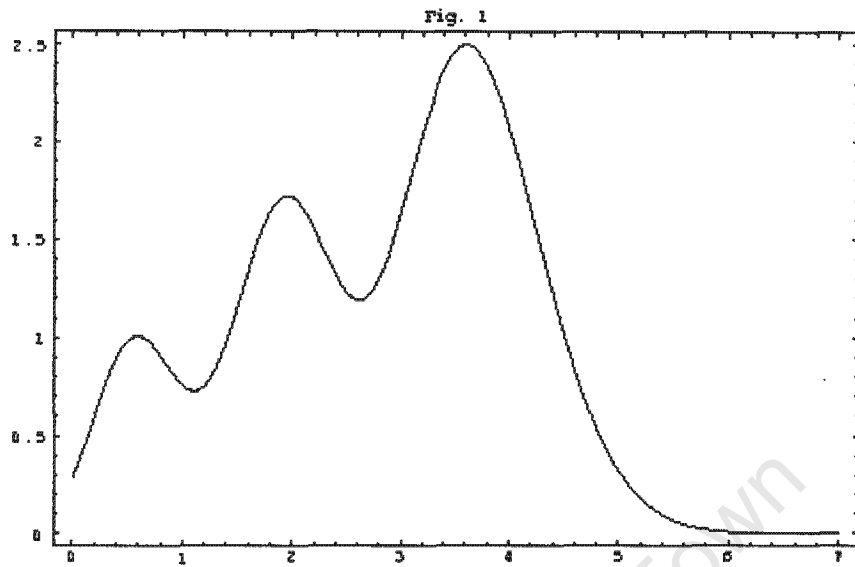


Figure B.1: The wave function for a perfect fluid model with $\gamma = 4/3$ (we have plotted the sum in eq. B.3.8 for $n \in [0, 10]$).

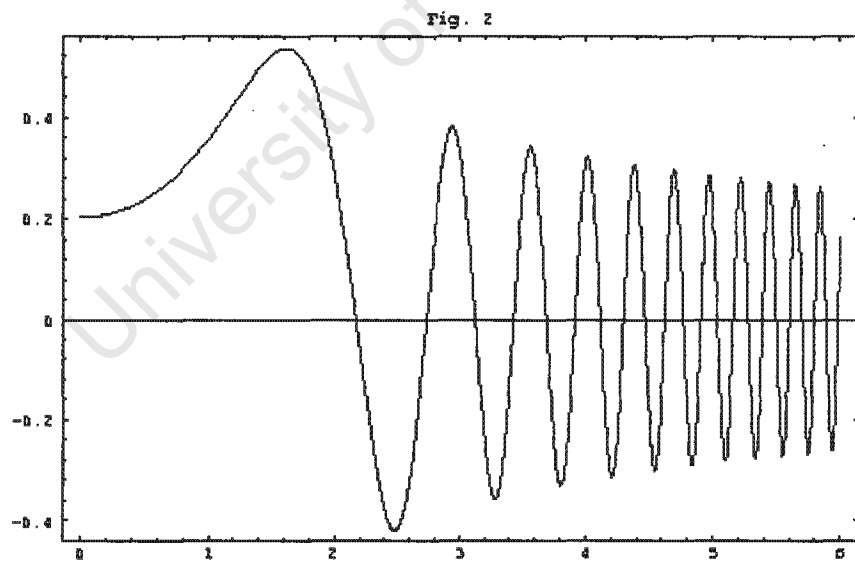


Figure B.2: The wave function for a perfect fluid model with $\gamma = 0$ (we have plotted eq. B.3.10 for $d_2 = 0$ and $a_0 = 1$).

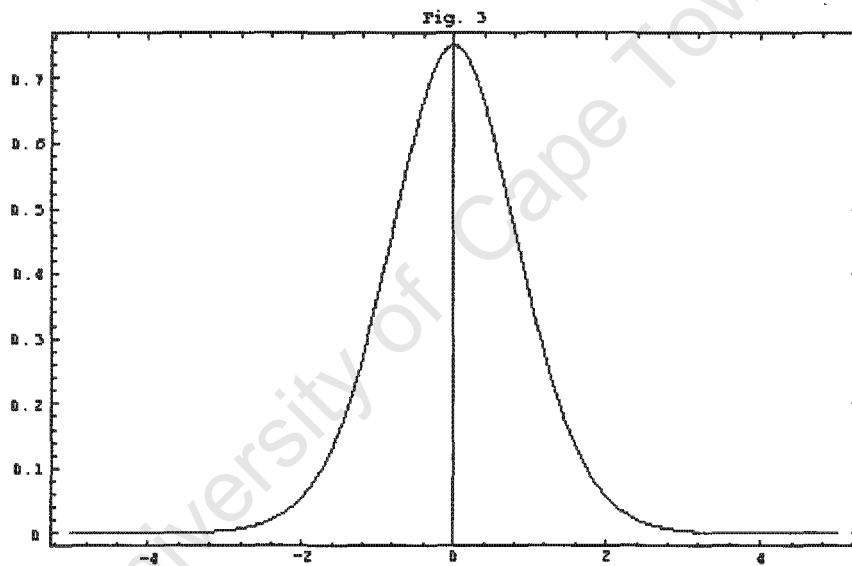


Figure B.3: The potential $V(\phi) = \Omega \cosh^{2n} \lambda\phi$ for $\gamma = 1/2$.

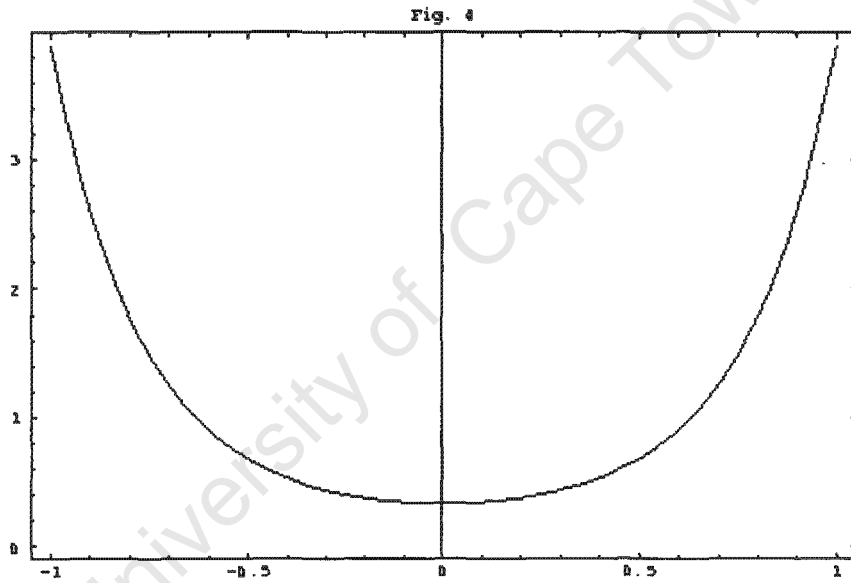


Figure B.4: The potential $V(\phi) = \Omega \cosh^{2n} \lambda\phi$ for $\gamma = 4/3$.

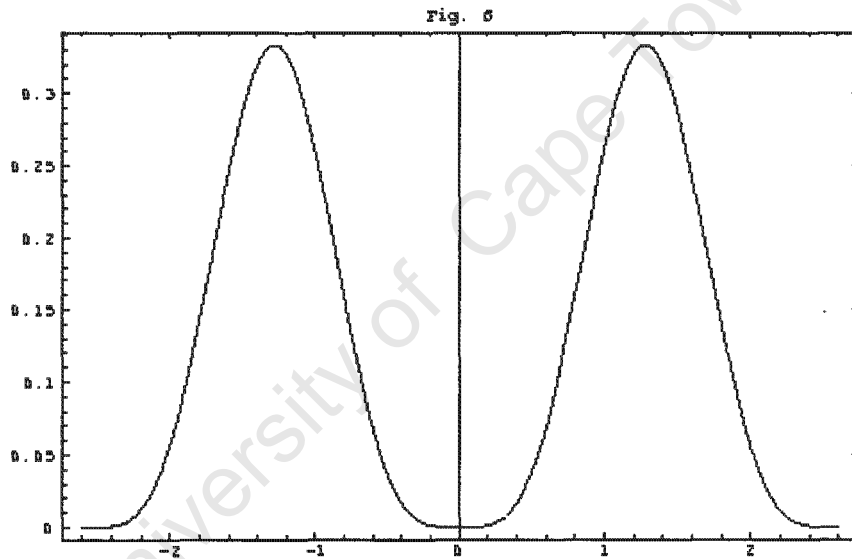


Figure B.5: The potential $V(\phi) = \Omega \cos^{2n} \lambda\phi_2$ for $\gamma = 4/3$ and $\lambda\phi_2 \rightarrow \lambda\phi - \pi/2$.

Appendix C

Classical and quantum wormholes with perfect fluids and scalar fields

Appeared in *Mod. Phys. Lett. A* No 18 (1996) 1453-1465.

A. Carlini \diamond ^{† 1} D.H. Coule \diamond and D.M. Solomons ^{* 2}

\diamond NORDITA, Blegdamsvej 17, DK-2100 Copenhagen Ø, Denmark

[†]Tokyo Institute of Technology, Physics Department,
Oh-Okayama, Meguro-ku, Tokyo 152, Japan

^{*}Department of Applied Mathematics, University of Cape Town,
Rondebosch 7700, South Africa

Abstract

Euclidean wormholes are obtained by the analytic continuation of closed recollapsing Friedmann Robertson Walker universes. We demonstrate this for a perfect fluid satisfying the strong energy condition. The quantum versions of such wormholes are consistent with the Hawking-Page (HP) conjecture for quantum wormholes as solutions of the Wheeler-DeWitt equation. We contrast this with a classical change of signature approach which,

¹Email: carlini@th.phys.titech.ac.jp

²Email: deon@maths.uct.ac.za

although might be consistent with the existence of classical wormholes for a given definition of the energy-momentum tensor of the fluid, upon quantization gives everywhere oscillatory wavefunctions which do not satisfy the HP conjecture.

C.1 Introduction

One possible solution to the cosmological constant (Λ) problem that had attracted a lot of interest in the recent years was due to the idea that wormhole solutions can lead Λ to become a dynamical variable with a distribution function $P(\Lambda)$ [28] - for a review of this proposal see, e.g., Ref. [242]. It was suggested that this function is peaked, due to de Sitter instantons, with the Baum-Coleman-Hawking factor $P(\Lambda) \sim \exp(1/\Lambda)$, so predicting $\Lambda \rightarrow 0$ [28, 7, 75]. Wormholes are used in two distinct ways in such arguments. Firstly they are used to justify why Λ should be treated as a dynamical quantum variable instead of a usual classical variable. This is the most important aspect, as it allows one to make predictions of the possible values of Λ . Wormholes have further been used in connecting many universes together, which produces a further exponentiation [28], i.e.

$$P(\Lambda) \sim \exp(\exp(1/\Lambda)) \quad (\text{C.1.1})$$

This is only useful if the first factor $\sim 1/\Lambda$ is correct (see, e.g. [184]). In other words, this aspect of wormholes only exaggerates any underlying behaviour. In general, Euclidean wormholes can represent quantum tunnelling between different topology regardless of their possible influence on the value of Λ . Classical wormhole solutions and their dependence on the kind of matter source might also be relevant to the saddle point evaluation of the (Euclidean) path integral of interacting quantum gravity.

An open and interesting issue is whether Euclidean wormholes can occur for fairly general matter sources. It is well known that classical wormholes can occur if the Ricci tensor has a negative eigenvalue: this is a necessary but not sufficient condition for their existence [76]. This condition is fairly restrictive, for example it excludes real scalar fields from being a suitable matter source for wormholes.

In simple Friedmann-Robertson-Walker (FRW) models, wormholes are typically described by a constraint equation of the form

$$\frac{\dot{a}^2}{a^2} = \frac{1}{a^2} - \frac{\text{const.}}{a^n} \quad (\text{C.1.2})$$

where a is the scale factor in the (spatially closed) line element $ds^2 = dt^2 + a^2 d\Omega_3^2$, and the derivative is with respect to the Euclidean time t .

In order to have an asymptotically Euclidean (AE) wormhole it is necessary that \dot{a}^2 remains positive at large a , and this requires $n > 2$. This wormhole represents two separate

Euclidean regions connected together by a throat where $\dot{a} = 0$, and the throat size a_0 is finite. Typical cases are $n = 6$ (axion) and $n = 4$ (conformal scalar field). Using the conformal time τ defined by $dt = a d\tau$, the typical solution of eq. C.1.2 is (see also Ref. [248])

$$a^{n/2-1} \sim (\text{const})^{1/2} \cosh \left[\frac{(n-2)}{2} \tau \right] \quad (\text{C.1.3})$$

One sees the typical wormhole shape, e.g. $a \sim \cosh(\tau)$ for the conformal scalar ($n = 4$) case. If a cosmological constant was included it would dominate for large a giving, in total, a “dumb-bell” shape.

C.2 Carlini-Mijić wormholes

C.2.1 Perfect fluid source

Carlini and Mijić [25] expanded the number of possible wormhole solutions by considering an analytic continuation of closed FRW universes.³ For a perfect fluid equation of state

$$p = (\gamma - 1)\rho \quad (\text{C.2.1})$$

(where p and ρ are, respectively, the pressure and energy density of the fluid), recollapsing closed universes require that the strong energy condition be satisfied, i.e. that $\gamma > 2/3$. It is the continuation of this theory to the Euclidean domain which then gives wormhole solutions. To see this one can consider the Friedmann equation in Euclidean space

$$\frac{\dot{a}^2}{a^2} = \frac{1}{a^2} - \rho \quad (\text{C.2.2})$$

The conservation equation for ρ in the Lorentzian region is given by

$$\dot{\rho} + 3(\rho + p)\frac{\dot{a}}{a} = 0 \quad (\text{C.2.3})$$

and with the usual equation of state $p = (\gamma - 1)\rho$ it has solution $\rho = \rho_0/a^{3\gamma}$. This solution also occurs in Euclidean space if the equation of state (C.2.1) and the conservation eq. (C.2.3) hold the same in Euclidean space (after the analytic continuation of $t \rightarrow it$).

Substituting for ρ into the Friedmann equation (C.2.2) gives

$$\frac{\dot{a}^2}{a^2} = \frac{1}{a^2} - \frac{\rho_0}{a^{3\gamma}} \quad (\text{C.2.4})$$

³A similar idea can also be found in Ref. [248].

which now has the form of the wormhole equation (C.1.2), with the simple correspondence $3\gamma = n$. Classical Euclidean wormholes are therefore possible for any $\gamma > 2/3$ (i.e. when the strong energy condition is satisfied) which is a generalization of the previously found axion ($\gamma = 2$) and conformal scalar ($\gamma = 4/3$) field cases. One can also easily evaluate the Ricci tensor from the Einstein equations, with the energy-momentum tensor for the fluid given by $T_{ab} = (\rho + p)U_a U_b + p g_{ab}$ (where U_a is the four velocity of the fluid, such that $U_a U^a = \pm 1$ in the Euclidean and Lorentzian regions, respectively, and g_{ab} is the spatially closed FRW metric). The result, valid both in the Euclidean and the Lorentzian regions, is that $R_0^0 = (2 - 3\gamma)\rho/2$, and clearly only for $\gamma > 2/3$ can the Ricci tensor have a negative eigenvalue and allow for the possibility of wormholes, cf. Ref. [76].

C.2.2 Scalar field source

Using an adaptation of the work of Ellis and Madsen [155], one can use a scalar field which simulates the equation of state with a certain value of γ . In Lorentzian space such a realization requires a potential of the form [25]

$$V(\phi) = \frac{(2 - \gamma)}{2a_0^2} \cosh^{\frac{6\gamma}{3\gamma-2}} \frac{(3\gamma - 2)}{\sqrt{2\gamma}} \phi \quad (\text{C.2.5})$$

where a_0 is an arbitrary constant which represents the maximum size of the closed universe for $\gamma > 2/3$. In order to obtain a classical wormhole with this potential it is necessary to also analytically continue the scalar field to an imaginary value, i.e. $\phi \rightarrow i\phi$,⁴ so that the Euclidean potential will be as in eq. (C.2.5) with \cosh replaced by \cos , and a_0 becomes the throat size of the corresponding wormhole.

Again one finds that only for $\gamma > 2/3$ can a classical AE wormhole solution be obtained.

For later use, we remark that provided the classical equations are valid the scalar potential $V(\phi)$ can be re-written in terms of the scale factor a , such that

$$V(\phi) \equiv V(a) = \frac{V_m}{a^{3\gamma}} \quad (\text{C.2.6})$$

where the constant $V_m = (1 - \gamma/2)a_0^{3\gamma-2}$.

⁴This analytic continuation is 'asymmetric' with respect to that for the time coordinate, in other words, in going from Lorentzian to Euclidean signature, one should Wick rotate $\phi \rightarrow +i\phi$ and $t \rightarrow -it$, cf. [95]

C.3 Quantum wormholes

C.3.1 Perfect fluid source

In a different vein, because the number of known wormhole solutions had appeared so limited, Hawking and Page (HP) considered that solutions of the Wheeler-DeWitt (WDW) equation could more generally represent wormholes [248]. For such wormholes, they suggested that the quantum mechanical wavefunction Ψ should decay exponentially for large scale factor a , so as to represent Euclidean space, and that Ψ be well behaved as $a \rightarrow 0$, so that no singularities are present.⁵ Because the WDW equation is independent of the lapse chosen, the Euclidean regime is already ‘included’ in the formalism. Thus, the quantum versions of the Carlini-Mijić (CM) wormholes should be found with no need of any explicit continuation.

Quantization of the constraint equation (C.2.4) gives the WDW equation (see, e.g., Refs. [197, 88])

$$\left(a^2 \frac{d^2}{da^2} + qa \frac{d}{da} + \rho_0 a^{6-3\gamma} - a^4 \right) \Psi(a) = 0 \quad (\text{C.3.1})$$

where q represents part of the factor ordering ambiguities.

We can get some idea as to when an Euclidean domain occurs at large a by considering the sign of the potential

$$U(a) \equiv \rho_0 a^{4-3\gamma} - a^2 < 0 \quad (\text{C.3.2})$$

in the analogous equation (setting the unimportant, in this regard, factor $q = 0$)

$$\left[\frac{d^2}{da^2} + U(a) \right] \Psi(a) = 0 \quad (\text{C.3.3})$$

When $U > 0$, oscillating solutions occur which represent Lorentzian metrics. Therefore, in order to obtain a wormhole (an AE regime for large scale factor) we require $U < 0$. Returning to our eq. (C.3.2), this occurs (in the usual case of positive energy density, $\rho_0 > 0$), for $2 > 4 - 3\gamma$, i.e. for $\gamma > 2/3$ (see Fig. 1).

This strong energy condition is the same as that obtained by CM for the occurrence

⁵Note that, on choosing the HP boundary condition for wormholes, one might be losing other interesting properties of the wave function, such as the prediction of an early inflationary epoch, which can instead be obtained by choosing other boundary conditions, such as the no-boundary proposal of Hartle and Hawking [91] or the Tunneling one [231], see also [22].

of wormhole solutions. Kim and Page [120] found that quantum wormholes are incompatible with a cosmological constant. However we have here a stronger condition: perfect fluid matter sources violating the strong energy condition are incompatible with wormholes obeying the HP conditions. The presence of any matter source with $\gamma < 2/3$ will eventually dominate for large a and prevent the AE wormhole.

A quantum wormhole also requires suitable behaviour for small a . As $a \rightarrow 0$ we can ignore the a^4 term in eq. (C.3.1), since $4 > 6 - 3\gamma$ when $\gamma > 2/3$. In this case the WDW equation (C.3.1) (for $\gamma \neq 2$) simplifies to a Bessel equation with solution

$$\Psi(a) \simeq a^{(1-q)/2} \left[c_1 J_\nu \left(\frac{2\sqrt{\rho_0}}{3(2-\gamma)} a^{3-3\gamma/2} \right) + c_2 Y_\nu \left(\frac{2\sqrt{\rho_0}}{3(2-\gamma)} a^{3-3\gamma/2} \right) \right] \quad (\text{C.3.4})$$

where we have defined $\nu \equiv (1-q)/3(2-\gamma)$. In order to satisfy the wormhole boundary condition we should choose the J Bessel function. For the particular case $\gamma = 2$, the solution of eq. (C.3.1) (with $q = 1$) is a linear combination of Bessel functions, $J_{\pm i\sqrt{\rho_0}/2}(ia^2/2)$, which oscillates an infinite number of times at the origin (see [95]), and therefore cannot satisfy the required regularity condition of HP.

Although the WDW is an ordinary differential equation, it is still not straightforward to obtain analytic solutions for all γ . Instead of proceeding by finding approximate WKB solutions, we can still emphasize important properties that any solution in the range $2/3 < \gamma < 2$ will have⁶ by considering the exactly soluble case of $\gamma = 4/3$. This is the case of a radiation (or, equivalently, that of a conformally coupled scalar field) dominated FRW ansatz, which allows eq. (C.3.1), for $q = 0$, to be written as (cf. [80])

$$\left(\frac{d^2}{da^2} + \rho_0 - a^2 \right) \Psi(a) = 0 \quad (\text{C.3.5})$$

This is in the form of a parabolic cylinder equation with solutions in terms of confluent hypergeometric functions (see, e.g., Ref. [1])

$$\begin{aligned} \Psi(a) \simeq \exp(-a^2/2) & \left[c_3 \cdot {}_1F_1(1/4(1-\rho_0); 1/2; a^2) \right. \\ & \left. + c_4 \cdot {}_1F_1(1/4(3-\rho_0); 3/2; a^2) \cdot a \right] \end{aligned} \quad (\text{C.3.6})$$

For $\rho_0 > 1$ and $c_4 = 0$ we get a regular oscillation for small a and an Euclidean regime for large a , see Fig. (2).

⁶The upper boundary $\gamma < 2$ is dictated by the requirement that the sound wave velocity of the fluid must be smaller than the speed of light.

C.3.2 Scalar field source

If wormholes could only occur when the strong energy condition is satisfied, they would still be rather restrictive. Especially since the strong energy condition is expected to be violated in the early universe and in such processes as evaporating black holes. However, working with the scalar field model with potential $V(\phi)$ given by eq. (C.2.5), it can be shown that quantum wormholes exist even when the strong energy condition is violated, except for the cosmological constant $\gamma = 0$ case [22]. These wormholes can satisfy the HP conditions up to an arbitrarily large size.

C.4 Classical signature change

C.4.1 Perfect fluid source

There is, however, a different approach based on ‘classical change of signature’ [55]. This is also closely related to possible topology fluctuations because the ‘no-go’ theorems [72] could be circumvented.

The metric for a FRW universe is taken to be of the form

$$ds^2 = -\epsilon dt^2 + a^2 \left[\frac{dr^2}{1 - kr^2} + r^2 d\Omega_2^2 \right] \quad (\text{C.4.1})$$

Here ϵ represents the signature change: $\epsilon = 1$ for usual Lorentzian space and $\epsilon = -1$ in Euclidean space. The three dimensional spacelike sections at $t = \text{const}$ are flat, open or closed if $k = 0, -1$ or $+1$, respectively.

We first consider a perfect fluid with energy-momentum tensor defined as [55]

$$T_{ab} = (\rho + \epsilon p)U_a U_b + p g_{ab} \quad (\text{C.4.2})$$

where, as usual, U_a is the four velocity of the fluid (such that $U_a U^a = -\epsilon$) and g_{ab} is the metric of eq. (C.4.1). The Friedmann equation turns out to be (cf. Ref. [55])

$$\frac{\dot{a}^2}{a^2} = \rho - \frac{\epsilon k}{a^2} \quad (\text{C.4.3})$$

and the energy conservation equation is

$$\dot{\rho} + 3(\rho + \epsilon p)\frac{\dot{a}}{a} = 0 \quad (\text{C.4.4})$$

The idea of classical signature change is that \dot{a}^2/a^2 should remain positive so that the need of analytic continuation to imaginary time is excluded. This provides a criteria for when the signature change occurs (for $k \neq 0$): $\epsilon = \text{sign}(k)$ when $\rho > 1/a^2$, while $\epsilon = -\text{sign}(k)$ when $\rho < 1/a^2$.

However, in order that the junction conditions be satisfied (that the scale factor and the energy density are continuous through the surface Σ of change of signature), one must have $k = 0$ (see Ref. [55]). The perfect fluid matter source with the energy-momentum tensor (C.4.2), from the outset, cannot allow for the possibility of a classical Euclidean wormhole.

One can, however, try to quantize the constraint (C.4.3) and look for “off-shell” solutions with $k = 1$. Then the WDW equation corresponding to the Friedmann eq. (C.4.3) can be obtained following the methods of Martin [160] (see also Ref. [56])⁷

$$\left(a^2 \frac{d^2}{da^2} + qa \frac{d}{da} + \rho a^6 - k\epsilon a^4 \right) \Psi(a) = 0. \quad (\text{C.4.5})$$

Substituting from the conservation equation for ρ (for the case of ρ continuous and with unique functional form in the Euclidean and Lorentzian manifolds), gives the WDW potential (cf. eq. (12))

$$U \equiv \rho_0 a^{4-3\gamma} - k\epsilon a^2 \quad (\text{C.4.6})$$

The main idea of classical signature change is to choose the signature variable ϵ in such a way that U remains positive everywhere. This results (for any k , in particular for $k = 1$) in purely oscillatory wavefunctions, and no instanton-like (‘classically forbidden’) behaviour of the form $\sim \exp(-S)$ is present.⁸

The impossibility of quantum wormholes can also be seen directly by looking at the WDW potential: in order that the WDW can have well defined (i.e. C^2 differentiable) solutions, the potential U of eq. (C.4.6) should be continuous, thus requiring $k = 0$ also “off-shell”.

⁷Note that, although the idea of classical signature change is that Euclidean regions can be described by the classical equations without the need of analytical continuations, these equations can in turn be quantized. But now also with the prescription $p_a \rightarrow -i\hbar\partial_a$ in the Euclidean domain. Because the signature of the metric is no longer considered fixed the resulting WDW equation differs from the usual “lapse independent” one, cf. Ref. [88].

⁸In principle, one could be ‘perverse’ and choose the signature change to keep \dot{a}^2/a^2 negative, so ensuring an $\sim \exp(-S)$ type behaviour everywhere. But this contradicts the original motivation of classical signature change.

Neither classical nor quantum wormhole solutions are thus possible in the context of the classical signature change model with the energy-momentum tensor of the form (C.4.2).

Changing T_{ab}

At this stage, we should point out that there is still some freedom in defining the energy momentum tensor for the perfect fluid: the main requirements are expected to be ‘smoothness’ of T_{ab} at the junction surface Σ and agreement with its standard expression in the Lorentzian region. Besides the [55] choice, another possible tensor is provided by the expression

$$T_{ab} = \epsilon(\rho + p)U_a U_b + pg_{ab} \quad (\text{C.4.7})$$

whose main property is to have $-\rho, p, p, p$ as eigenvalues in both the Euclidean and Lorentzian signature regions.

Repeating the calculations leading to eqs. (C.4.3)-(C.4.4), one can easily check that the Friedmann equation for a FRW universe with the matter content of eq. (C.4.7) becomes

$$\frac{\dot{a}^2}{a^2} = \epsilon \left(\rho - \frac{k}{a^2} \right) \quad (\text{C.4.8})$$

while the energy conservation equation is given again by the (standard) equation (C.2.3) (which is the same in both signature regions).

This time, positivity and continuity of \dot{a}^2/a^2 can be easily seen to be guaranteed by the condition that $\rho|_{\Sigma} = (k/a^2)|_{\Sigma}$ at the junction surface ($a|_{\Sigma} = a_0$), which is perfectly consistent with the existence of a closed universe ($k = 1$) (provided that, as usual, $\rho > 0$). In other words, the extrinsic curvature (and \dot{a}) must be zero on Σ , and the change of signature is of the *strong* type [56]. Furthermore, for $k = 1$, the signature will be Lorentzian ($\epsilon = 1$) when $\rho > 1/a^2$, and Euclidean ($\epsilon = -1$) when $\rho < 1/a^2$.

In particular, for continuous p, ρ and equation of state (C.2.1), the solution of the conservation eq. (C.2.3) is given by $\rho = \rho_0/a^{3\gamma}$ (for both signatures). Consequently the Friedmann eq. (C.4.8) in Euclidean space is again exactly of the form (C.1.2), and one has the same Euclidean wormhole solutions (with throat size a_0) as in the CM case, i.e. when the strong energy condition is satisfied.⁹ Moreover, the solution of the same Friedmann

⁹Evaluating, as in the CM case, the Ricci tensor from the Einstein equations and with the energy-momentum tensor (C.4.7), gives once more $R_0^0 = (2 - 3\gamma)\rho/2$, which is negative for $\gamma > 2/3$.

equation in Lorentzian space clearly represents a closed and expanding FRW universe with maximum size a_0 . What the change of signature approach is suggesting in this case, is that in principle one could have a change of signature also at large scale factor, and that the ‘continuation’ of the closed universe at its maximum size is an AE wormhole. The difference with respect to the standard CM approach is that, in the context of the classical signature change model, there is no need of resorting to any continuation into imaginary time.

One can then quantize in a similar fashion the constraint eq. (C.4.8) for the energy-momentum tensor (C.4.7) to obtain the following WDW equation (cf. Ref. [160])

$$\left[a^2 \frac{d^2}{da^2} + qa \frac{d}{da} + \epsilon(\rho a^6 - ka^4) \right] \Psi(a) = 0. \quad (\text{C.4.9})$$

where now, substituting from the conservation equation for ρ (and with $q = 0$), the potential U is given by

$$U \equiv \epsilon(\rho_0 a^{4-3\gamma} - ka^2) \quad (\text{C.4.10})$$

Also in this case, as for when the matter content was described by eq. (C.4.2), the classical change of signature picture requires that we choose ϵ such that U will be positive everywhere (this time U is continuous for $k = 1$, provided the classical junction conditions hold). This will give again purely oscillatory wavefunctions everywhere, which do not satisfy the HP conditions for the existence of quantum wormholes.

C.4.2 Scalar field source

With a scalar field matter source the Friedman equation now has the form

$$\frac{\dot{a}^2}{a^2} = \dot{\phi}^2 + \epsilon \left(V(\phi) - \frac{k}{a^2} \right) \quad (\text{C.4.11})$$

Strictly speaking, this equation should be justified by a rigorous action principle. Embacher [56] has presented some possible alternative Friedman equations being derived from different fundamental Lagrangians. The property of oscillatory behaviour seems inherent in all of them, cf. the actions S_7 and S_8 in Ref. [56].

Using the usual canonical quantization methods, the WDW equation corresponding to the Friedman equation (C.4.11) is given by (cf. Ref. [160])

$$\left[a^2 \frac{\partial^2}{\partial a^2} + qa \frac{\partial}{\partial a} - \frac{\partial^2}{\partial \phi^2} + \epsilon(a^6 V(\phi) - a^4) \right] \Psi(a, \phi) = 0 \quad (\text{C.4.12})$$

Again the ϵ term conspires to keep the WDW potential

$$U \equiv \epsilon(a^6 V(\phi) - a^4) \quad (\text{C.4.13})$$

of the same sign. This will result in the wavefunction being oscillatory in the “time variable” a , after being solved by some appropriate method (cf. Ref. [88]). Explicit solutions displaying this oscillatory behaviour for the case of $V(\phi) = \text{const}$ are given in Ref.[160]

One can also have an idea of the behaviour of the WDW wave functional considering the simplified model in which the potential $V(\phi)$ is substituted by the classically equivalent potential $V(a)$ into the Friedmann equation (C.4.11). In doing so, i.e. assuming the existence of the fixed relationship (C.2.6) between ϕ and a , one is effectively ‘freezing out’ the scalar field degree of freedom.

The WDW equation obtained from this modified Friedmann equation will have the same form as eq. (C.4.5), but (for $k = 1$) with the potential (cf. Ref. [160])

$$U = \epsilon(V_m a^{4-3\gamma} - a^2) \quad (\text{C.4.14})$$

Again, the spirit of classical signature change is to use the signature change variable ϵ such that $U > 0$ everywhere.

The choice $\gamma < 2/3$ seems more physically reasonable in this model. In such cases the usually forbidden region at small scale factors becomes classically allowed by taking $\epsilon = -1$ there, and $\epsilon = 1$ for large scale factor. This case agrees with the original motivation of classical signature change which was to avoid the need for Euclidean time during the early and presumably small universe [55].

On the other hand, for $\gamma > 2/3$ a classical signature change would allow the existence of a classical description beyond the usual maximum size of a closed universe. This appears to be suspect on physical grounds, especially if we were dealing with large universes, but it might be justified by considering such closed universes to be of order of the Planck size.

In both cases, the resulting quantized model of signature change will give wavefunctions oscillating everywhere, so preventing the HP conditions for the existence of quantum wormholes to be satisfied.

C.5 Conclusions

Using a perfect fluid matter source we have found that classical wormhole solutions (obtained by an analytic continuation) occur only when the strong energy condition is satisfied. The quantum analogues of such wormholes agree with the HP conjecture for conditions to be satisfied by quantum wormholes.

We have briefly mentioned that quantum wormholes (but not classical ones) can also be obtained for violations of the strong energy condition if a scalar field matter source is used. The scalar potential $V(\phi)$, obtained by Carlini and Mijić, that in a sense simulates a perfect fluid with a certain value of γ , can be used for such a purpose.

In the change of signature approach, no classical Euclidean wormhole solutions are possible for a perfect fluid matter source with the energy-momentum tensor of Ref. [55]. A similar classical signature change approach, based on a modified energy-momentum tensor for the perfect fluid, can instead reproduce the classical CM solutions for a closed Lorentzian expanding universe ($\gamma > 2/3$) which is ‘continued’ at its maximum radius into an AE wormhole, but with no need of any imaginary time.

At the quantum level, however, the classical change of signature model tries to entirely avoid the presence of classically forbidden regions where the wave function would behave exponentially. Thus, the WDW wave functions are oscillating everywhere, and there are no quantum wormhole solutions in the sense of HP for any given choice of the energy-momentum tensor.

Although the classical signature change gives oscillatory wavefunctions, there is still need of an explanation of why one should choose \dot{a}^2 positive in eqs. (C.4.3), (C.4.8) and (C.4.11). As previously mentioned, one could choose the opposite condition and get an “everywhere forbidden” behaviour (cf. Ref. [57], where it is suggested that there is some preponderance of Lorentzian over Euclidean behaviour, while oscillations between the two cases are constantly occurring). An understanding of this point is required before one could fully justify the use of classical signature change in obviating the need for quantum wormhole behaviour.

The difference between purely oscillatory and exponential wavefunctions will have a crucial effect on arguments setting $\Lambda \rightarrow 0$. Once the exponential peak is lost, one would expect wider predictions for Λ if it is given by a distribution function $P(\Lambda)$. Indeed, in

the quantization scheme of Ref. [160] the classical signature change approach seems only compatible with the tunneling boundary condition [160], which would give larger values of Λ [33].

Of course there are also a number of other important and still unresolved issues, such as those concerning the viability of the WDW quantization scheme for the classical signature change model and the proper consideration of the signature variable within a more general action principle (see, e.g., Refs. [56] and [81]). Should the signature change variable also be treated as a dynamical degree of freedom? Finally, if signature change is possible, it would then be interesting to investigate its relevance for the closely related topic of topology change.¹⁰ We hope to address these and related problems in a future publication.

Acknowledgements

We would like to thank Prof. G.F.R. Ellis for his continued interest and encouragement during the course of this work. A.C.'s research was mainly supported by an EEC fellowship in the 'Human Capital and Mobility' program, under contract No. ERBCHBICT930313, and, since February 1996, by the JSPS postdoctoral fellowship No. P95196.

¹⁰Both signature and topology change are expected to produce similar mild singularities, see, e.g., Refs. [55] and [101].

Appendix D

Spatially Homogeneous Cosmologies: Geometrical Setting

We present a summary of the synthesis provided by Ellis, Siklos and Wainwright *Geometry of cosmological models* in [235] pages 1-50.

A four-dimensional space-time $(\mathcal{M}, g_{\mu\nu})$ is said to be *spatially homogeneous* if it possesses an r -dimensional isometry group $G^{(r)}$ (the invariance group of the metric $g_{\mu\nu}$) that acts transitively on a one-parameter family of spacelike hypersurfaces, the orbits of the group¹ (so that $r \geq 3$), which provides a natural slicing of the space time. At any point q on any such hypersurface Σ there are (at least) three nonzero linearly independent Killing vector fields tangent to Σ . Since a Killing vector field ξ^μ is completely determined by the values of ξ^μ and $\nabla_\mu \xi^\nu$ at any point q of Σ , there can be at most $r_{max} \doteq \frac{1}{2}n(n+1)$ linearly independent Killing vector fields on a manifold of dimension n (see Appendix C.3 in Wald 84 [237]); here, this means $3 \leq r \leq 6$. When $r = r_{max}$, the Riemann space has constant curvature. Furthermore, a theorem due to Fubini states that a Riemannian space (for $n > 2$) cannot admit an isometry group of dimension $r = \frac{1}{2}n(n+1) - 1$ (see [46]); here, this implies that the only possible values of r are 3, 4 and 6. If $r = 6$, the space time is not only spatially homogeneous but also isotropic, that is, locally spherically symmetric, and belongs to the FLRW class, which features maximally symmetric spacelike sections, i.e.

¹The orbit of a point p under a group $G^{(r)}$ is the set of points into which p is moved by the action of all elements of the group.

sections of constant curvature.² If $r = 4$, the space time is locally rotationally symmetric (LRS); there exists a three-parameter subgroup $\overline{G}^{(3)}$ that acts either *simply* or *multiply* transitively on the spacelike hypersurfaces: The latter case includes the Kantowski-Sachs cosmological models (the orbits of the group are two-dimensional, maximally symmetric, and with positive constant curvature); the former corresponds to LRS Bianchi models and thus points to the last possible value of r , namely $r = 3$, which corresponds to the Bianchi class. Thus, if we set aside the Kantowski-Sachs models, we are left with isometry groups that act *simply* transitively on the spacelike hypersurfaces Σ , i.e. such that $\dim G = \dim \Sigma = 3$. In the light of the preceding discussion we can state a definition of Bianchi cosmologies: *A Bianchi cosmology is a model the metric of which admits a three-dimensional group of isometries that acts simply transitively on spacelike hypersurfaces Σ , which are surfaces of homogeneity in space time.* The complete list of Bianchi cosmologies is obtained by classifying the three-parameter isometry groups, that is, the three-dimensional real Lie algebras generated by the associated Killing vector fields; the outcome is nine nonequivalent Bianchi types – or ten equivalence classes – named according to Bianchi's own terminology.

We sketch the classification procedure according to Wahlquist and Bher, Ellis and MacCallum, and Siklos [151, 152, 152, 108, 5]. Suppose that X_i for $i = 1, 2, 3$ form a basis of a three-dimensional Lie algebra with structure constants C_{ij}^k , which are defined through the commutators $[X_i, X_j] = C_{ij}^k X_k$ (they are antisymmetric and satisfy the Jacobi identity). Given C_{ij}^k we can define a three-vector a^i and a symmetric 3×3 matrix n^{ij} by $a_i := \frac{1}{2} C_{li}^l$ and $n^{ij} = \epsilon^{ijk} (\frac{1}{2} C_{kl}^j - \delta_k^j a_l)$ respectively, where ϵ^{ijk} is the unique totally antisymmetric tensor satisfying $\epsilon^{ijk} \epsilon_{ijk} = 3! = 6$. It is easy to show that the structure constants can be written as $C_{ij}^k = n^{kl} \epsilon_{lij} + 2\delta_{[i}^k a_{j]}$. Substitution of this expression into the Jacobi identity yields the simple result $n^{ij} a_j = 0$. According to Ellis and MacCallum, the classification now gives two broad classes: *class A* ($a_i = 0$) and *class B* ($a_i \neq 0$); the resulting Lie algebras are divided into several types according to the rank and the modulus of the signature of n^{ij} . In class A there exists precisely six distinct Lie algebras whereas in class B there are only four possible values for the rank and the signature of n^{ij} . Some types (VI and VII) can be subclassified with the help of a further invariant h , which can be determined by the formula $a_i a_j = \frac{1}{2} h n^{kr} n^{ls} \epsilon_{rsi} \epsilon_{klj}$. The resulting algebraic classification is summarized in

²Note that in the case of space times ($n = 4$), the ten-parameter Poincaré isometry group of flat space is an example of $G^{(10)}$; Minkowski and de Sitter space-times are maximally symmetric.

a	n_1	n_2	n_3	Bianchi type	p	q	NEC	WEC
0	0	0	0	I	0	1	\mathcal{N}	\mathcal{N}
0	+1	0	0	II	3	2	\mathcal{N}	\mathcal{N}
0	0	+1	-1	VI_0	5	3	\mathcal{N}	\mathcal{N}
0	0	+1	+1	VII_0	5	3	\mathcal{N}	\mathcal{N}
0	+1	+1	+1	$VIII$	6	4	\mathcal{N}	\mathcal{N}
0	+1	+1	+1	IX	6	4	\mathcal{Y}	\mathcal{N}

Table D.1: The Bianchi types for *class A*. Null Energy Condition (NEC) violation for bounce behaviour in General Relativity is indicated with \mathcal{N} , otherwise \mathcal{Y} . Similarly for the Weak Energy Condition (WEC).

a	n_1	n_2	n_3	Bianchi type	p	q	NEC	WEC
1	0	0	0	V	3	1	\mathcal{N}	\mathcal{N}
1	0	0	+1	IV	5	3	\mathcal{N}	\mathcal{N}
1	0	+1	-1	III or VI_{-1}	5	3	\mathcal{N}	\mathcal{N}
$\sqrt{-h}$	0	+1	-1	VI_h ($h < 0$)	5	3	\mathcal{N}	\mathcal{N}
\sqrt{h}	0	+1	+1	VII_h ($h > 0$)	5	3	\mathcal{N}	\mathcal{N}

Table D.2: The Bianchi types for *class B*. Strong Energy Condition violation for bounce behaviour in General Relativity is indicated with \mathcal{N} , otherwise \mathcal{Y} . Similarly for the Weak Energy Condition (WEC).

Table D.1 and Table D.2 (n_i for $i = 1, 2, 3$ denotes the diagonal elements of the symmetric matrix n^{ij} ; a is the nonzero component of the vector a_i obtained after a suitable rotation of axis and rescaling; the number p refers to the dimension of the orbits of the group—it is related to the automorphism degrees of freedom—; and the number q describes the degree of generality of the most general vacuum solution of each group type.)

Bibliography

- [1] M. Abramowitz and I.A. Stegun, *Handbook of mathematical functions*, Dover, New York, 1965.
- [2] K. Akama, *An early proposal of 'brane world'*, Lect. Notes Phys. **176** (1982), 267, [hep-th/0001113]; V.A. Rubakov and M.E. Shaposhnikov, *Do We Live Inside a Domain Wall?*, Phys. Lett. B **125** (1983) 136; M. Visser, *An Exotic Class of Kaluza-Klein Models*, Phys. Lett. B **159** (1985) 22 [hep-th/9910093]; G.W. Gibbons and D.L. Wiltshire, *Space-Time as a Membrane in Higher Dimensions*, Nucl. Phys. B **287** (1987) 717 [hep-th/0109093]; E. Witten, *Strong Coupling Expansion of Calabi-Yau Compactification*, Nucl. Phys. B **471** (1996) [hep-th/9602070]; I. Antoniadis, *A possible new dimension at a few TeV*, Phys. Lett. B **246** (1990) 377; N. Arkani-Hamed, Dimopoulos and G. Dvali, *The hierarchy problem and new dimensions at a millimeter*, Phys. Lett. B **429** (1998) 263 [hep-th/9803315]; K. Dienes, E. Dudas and T. Ghergetta, *Extra spacetime dimensions and unification*, Phys. Lett. B **436** (1998) [hep-th/9803466]; I. Antoniadis, N. Arkani-Hamed, S. Dimopoulos and G. Dvali, *New dimensions at a millimeter and a Fermi and superstrings at a TeV*, Phys. Lett. B **436** (1998) 257 [hep-ph/9804398]; G. Shiu and S.H. Tye, *TeV scale superstring and extra dimensions*, Phys. Rev. D **58** (1998) 106007 [hep-th/9805157]; K. Dienes, E. Dudas and T. Gherghetta, *Grand Unification at intermediate mass scales through extra dimensions*, Nucl. Phys. B **537** (1999) [hep-th/9806292]; Z. Kakushadze and S.H. Tye, *Brane World*, Nucl. Phys. B **548** (1999) 180 [hep-th/9809147]; K. Benakli, *Phenomenology of low quantum gravity scale models*, Phys. Rev. D **60** (1999) 104002 [hep-ph/9809582]; C.P. Burgess, L.E. Ibanez and F. Quevedo, *Strings at the intermediate scale or is the fermi scale*

- dual to the Planck scale?*, Phys. Lett. B **447** (1999) 257 [hep-ph/9810535]; S. Forste, Z Lalak, S Lavignac and H-P Nilles Phys. Lett. B. **481** (2000) 360; see [189].
- [3] R. Bach, *Zur weylschen relativitatstheorie und der weylschen erweiterung des krümmungstenorbegriffs*, Math. Z. **9** (1921), 110–35.
- [4] J.D. Barrow and S. Cotsakis, Phys. Lett. B **214** (1988), 515, S. Cotsakis, Phys. Rev. D **47** (1993) 1437; *ibid*, **49**(1995) 6199.
- [5] J.D. Barrow and H. Sirousse-Zia, *Mixmaster cosmological model in theories of gravity with a quadratic lagrangian*, Phys. Rev. D **39** (1986), 2187–2191, erratum in Phys. Rev. D. **41** (1990), 1362.
- [6] M. Bartelmann, Strong and weak lensing by galaxy clusters, 2002, Invited Review at “Matter and Energy in Clusters of Galaxies”, Taipei 2002, see [astro-ph/0207032].
- [7] E. Baum, Phys. Lett. B **133** (1983), 185.
- [8] B. Bertotti, Proc. Roy. Soc. Lond. **A294** (1966), 195.
- [9] P. Binetruy, C. Deffayet, and D. Langlois, Nucl. Phys. B **462** (1999), 34, N. Kaloper, Phys. Rev. D **61**, 064003 (2000); t. Nihei, Phys. Lett. B **465**, 81 (1999); D.N. Vollick, Class. Quantum Grav. **18**, 1 (2001); L. Mendes and A.R.Liddle, Phys. Rev. D **62**, 103511 (2000); E.J. Copeland, A.R. Liddle and J.E. Lidsey, Phys. Rev. D **64**, 023509 (2001); Phys. Rev. D **63** 103505 (2001); S. Tsujikawa, K. Maeda and S. Mizuno Phys. Rev. **63** , 123511 (2000); K. Maeda, astro-ph/0012313; S. Mukohyama, T. Shiromizu and K. Maeda, Phys. Rev. D **61**, 024028 (2000); *Erratum: ibid.* D **63** 029901 (2001).
- [10] R.D. Blandford and R. Narayan, Ann. Rev. Ast. **30** (1992), 311.
- [11] D.G. Boulware, *Quantum field theory in spaces with closed time-like curves*, Phys.Rev. D **46** (1992), 4421–4441.
- [12] P. Bowcock, C. Charmousis, and R. Gregory, Class. Quantum Grav. **17** (2000), 4745.
- [13] P. Brax and C. van de Bruck, *Cosmology and brane worlds: A review*, Class.Quant.Grav. **20** (2003), R201–R232, [hep-th/0303095].

- [14] R. Brustein and R. Madden, *Graceful exit and energy conditions in string cosmology*, Phys. Lett. B **410** (1997), 110, see [hep-th/9702043].
- [15] ———, *A model of graceful exit in string cosmology*, Phys. Rev. D **57** (1998), 712–724, [hep-th/9708046].
- [16] R. Brustein and P. Steinhardt, Phys. Lett. B **302** (1993), 196.
- [17] R. Brustein and G. Veneziano, Phys. Lett. B **329** (1994), 429, N. Kaloper, R. Madden and K.A. Olive, Nucl. Phys. B **452**, 677 (1995); R. Easther, K. Maeda and D. Wands, Phys. Rev. D **53**, 4247 (1996).
- [18] R. Caldwell, M. Kamionkowski, and N. Weinberg, *Phantom energy and cosmic doomsday*, Phys.Rev.Lett. **91** (2003), 071301, [astro-ph/0302506].
- [19] A. Campos and C. Sopena, Phys. Rev. D **63** (2001), 104012, Phys. Rev. D **64**, 104011 (2001).
- [20] V.F. Cardone and M. Sereno, *Gravitational lensing by spherically symmetric lenses with angular momentum*, to appear, 2002.
- [21] A. Carlini, SISSA preprint 65/92/A, 1993.
- [22] A. Carlini, D.H. Coule, and D.M. Solomons, *Euclidean quantum wormholes with scalar fields*, Int. Journal of Mod. Phys. A **20** (1997), 3517–3544.
- [23] A. Carlini and M. Martellini, Class. Quantum Grav. **9** (1992), 629.
- [24] A. Carlini and M. Mijić, SISSA preprint 91A, 1990.
- [25] ———, *Spacetime wormholes as analytic continuation of closed expanding universes*, SISSA preprint 91A, 1991, A. Carlini, *Spacetime wormholes with a scalar field: a new set of exact solutions*, SISSA preprint 65/92/A (1992); A. Carlini and M. Martellini, Class. Quantum Grav. **9**, 629, (1992).
- [26] B.J. Carr and J.E. Lidsey, Phys. Rev. D **48** (1993), 543.
- [27] C. Cartier, E.J. Copeland, and R. Madden, *The graceful exit in pre-big bang string cosmology*, JHEP **0001** (2000), 035, see [hep-th/9910169].

- [28] S. Coleman, Nucl. Phys. B **310** (1988), 643, S.W. Hawking, *Phys. Lett. B* **134**, (1983), 403; E. Baum, *Phys. Lett. B* **133**, (1983), 185.
- [29] C.B. Collins and S.W. Hawking, *Astrophys. J.* **180** (1973), 137, *Mon. Not. R. Astr. Soc.* **162**, 307 (1973).
- [30] S. Cotsakis, *Mathematical problems in higher order gravity and cosmology. a talk presented at the eighth marcel grossmann meeting, jerousalem, june 22-27*, [gr-qc/9712046], 1997.
- [31] D.H. Coule, *Mod. Phys. Lett A* **10** (1989).
- [32] ———, *Class. Quantum Grav.* **9** (1992), 2353.
- [33] ———, *Mod Phys. Lett A* **10** (1995), 1989.
- [34] D.H. Coule and K. Maeda, *Class. Quantum Grav.* **7** (1990), 955.
- [35] D.H. Coule and D.M. Solomons, *Can quantum wormholes really help set $\lambda \rightarrow 0$?*, University of Cape Town preprint (1993).
- [36] C.P. Burgess C.P. and S. Hagan, *Phys. Rev. D* **43** (1991), 1869, Brown J.D., Burgess C.P., Kshirsagar A., Whiting B.F. and York J.W., *Nucl. Phys. B* **328**, (1989), 213; Twamley J. and Page D.N., *Nucl. Phys. B* **378**, (1992), 247.
- [37] G. de Risi and M. Gasperini, *Low-energy graceful exit in anisotropic string cosmology backgrounds*, *Phys. Lett. B* **521** (2001), 335-342, see [hep=th/0109137].
- [38] V. de Sabbata and C. Sivaram, *Gravitation and modern cosmology: the cosmological constant problem*, Plenum Press, New York, 1991, eds. A. Zichichi, V. de Sabbata and N. Sanchez.
- [39] R. Dicke and P. J. E. Peebles, *General relativity*, ch. The Big Bang Cosmology: Enigmas and Nostrums, Cambridge University Press, 1979, ed. S. W. Hawking and W. Israel.
- [40] S. Djorgovsky and H. Spinrad, *Ap. J.* **282** (1984), L1.

- [41] G. Dvali and S.-H. H. Tye, *Brane inflation*, Phys. Lett. B **450** (1999), 72, [hep-th/9812483].
- [42] C.C. Dyer and L.M. Oattes, *Astrophys. J.* **326** (1988), 50.
- [43] C.C. Dyer and D.C. Roeder, *Astrophys. J. Lett.* **180** (1973), L31.
- [44] D. A. Easson and R. H. Brandenberger, *Universe generation from black hole interiors*, JHEP **0106** (2001), 024, [hep-th/0103019].
- [45] J. Ehlers, *Contributions to the relativistic mechanics of continuous media*, Gen. Rel. Grav. **25** (1993), 1225.
- [46] L.P. Eisenhart, *Riemannian geometry*, sixth ed., Princeton University Press, Princeton, 1966.
- [47] G. F. R. Ellis, *General relativity and cosmology, proc. int. school of physics "enrico fermi" (varenna) course xlvii*, ch. Relativistic Cosmology, pp. 104–179, Academic Press, 1971, ed. R K Sachs.
- [48] G.F.R. Ellis, *Math. Phys.* **8** (1967), 1171.
- [49] G.F.R. Ellis, B.A.C.C. Bassett, and P.K.S. Dunsby, *Lensing and caustic effects on cosmological distances*, *Class. Quantum Grav.* **3** (1997), 2233, [gr-qc/9801092].
- [50] G.F.R. Ellis and M. Jaklitsch, *Astrophys. Journ.* **346** (1989), 601–606.
- [51] G.F.R. Ellis, D.H. Lyth, and M. Mijić, *Phys. Lett. B* **271** (1991), 52.
- [52] G.F.R. Ellis, D.C. Roberts, D. Solomons, and P.K.S. Dunsby, *A solution to the graceful exit problem in pre-big bang cosmology*, *Phys. Rev. D.* **62** (2000), 084004, see [gr-qc/9912005].
- [53] G.F.R. Ellis and D.M. Solomons, *Caustics of compensated spherical lens models*, *Class. Quantum Grav.* **15** (1998), 2381–2396.
- [54] G.F.R. Ellis and W.R. Stoeger, *Classical Quant. Grav.* **4** (1987), 1697.

- [55] G.F.R. Ellis, A. Sumeruk, D. Coule, and C. Hellaby, *Class. Quantum Grav.* **9** (1992), 1535, G.F.R. Ellis, *Gen. Rel. Grav.* **24**, 1047, (1992).
- [56] F. Embacher, *Phys. Rev D* **51** (1995), 6764.
- [57] ———, *Phys. Rev D* **52** (1995), 2150.
- [58] C. Bennett *et al*, *First year wilkinson microwave anisotropy probe (wmap) observations: Foreground emission*, to appear in *ApJ* (2003), [astro-ph/0302208].
- [59] A. Feinstein, *Exact inflationary solutions from a superpotential*, 2000, [gr-qc/0005015].
- [60] H.A. Feldman, V.F. Mukhanov, and R.H. Brandenberger, *Theory of cosmological perturbations. part 1: Classical perturbations. part 2: Quantum theory of perturbations. part 3: Extensions*, *Phys. Rept.* **215** (1992), 203, and D.H. Lyth and A. Riotto, *Particle physics models of onflation and the cosmological density perturbation*, *Phys. Rept.* **314** (1999) [hep-ph/9807278].
- [61] S. Foffa, *Pre-big bang on the brane*, *Phys. Rev. D* **66** (2002), 063512, [hep-th/0207103]; also see *Bouncing pre-big bang on the brane* [hep-th/0304004].
- [62] S. Foffa, M. Maggiore, and R. Sturani, *Loop corrections and graceful exit in string cosmology*, *Nucl.Phys. B* **552** (1999), 395–419, see [hep-th/9903008].
- [63] B. Fort, 1990, in [164].
- [64] B. Fort, J.-F. Le Borgne, Y. Mellier, G. Soucail, and R. Pello, 1990, in [164].
- [65] B. Fort and Y. Mellier, *Astron. Astrophys. Rev.* **5** (1994), 239.
- [66] T. Fukuyama and M. Morikawa, *Class. Quantum Grav.* **7** (1990), 823, L.J. Garay and J. García-Bellido, *Nucl. Phys. B* **400**, (1993), 416.
- [67] L.J. Garay, *Phys. Rev. D* **48** (1993), 1710.
- [68] L.J. Garay, J.J. Halliwell, and G.A. Mena Marugán, *Phys. Rev. D* **43** (1991), 2572.

- [69] M. Gasperini, *Lectures at vi seminario nazionale di fisica teorica*, 1999, see [hep-th/9907067] and also [<http://www.to.infn.it/~gasperin/>].
- [70] M. Gasperini and G. Veneziano, *Phys. Lett. B* **277** (1992), 256.
- [71] ———, *Astropart. Phys.* **1** (1993), 317.
- [72] R.P. Geroch, *J. Math. Phys.* **8** (1967), 782, Tipler F.J., *Ann. Phys. (N.Y.)* **108**, (1977), 1.
- [73] G. W. Gibbons, *Quantum gravity/string/m-theory as we approach the 3rd millenium*, (1998).
- [74] G.W. Gibbons and L.P. Grishchuk, *Nucl. Phys. B* **313** (1989), 736.
- [75] S. Giddings and A. Strominger, *Nucl. Phys. B* **306** (1988), 890, Shoen R. and Yau, S.T., *Commun. Math. Phys.* **79**, (1982), 281; Cheeger J. and Grommol D., *Ann. Math.* **96**, (1972), 413.
- [76] ———, *Nucl. Phys. B* **306** (1988), 890.
- [77] S.B. Giddings and A. Strominger, *Nucl. Phys. B* **321** (1989), 481.
- [78] M. Giovannini, *Phys. Rev. D* **65** (2002), 124019, C. Grojean, F. Quevedo, G. Tasinato, I. Zavala, *JHEP*, *Branes on Charged Dilatonic Backgrounds: Self-Tuning, Lorentz Violations and Cosmology* **0108** (2001) 005 [hep-th/0106120]; C.P. Burgess, F. Quevedo, S.-J. Rey, G. Tasinato and I. Zavala, *Cosmological Spacetimes from Negative Tension Brane Backgrounds*, *JHEP* **0210** (2002) 028 [hep-th/0207104].
- [79] M. Goliath and G.F.R. Ellis, *Homogeneous cosmologies with cosmological constant*, *Phys. Rev. D* **60** (1999), 023502, [gr-qc/9811068].
- [80] P.F. Gonzalez-Diaz, *Mod. Phys. Lett. A* **5** (1990), 1307.
- [81] J. Greensite, *Phys. Lett. B* **300** (1993), 34, A. Carlini and J. Greensite, *Phys. Rev. D* **49**, 866, (1994).
- [82] L.P. Grishchuk and L.V. Rozhansky, *Phys. Lett. B* **234** (1990), 9.

- [83] C. Gunnarsson, *Gravitational lensing of the most distant known supernova, sn1997ff*, Proceedings of New Trends in Theoretical and Observational Cosmology (Tokyo), Sept. 2001, see [astro-ph/0112340].
- [84] A. Guth, *The inflationary universe*, Vintage, London, 1998.
- [85] S.D.J. Gwyn and F.D.A. Hartwick, *Astrophys. J.* **468** (1996), L77, (see also <http://astrowww.phys.uvic.ca/grads/gwyn/pz/hdfn/spindex.html> and <http://opposite.stsci.edu/pubinfo/pr/96/01.html>).
- [86] F. Hadrovic and J. Binney, *Gravitational lensing and the angular-diameter distance relation*, [astro-ph/9708110]; submitted to MNRAS, 1997.
- [87] J.J. Halliwell, *Phys. Lett. B* **185** (1987), 341, A.B. Burd and J.D. Barrow, *Nucl. Phys. B* **308**, (1988), 929; J.D. Barrow and K. Maeda, *Nucl. Phys. B* **341**, (1990), 294; A.L. Berkin and K. Maeda, *Phys. Rev. D* **44**, (1991), 1691.
- [88] ———, *Quantum cosmology and baby universes*, World Scientific, Singapore, 1991.
- [89] F. Hammer, M. Cailloux, B. Fort, and O. le Fèvre, *Astrophys. J.* **399** (1992), L125.
- [90] J.B. Hartle and S.W. Hawking, *Phys. Rev. D* **28** (1983), 2960, S.W. Hawking, *Nucl. Phys. B* **239**, 257 (1984); S.W. Hawking and D.N. Page, *Nucl. Phys. B* **264**, 185 (1986).
- [91] ———, *Phys. Rev. D* **28** (1983), 2960.
- [92] S. W. Hawking and G. F. R. Ellis, *The large-scale structure of space-time*, Cambridge University Press, 1973.
- [93] S.W. Hawking, *Phys. Rev. D* **37** (1988), 904.
- [94] S.W. Hawking and D.N. Page, *Nucl. Phys. B* **264** (1986), 185.
- [95] ———, *Phys. Rev. D* **42** (1990), 2655.
- [96] R.M. Hawkins and J.E. Lidsey, *Inflation on a single brane—exact solutions*, *Phys. Rev. D.* **63** (2001), 041301, [gr-qc/0011060].

- [97] J.N. Hewitt, E. L. Turner, D.P. Schneider, B.F. Burke, G.I. Langston, and C. R. Lawrence, *Nature* **333** (1988), 537, J.N. Hewitt, B.F. Burke, E.L. Turner, D.P. Schneider, C.R. Lawrence, G.I. Langston and J.P. Brody, in [169].
- [98] S. Hiano, C. Herdeiro, and R. Kallosh, *String theory and hybrid inflation/acceleration*, *JHEP* **0112** (2001), 027, [hep-th/0110271]; K. Dasgupta, C. Herdeiro, S. Hirano and R. Kallosh, *Inflationary Model and M-Theory* [hep-th/0203019].
- [99] D.E. Holz and R.M. Wald, *A new method for determining cumulative gravitational lensing effects in inhomogeneous universes*, *Phys.Rev. D* **58** (1998), 063501, see [astro-ph/9708036].
- [100] P. Horava and E. Witten, *Nucl. Phys. B* **460** (1996), 506, *Nucl. Phys. B* **475**, 94 (1996).
- [101] G.T. Horowitz, *Class. Quantum Grav.* **8** (1991), 587, G.T. Horowitz, in *Proceedings of the Sixth Marcel Grossman Meeting*, (World Scientific, Singapore, 1992).
- [102] W. Hu, see [astro-ph/0105424], to appear in *Astrophys. J. Lett.*, 2001.
- [103] ———, *Phys.Rev. D* **64** (2001), 083005, see [astro-ph/0105117].
- [104] ———, *Dark synergy: Gravitational lensing and the cmb*, *Phys.Rev. D* **65** (2002), 023003.
- [105] Daisuke Ida, *Brane-world cosmology*, *JHEP* **0009** (2000), 014, [gr-qc/9912002].
- [106] M.M. Sheikh Jabbari and H. Arafai, *Different d-brane interactions*, *Phys. Lett. B* **394** (1997), 288–296, [hep-th/9608167]; *Classification of D-brane angles*, *Phys. Lett. B* **420** (1998) [hep-th/9710121]; J. García-Bellido, R. Rabadán, F. Zamora, *Inflationary Scenario from branes at Angles*, *JHEP* **01** (2002) 036 [hep-th/0112147]; N. Jones, H. Stoica and S.H. Tye, *Brane interaction as the origin of inflation*, [hep-th/0202163]; M. Gomez-Reino and I. Zavala, *Recombination of intersecting D-branes and cosmological inflation*, *JHEP* **0209** (2002) 020 [hep-th/0207278].

- [107] A. Jakobek, K. A. Meissner, and M. Olechowski, *New brane solutions in higher order gravity*, Nucl.Phys. B **645** (2002), 217–236, see [hep-th/hep-th/0206254].
- [108] R. T. Jantzen, *Cosmology of the early universe*, World Scientific, Singapore, 1984, eds. R. Ruffini and L. Z. Fang.
- [109] D.P. Jatkar, S. Bhattacharya, D. Choudhury, and A.A. Sen, *Brane dynamics in randall-sundrum model, inflation and graceful exit*, Class. Quantum Grav. **19** (2002), 5025–5038, see [hep-th/0103248].
- [110] R. Colistete Jr. and N. Pinto-Neto, *Graceful exit from inflation using quantum cosmology*, Phys. Lett. A **290** (2001), 219–226.
- [111] M. Olechowski and K. A. Meissner, *Domain walls without cosmological constant in higher order gravity*, Phys.Rev.Lett. **86** (2001), 3708–3711, see [hep-th/0009122]; *Brane localization of gravity in higher derivative theory* Phys.Rev. D **65** (2002) 064017 [hep-th/0106203].
- [112] T. Kaluza, Sitzungsber. Preuss. Akad. Wiss. Berlin (Math. Phys.) **K1** (1921), 966, O. Klein, Z. Phys. **37**(1926) 895.
- [113] P. Kanti, I.I. Kogan, K.A. Olive, and M. Pospelov, Phys. Lett. B **468** (1999), 31, [hep-ph/9909481]; C. Csaki, M. Graesser, C. Kolda and J. Terning, Phys. Lett. B **462**, 34 (1999), [hep-ph/9906513]; C. Csaki, M. Graesser, L. Randall and J. Terning, Phys. Rev. D **62**, 04015 (2000), [hep-ph/9911406]; E. E. Flanagan, S. H. Tye and I. Wasserman, Phys. Rev. D **62**, 044039 (2000), [hep-ph/9910498]; J. M. Cline, C. Grojean and G. Servant Phys. Rev. Lett. **83**, 4245 (1999), [hep-ph/9906523]; P. Binetruy, C. Deffayet and D. Langlois, Nucl. Phys. B **565**, 269 (2000), [hep-th/9905012].
- [114] P. Kanti, J. Rizos, and K. Tamvakis, *Singularity-free cosmological solutions in quadratic gravity*, Phys.Rev. D **59** (1999), 083512.
- [115] R. Kantowski and R. K. Sachs, J. Math. Phys. **7** (1967), 443.
- [116] V. Kaplunovsky, Phys. Rev. Lett. **55** (1985), 1036.

- [117] R. Kayser, J. Surdej, J.J. Condon, K.I. Kellermann, P. Magain, M. Renny, and A. Smette, *Astrophys. J.* **364** (1990), 15.
- [118] A. Kehagias and E. Kiritsis, *Mirage cosmology*, *JHEP* **9911** (1999), 022, [hep-th/9910174].
- [119] S.P. Kim, *Phys. Rev. D* **46** (1992), 3403.
- [120] S.P. Kim and D. N. Page, *Phys. Rev. D* **45** (1992), R3296.
- [121] D. Klemm, *Topological black holes in weyl conformal gravity*, *Class. Quantum Grav.* **15** (1998), 3195–3201, also see more recent publications O. Barabash and Yu. Shtanov *Newtonian Limit of Conformal Gravity* *Phys. Rev. D* **60** (1999) 064008 [astro-ph/9904144]; A. Edery, A. A. Méthot, M. B. Paranjape *Gauge choice and geodesic deflection in conformal gravity* *Gen. Rel. Grav.* **33** (2001) 2075-2079 [astro-ph/0006173].
- [122] J.-P. Kneib, R.S. Ellis, I. Smail, W.J. Couch, and R.M. Sharples, *Ap. J.* **471** (1996), 643–656.
- [123] L. Kofman, R. Kallosh, and A.D. Linde, *Pyrotechnic universe*, *Phys. Rev. D* **64** (2001), 123523, [hep-th/0104073]; R. Kallosh, L. Kofman, A.D. Linde and A.A. Tseytlin, *BPS branes in cosmology*, *Phys. Rev. D* **64** (2001) 123524 [hep-th/0106241].
- [124] E.W. Kolb and M.S. Turner, *The early universe*, Addison Wesley, Redwood City, CA, 1990.
- [125] K. Koyama, *Cmb anisotropies in brane worlds*, (2003), [astro-ph/0303108]; C. Csaki, M. Graesser, L. Randall and J Terning, *Phys. Rev. D* **62**, 045015 (2000); K. Koyama, *Phys. Rev. D* **66** 084003 (2002); T. Wiseman, *Class. Quantum Grav.* **19**, 3083 (2002); S. Kanno and J. Soda, *Phys. Rev. D* **66**, 083506 (2002); K. Koyama and J. Soda, *Phys. Rev. D* **65**, 023514 (2002); T. Shiromizu and K. Koyama, *Phys. Rev. D*, in press.
- [126] A. Krasinsky, *Inhomogeneous cosmological models*, Cambridge University Press, Cambridge, 1997.

- [127] P. Kraus, *JHEP* **991** (1999), 011.
- [128] M. Kriele, W. Hasse, and V. Perlick, *Class. Quantum Grav.* **13** (1996), 1161.
- [129] K. Kuchar, *General relativity and relativistic astrophysics*, World Scientific, Singapore, 1993, ed. Kunstatter and others.
- [130] J.H. Kung, *Gen. Rel. Grav.* **27** (1995), 35, M.L. Fil'chenkov, *Phys. Lett. B* **354**, (1995), 208; N.A. Lemos, *Radiation dominated quantum Friedmann models*, e-print archive [gr-qc/9511082], (1995).
- [131] D. Langlois, *Brane cosmology: an introduction*, Proceedings of the YITP workshop on **Braneworld—Dynamics of spacetime boundary** (Paris), 2002, see [hep-th/0209261]; *Prog.Theor.Phys.Suppl.* **148** (2003) 181-212.
- [132] R.J. Lavery and J.P. Henry, *Ap. J.* **329** (1988), L21.
- [133] C.R. Lawrence, D.P. Schneider, M. Schmidt, C.L. Bennett, J.N. Hewitt, B.F. Burke, E.L. Turner, and J.E. Gunn, *Science* **223** (1984), 46.
- [134] J.E. Lidsey, *Class. Quantum Grav.* **8** (1991), 923, B. J. Carr and J. E. Lidsey, *Phys. Rev. D* **48**, 543 (1993).
- [135] ———, *Class. Quantum Grav.* **11** (1994), 1211.
- [136] J.E. Lidsey, A.R. Liddle, E.W. Kolb, E.J. Copeland, T. Barreiro, and M. Abney, *Reconstructing the inflaton potential: An overview*, *Rev. Mod. Phys.* **69** (1977), 373.
- [137] J.E. Lidsey, D. Wands, and E.J. Copeland, *Superstring cosmology*, *Phys. Rept.* **337** (2000), 343–492, see [hep-th/9909061].
- [138] A. Linde, *JETP Lett.* **60** (1984), 211.
- [139] ———, *Hybrid inflation*, *Phys. Rev. D.* **49** (1994), 748, see [astro-ph/9307002].
- [140] A.D. Linde, *A new inflationary universe scenario: A possible solution of the horizon, flatness, homogeneity, isotropy and primordial monopole problems*, *Phys. Lett. B* **108** (1982), 389, A. Albrecht and P.J. Steinhardt, *Cosmology for Grand*

- Unification Theories with Radiatively Induced Symmetry Breaking*, Phys. Rev. Lett. **48** (1982) 1220; also see reviews A.R. Liddle and D.H. Lyth, *Cosmological Inflation and Large-Scale Structure*, Cambridge University Press (2000); P.J. Peebles, *Principles of Physical Cosmology*, Princeton, USA; Univ. Pr. (1993); R.H. Brandenberger, *Principles, progress and problems in inflationary cosmology*, AAPPS Bull. **11** (2001) 20 [astro-ph/0208103]; J. Garcia-Bellido, *20+ years of inflation*, Nucl.Phys.Proc.Suppl. **114** (2003) 13-26 [hep-ph/0210050].
- [141] ———, *Particle physics and inflationary cosmology*, Harwood, Chur, Switzerland, 1990.
- [142] ———, *Inflationary theory vs. the ekpyrotic/cyclic scenario*, 2002, a talk at Stephen Hawking's 60th Birthday Conference, Cambridge University, no. SU-ITP-02-25, [hep-th/0205259].
- [143] E.V. Linder, *Averaging inhomogeneous universes: Volume, angle, line of sight*, see [astro-ph/9801122], 1998.
- [144] A. Lukas, Phys. Lett. B **347** (1995), 13.
- [145] A. Lukas, B.A. Ovrut, K.S. Stelle, and D. Waldrum, Phys. Rev. D **59** (1999), 086001.
- [146] R. Lynds and V. Petrosian, BAAS **18** (1986), R1014.
- [147] R. Maartens, Phys. Rev. D **62** (2000), 084023, [hep-th/0004166]; *Geometry and Dynamics of the Brane-World*, [gr-qc/0101059] (2001).
- [148] ———, *Brane-world cosmological perturbations: a covariant approach*, Prog.Theor.Phys.Suppl. **148** (2002), 213, [gr-qc/0304089]; B. Gumjudpai, R. Maartens and C. Gordon, *Density perturbations in a brane-world universe with dark radiation* (2003) [gr-qc/0304067]; N. Deruelle, *Cosmological perturbations of an expanding brane in an anti-de Sitter bulk: a short review*, Astrophys.Space Sci. **283** (2003) 619-626 [gr-qc/0301035].

- [149] R. Maartens, V. Sahni, and T.D. Saini, *Phys. Rev. D* **63** (2001), 063509, A.V. Toporensky, *Class. Quant. Grav.* **18**, 2311-2316 (2001); M.G. Santos, F. Vernizzi, P.G. Ferreira, *Phys. Rev. D*, **64**,063506 (2001).
- [150] R. Maartens, D. Wands, B. A. Bassett, and I. P. C. Heard, *Phys. Rev. D* **62** (2000), 041301.
- [151] M. A. H. MacCallum, *Cosmological models from a geometric point of view*, Cargèse Lectures in Physics, vol. 6, Gordon and Breach, New York, 1973, ed. E. Schatzman.
- [152] ———, *General relativity: an einstein centenary survey*, Cambridge University Press, Cambridge, 1979, eds. S. W. Hawking and W. Israel.
- [153] R. Madden, N. Kaloper, and K.A. Olive, *Towards a singularity free inflationary universe?*, *Nucl. Phys. B* **452** (1995), 677, see [hep-th/9506027].
- [154] ———, *Axions and the graceful exit problem in string cosmology*, *Nucl. Phys. B* **371** (1996), 34–40, see [hep-th/9510117].
- [155] M. Madsen and G.F.R. Ellis, *Class. Quantum Grav.* **8** (1991), 667.
- [156] P. Magain, J. Swings, J.-P. Kneib, U. Borgeest, R. Kayser, H. Kühr, S. Refsdal, and M. Remy, *Nature* **334** (1988), 327.
- [157] J. Maharana, M. Gasperini, and G. Veneziano, *Nucl. Phys. B* **472** (1996), 1996, M. Gasperini and G. Veneziano, *Gen. Rel. Grav.* **28**, 1301 (1996); M. Gasperini, *Int. J. Mod. Phys. A* **13**, 4779 (1998); M. Cavagliá and C. Ungarelli, *Class. Quantum Grav.* **16**, 1401 (1991).
- [158] J.M. Maldacena, *The large n limit of superconformal field theories and supergravity*, *Adv. Theor. Math. Phys.* **2** (1998), 231, [*Int. J. Theor. Phys.* **38** (1999) 1113] [hep-th/9711200]; O. Aharony, S.S. Gubser, J.M. Maldacena, H. Ooguri and Y. Oz, *Large N field theories, string theory and gravity* *Phys. Rept.* **323** (2000) 183 [hep-th/9905111]; G. 't Hooft, *Dimensional Reduction in Quantum Gravity* [pr-qc/9310026]; L. Susskind, *The World as a hologram* *J. Math. Phys.* **36** (1995) 6377 [hep-th/9409089].

- [159] P. D. Mannheim and D. Kazanas, *Exact vacuum solutions to conformal weyl gravity and galactic rotation curves*, *Astrophys. J.* **342** (1989), 635–638.
- [160] J. Martin, *Phys. Rev. D* **49** (1994), 5086.
- [161] J. Martin, P. Peter, N. Pinto-Neto, and D.J. Schwarz, *Passing through the bounce in ekpyrotic models*, *Phys. Rev. D* **65** (2002), 123513, [hep-th/0112128].
- [162] G.A. Mena Marugán, *Class. Quantum Grav.* **11** (1994), 2205.
- [163] N.E. Mavromatos, G.A. Diamandis, B.C. Georgalas, and E. Papantonopoulos, *On 'graceful exit' from inflationary phase in two-dimensional liouville string cosmology*, *Phys. Lett. B* **461** (1999), 57–65, see [hep-th/9903045].
- [164] Y. Mellier, B. Fort, and G. Soucail (eds.), *Gravitational lensing* Lecture Notes in Physics, vol. 360, Springer, Berlin, 1990.
- [165] Y. Mellier, G. Soucail, B. Fort, J.-F. le Borgne, and R. Pello, 1990, in [164].
- [166] E. Moertsell, A. Goobar, and L. Bergstroem, *Astrophys. J.* **559** (2001), 53, [astro-ph/0103489].
- [167] E. Moertsell, A. Gunnarsson, and A. Goobar, *Astrophys. J.* **561** (2001), 106.
- [168] V. Moncrief and C. Teitelboim, *Phys. Rev. D* **6** (1972), 966.
- [169] J.M. Moran, J.N. Hewitt, and K.Y. Lo, *Gravitational lenses*, Lecture Notes in Physics, vol. 330, Springer-Verlag, 1989.
- [170] S. Mukherji and M. Peloso, *Bouncing and cyclic universes from brane models*, *Phys. Lett. B* **547** (2002), 297–305, [hep-th/0205180].
- [171] N. Mustapha, B.A.C.C. Bassett, C. Hellaby, and G.F.R. Ellis, *The distortion of the area distance-redshift relation in inhomogeneous isotropic universes*, *Class. Quantum Grav.* **15** (1997), 2363, [gr-qc/9708043].
- [172] Y.S. Myung, *Bouncing and cyclic universes in the charged ads bulk background*, [hep-th/0208086]; Y. Shtanov, *Bouncing Braneworlds* [gr-qc/0208047]; Ph. Brax and

- D.A. Steer, *A comment on bouncing and cyclic branes in more than one extra-dimension* [hep-th/0207280]; H. Liu, *Exact Global Solutions of Brane Universes and Big Bounces* Phys.Lett. B560 (2003) 149-154 [hep-th/0206198]; C. Gordon and N. Turok, *Cosmological Perturbations through a General Relativistic Bounce* Phys.Rev. D **67** (2003) 123508 [hep-th/0206138]; S. Kachru and L. McAllister, *Bouncing Brane Cosmologies from Warped String Compactifications* JHEP 0303 (2003) 018 [hep-th/0205209]; S. and M. Peloso, *Bouncing and cyclic universes from brane models*, Phys. Lett. B **547** (2002) 297–305 [hep-th/0205180]; P. Peter and N. Pinto-Neto, *Primordial perturbations in a non singular bouncing universe model* Phys. Rev. D **66** (2002) 063509 [hep-th/0203013]; R.H. Brandenberger, S.E. Joras and J. Martin, *Trans-Planckian Physics and the Spectrum of Fluctuations in a Bouncing Universe*, Phys. Rev. D, **66** (2002) 083514 [hep-th/0112122].
- [173] R. Nityanda, 1990, in [164].
- [174] D. Nolte, F. Quevedo, G. Rajesh, C.P. Burgess, M. Majumdar, and R.J. Zhang, *The inflationary brane-antibrane universe*, JHEP **07** (2001), 047, [hep-th/01005204].
- [175] A.A. Nucita, A. Qadir, F. de Paolis, and G. Ingrosso, *A note on gravitational wave lensing*, Astron. Astrophys. **394** (2001), 749–752.
- [176] D.N. Page, J. Math. Phys. **32** (1991), 3427.
- [177] A. Pais and G. F. Uhlenbeck, *On field theories with non-localized action*, Phys.Rev. **79** (1950), 145–165.
- [178] E. Papantonopoulos and I. Pappa, *Inflation induced by vacuum energy and graceful exit from it*, Mod. Phys. Lett. A **16** (2001), 2545–2555, see [gr-qc/0103101].
- [179] C. Park and S.-J. Sin, *Moving domain walls in ads_5 and graceful exit from inflation*, Phys. Lett. B **485** (2000), 239–245, see [hep-th/0005013].
- [180] R. Pello-Descayre, G. Soucail, B. Sanahuja, G. Mathez, and E. Ojero, Astron. Astrophys. **190** (1988), L11–L14.

- [181] R. Penrose, *Phys. Rev. Lett.* **14** (1965), 57, S. Hawking, *Proc. R. Soc. London A* **300**, 182 (1967).
- [182] ———, *Techniques of differential topology in relativity*, Society for Industrial and Applied Maths, Philadelphia, 1972.
- [183] ———, *General relativity: An einstein centenary*, Cambridge Univ. Press, Cambridge, 1979, eds. S. Hawking and W. Israel, *M. Markov, JETP Lett.* **36**, 265 (1982); **46**, 431 (1987); V. Ginsburg, V. Mukhanov and V. Frolov, *Sov. Phys. JETP* **67**, 649 (1988).
- [184] J. Polchinsky, *Phys. Lett. B* **219** (1989), 251.
- [185] ———, *String theory, two volumes*, Cambridge University Press, Cambridge, 1999.
- [186] W. H. Press and J. E. Gunn, *Ap. J.* **185** (1973), 397.
- [187] L. Querella, *Variational principles and cosmological models in higher-order gravity*, Ph.D. thesis, Université de Liège, 1999.
- [188] F. Quevedo, B. de Carlos, J.A. Casas, and E. Roulet, *Model-independent properties and cosmological implications of the dilation and moduli sectors of 4-d strings*, *Phys. Lett. B* **318** (1993), 447–456, [hep-ph/9308325]; T. Banks, D.B. Kaplan and A.E. Nelson, *Cosmological implications of dynamical supersymmetry breaking*, *Phys. Rev. D* **49** (1994) 779 [hep-ph/9308292].
- [189] L. Randall and R. Sundrum, *An alternative to compactification*, *Phys. Rev. Lett.* **83** (1999), 4690, and page 3370 for the two-brane scenario, see also [hep-th/9906064]; R. Cardenas, I. Quiros and R. Bonal, *Bouncing open universes embeddable in a distorted Randall-Sundrum brane scenario* [gr-qc/0105080v1] (2001); E. Prodanov, *Bouncing branes* [hep-th/010315v1] (2001); I. Kogan, S. Mouslopoulos, A. Papazoglou and G. Ross, *Multigravity in six dimensions: Generating bounces with flat positive tension branes* [hep-th/0107086v3] (2001).
- [190] B. Ratra, *Phys. Rev. D* **40** (1989), 3939.
- [191] A. Raychaudhuri, *Relativistic cosmology*, *Phys. Rev.* **98** (1955), 1123.

- [192] S. Refsdal and J. Surdej, Rep. Prog. Phys. **56** (1994), 117.
- [193] S. Rey, Phys. Rev. Lett. **77** (1996), 1929.
- [194] R.J. Riegert, *Classical and quantum conformal gravity*, Ph.D. thesis, University of California, San Deigo, 1986.
- [195] A.G. Riess et al., Astrophys. J. **560** (2001), 49, [astro-ph/0104455].
- [196] A.A. Ruffa, Astrophys. J. (1999), L31.
- [197] M. Ryan, *Hamiltonian cosmology*, Springer-Verlag, Berlin, 1972, B.S. DeWitt, Phys. Rev. **160**, 1113, (1967), Peleg Y., *Quantum dust black holes*, e-print archive [hep-th/9307057], (1993).
- [198] H.J. Schmidt S. Kluske, *Towards a no hair theorem for higher order gravity*, Astron. Nachr. **317** (1996), 337–348, see [gr-qc/9503021]; see also *The de Sitter space-time as attractor solution in higher order gravity* to appear in R. Santilli, G. Sardanashvili (Eds.) *New frontiers in gravitation* Hadronic Press. [gr-qc/9501032].
- [199] S. D. Odintsov S. Nojiri, *Brane-world cosmology in higher derivative gravity or warped compactification in the next-to-leading order of ads/cft correspondence*, JHEP **0007** (2000), 049, see [hep-th/0006232].
- [200] T. D. Saini, S. Raychaudhury, V. Sahni, and A. A. Starobinsky, *Reconstructing the cosmic equation of state from supernovae distances*, Phys.Rev.Lett. **85** (2000), 1162–1165.
- [201] A.K. Sanyal, Int. J. Mod. Phys. A **10** (1995), 2231.
- [202] P. Schneider, J. Ehlers, and E.E. Falco, *Gravitational lenses*, Springer-Verlag, Berlin, 1992.
- [203] S. Seitz and P. Schneider, Max-Planck-Institut Preprint MPA (1993), 775.
- [204] U. Seljak, Astrophys. J. **463** (1996), 1.
- [205] M. Sereno, *Gravitational lensing by spinning and escaping lenses*, Phys. Lett. A **305** (2002), 7–11, [astro-ph/0209148].

- [206] I.L. Shapiro, *The graceful exit from the anomaly-induced inflation: Supersymmetry as a key*, Int. J. Mod. Phys. D **11** (2002), 1159–1170, see [hep-ph/0103128].
- [207] I.L. Shapiro and J. Sola, *A modified starobinsky's model of inflation: Anomaly-induced inflation, susy and graceful exit*, talk given at SUSY 2002: the 10th International Conference on Supersymmetry and Unification of Fundamental Interactions, DESY, Hamburg, Germany, June 17–23; also at GRG 11: International Conference on Theoretical and Experimental Problems of General Relativity and Gravitation, Tomsk, Russia, July 1–8 2002, see [hep-ph/0210329].
- [208] ———, *Massive fields temper anomaly-induced inflation: the clue to graceful exit?*, Phys. Lett. B **530** (2002), 10–19, see [hep-ph/0104182]; see also A.A. Starobinsky *Phys. Lett. B* **91** (1980) 99.
- [209] E.J. Shaya, P. Teyssandier, F. Hammer, I.M. Goia, et al., *Astrophys. J.* **491** (1997), 477.
- [210] T. Shiromizo, K. Maeda, and M. Sasaki, *Phys. Rev. D* **62** (2000), 024012.
- [211] L. Smolin, *Did the universe evolve?*, *Class. Quantum. Grav.* **9** (1992), 173, *The Life of the Cosmos* (Oxford University Press, 1997).
- [212] G.F. Smoot et al., *Structure in the cobe dmr first year maps*, *Astrophys. J.* **396** (1992), L1, C.L. Bennet and others., *4-year COBE DMR cosmic microwave background observations: maps and basic results* *Astrophys. J.* **464** (1996) L1 [astro-ph/9601067]; C.B. Netterfield and others., *A measurement by BOOMERANG of multiple peaks in the angular power spectrum of the cosmic microwave background*, *Astrophys. J.* **571** (2002) 604–614 [astro-ph/0104460]; C. Pryke and others., *Cosmological parameter extraction from the first season of observations with DASI*, *Astrophys. J.* **568** (2002) 46–51 [astro-ph/0104490]; R. Stomper and others., *Cosmological implications of the MAXIMA-I high resolution cosmic microwave background anisotropy measurement*, *Astrophys. J.* **561** (2001) L7–L10 [astro-ph/0105062].
- [213] J. Soda and S. Kawai, *Evolution of fluctuations during graceful exit in string cosmology*, *Phys. Lett. B* **460** (1999), 41–46, see [gr-qc/990303017].

- [214] D.M. Solomons, P.K.S. Dunsby, and G.F.R. Ellis, *No bounce behaviour in spatially homogeneous cosmologies*, submitted to Phys. Rev. D, [gr-qc/0103087], 2002.
- [215] ———, *Bounce behaviour in higher derivative kantowski-sachs cosmologies*, (2003).
- [216] G. Soucail, B. Fort, Y. Mellier, and J.P. Picat, *Astron. Astrophys.* **172** (1987), 14.
- [217] G. Soucail, Y. Mellier, B. Fort, G. Marthez, and F. Hammer, *Astron. Astrophys.* **184** (1987), L7.
- [218] G. Soucail, Y. Mellier, B. Fort, G. Mathez, and M. Cailloux, *Astr. Ap.* **191** (1988), L19.
- [219] C.C. Steidel and W.L.W. Sargent, *Astron. J.* **99** (1990), 1693.
- [220] P.J. Steinhardt, J. Khoury, B.A. Ovrut, and N. Turok, *The ekpyrotic universe: Colliding branes and the origin of the hot big bang*, *Phys. Rev. D* **64** (2001), 123522, J. Khoury, B.A. Ovrut, N. Seiberg, P.J. Steinhardt and N. Turok, *Phys. Rev. D* **66** (2002) 046005, [hep-th/0109050].
- [221] P.J. Steinhart and N. Turok, *A cyclic model of the universe*, [hep-th/0111030]; J. Khoury, B.A. Ovrut, N. Seiberg, P.J. Steinhart and N. Turok, *From big crunch to big bang*, *Phys. Rev. D* **65** (2002) 086007 [hep-th/0108187].
- [222] K. S. Stelle, *Renormalization of higher-derivative quantum gravity*, *Phys. Rev. D* **16** (1977), 953–969.
- [223] W. R. Stoeger, R. Maartens, and G. F. R. Ellis, *Astrophys. J.* **443** (1995), 1.
- [224] A. Strominger, *The ds/cft correspondence*, *JHEP* **0110** (2001), 034, [hep/th/0106113]; L. Dyson, J. Lindsay and L. Susskind, *Is there really a de Sitter/CFT duality?*, *JHEP* **0208** (2002) 045 [hep-th/0202163].
- [225] D.R. Taylor and R. Maartens, *Almost-homogeneity of the universe in higher-order gravity*, *Gen. Rel. Grav.* **27** (1995), 1309, see [gr-qc/9511043].
- [226] R. C. Tolman, *Relativity thermodynamics and cosmology*, Oxford University Press, Oxford, 1934, Dover 1987.

- [227] A.V. Toporensky and V.O. Ustiansky, *Dynamics of bianchi ix universe with massive scalar field*, [gr-qc/9907047], 1999.
- [228] A.A. Tseytlin, *Mod. Phys. Lett. A* **6** (1991), 1721.
- [229] S.H. Tye, G. Shiu, and I. Wasserman, *Rolling tachyon in brane world cosmology from superstring field theory*, 2003, [hep-th/0207119]; J.M. Cline, H. Firouzjahi and P. Martineau, *Reheating from tachyon condensation*, *JHEP* **0211** (2002) 041 [hep-th/0207156], p. 083517.
- [230] G. Veneziano, *Phys. Lett. B* **265** (1991), 287, M. Gasperini and G. Veneziano, *Astropart. Phys.* **1**, 317 (1993); *Mod. Phys. Lett. A* **8**, 3701 (1993); *Phys. Rev. D* **50**, 2519 (1994). An updated collection of papers on the pre-big bang scenario is available at <http://www.to.infn.it/~gasperin>.
- [231] A. Vilenkin, *Phys. Rev. D* **30** (1984), 549, A.D. Linde, *Sov. Phys. JETP* **60**, 211, (1984); V.A. Rubakov, *Phys. Lett. B* **148**, 280, (1984); Y.B. Zeldovich and A.A. Starobinski, *Sov. Astron. Lett.* **10**, 135, (1984).
- [232] ———, *Phys. Rev. D* **46** (1992), 2355.
- [233] ———, *Phys. Rev. D* **30** (1994), 509, A.D. Linde, *Sov. Phys. JETP* **60**, 211 (1984); Y. Zel'dovich and A.A. Starobinski, *Sov. Astron. Lett.* **10**, 135 (1984); V.A. Rubakov, *Phys. Lett. B* **148**, 280 (1984).
- [234] A. Vilenkin and A. Borde, *Phys. Rev. Lett.* **72** (1994), 3305.
- [235] J. Wainwright and G. F. R. Ellis, *Dynamical systems in cosmology*, Cambridge University Press, 1997.
- [236] R. Wald, *Phys. Rev. D* **28** (1982), 2118.
- [237] R.M. Wald, *General relativity*, The University of Chicago Press, Chicago, 1984.
- [238] J. Wambsganss, *The search for matter with gravitational lensing*, Frontier Group, 2002, To appear in *Where's the Matter? Tracing Bright and Dark Matter with the New Generation of Large Scale Surveys*, ed. M. Treyer & L. Tresse.

- [239] D.W. Weedman, R.J. Weymann, R.F. Green, and T.M. Heckman, *Ap. J.* **255** (1982), L5.
- [240] S. Weinberg, *Gravitation and cosmology*, Wiley, New York, 1972.
- [241] ———, *Ap. J.* **208** (1976), L1.
- [242] ———, *Rev. Mod. Phys.* **61** (1989), 1.
- [243] B. Whitt, *Phys. Lett. B* **145** (1984), 176, M. Mijić, M. Morris and W Suen, *Phys. Rev. D* **34**, 2934 (1986); J. Barrow, *Phys. Lett. B* **183**, 285 (1987).
- [244] E. Witten, *Quantum gravity in de sitter space*, This article is an expanded version of a lecture at Strings 2001 in Mumbai [hep-th/0106109]; T. Banks, *Cosmological breaking of supersymmetry or Little Lambda goes back to the future, II* [hep-th/0007146]; T. Banks and W. Fischler, *M-Theory observables for cosmological space-times* [hep-th/0102077]; J.M. Maldacena and C. Núñez, *Supergravity description of field theories on curved manifolds and a no-hp theorem*, *Int. J. Mod. Phys. A* **16** (2001) 822 [hep-th/0007018], 2001.
- [245] D. Youm, *Mod. Phys. Lett. A* **16** (2001), 937–946, *Nucl. Phys. B* **576**, 106 (2000), [hep-th/9911218]; *Localization of Gravity on Dilatonic Domain Walls: Addendum to “Solitons in Brane Worlds”* *Nucl.Phys. B* **596** (2001) 289-295 [hep-th/0007252]; *Nucl. Phys. B* **589**, 315 (2000), [hep-th/0002147]; K. Maeda and D. Wands, *Phys. Rev. D* **62** 124009 (2000), [hep-th/0008188]; A. Mennim and R.A. Battye, [hep-th/0008192]; C. Barcelo and M. Visser *JHEP* **0010** 019 (2000), [hep-th/0009032].
- [246] M. Zaldarriaga, *Phys. Rev. D.* **62** (2000), 063510, in press.
- [247] M. Zaldarriaga and U. Seljak, *Phys. Rev. D.* **59** (1999), 123509, in press, [astro-ph/0105117].
- [248] A. Zhuk, *Phys. Lett. A* **176** (1993), 176.